PB80-187842

Sulfur Dioxide Oxidation in Scrubber Systems

Virginia Univ.
Charlottesville. Dept. of Chemical Engineering

Prepared for

Industrial Environmental Research Lab.
Research Triangle Park, NC

Apr 80

U.S. Department of Commerce
National Technical Information Service
NTIS

United States
Environmental Protection
Agency

Industrial Environmental Research
Laboratory
Research Triangle Park NC 27711

EPA-600/7-80-083
April 1980

PB80-187842

EPA

Sulfur Dioxide Oxidation in Scrubber Systems

Interagency Energy/Environment R&D Program Report

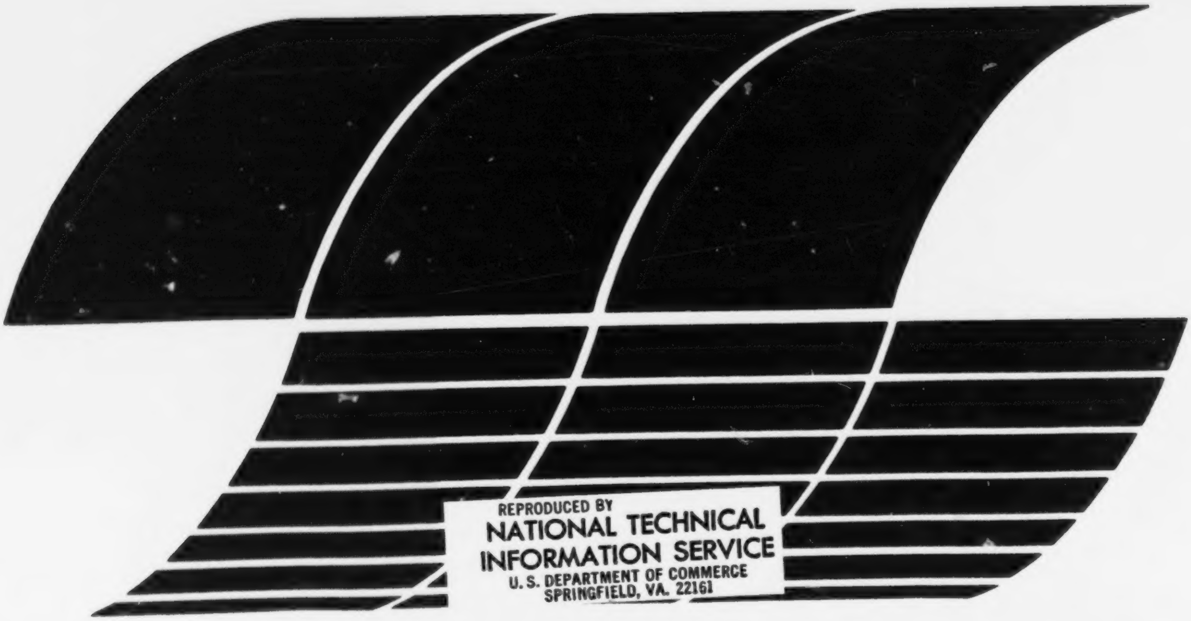

REPRODUCED BY
NATIONAL TECHNICAL
INFORMATION SERVICE
U. S. DEPARTMENT OF COMMERCE
SPRINGFIELD, VA. 22161

RESEARCH REPORTING SERIES

Research reports of the Office of Research and Development, U.S. Environmental Protection Agency, have been grouped into nine series. These nine broad categories were established to facilitate further development and application of environmental technology. Elimination of traditional grouping was consciously planned to foster technology transfer and a maximum interface in related fields. The nine series are:

1. Environmental Health Effects Research
2. Environmental Protection Technology
3. Ecological Research
4. Environmental Monitoring
5. Socioeconomic Environmental Studies
6. Scientific and Technical Assessment Reports (STAR)
7. Interagency Energy-Environment Research and Development
8. "Special" Reports
9. Miscellaneous Reports

This report has been assigned to the INTERAGENCY ENERGY-ENVIRONMENT RESEARCH AND DEVELOPMENT series. Reports in this series result from the effort funded under the 17-agency Federal Energy/Environment Research and Development Program. These studies relate to EPA's mission to protect the public health and welfare from adverse effects of pollutants associated with energy systems. The goal of the Program is to assure the rapid development of domestic energy supplies in an environmentally-compatible manner by providing the necessary environmental data and control technology. Investigations include analyses of the transport of energy-related pollutants and their health and ecological effects; assessments of, and development of, control technologies for energy systems; and integrated assessments of a wide range of energy-related environmental issues.

EPA REVIEW NOTICE

This report has been reviewed by the participating Federal Agencies, and approved for publication. Approval does not signify that the contents necessarily reflect the views and policies of the Government, nor does mention of trade names or commercial products constitute endorsement or recommendation for use.

This document is available to the public through the National Technical Information Service, Springfield, Virginia 22161.

TECHNICAL REPORT DATA
(Please read Instructions on the reverse before completing)

1. REPORT NO. EPA-600/7-80-083	2.	3. RECIPIENT'S ACCESSION NO. PB 80 187842
4. TITLE AND SUBTITLE Sulfur Dioxide Oxidation in Scrubber Systems		5. REPORT DATE April 1980
		6. PERFORMING ORGANIZATION CODE
7. AUTHOR(S) J. L. Hudson		8. PERFORMING ORGANIZATION REPORT NO.
9. PERFORMING ORGANIZATION NAME AND ADDRESS University of Virginia Department of Chemical Engineering Charlottesville, Virginia 22901		10. PROGRAM ELEMENT NO. EHE624
		11. CONTRACT/GRANT NO. Grant No. R805227
12. SPONSORING AGENCY NAME AND ADDRESS EPA, Office of Research and Development Industrial Environmental Research Laboratory Research Triangle Park, NC 27711		13. TYPE OF REPORT AND PERIOD COVERED Final; 7/77-6/79
		14. SPONSORING AGENCY CODE EPA/600/13

15. SUPPLEMENTARY NOTES IERL-RTP project officer is Robert H. Borgwardt, Mail Drop 65, 919/541-2336.

16. ABSTRACT The report relates the liquid-phase oxidation kinetics of bisulfite and sulfite anions (determined in bench scale experiments) to conditions representative of limestone scrubbers used for flue gas desulfurization. The chemical reaction rates were determined for clear solutions and slurries of calcium sulfite when gas-to-liquid transfer of oxygen was not a limiting resistance. From the experimental results, a mathematical model was developed for the overall oxidation rate of calcium sulfite slurries, including solids dissolution and chemical reaction. The overall rate is shown to decline with increasing pH due to the reduced solubility of calcium sulfite; the solid dissolution rate is thus the limiting factor at high pH. The homogeneous chemical oxidation rate is 1.5 order and increases with pH. Organic acids inhibit the oxidation reaction, especially glycolic acid. Manganese and iron catalyze the oxidation reaction even in the presence of organic inhibitors.

17. KEY WORDS AND DOCUMENT ANALYSIS

a. DESCRIPTORS		b. IDENTIFIERS/OPEN ENDED TERMS	c. COSATI Field/Group	
Pollution	Desulfurization	Pollution Control	13B	07D
Sulfur Dioxide	Mathematical Models	Stationary Sources	07B	12A
Oxidation	Sulfites	Calcium Sulfite		
Scrubbers	Calcium Inorganic	Glycolic Acid	07A, 13I	
Calcium Carbonates	Compounds			
Flue Gases	Organic Acids		21B	

18. DISTRIBUTION STATEMENT Release to Public	19. SECURITY CLASS *(This Report)* Unclassified	21. NO. OF PAGES
	20. SECURITY CLASS *(This page)* Unclassified	22. PRICE

EPA Form 2220-1 (9-73)

EPA-600/7-80-083

April 1980

Sulfur Dioxide Oxidation in Scrubber Systems

by

J.L. Hudson

University of Virginia
Department of Chemical Engineering
Charlottesville, Virginia 22901

Grant No. R805227
Program Element No. EHE624

EPA Project Officer: Robert H. Borgwardt

Industrial Environmental Research Laboratory
Office of Environmental Engineering and Technology
Research Triangle Park, NC 27711

Prepared for

U.S. ENVIRONMENTAL PROTECTION AGENCY
Office of Research and Development
Washington, DC 20460

ABSTRACT

This study relates the liquid phase oxidation of bisulfite and sulfite anions to sulfate to the conditions in lime/limestone scrubbing systems such as those used for removal of sulfur dioxide from power plant stack gases.

Experiments were carried out for the oxidation in both calcium sulfite and sodium sulfite clear solutions and in calcium sulfite slurries. In the slurry studies, both the rate of chemical reaction and the rate of solid to liquid mass transfer were investigated, but with both slurries and clear solutions, the experiments were run so that gas to liquid transfer of oxygen was not a limiting resistance. A mathematical model for the dissolution of solid particles and liquid phase chemical reaction was developed in conjunction with these experimental results. The oxidation was carried out over a pH range of 4.0 to 5.5 (although some experiments were at pH 6 and pH 11), at temperatures of 25°C to 50°C, and in the presence of iron and manganese catalysts and several organic acid inhibitors. Batch reactors were used for the slurry studies and for the slower clear solution oxidations while a flow reactor was employed for faster clear solution reactions.

Although under special combinations of catalyst, pH, and organic acid, the order was as low as one or rose to two, the homogenous chemical oxidation rate of calcium sulfite oxidation is 1.5 order over most of the range of conditions. The rate increases strongly with increasing pH. Of the organic acids studied, glycolic is the strongest inhibitor, followed by adipic and succinic. Citric and acetic acids are less inhibitory than the others. Both manganese and iron catalyze the reaction even in the presence of the organic acid inhibitors. Oxygen concentration varied over a large range; its order is 0.5 in the rate expression for the manganese catalyzed oxidation at higher pH.

In a three phase slurry oxidation the overall reaction of sulfite to sulfate declines with increasing pH; this decrease is caused by the sharply reduced calcium sulfite solubility with increasing pH. This calcium sulfite solubility was determined in independent experiments.

The results of the mathematical model for the dissolution and reaction of calcium sulfite particles compare well with results of the three phase slurry oxidations.

CONTENTS

Abstract ii
Figures v
Tables viii

1. Introduction 1
   A. General Considerations 1
   B. Background Literature 3

2. Experiments 32
   A. Apparatus 33
      1. Batch Reactor 33
      2. Flow Reactor 37
   B. Procedure 44
      1. Rate from Concentration Measurements 44
      2. Rate from pH Measurements 46
      3. Rates from Temperature Measurements 46
   C. Analysis of Calcium Sulfite 48
   D. Equilibrium Relationship for S^{4+} Species 50
   E. Iodometric Titration 50
   F. Analysis of Data 52
      1. Analysis of a Single Experiment 52
      2. Multiple Regression Analysis 53
      3. Analysis of pH Method Data 61
      4. Analysis of Flow-Thermal Method 64

3. Oxidation in Calcium Sulfite Solutions 69
   A. $CaSO_3$ Oxidation (No organic acids) 70
   B. $CaSO_3$ Oxidation in the Presence of Organic Acids .. 71
      1. Succinic Acid 83
         a. Effect of pH on the rate of oxidation 83
         b. Effect of succinic acid concentration 85
      2. Adipic Acid 90
      3. Glycolic Acid 90
      4. Comparison of Rates of Oxidation with Succinic Acid, Adipic Acid, Glycolic Acid, Citric Acid, and Acetic Acid 96
      5. Effect of Catalysts--Manganese and Iron 107
         a. Succinic Acid 107
         b. Glycolic Acid 111

   C. Reaction in Liquor from Penberthy Oxidation Runs at Shawnee 118
   D. Dependence of Oxidation Rate on Stirring Speed and Oxygen Flow Rate 122
   E. Rate of $CaSO_3$ Oxidation at High Catalyst Concentrations by Flow-Thermal Method 133

4. Oxidation in Slurries 139
A. Experiment 140
1. Solubility Studies 140
a. Theoretical Analysis 140
b. Experimental Results 141
2. Oxidation in Calcium Sulfite Slurries 143
3. Oxygen Flow Rate Studies 143
4. pH and Temperature Studies 146
5. Slurry Density Studies 153
6. Catalyzed Slurry Oxidation Studies 153
7. Liquid Phase Slurry Behavior 161
8. pH Behavior During Reaction 161
9. Slurry Reactions with and without pH Controller 161
10. Liquid phase Catalyst Studies 171
B. Mathematical Model 171
1. General Description of Model 171
2. Physical Description of Particles 174
a. Electron Micrograph 174
b. Particle Size Distribution 175
3. Derivation of the Spherical Model 175
4. Solutions of the Spherical Model 179
5. Derivation of the Flat Plate Model 192

5. Oxidation in Sodium Sulfite Solutions 194
A. Na_2SO_3 Oxidation 195
1. Manganese Catalyst 195
B. Na_2SO_3 Oxidation with Succinic Acid Buffer 195
1. Iron Catalyst 195
2. Manganese Catalyst 208
3. Mixed Catalysts 217
C. Rate of Na_2SO_3 Solution Oxidation by the Flow-Thermal Method 221

6. Conclusion 227

References 233

FIGURES

Number Page

1-1 Effect of pH on the Relative Concentrations of Sulfur (4+) Species in Solution 4
1-2 Electron Micrograph of Calcium Sulfite Particles - Sulfite and Sulfate Particles 8
1-3 Electron Micrograph of Calcium Sulfite Particle Individual Agglomerate 8
1-4 Comparison of Gladkii's Figure 6 with Figure 5 23
1-5 Comparison of Slurry Oxidations at 50°C. 24
1-6 Comparison of Gladkii's Figure 6 with Soviet Slurry Oxidation Rate Expression 26
1-7 Determination of Soviet Reaction Order 27
1-8 Comparison of Slurry Oxidations at 40°C. 29

2-1 Experimental Apparatus 34
2-2 Reaction Vessel. 35
2-3 Tubular Flow Reactor 38
2-4 REPORT and CURVIT Programs 54
2-5 Element of Reacting Fluid. 66
2-6 Sample Output for Flow Reactor 68

3-1 Rate of Calcium Slufite Oxidation; no added catalyst . . . 72
3-2 Rate of Calcium Sulfite Oxidation; [Mn] = 0.6 ppm. 76
3-3 Rate of Calcium Sulfite Oxidation; [Mn] = 0.53 ppm, [Fe] = 1.02 ppm 77
3-4 Rate of Calcium Sulfite Oxidation; variable [Mn] 79
3-5 Rate of Calcium Sulfite Oxidation; variable [Mn], ($[S^{4+}]$ = 0.0037 mol/ℓ). 80
3-6 Effect of Temperature on the Rate Constant 81
3-7 Effect of pH on Rate of Reaction 86
3-8 Concentration Sulfur (4+) Versus Time for Various Concentrations of Succinic Acid 87
3-9 Concentration Sulfur (4+) Versus Time, Run 566, 0.2M Succinic Acid 88
3-10 The Inhibition of the Sulfite Oxidation Due to Succinic Acid. 89
3-11 Initial Rate Versus Succinic Acid Concentration. 91
3-12 The Inhibition of the Sulfite Oxidation Due to Adipic Acid. 94
3-13 Concentration S^{4+} vs Time for Various Concentrations of Glycolic Acid, pH = 4.0 97
3-14 Inhibition of the Sulfite Oxidation due to Glycolic Acid . 98
3-15 The pH Effect on the Inhibition of the Sulfite Oxidation Due to Glycolic Acid. 99
3-16 Effect of Glycolic Acid on Rate of Oxidation of $CaSO_3$, at T=50°C, pH=4.0, $[S^{4+}]$=0.01M 102
3-17 Comparative Strength of Various Organic Acids as Inhibitors at 0.2M. 103

FIGURES (continued)

3-18 Comparative Strength of Various Organic Acids as Inhibitors at 0.01M . . . 104
3-19 Sulfur (4+) Concentration vs Time for Various Mn Concentrations . . . 110
3-20 Effect of Mn on Oxidation Rate of Succinic Acid Buffered CaSO$_3$ Solutions for $[S^{4+}]$=0.01M, T=50°C, pH=5.0 . . . 113
3-21 Concentration Sulfur (4+) vs Time, 1000 ppm Glycolic Acid, Various Concentrations of Mn . . . 114
3-22 Effect of Mn Addition to Glycolic Acid Inhibited CaSO$_3$ Oxidation; rate at $[S^{4+}] = 0.01M$ . . . 116
3-23 Effect of Mn Addition to Glycolic Acid Inhibited CaSO$_3$ Oxidation; Rate at $[S^{4+}] = 0.01$ M . . . 117
3-24 Stirring Speed = 215 rpm . . . 123
3-25 Stirring Speed = 1800 rpm . . . 124
3-26 Rate at $[S^{4+}] = 0.01$ M vs Stirring Speed . . . 128
3-27 1.4 Order Rate Constant vs Mn Concentration in CaSO$_3$ Filtrate Oxidations . . . 132
3-28 Representative T vs t Results for CaSO$_3$ Oxidation . . . 134
3-29 Effect of [Mn] on CaSO$_3$ Oxidation Rate . . . 136

4-1 Solubility of Calcium Sulfite at 40°C . . . 142
4-2 Effect of Slurry Density on Oxidation Rate . . . 144
4-3 Typical Slurry Reaction Curve . . . 145
4-4 Effect of Mn Catalyst on Slurry Oxidation Rate . . . 147
4-5 Slurry Oxidation, pH = 4.5 . . . 148
4-6 Slurry Oxidation, pH = 4.7 . . . 149
4-7 Slurry Oxidation, pH = 5.0 . . . 150
4-8 Effect of pH on Slurry Oxidation Rates . . . 151
4-9 Slurry Oxidation, pH = 4.5 . . . 154
4-10 Slurry Oxidation, pH = 4.5 . . . 155
4-11 Catalyzed and Uncatalyzed Oxidations at 50°C . . . 158
4-12 Effect of Catalyst on pH Behavior (40°C) . . . 159
4-13 Effect of Catalyst on pH Behavior (50°C) . . . 160
4-14 Slurry Oxidation, 200 ppm Mn, pH = 5.0 . . . 164
4-15 Slurry Oxidation, 200 ppm Mn, pH = 4.5 . . . 165
4-16 Slurry Oxidation, 200 ppm, pH = 5.0 . . . 166
4-17 Slurry Oxidation, pH = 5.0 . . . 167
4-18 pH Behavior During Slurry Oxidations; Effect of Slurry Density . . . 168
4-19 pH Behavior During Slurry Oxidations; Effect of Initial pH . . . 169
4-20 pH Behavior During Slurry Oxidations; Highly Catalyzed Runs . . . 170
4-21 Slurry Oxidation with No Mn Added . . . 172
4-22 Liquid Phase Catalyst Behavior During Slurry Oxidations . . . 173
4-23 B-30 Program and Sample Calculation . . . 181
4-24 Determination of ke from Highly Catalyzed Slurry Data (2000 ppm Mn added) . . . 187
4-25 Comparison of Total S^{4+} from Model to Experimental Slurry Oxidation Data for No Added Mn . . . 188

FIGURES (continued)

4-26 Comparison of Model to Experimental Data for 6.66 ppm Mn Added. 189
4-27 Comparison of Model to Experimental Data for 200 ppm Mn Added 190
4-28 Comparison of Liquid S^{4+} from Model to Experimental Slurry Oxidation Data for No Mn Added. 191
4-29 Computer Predicted Liquid $[S^{4+}]$ Profiles 193

5-1 Dependence of Rate on Sulfite Concentration. 197
5-2 Dependence of Rate on Manganese Concentration. 198
5-3 Sulfur S^{4+} Concentration vs Time for Iron Catalyzed Na_2SO_3 Oxidations. 200
5-4 Rate at $[S^{4+}]$ = 0.028 mol/ℓ vs Concentration Iron Added for Sodium Sulfite Oxidations 203
5-5 Sulfur (4+) Concentration vs Time for Iron Catalyzed Oxidations at Various Temperatures Using Na_2SO_3 204
5-6 Activation Energy Determination for Fe Catalyzed Na_2SO_3 Oxidations. 206
5-7 Rate at $[S^{4+}]$ = 0.028 M vs Concentration Fe. 210
5-8 Sulfur (4+) Concentration vs Time for Manganese Catalyzed Oxidations of Na_2SO_3 Solutions. 213
5-9 Rate at $[S^{4+}]$ = 0.028 M vs Concentration Mn. 215
5-10 Reduced Sulfur (4+) Concentration vs Time for Comparison of Oxidation Reactions. 218
5-11 Comparison of Mn Added Only to Oxygen Side or Only to Sulfur Side 226

LIST OF TABLES

Number Page

1-1 Fly Ash Analysis 6
1-2 Limestone Analysis 9
1-3 Comparison of Literature of Sulfite Dioxide Oxidation. . . 15

2-1 Analysis of Calcium Sulfite Solid. 49

3-1 Rate of Calcium Sulfite Oxidation; No added catalyst ($pH = 4.6$). 73
3-2 Rate of Calcium Sulfite Oxidation; [Mn] = 0.6 ppm. 74
3-3 Rate of Calcium Sulfite Oxidation; Added Mn and Fe 75
3-4 Rate of Calcium Sulfite Oxidation; variable [Mn] 78
3-5 Effect of Temperature on Rate Constant 82
3-6 Effect of pH on Succinic Acid Buffered $CaSO_3$ Solutions . . 84
3-7 Effect of Succinic Acid on Oxidation Rate. 92
3-8 Results of Order and Rate Determination Analysis of Data for Calcium Sulfite Oxidation with Varying Concentrations of Adipic Acid. 93
3-9 Results of Order and Rate Determination Analysis of Data for Calcium Sulfite Oxidations with Varying Concentrations of Glycolic Acid Added 95
3-10 Effect of Glycolic Acid on Oxidation Rate of Calcium Sulfite 100
3-11 Results of Order and Rate Determination Analysis of Data for Calcium Sulfite Oxidations with Varying Concentrations of Glycolic Acid Added 101
3-12 Effect of Organic Acids on Oxidation Rate of Calcium Sulfite 105
3-13 Catalyst Impurity Levels in $CaSO_3$ Solutions. 108
3-14 Effect of Mn Impurity on Oxidation Rate. 109
3-15 Effect of Mn Concentration on Oxidation Rate of Succinic Acid Buffered $CaSO_3$ Solutions 112
3-16 Effect of Manganese Addition to Glycolic Acid Inhibited Runs. 115
3-17 Oxidation of Sulfite Solutions 119
3-18 Supplemental Analysis of Shawnee Sample. 121
3-19 Effect of Stirring Speed - No added catalyst 125
3-20 Effect of Stirring Speed on Reaction Rate Constant - 0.5 ppm Mn. 127
3-21 Effect of Oxygen Flow Rate on Oxidation in Unsaturated Solutions 129
3-22 Results of Filtrate Oxidations; $pH_I = 4.5$, $T = 40°C$. . . . 131
3-23 Effect of High Mn Concentration on $CaSO_3$ Oxidation Rate . . 137
3-24 Effect of pH on the Rate of Mn Catalyzed $CaSO_3$ Oxidation. . 138

4-1 Results of Studies Showing Effect of Initial pH on Oxidation. 152

LIST OF TABLES (continued)

4-2 Effect of Slurry Load on Oxidation Rate at 40°C 156
4-3 Effect of Catalyst on Slurry Oxidation Rate 157
4-4 Experiments Made in Mn Catalyst Study 162
4-5 Experimental Conditions Used in Slurry Oxidations Shown in Figures 4-5 to 4-7, 4-9, 4-10, 4-14 to 4-17. 163
4-6 Size Distribution of Calcium Sulfite Particles (Coulter Method). 176

5-1 Na_2SO_3 Oxidation. 196
5-2 Results of Sodium Sulfite Oxidation with Iron Catalyst Added. 202
5-3 Results of Iron Catalyzed Reactions at Various Temperatures Using Sodium Sulfite 205
5-4 Results of Sodium Sulfite Oxidations with Varying Initial Sulfite Concentration and 5 ppm Iron Added 207
5-5 MULTREG Results for Iron Catalyzed Na_2SO_3 Oxidations. . . . 209
5-6 Results of Sodium Sulfite Oxidations with Manganese Added . 211
5-7 Regression Analysis of Manganese Catalyzed Na_2SO_3 Oxidations 216
5-8 Results of Sodium Sulfite Oxidations with Iron and Manganese Added. 219
5-9 Multiple Regression Results for Mixed Catalyst Sodium Sulfite Oxidations 220
5-10 Effect of [Mn] on Na_2SO_3 Oxidation Rate 223
5-11 Effect of pH on Na_2SO_3 Oxidation Rate 224

SECTION 1

I. Introduction

  A. General Considerations

  B. Background Literature

INTRODUCTION

A. General Considerations

In the removal of sulfur oxides from stack gases by any of the scrubbing methods, a fraction of the sulfur compounds is oxidized to sulfates. This oxidation occurs whether the scrubbing agent is a slurry (lime/limestone systems) or a clear solution (double alkali or other such systems). Furthermore, the oxidation occurs not only in the absorber, but also in other sections of the system, such as in the hold tanks.

In lime/limestone scrubbing systems SO_2 oxidation is important for several reasons. (The species actually taking part in the reaction is either a bisulfite or sulfite ion depending on the pH of the solution; however, it is convenient and it is common practice to refer to sulfur dioxide or calcium sulfite oxidation.) The oxidation in the scrubbing system can increase the degree of supersaturation of calcium sulfate, leading to an increase in the rate of gypsum scale formation (183, 30). Thus, it is important to limit calcium sulfite oxidation in some systems. On the other hand, calcium sulfate is preferable to calcium sulfite from the standpoint of solids disposal since the sulfate has a higher settling velocity than the sulfite and the sulfate also has a higher compaction and a lower chemical oxygen demand (31-36). The latter is important from water pollution considerations. Therefore, in some limestone scrubbing systems it may be desirable to promote or inhibit oxidation.

Oxidation in lime/limestone systems, both in the scrubber and in the hold tanks, is a very complicated process. The rate of oxidation can depend on chemical kinetics since the rates of liquid phase reactions of sulfite ion and bisulfite ion vary with concentration, with the presence of catalysts or inhibitors, and with the type of oxidizing agents, viz., oxygen or nitrogen oxides. (It should be noted that very small concentrations of some catalysts can influence the reaction greatly and that, therefore, many reactions which are supposedly being run without catalysts are in fact being catalyzed by impurities present.) The rate of oxidation is also influenced by phase and chemical equilibria. There are three phases present in the scrubbing system, solid, liquid, and gas. Both the phase equilibria and chemical equilibria are strongly dependent on pH. For example, lowering the pH in the presence of calicium sulfite increases the solubility and, therefore, increases the concentration of dissolved sulfur containing species. This can increase the rate of oxidation under some conditions, particularly, say, in a hold tank. However, a lowering of the pH of scrubbing liquor in the absorber converts sulfite ion to bisulfite ion; this would lower the rate of oxidation since sulfite ion is oxidized much more quickly than bisulfite ion in a clear liquor (but not in a slurry where solubility effects are important). Finally, the rate of oxidation can be influenced or controlled by mass transfer, viz., by the rate of transfer of oxygen to the liquor and by the rate of dissolution of solid particles.

The complex sulfur dioxide oxidation process was broken down into steps and each step studied separately. The oxidation of calcium sulfite and sodium sulfite clear solutions was inventigated as a function of manganese and iron catalysts, pH, temperature, and organic acid inhibitors. The rate of dissolution of calcium sulfite particles in a stirred liquid was determined and this information, along with the kinetic rate results, were used as a basis for a mathematical model for the dissolution and reaction of calcium sulfite particles. Measurements were then made on the rate of oxidation in calcium sulfite slurries and the results compared to predictions of the model.

B. Background Literature

Atmospheric sulfur dioxide affects our lives in many ways. It is a health hazard (9, 10), corroder of structures (94) and equipment, visibility impairer (106), and habitat modifier (88, 166). Man's activities of smelting and burning fossil fuels among others have significantly altered the world sulfur budget (97), threatened his health (10, 57), and now require control (60, 61).

Control methods include: wet scrubbing, dry sorbents (furnace injection) (144, 161), catalytic oxidation (5, 27, 37, 38, 73, 121, 123, 146, 164), dry filters (and baghouse add-ons) (1), and fuel precleaning (111).

Today, wet scrubbing is the most widespread method (59) for cleaning SO_2 from stationary sources. When the SO_2 enters any scrubbing liquor, the following equilibria are set up (154):

$$SO_2 + H_2O \rightleftharpoons SO_2 \cdot mH_2O \rightleftharpoons HSO_3^- + H^+ \rightleftharpoons SO_3^{2-} + H^+$$

$$\text{low} \longrightarrow \text{pH} \longrightarrow \text{high}$$

These relationships are shown graphically in Figure 1-1. Water-only scrubbing is ineffective. Removing the H^+ in the last two equilibria above effectively shifts the concentrations to the right, thereby sequestering the sulfur dioxide as bisulfite on sulfite anions. All of the scrubbing methods

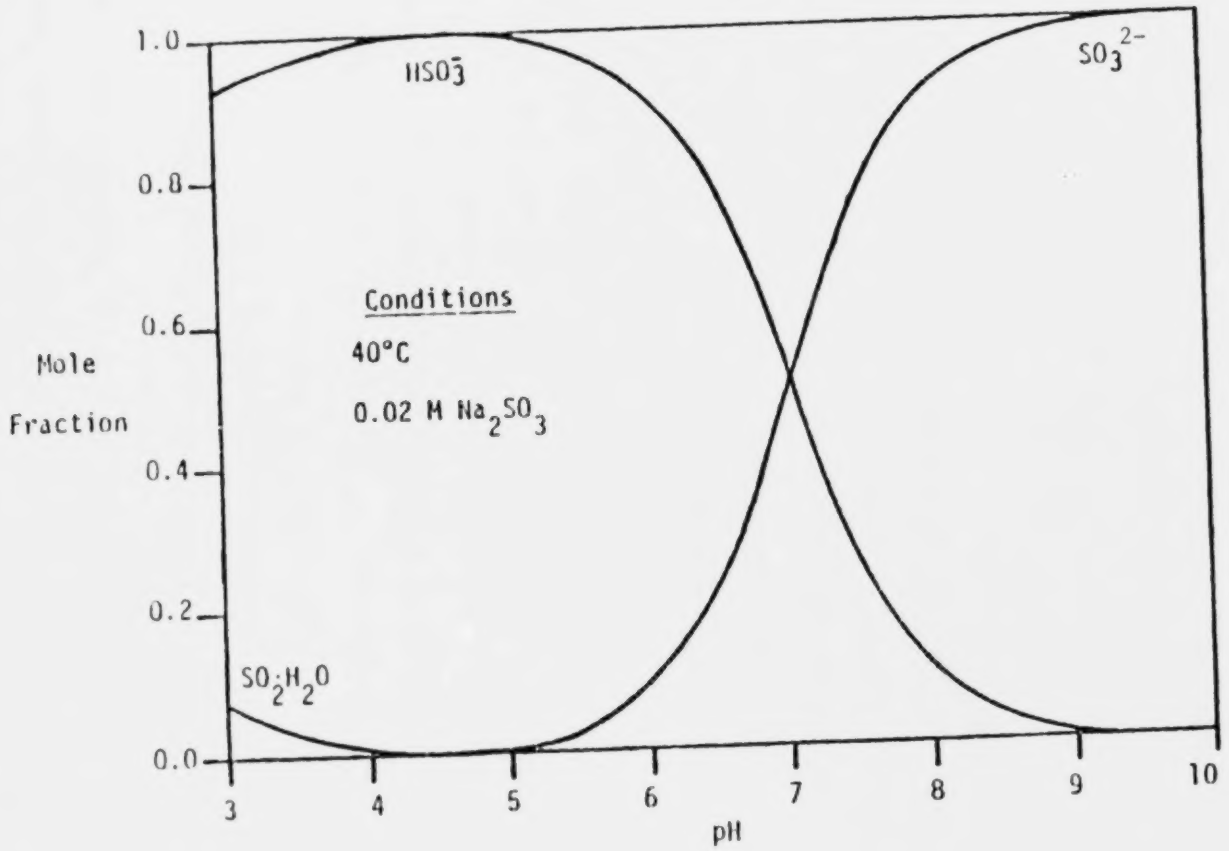

Figure 1-1. Effect of pH on the Relative Concentrations of Sulfur (4+) Species in Solution.

turn on this principle of tying up hydronium ion by the addition of many kinds of alkalis (eg. $CaCO_3$, CaO, NaOH, NH_3). The resulting sulfite/bisulfite solution can be discarded (these are "throwaway" processes) or regenerated (132, 177). Overall, the scrubbing process consists of: Gas-Liquid mass transfer from the stack gas, equilibria and reaction in the scrubbing mixture, modulation by Solid-Liquid transfer of absorbents (and possible Liquid-Solid transfer of products).

The Gas-Liquid mass transfer is accomplished in several ways (90): spray tower, venturi (89, 98, 175), packed bed (159) and turbulent contact (moving ball) absorber (113). The efficiency of the G-L contacting step has been the subject of much study to assess major resistances (120, 178) and control them (142). Since SO_2 is chemically transformed as it enters (102) the liquid surface (from bubbles (104) or surface films (11, 46, 58)), the rates are best treated as absorption with reaction and described by parallel approaches viz., film theory (47, 85, 157), penetration theory (40, 41), or surface renewal (51, 52, 143).

From coal fired boilers, stack gas entering the scrubber carries (53) 4 to 7% O_2; various oxides of nitrogen; CO_2, CO, and organic residues; as well as inorganic residues entrained as fly ash (including chloride (29, 114) and metals (105) as well as inert particulates (64, 77). Some scrubbing methods remove particulates (69) as well as sulfur oxides, but these particulates (inorganic and other coal debris) influence the scrubbing process as catalysts and inhibitors of sulfite oxidation. See Table 1-1.

The sulfur oxides rapidly (23) form a potentially reactive mixture described by the SO_2 dissociation equilibrium (99). The first ionization constant being 1.74×10^{-2} (167), the second 6.24×10^{-8} (189). The equilibria have been studied for SO_2/water systems (137, 169, 170) and scrubbing systems (124, 144).

TABLE 1-1. FLY ASH ANALYSIS

Chemical Analysis

Component	Weight Percent
Al_2O_3	20-30
Fe_2O_3	12-23
CaO	2-7
MgO	0.5-1.5

The most common absorbents (solids) are lime, limestone and dolomite found as crystalline aggregates (see Figures 1-3 and 1-2) and solid mixtures (78). Their solubility has been determined (65, 82) and noted in scrubber operation (29, 70). These soluble minerals provide the carbonates and hydroxides to fix the SO_2 in solutions. An analysis (43, 79) is given in Table 1-2.

The dissolved sulfur species HSO_3^- and SO_3^{2-} are subject to oxidation in solution by dissolved oxygen producing SO_4^{2-}. This gypsum is produced in lime/ limestone throwaway processes and can lead to supersaturation in all calcium-based processes causing scaling (29, 56, 77). Scale formation can be controlled by additive controlled oxidation (below 20%) (29) and gas pretreatments. The oxidation occurs along the trajectory of the SO_2 as it enters the absorbing solution (127). Hydrodynamic conditions (151, 168) and mass transfer to the solution (169, 170) determine the region where reaction occurs. The limit of this region, called the reaction plane, determines what theory best describes the rate of absorption (80, 120). For instance, when the film is large (equal or greater than the diameter of the small particles of solid), dissolution can occur in the reacting zone, further increasing reaction and enhancing absorption (138).

One approach to scaling control is limitation of oxidation by the addition of an inhibitor (50, 77, 147). Many organic materials (especially those bearing hydroxyl groups) inhibit the oxidation. This action is not likely to be true catalysis (20, 50, 140), hence the inhibitors may be subject to consumption and would require replacement. Factors to consider with regard to inhibitors are:

-- Inhibitor must be water-soluble.

-- Its actions may be modeled well enough to limit oxidation in part of the system.

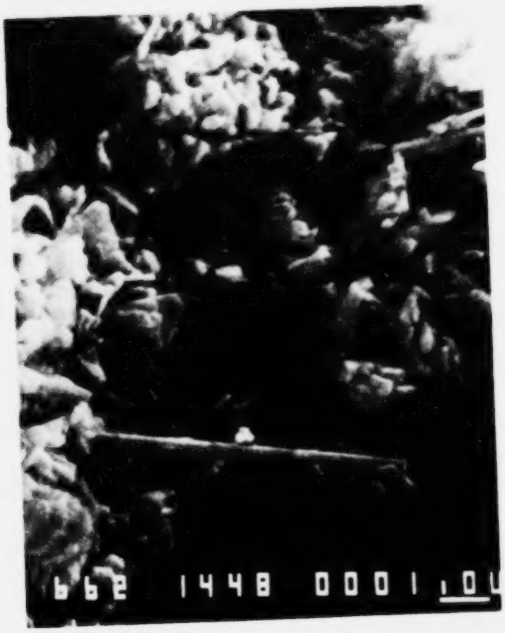
662 1448 0001 10U

Figure 1-2. Electron Micrograph of Calcium Sulfite Particles - Sulfite and Sulfate Particles

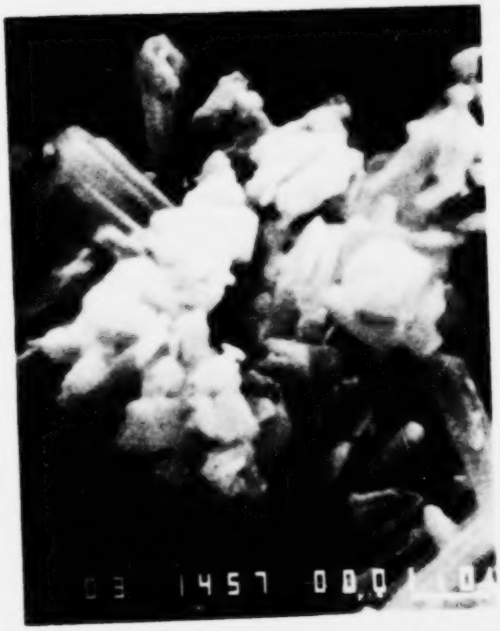
03 1457 0001

Figure 1-3. Electron Micrograph of Calcium Sulfite Particle - Individual Agglomerate

TABLE 1-2. LIMESTONE ANALYSIS

Chemical Analysis

Component	Weight Percent
Al_2O_3	6.01
Fe_2O_3	0.19
MnO	0.06
CaO	55.5
Cl	0.004
Cu	0.00044
Cr	0.00011
As	0.0002
Hg	$6x10^{-6}$

-- Products formed from inhibitors may also retard (or promote) the oxidation.

-- The contacting method in the scrubber changes the effectiveness of inhibitors (43).

-- Fly ash may contain phenolic organic residues active as inhibitors.

Recently organic acids used to enhance limestone solubility were identified as rate retarders. The most extensive set of experiments dealing with the organic acid effect of both the sodium and the calcium sulfite oxidation are reported by Hatfield, Kim and Mullins (81). It was reported that in the sodium system, organic acids promoted the sulfite oxidation with the order being: adipic > glycolic > no acid. However, in the calcium system organic acids were found to reduce the oxidation with the order being: glycolic > adipic > no acid. The results dealing with the calcium system are comparable to the results of the present work, dealing with the comparative inhibitory strength of the organic acids. The relative strength was: glycolic > adipic > succinic > no acid.

There are large discrepancies between the current results and those of Hatfield et al. for the rate of oxidation of the sulfite. Hatfield et al. reported that the sulfite oxidation goes toward completion in several hours, but the results of this work show that the sulfite goes to sulfate in a matter of minutes (usually less than 20 minutes even with inhibitors added). Hatfield et al. added $CaCO_3$ (calcium carbonate) to the reaction mixture for pH control and used an oxygen flow rate of only 20 ml/min. The present experiments used the addition of NaOH for pH control and a flow rate of oxygen at 3 ℓ/min to maintain O_2 saturation in the reactor. This suggests that while the $CaCO_3$ or the NaOH may have an effect on the sulfite oxidation, the experiments by Hatfield et al. were oxygen limited (controlled by the oxygen flow rate rather than the sulfite oxidation kinetics). These workers also determined the rate of reaction to increase with pH, which is in agreement with the current findings.

In a recent work Altwicker (8) found hydroquinone caused a changing reduction in the oxidation rate which he attributed to inhibitor in the reaction plane being consumed quicker than it could be replenished, casting doubt on the sulfite method for measuring interfacial area in contactors.

The scaling problem is greatest in the scrubber and mist eliminator. By inducing oxidation elsewhere in the system, supersaturation in SO_4^{2-} will not happen. For this reason various approaches to forced oxidation in the holding tank beneath the scrubber have been studied (29, 71). For example: forced oxidation of the calcium sulfite reaction product in both lime and limestone FGD systems has been successfully demonstrated in 10 megawatt prototype units at the Shawnee Test Facility. The oxidized gypsum product (74) results in less disposal volume and settles by an order-of-magnitude faster than the unoxidized material. It filters to better than 80% solids and handles like moist soil compared with the unoxidized material which filters only to about 50 to 60% solids and is thixotropic (83).

Improved settling is treated elsewhere as well (110, 124, 132, 161), and good sulfate removal has been discussed (29). The problem of scrubber scaling is eliminated in sodium-based liquors (56, 77, 110, 132, 161), but the added cost of sodium absorbents (49, 69, 110) necessitates regeneration of the "alkali values" of the sodium absorbent usually with a calcium base (lime/limestone) that is discarded.

Recovery oriented, sulfur-concentrating processes are usually gaseous (27, 128, 165), but some processes (55, 92) use a liquor, operating by electrolytic regeneration (92). The most prominent (68, 77, 103) two loop process is the double alkali process (dual alkali), featuring (56, 96, 110) efficient, higher pH scrubbing with sodium liquor at low L/G rates, reduced scaling, and thorough limestone utilization, but may have disposal problems.

Other companies which have utilized liquid phase oxidation in wet scrubber flue gas desulfurization processes include Babcock and Wilcox (magnesia-base wet scrubbing) (13), Wellman-Lord, Stone and Webster/Ionics (63), Aerojet-General Corporation (zinc oxide process) (6,92), and Monsanto (CALSOX system) (87). There are many other systems including ones based on magnesia (100, 158).

Many models for the physical and chemical events underlying these removal processes have emerged beginning with the equilibria among the solution ionics (133) and a generalization of the oxidation in solution (109, 153). The real challenge is in formulating (47) the complex equilibria, dissolution rates, absorption rates (40), and reaction rates in a way suitable for computing concentration profiles, removal rates and efficiences, and absorbent efficiencies in the scrubber (114) and holding tank (175).

Any description requires the reaction kinetics of sulfite oxidation in solution. Indeed, this topic has been the subject of multifaceted research for 132 years yielding sure findings only slowly.

The oxidation is a free radical chain process subject to photochemical initiation, the quantum efficiency of which is 5×10^4 (16). The impurity level of the work that produced this figure raises doubt about its validity. Further work shows no influence of UV on the oxidation rate in aerosols of low pH (95). The most careful photochemical study concluded that there is no simple relation between the light absorbed and the rate (112).

Experiments using various surfaces and particulate additives (86) found no variation with contact area of catalyst. This well establishes the reaction as a case of homogeneous catalysis. Other workers (20) who exceeded solubility limits of catalyst suggested the subsequent particles might have provided sites for heterogeneous catalysis, but this is not the case (18).

The effect of impurities is dramatic. The sensitivity of the reaction rate to stray metal ions is the hallmark of the reaction, but inorganic anions (188) as well as organic molecules affect the rate (although in the opposite way). In fact, the bane of much experimental work was rubber in the apparatus (48, 115, 140, 171). Pure gum rubber stops the reaction (112) giving evidence that the sulfur vulcanizing chemicals are not the cause. The degree of inhibition by hydrocarbons is so sensitive that oxidation has been suggested as a semiquantitative analysis for their presence (152). This sensitivity is an important consideration for operations in rubber-lined slurry handling equipment, such as those at Shawnee Valley.

The acceleration of the rate by metals is extreme: 10^{-12} M copper ion added during sulfite oxidation increased the rate (171). Many metals have been studied:

Co	7, 21, 42, 44, 54, 95, 107, 108, 109, 130, 126, 149, 163, 185, 187
Cu	7, 17, 21, 66, 84, 95, 109, 150, 140, 172
Mn	21, 42, 48, 75, 86, 93, 95, 179
Fe	21, 39, 84, 86, 93, 95, 140
Mg	21, 42, 179
Ni	21, 93, 140
Al	21, 39
Zn	21, 179
Ca	179
NH_4^+	21, 45, 95, 115, 140, 152

General comparisons have tested their relative effectiveness:

Co, Ni > Cu > Fe ref 140
Mn > Co, Ni > Fe, Cu > Mg, Zn, Na, NH_4^+ ref 21
Mn >> Zn, Mg > Ca ref 179
Mn > Cu > Fe > Co, NH > Na > uncat. ref 95
329 199 167 49 49 4 3 = Relative strength
Mn ∿ 7000 x Mg ref 42

The most effective catalysts are clearly manganese and cobalt with iron giving a notable effect. The metal showing the least effect is sodium (21, 91, 95). For this reason, the spectator ion is nearly always chosen as sodium. Ammonium, a constituent in many natural systems, increases the rate of oxidation. The probable cause is not catalysis, but rather its effect on pH may merely shift the equilibrium toward sulfite which is most rapidly oxidized. Several workers (20, 45, 136, 150, 152) have considered nonmetallic catalysis and mechanistic interactions of sulfur compounds. The very few experiments have no salient results.

One curious observation is that sulfate formed by the reaction has less effect than initially added sulfate upon the reaction rate (111, 134). No satisfactory answer exists (42, 66, 141), but control of the position of the sulfur species equilibrium is one candidate. An early controversy concerned bisulfite oxidation rates increasing with dilution (17, 115, 119). The spurious effect was due to decreased oxygen mass transfer at higher concentrations (140).

The oxidation in all pH ranges has been studied with wide concentration changes of sulfur species and catalyst and some slight changes of oxygen concentration. Many of the important results in the literature are compared on Table 1-3. Although no firm results stand out, the many contrasts serve to

TABLE 1-3. COMPARISON OF THE LITERATURE OF SULFUR DIOXIDE OXIDATION

Reference	Year	S Species	Conc, M	Order	O_2 Conc, M	Order	Cat Ident	Conc, M	Order	Contacting Method	Temp	pH	k	Comments
Hoather & Goodeve[86]	1934	H_2SO_3	$5\text{-}50\times10^{-4}$ 2.5×10^{-6}	1 0	2×10^{-3}	1 0	- Mn	- $3\times10^{-6}\text{-}8\times10^{-5}$	- 2	stirring	40°C 35°C	7 5	- -	impurity likely
Coughanowr & Krause[48]	1965	$SO_2 \cdot H_2O$	1.7×10^{-3} 1.9×10^{-3}	0 0	$3\text{-}6\times10^{-4}$ $4\text{-}8\times10^{-4}$	0 0	Mn	2.7×10^{-4} $1.8\times10^{-3}\text{-}0.18$	2 2	stirring H & R "T"	25°C	-	$.03\text{-}221\times10^{-7}\ \frac{\text{mole}}{\text{l sec}}$	
Walter[179]	1972	$SO_2 \cdot H_2O$	0.009	0	1.2×10^{-3}	0	Mn Mg	$1.8\text{-}9\times10^{-5}$ $0.036\text{-}0.82$	2 0.7	stirring	25°C	-	$1.3\text{-}16\times10^{-10}\ \frac{\text{mole}}{\text{l sec}}$ $0.3\text{-}2.46\times10^{-9}\frac{\text{mole}}{\text{l sec}}$	Ea $32\frac{\text{kcal}}{\text{mole}}$, obs. mass trans limit
Powell[135]	1973	HSO_3^-	0.03-.09	1	1.2×10^{-3}	-	-	-	-	stirring	25°C	1-2	$1.66\times10^{-5}\text{sec}^{-1}$	inert apparatus, DDI
Catipovic[42]	1974	HSO_3^- SO_3^{2-}	.001-.01 0.009	0 1	1.1×10^{-3}	- -	Mn -	$6.6\text{-}19.9\times10^{-6}$ -	1 -	stirring	25°C	1-4 11.1	$6.9\text{-}29.4\times10^{-8}\frac{\text{m}}{\text{l sec}}$ 0.053sec^{-1}	gave great care to purity of mat'ls, Ea 18.7 kcal/mole
Chen & Barron[44]	1972	SO_3^{2-}	.009-.03	3/2	$1\text{-}4\times10^{-4}$	0	Co	$10^{-7}\text{-}3\times10^{-6}$	1/2	H & R	25°C	9-10	$3.2\text{-}66\times10^{-5}\frac{\text{mole}}{\text{l sec}}$	Ea 17.5 kcal/mole
Barron & O'Hearn[19]	1966	SO_3^{2-}	0.04-0.4	3/2	0-0.003	0	Cu	10^{-4}	1	H & R	25°C	-	1200 1/g mole sec	Ea 18.3 kcal/mole
Linek & Mayrhoferova[108]	1970	SO_3^{2-}	0.25-0.8	0	$2\text{-}11\times10^{-4}$	1-2	Co	$0\text{-}10^{-3}$	1/2	stirring	25°C 35°C	8-9	$19.3\ \text{sec}^{-1}$	no effect due to stirring at high speed
Alper[7]	1973	SO_3^{2-}	0.8 0.5-1.0	0	$.3\text{-}2\times10^{-3}$ $1\text{-}8\times10^{-3}$	2 1	Cu Co	10^{-3} $4\times10^{-5}\text{-}10^{-3}$	1	stirring Pack col	25°C 30°C	9.2 8.3	-	stirring changed O_2 order
Reinders & Vles[140]	1925	SO_3^{2-}	0.06	1	1.1×10^{-3}	-	Cu	$10^{-5}\text{-}10^{-3}$	1	stirring	25°C	10	-	NH_4^+ present
Fuller & Crist[66]	1941	SO_3^{2-}	0.01-0.05	1	1.1×10^{-3}	-	- Cu	- $10^{-9}\times10^{-4}$	- 1	stirring	25°C	8.7	$0.013\ \text{sec}^{-1}$ 2.5×10^{6} 1/mole sec	no effect of added acid inh drops rate to 10^{-5}
Phillips & Johnson[131]	1959	SO_3^{2-}	.001-1.0	1 0	$1\text{-}7\times10^{-4}$	2 1	Cu Cu, Versene	10^{-5}	-	low turb high turb	30°C	9.2	-	Versene likely effect on mech
DeWaal & Okeson[54]	1966	SO_3^{2-}	0.8	1	1.1×10^{-3}	1	Co	10^{-3}	-	Wet wall	30°C	7-9	$50 — 10^{4}\text{sec}^{-1}$	Cat solubility exceeded Ea 12 kcal/mole
Wesselingh & Van't Hoog[185]	1970	SO_3^{2-}	0.8	-	$1\text{-}11\times10^{-4}$	2	Co	4×10^{-4}	1	Wet wall	30°C	8.5	-	Ea 10.53 kcal/mole absorption indep of hydrodynamics
Linek & Tvrdik[109]	1971	SO_3^{2-}	0.3-0.8	0	6.4×10^{-4} 5×10^{-4}	1 2	Co	$5\times10^{-6}\text{-}10^{-3}$	1	Stirring Wet Wall	25°C 33°C	7-9	$1\text{-}5\times10^{4}\ \text{sec}^{-1}$	O_2 order change sharp Ea 15 kcal/mole
Reith & Beek[141]	1973	SO_3^{2-}	0.8	0	1.1×10^{-3}	2	Co	$8.8\times10^{-6}\text{-}10^{-3}$	1	Wet Wall	30°C	7-9	1.43×10^{5} 1/mole sec	added $SO_4^{=}$: no effect Ea 12.4 kcal/mole
Sawicki & Barron[148]	1973	SO_3^{2-}	0.1-0.3	-	$.3\text{-}3\times10^{-3}$	1 2	Co	$5\times10^{-7}\text{-}10^{-4}$	1/2	Wet Wall	25°C	10	2.3×10^{6} 1/mole sec	O_2 order switches with Cat Conc
Onda[129]	1972	SO_3^{2-}	0.3-1	-	$2\text{-}11\times10^{-4}$	2— 1	Co	$10^{-9}\text{-}5\times10^{6}$	-	Pack col	30°C	8.5	-	O_2 order change gradual
Yagi & Inoe[187]	1962	SO_3^{2-}	0.008	1	$1\text{-}15\times10^{-4}$	1 -	- Co	- $0.5\text{-}7.0\times10^{-7}$	- 1	bubbling	20°C	8-9	$-1.4\frac{\text{mole}}{\text{l}\cdot\text{sec}}$ S O +.4 $1+1.46\times10^{-7}$ Cat S O	

define the main kinetic questions. The only problem comes from the varying conditions in the experiments which render some data uncomparable.

The order in sulfur is usually zero or one, but this depends on the pH range. For low pH the HSO_3^- order seems to be 0: at high pH the SO_3^{2-} order may be one. There are also changing order results.

The oxygen order is the most controversial and has the most complicated fluctuations. The order has been observed to shift from zero to two as the sulfite concentration changes (12), switch between one and two as the catalyst concentration increases (148), and to vary as its own concentration changes (129). Whether the change is gradual (129) or abrupt (109) is a question.

Catalyst dependence is stronger than that of the reactants, but the value is unsettled. Mn and Co produce orders of magnitude change in the reaction rate by variations of only a few ppm in their concentrations (48). Mg, conversely, produces a sluggish, but steady, increase in the oxidation rate as its concentration changes over orders of magnitude (42).

Experiments on the pH are scattered widely in the literature. The treatment by Fuller and Crist is worthy of note (66). (Linek and Tvrdik also treat the subject well). (109). Because the effect of pH is so closely linked with the sulfurous solution equilibrium, no clear chemical trends emerge. At extremely high pH (>12), however, the rate is depressed (19, 115, 190). This behavior is sometimes due to reduction in oxygen solubility (118). Nevertheless there appears to be a genuine chemical effect, for the rate reduction occurs as well for oxygen already in solution (101).

The energetics of the reaction are not as fully examined as the kinetics. All the works report operating temperatures between 20°C and 40°C. The low pH activation energy is around 20 kcal/mol, at high pH it is near 15 kcal/mol.

The published rates vary widely in first and second order kinetic equations. The values appearing in Table 1-3 are for conditions of low pH where half-lives of a day are common as well as instances of high pH reacting to half concentration in 0.01 sec and less.

In the low pH reaction, the stirring also causes discrepancies. Schultz and Gaden (155) report a decreasing reaction rate with increased stirrer speed. This finding touched off studies (131) that have still not resolved the ambiguity. Also at low pH no true (86) induction period has been observed, although start up lags due to physical causes do occur (152). At high pH an induction period up to 2 sec is possible (48).

The above questions all touch on the molecular activity making up the reaction mechanism. And, just as these specific questions remain open, the final elucidation of the oxidation mechanism remains to be done. It is generally accepted (66) that the oxidation proceeds by a free radical chain-- with or without metal participation. Many aqueous sulfur radicals possibly involved are characterized (190). The early suggestions by Haber (76) and Titoff (171) have given way to the proposed mechanism of Abel (2, 3, 4) and Backstrom (14, 15, 16). A few points of interest to all mechanisms are: the oxygen atom transferred does not come from the solvent (186), the uncatalyzed reaction occurs by initiation other than by stray metal ions (66), the activation energies in the catalyzed reaction agree closely with those for some metal-ligand substitutions of the catalyst (108). The results of some recent oxidation studies in slurries have given better definition to the oxidation problems.

Ramachandran and Sharma proposed a model for gas absorption in a three phase slurry system. An instantaneous chemical reaction was assumed to occur in the liquid boundary layer surrounding the solid particles. Two cases were examined in their model. The first case assumed that solid dissolution was unimportant in the rate of gas absorption. The second case assumed that solid dissolution into the liquid phase was an important factor. Results from the second case showed the rate of gas absorption to be proportional to the square root of the concentration of the solids present.

Bjerle, Bengtsson, and Farnkvist (28) conducted an experimental examination of $CaCO_3$ slurry oxidation in a laminar jet absorber at 25°C and 45°C and pH 8.5. In their weak (2%) slurry they found the SO_2 mass transfer coefficient to be nearly that in an otherwise identical clear solution (clear $k_{SO_2} = 1.19 \times 10^{-4}$ *vs* slurry k: 1.38×10^{-4} mol/(cm^2sec atm).

Uchida, Wen and colleagues have conducted a series of studies on slurry oxidation. In 1975 (184), using a continuous stirred tank reactor to study the oxidation of sodium and calcium sulfite solutions by air, they found that for sodium sulfite concentrations of 0.1 M, the reaction was mass-transfer limited up to at least 700 rpm impeller speed. The absorption rate was a function of both gas velocity and impeller speed. They also found that the rate of oxidation showed a dependency which was slightly greater than first order in impeller speed and oxygen concentration, slightly less than zero order in hydronium ion concentration, and independent of sulfite concentration.

In oxidizing calcium sulfite solutions, it was determined that the oxidation was first order in sulfite, and reacted faster at pH 4 than pH 7. Addition of copper had no catalytic effect on the reaction. Finally, they found that a 2 g/ℓ calcium sulfite slurry reacted much faster at pH 7 than the saturated solution.

In 1977, (174) Uchida and Wen extended the model, applying it to six cases: I) no solid dissolution in the liquid film near Gas-Liquid interface;

(a) reaction plane near the gas surface, b) reaction plane near solid surfaces, (c) reaction plane near the G-L surface and the bulk is constant at saturation. II) Solid dissolution considerable in the liquid film near the G-L interface; (a) reaction plane near G-L interface and $[S^{4+}]_{bulk}$ at saturation value, (b) reaction plane is near G-L interface and is less than saturation, (c) reaction plane surrounds the solid particles. Concentration profiles and tests for each case are given and a numerical example is shown by Uchida and Wen.

In a closely related study, Sada, Kumazawa, and Butt (145) modeled sulfur dioxide oxidation and reaction in a $Mg(OH)_2$ (0.5 to 10 at wt%) slurry using the film theory. They took exception to Uchida's driving force for dissolution and recast the equations in terms of $([S^{4+}]_{surface} - [S^{4+}])$ and used a different mass transfer coefficient for the liquid film and the bulk.

A recent work by Uchida (173) was a deeper experimental study of limestone slurry absorption of SO_2. He found particle size of the solid to influence the SO_2 absorption rate indicating that the solid dissolution rate is important.

In a TVA report (134), slurry oxidation was studied in a spinning cup oxidizer. The degree of oxidation was determined by infrared analysis of the solids. Various salts were added to the solution and it was found that manganese and iron compounds were strong catalysts, nickel and vanadium had no effect, and cobalt, copper and thiosulfate ions suppressed the reaction. Tests also confirmed the fact that oxidation was faster at the lower pH values.

Representative (30) of the extensive (31-38) articles by Borgwardt, is an interesting study of unsaturated (with respect to SO_4^{2-}) closed loop scrubber operation at the pilot plant scale. The key to stable no-scale (undersaturated in SO_4^{2-}) operation is limiting the oxidation of S^{+4} to 20%. In this way the sulfate that is formed is cleared from the system as a solid solution with the precipitating sulfite.

In another case, enhanced oxidation was examined. Using a pilot scale scrubbing system with a forced oxidation tank, Borgwardt (29) found the oxidation of calcium sulfite was limited by the mass transfer of oxygen from the injected air into the liquid. The pH in the oxidation tank was 4.5. The mass transfer limitation was eliminated by increasing the residence time of oxygen in the reactor. An air stoichiometry of 2.6 was used in this investigation. The product solids have improved settling and dewatering characteristics.

In a work similar to the current one, Gladkii at the State Scientific Research Institute of Industrial and Sanitary Gas Cleaning at Moscow (70) found results of immediate application. For this reason the following description and comparison is more thorough. Slurries of calcium sulfite were oxidized in an agitated bubbler reactor. The initial concentration varied from 300-1800 ppm, and temperature ranged from 40°C to 62°C. Iodometric titrations were used to find the total sulfite concentration, and the pH was monitored continuously. The authors found that the reaction was in the kinetic-limiting regime above 700 rpm, since agitator speed, size and concentration of solids, and quantity of air did not effect the oxidation rate. The reaction began with an initial drop in pH from 6.8 to about 5.8, followed by a long stretch where pH remained constant, and finally a sharp drop to pH 3.2 at the end of the reaction. During the first pH drop the reaction rate accelerated due to the increased concentration of bisulfite in solution. In the constant pH region the oxidation rate also remained constant. The final pH drop reflected the depletion of the solid sulfite, and the rate order in bisulfite.

The authors then varied the initial pH of the reacting solution from 3.6 to 6.0. The induction period of accelerating rate was not observed at initial pH values lower than 6.0. The rate during the constant pH period was used as a measure of reaction velocity and it was found that this velocity reached a maximum at pH 4.5. Both of these facts (the induction period and the rate maximum) are used to support the contention that the dominant reacting species is the bisulfite ion.

Another significant result of the Russian research is an empirical correlation between pH, temperature, and the liquid phase concentration of a desaturated calcium sulfite solution. This equation is combined with the determined first-order rate in sulfite to give a rate constant equal to 0.85 ℓ/min at 40°C and an activation energy of 21.5± 0.5 kcal/mol.

The catalytic effect of manganese sulfate was then studied, and it was found that a concentration of 100 ppm $MnSO_4$ greatly accelerated the oxidation. Furthermore, it reduced the activation energy to 13.8 ± 0.5 kcal/mol and the order in sulfite to ½.

Some additional comments and comparisons with the current work at the University of Virginia are in order:

Comparison of Figure 5 and Figure 6 of ref (70): The rates given in Figure 5 were checked to determine if they agree with the rate vs. pH diagram in Figure 6. The rates in Figure 5 were taken as the linear portions of the C_{CaSO3} vs time curves for the various pH's. (Note that the $CaSO_3$ was given in grams of $CaSO_3$ per liter.) The results were as follows:

@ pH = 6

slope = $\frac{7.6 - 0}{0 - 80}$ = 0.095 g/(ℓ-min)

R = (0.095 g/ℓ-min) (1/120 g/(g-mol)

= 0.791 x 10^3 g-mol/(ℓ min)

@ pH = 5 R = 3.84 x 10^3 g-mol/(ℓ-min)

@ pH = 4.5 R = 4.58 x 10^3 g-mol/(ℓ-min)

@ pH = 3.6 R = 2.28 x 10^3 g-mol/(ℓ-min)

The points were plotted on Figure 1-4 showing good agreement with the published curve, with the exception of the point at pH = 4.5.

Comparison of Figure 6 and Figure 7 of ref (70): Using the line at 40°C, the concentrations of SO_2 were determined from Figure 7. These concentrations were then used to calculate the reaction velocity. The reaction velocity was then plotted on Figure 1-5. The equation used for calculation of the reaction velocity was:

$$w = k\ C_{SO_2}$$

where w = reaction velocity, gmol/(ℓ-min)

$$k = 0.85\ \text{min}^{-1}$$

Only concentrations taken between pH = 4.5 and pH = 6 were used for this comparison. In this pH range the SO_2 present will exist as HSO_3^-. At pH values of 4.5 and less, considerable $SO_2 \cdot H_2O$ will be present in the solution which will tend to give a lower specific reaction rate. Results were as follows:

@ pH = 6.0

C_{SO_2} = 7.94 x 10^{-4}

R = 0.85 (7.94 x 10^{-4})

= 6.75 x 10^{-4}

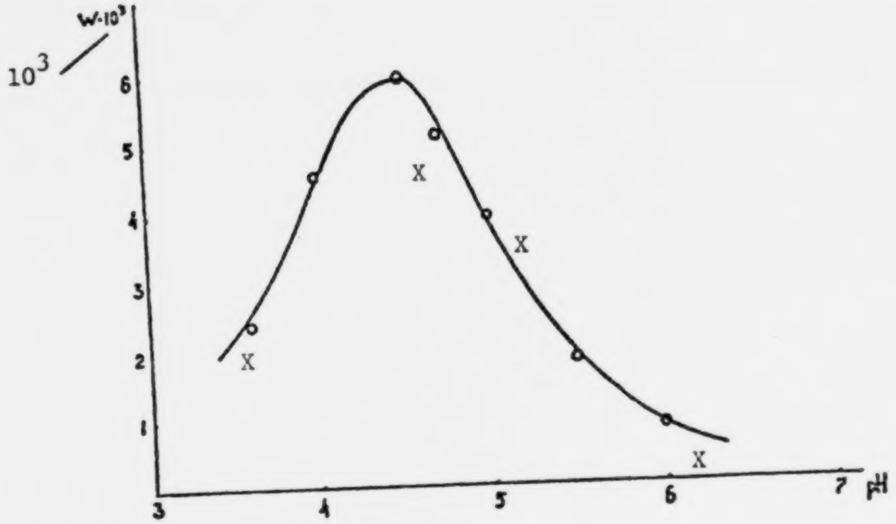

FIGURE 6.

Dependence of Reaction Velocity of Oxidation (V, mol/ℓ x min) on pH of Suspension at a Temperature of 40°C

X = Calculated points

o = Original points in paper

Figure 1-4. Comparison of Gladkii's Figure 6 with Figure 5 (70)

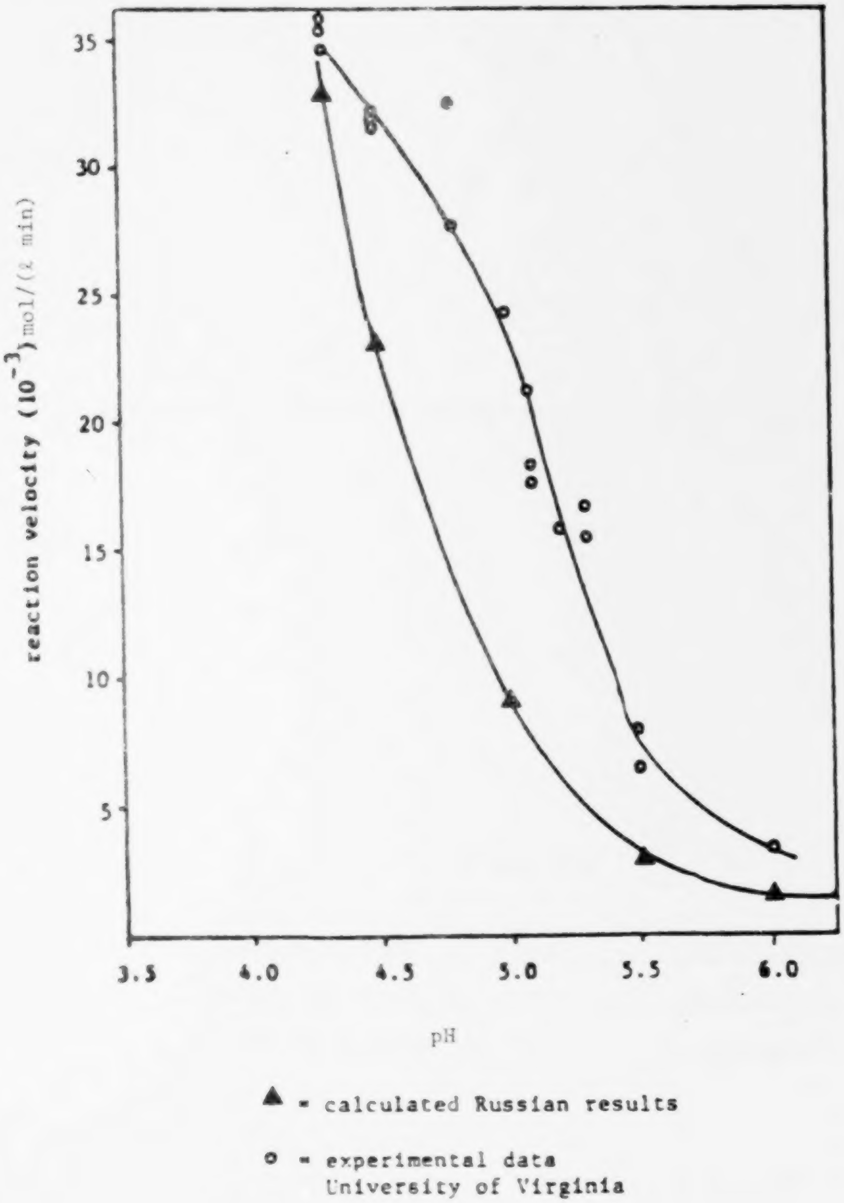

Figure 1-5. Comparison of Slurry Oxidations at 50°C

@ pH = 5.0 $R = 4.26 \times 10^{-3}$ g-mol/(ℓ-min)

@ pH = 4.7 $R = 0.85 \times 10^{-2}$ g-mol/(ℓ-min)

These results were then plotted in Figure 1-6 giving good agreement between the two curves except at pH = 4.7.

Comparison of Figure 7 and Figure 8 of ref (70): Assuming that the reaction being studied is first order, the rate expression can be given by

$$w = k \cdot C_{SO_2} \text{ g-mol/(ℓ-min)}$$

or

$$\log w = \log C_{SO_2} + \log k$$

This is in the form of $y = mx + b$ with a slope (m) equal to 1. However, the slope in Figure 8 is computed as 0.5.

A new graph of log w vs log C_{SO_2} was generated from the data given in Figures 6 and 7. Reaction velocities were obtained from Figure 6 and concentrations were obtained from Figure 7 at 40° C for various pH values.

pH	w	log w	log C
6	0.791×10^{-3}	---	-3.1
5.6	1.7×10^{-3}	-2.77	-2.8
5.3	2.6×10^{-3}	-2.59	-2.6
5	3.84×10^{-3}	-2.41	-2.2
4.7	5.5×10^{-3}	-2.25	-2.0

A new plot was made of log w vs log C_{SO_2} total on Figure 1-7. This plot shows a measured slope of 1.01 which is indicative of the reported first order reaction. The reaction rate was calculated from the first graph and found to be 0.85 which is in agreement with the published report. Therefore, Figure 8 as published must be in error.

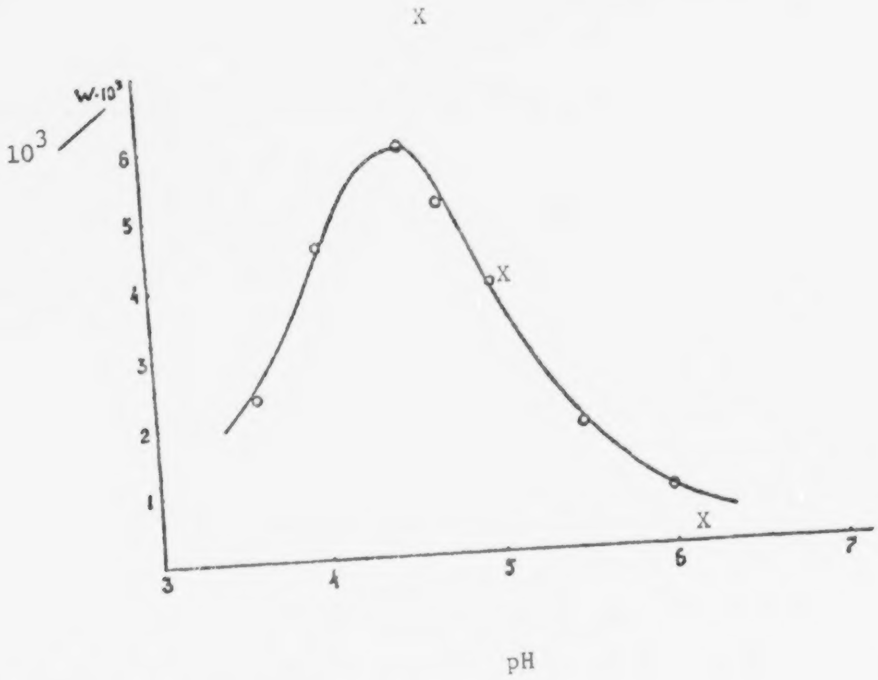

FIGURE 6.

Dependence of Reaction Velocity of Oxidation (V, mol/ℓ x min) on pH of Suspension at a Temperature of 40°C

X = Calculated points, section-B
o = Original points in paper

Figure 1-6. Comparison of Gladkii's Figure 6 with Soviet Slurry Oxidation Rate Expression (70)

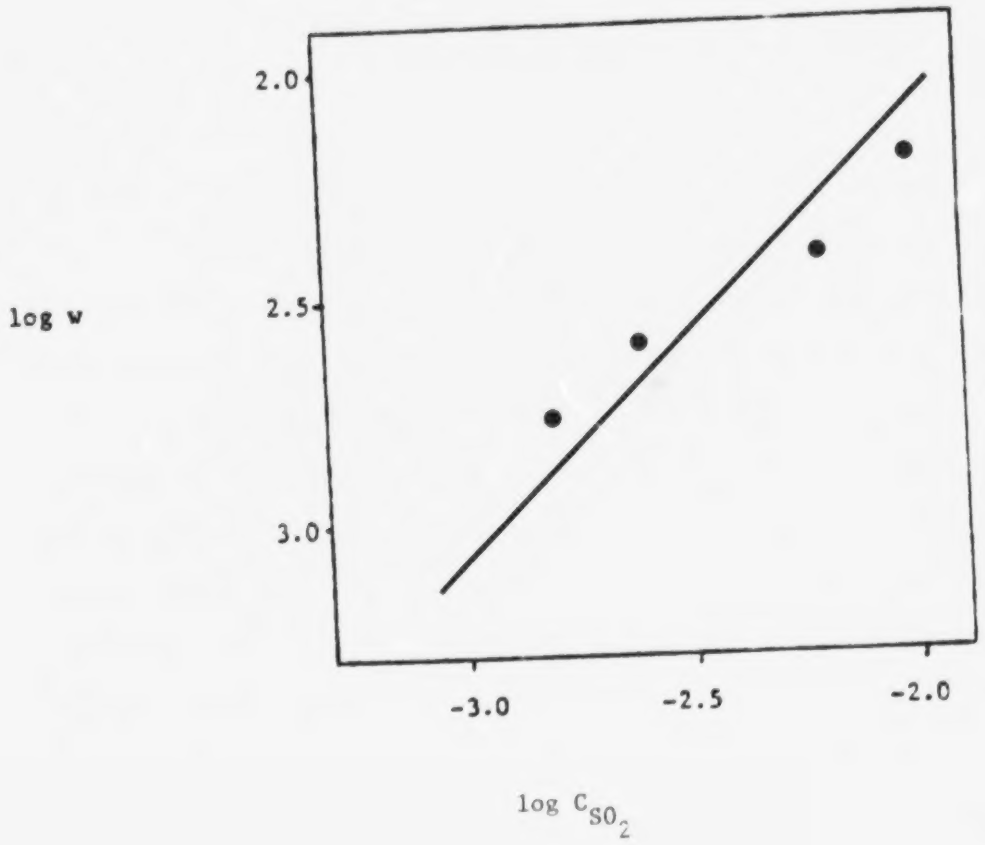

Figure 1-7. Determination of Soviet Reaction Order

Comparison of University of Virginia and Gladkii Data: Experimental data obtained at the University of Virginia are shown in Figure 1-5 along with the calculated Soviet results. It should be noted that since the calculated Soviet results at pH 5 and 40°C did not correlate with experimental data, the calculated results at 50°C and pH 5 are also suspect. The reaction rates at the University of Virginia are about twice those obtained by Gladkii.

Experiments in the current work have determined the reaction velocity of calcium sulfite oxidation in slurries at 40°C and various pH's. These results are shown in Figure 1-8 along with the reported Soviet experimental data. Again, the current reaction velocities exceed those reported by Gladkii.

Even though there is an extensive literature concerning S^{4+} oxidation, in the clear solution that surrounds the particles in slurries no certain explanation of the process has emerged. The following studies are representative.

Pritchett (136) measured temperature rise in a flow reactor carrying mixed oxygen and manganese, catalyzed sulfur dioxide solution (pH not given). He found no dependence on $[S^{4+}]$ but half order dependence on $[O_2]$ and a first order effect of $[Mn^{2+}]$. He found $MnSO_4$ more active than $MnCl_2$ and applied his results to O_2 absorption experiments. The most salient product of this work may well be the approach Pritchett took in relating the chain reaction mechanism of sulfite oxidation, borrowing methodology from biochemistry where cycles (such as chain intermediate regeneration) are more common.

In another flow/thermal study, Srivastana (163) obtained a curious result also reported elsewhere (7, 108, 129, 130, 131, 139). With no cobalt catalyst and below $[SO_3^{2-}] = 0.04$ M the rate depends on $[SO_3^{2-}]^n$ but n becomes zero above the sulfite concentration of 0.04 M. With catalyst added the "switch point" occurred when $[SO_3^{2-}] = 0.08$ M. The rate increased linearly with $[Co^{2+}]$ up to 3.4×10^{-5}M at which point cobaltous hydroxide precipitates. They

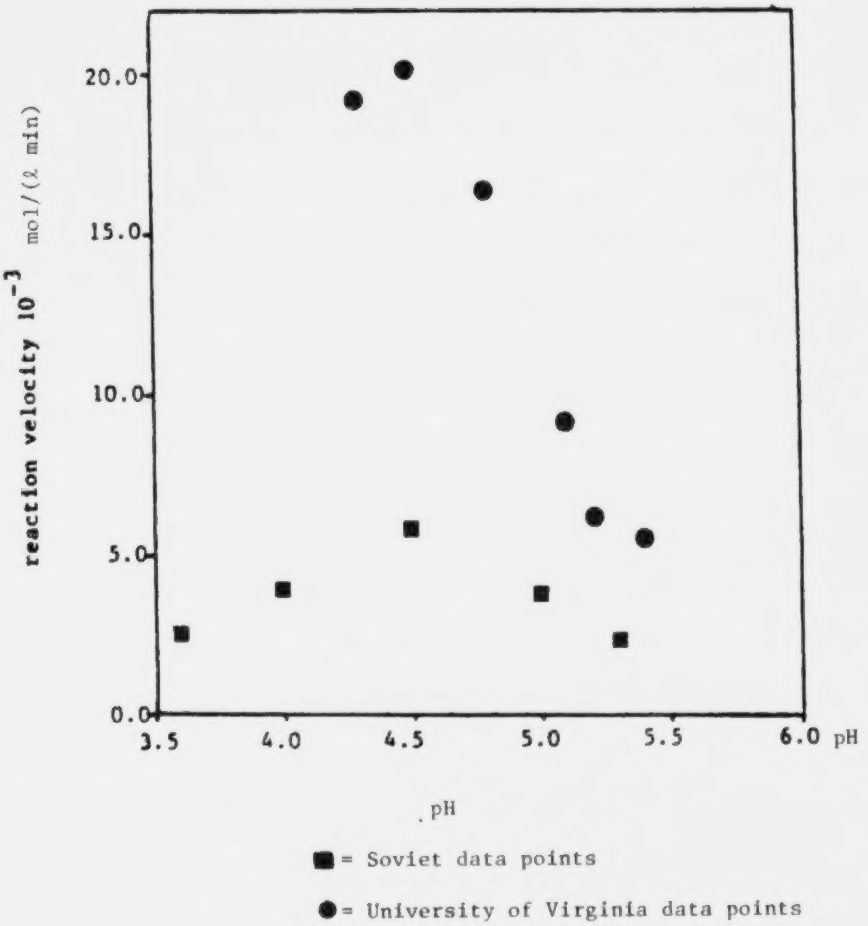

Figure 1-8. Comparison of Slurry Oxidations at 40°C

indicate (and use in further calculations) an oxygen dependence of one but do not support this finding in the report. They finally give an involved rate expression for the high pH oxidation.

In another work (67) in which the $[S^{4+}]$ dependence varies from low to high pH (3-8), Fuzzi examined stirred sulfur solutions open to the air. He found the order in sulfur to be 1 below pH 4 growing to 2 above pH 5. The dependence on Fe^{3+} was linear. Fuzzi found the overall rate to have a strong maximum with respect to pH at pH 4 which he attributed to a growing ratio of $HSO_3^-/SO_2 \cdot H_2O$ and a declining $[Fe^{3+}]$ as $Fe(OH)_3$ precipitated.

Another low pH study by Catipovic (42) assessed the effects of catalyst, pH and added sulfate. In a vigorously stirred batch reactor under a few millimeters O_2 pressure with no outlet he found: both Mg^{2+} and Mn^{2+} catalyzed oxidations are zero order in $[S^{4+}]$ on the pH range 1 to 4; Mn^{2+} is much more potent a catalyst than Mg^{2+}; added sulfate inhibited the reaction significantly. He noticed that the ratio of the rate constants with and without added sulfate plotted against the ratio of $[SO_4^{2-}]_{added}/[SO_4^{2-}]_{initial}$ expressed the results in dimensionless form. The activation energy with Mn catalyst was 18.7 kcal/mol.

In research which predated one of the experimental methods of current study, Bengtsson (24) studied the oxidation at intermediate pH (6-7.5). Bengtsson did experiments on the pH range 6 to 8.5 and $[SO_3^{2-}]$ from 3×10^{-5}M to 10^{-2}M by using a pH method as described in Section III. For the pH interval from 6.0 to 7.5 in order to simplify his eq. (3-11), Bengtsson made the following assumptions:

$[H^+] + [OH^-] << [HSO_3^-]$

$[H^+]^2 << K_3[HSO_3^-]$

$k_w << k_3[HSO_3^-]$

But these three in equalities are not valid once the pH value is lower than 6.0.

In Bengtsson's experiment, distilled water was first brought to temperature and loaded with O_2. Then 500 ml of this water were mixed with a buffered Na_2SO_3 solution in the reactor vessel. Then, 0.2 M H_2SO_4 brought the solution to the desired pH value. Finally, a certain amount of catalyst solution was added rapidly. The pH displacement produced by the oxidation registered on the recorder. It happens that by using the buffered Na_2SO_3 solution, he could neglect the oxidation before the catalyst addition because of the inhibiting effect of buffer. Note that the derivation of pH method should have considered this addition of buffer acid which is designated as [HA] in Section III. For the unbuffered condition, equation 3-10 could be simplified to be equation 3-11. This equations has been used for all of our unbuffered runs in which oxidation was started by supplying the oxygen instead of adding catalyst. The rate of sulfite oxidation found by Bengtsson is zero order with respect to oxygen and three-halves order with respect to sulfite. The dependence of the rate of oxidation on $[CO^{2+}]$ was half order. The activation energy in his rate constant was 57 kJ/mol.

The pH method which Bengtsson and Bjerle (25) developed was based on the fast equilibrium between sulfite and bisulfite, and only applies when bisulfite concentration is practically constant with pH. They used a value of ΔH_{298} = 2.9 kcal/mol to calculate equilibria relationships at a variety of temperatures. At pH values above 7.5, they tried an absorption method which depended on keeping the reaction plane within the diffusion film. This method proved less successful than the pH method.

SECTION 2

EXPERIMENTS

OUTLINE

II. Experiments

  A. Apparatus

    1. Batch Reactor

    2. Flow Reactor

  B. Procedure

    1. Rate from Concentration Measurements

    2. Rate from pH Measurements

    3. Rate from Temperature Measurements

  C. Analysis of Calcium Sulfite

  D. Equilibrium Relationship for S^{4+} Species

  E. Iodometric Titration

  F. Analysis of Data

    1. Analysis of a Single Experiment

    2. Multiple Regression Analysis

    3. Analysis of pH Method Data

    4. Analysis of the Flow-Thermal Method

SECTION 2

EXPERIMENTS

A. APPARATUS

1. Batch Reactor

The experimental apparatus was a batch-type stirred reactor with a continuous gas feed (Figure 2-1). A constant temperature was maintained by immersing the reactor in a Plexiglas water bath. The bath temperature was controlled by a Sargent-Welch Thermonitor, Model ST, employing two heating paddles totalling 750 watts. An auxiliary 125 watt heater was used to assist in obtaining the selected temperature. A stirring motor provided circulation of the water in the tank. Temperature was monitored with a thermometer calibrated against an NBS-certified thermometer to 0.1°C.

Materials for the reactor were carefully chosen to avoid possible contamination by metals and organic materials which might affect the reaction. A one liter Pyrex flask was used as the reactor (Figure 2-2). The flask had been fitted with five standard 24/40 necks to accommodate various equipment. The bottom of the flask had been flattened in order to make it more stable. The flask was securely fastened to a weighted base in order to reduce vibrations and movement in the water bath. Four indentations were made in the flask to act as baffles to increase the turbulence.

A Trubore glass bearing and stirring shaft was located in the center neck of the reaction flask in order to provide agitation of the reacting solution and allow the addition of gases to the reactor. All reactions were conducted at stirring speeds greater than 1500 rpm, requiring the addition of a film of

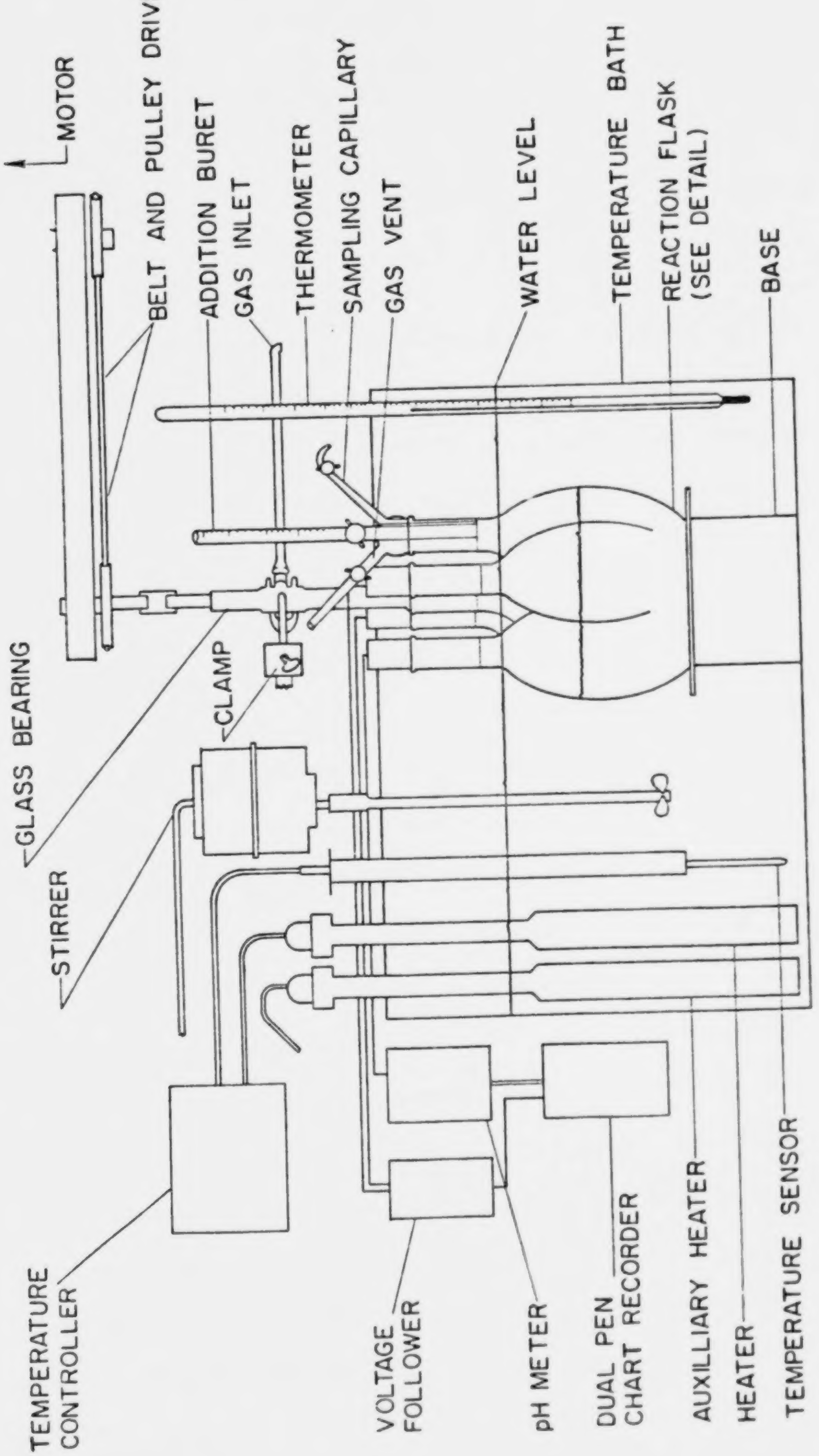
MOTOR
BELT AND PULLEY DRIVE
ADDITION BURET
GAS INLET
THERMOMETER
SAMPLING CAPILLARY
GAS VENT
WATER LEVEL
TEMPERATURE BATH
REACTION FLASK (SEE DETAIL)
BASE
GLASS BEARING
CLAMP
STIRRER
TEMPERATURE CONTROLLER
VOLTAGE FOLLOWER
pH METER
DUAL PEN CHART RECORDER
AUXILLIARY HEATER
HEATER
TEMPERATURE SENSOR

Figure 2-1. Experimental Apparatus

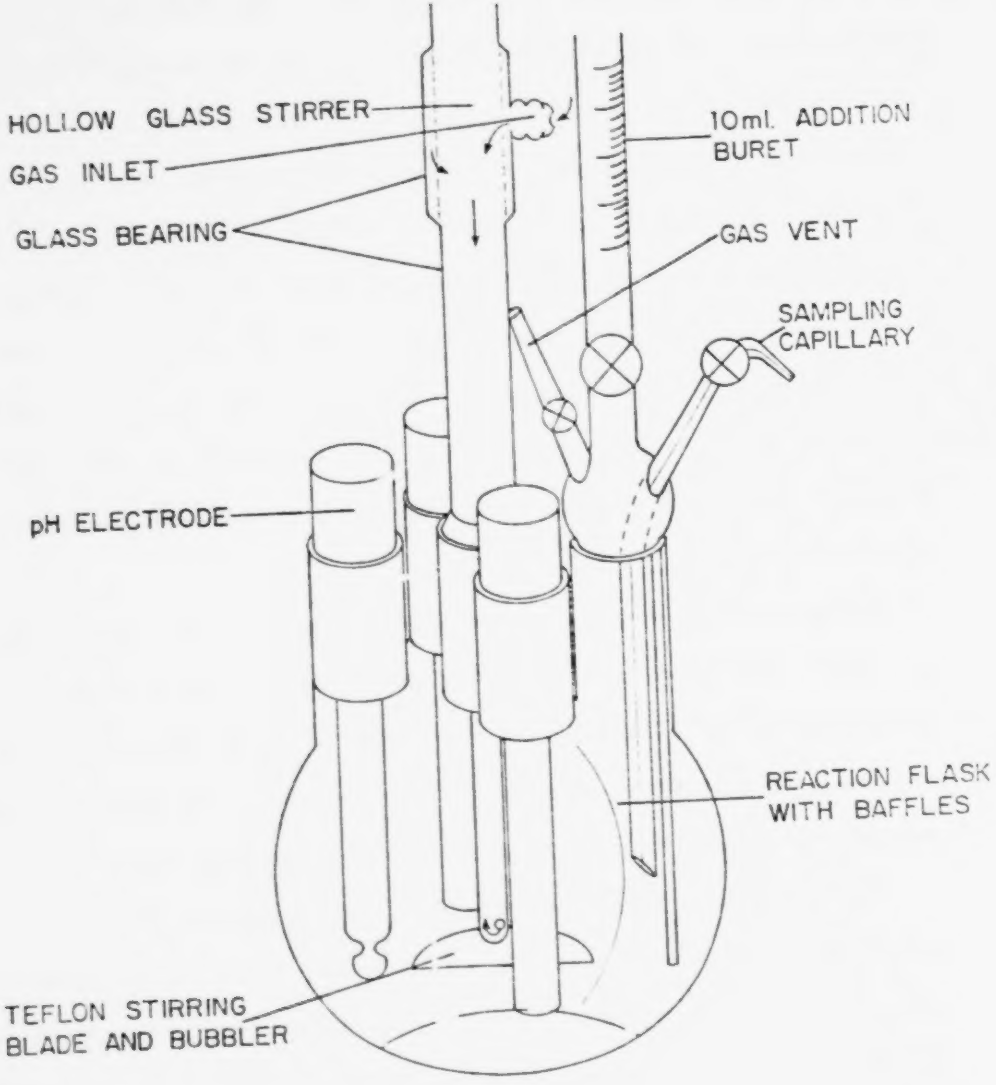
HOLLOW GLASS STIRRER
GAS INLET
GLASS BEARING
10ml. ADDITION BURET
GAS VENT
SAMPLING CAPILLARY
pH ELECTRODE
REACTION FLASK WITH BAFFLES
TEFLON STIRRING BLADE AND BUBBLER

Figure 2-2. Reaction Vessel

Dow-Corning High Vacuum Silicone Lubricant to the shaft to reduce friction. The lubricant was applied at least once a day following the removal of old material with acetone and a rinse with deionized water. Gases were introduced into the flask by means of a glass tube in the bearing, flowing through the hollow shaft, and were released into the reactor through a small hole located near the end of the shaft. A 7.5 cm Teflon stirring blade was fitted to the end of the shaft in order to agitate the reacting solution and improve gas dispersion throughout the reactor. A 1/25 hp, single-phase Teletype Corporation motor provided power to the shaft through a Plexiglas pulley and rubber o-ring drive belt arrangement. A Variac was used to set the stirring speed which was checked regularly with a strobe light tachometer. A short length of rubber tubing connected the pulley shaft to the glass shaft. This provided a means of facilitating the shaft alignment with respect to depth in the reactor and gas inlets.

A second neck of the flask was fitted with a pyrex glass sampling arm and gas vent. The sampling tube extended to within 0.7 cm of the reactor bottom, and it was of sufficient diameter to provide rapid sample taking. The sampling procedure consisted of closing off the gas vent stopcock and allowing the gas pressure to force the sample up through the sampling tube.

In the slurry oxidation reaction, this sampling tube was used for taking slurry samples. Clear solution samples were taken by using another sampling attachment which was composed of a glass tube, with a Micropore filter fitted on the outside end, leading to an aspirator. Filtered liquid samples from the slurry were thus drawn through the Micropore filter into a test tube under the pressure difference caused by the vacuum.

A glass combination electrode fitted in a special male 24/40 Teflon fitting occupied the third neck of the flask. The electrode was connected to a Radiometer Copenhagen PHM63 digital pH meter, which displayed the pH of the reacting solution. The pH changes of the solution during the course of the reactions were recorded on a Health-Schlumberger Model SR-206 dual pen strip chart recorder, when necessary.

In the unbuffered runs where constant pH was necessary, a pH controller operating base and acid pumps was added to the apparatus. Each pump was attached by Silastic tubing to a glass capillary tube fit with a 24/40 ground glass joint. This was placed in one of the necks of the reactor flask.

The sulfite concentration was measured by iodometric titration (See section 2-E) using a buret accurate to 0.002 ml. Pipettes used to measure iodine and sample aliquots wre calibrated to 0.001 ml gravimetrically. A total error was calculated.

All chemicals used in the reactions, with the exception of the calcium sulfite and gases, were reagent grade materials with catalytic impurities in concentrations of less than 0.0008%. The oxygen and nitrogen were 99.5% pure. The calcium sulfite used was very impure, and an analysis is included. (See Section C.) Water used in the reaction solution, either city water or distilled water, was passed through a purification system supplied by Hydro Service and Supplies, Inc., who claim the conductivity to be 18 x 10 18Ω-cm or better. The gas flow into the reactor was maintained at a constant flow of 3 ℓ/min. A rotameter was used to measure the flow and it had been calibrated using a wet-test meter.

2. Flow Reactor

The tubular flow reactor (Figure 2-3) is a coiled, inert tube situated between an efficient mixer at the inlet and throttling valve at the exit to maintain pressure in the tube. It is fed by oxygen and sulfur solution reser-

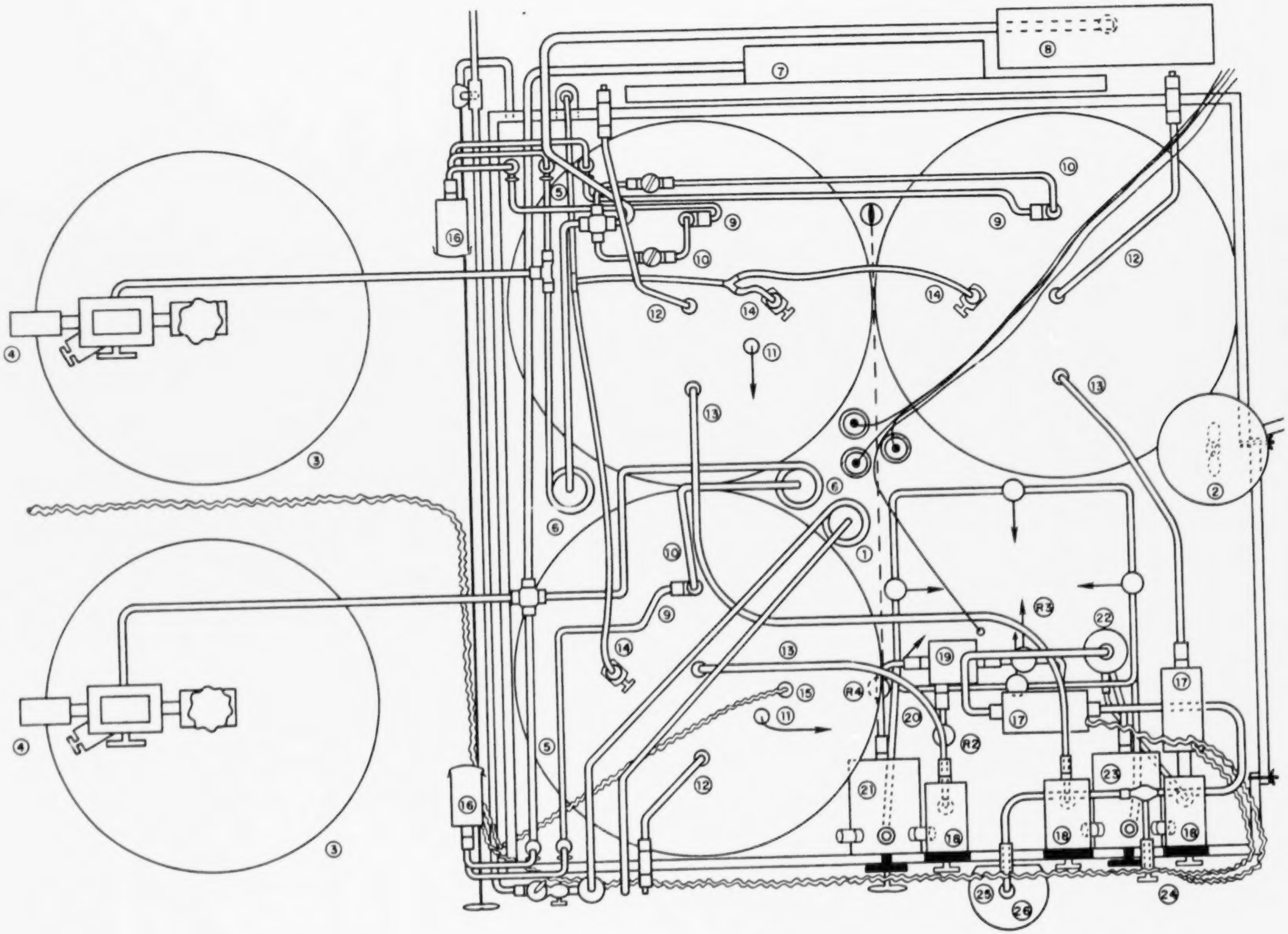
⑧
⑦
⑩
⑨
⑤
⑯
⑫
⑭
⑪
⑬
②
⑥
①
R3
㉒
⑲
⑰
R4
⑮
⑳
R2
㉑
⑱
㉓
㉔
㉕
㉖
③
④

Figure 2-3. Tubular Flow Reactor

voirs and ended by a second mixer where an iodine quench solution may be added. In the description that follows the circled numbers refer to points on Figure 2-3. The entire device is built in a water bath that maintains its temperature (hence the initial temperature of the reactants) to 0.002°C referred to a Fisher Calorimeter Thermometer (NBS certificate 141368). The water bath temperature controller is a Sargent-Welch "Thermonitor" of the phase-firing variety that provides excellent proportional, integral temperature control although it injects much electrical line noise. To assure temperature control operation well within the proportional band of the "Thermonitor," a copper cooling coil ① constantly passes city water through the vigorously stirred bath. The twin four-blade stirrer ② is externally mounted to separate the reactor from unnecessary vibration.

The flow circuit including the reactor tube begins with the gas cylinders ③ outside the thermostat. Both oxygen and nitrogen cylinders carry Matheson #3 regulators ④ (for high pressure delivery with fine--no droop--control). While these regulators proved superior to others tried, the combination of the low gas flowrate needed to displace the reactants from the reservoirs and the hysteresis (lockup) in the regulators necessitated a constant bleed stream ⑤ of each gas during experiments to maintain constant pressure over the reactants. Although the bleed stream did not pass through the reactant solutions, this constant expansion of compressed gases gave considerable Joule-Thompson cooling. To avoid cooling the reactants, all the inlet gas lines and valves are immersed in the thermostat and include helical coils

⑥. The stainless steel gas line tubing was well cleaned of contaminants before assembly. The oxygen-side pressure gauge ⑦ is a 12 in. Heise brand solid front (0-1500 PSI x 2 PSI). The nitrogen pressure gauge ⑧ is a 10 in.

J. P. Marsh type 100 Mastergauge (0-2000 PSI x 20 PSI). (The higher resolution oxygen gauge was indicated since $[O_2]$ in this reactor is calculated from the partial pressure of oxygen over the reactant solution.) By driving the reactants with equal pressure, it is easier to maintain nearly equal reactant flowrates resulting in less leftover reactant after an experimental run.

The reactant reservoirs come next. Because high pressure is involved, pressure vessel construction techniques were used for the outer stainless steel containers holding the four litre polyethylene reservoir bottles. The covers of the cylinders are fitted with: outlets ⑨ and inlets ⑩ for the gas supply; wire passage ⑪ for the reactant thermistors; solution filling ⑫ and withdrawal ⑬ tubes; overflow purge tubes ⑭ , and for the oxygen cylinder, egress for the fiberoptic flowmeter cable ⑮ .

The gas outlets all proceed to protective mufflers ⑯ . The nitrogen inlet tubes ⑩ for the sulfur and iodine reservoirs terminate in the space above the solution bottle while the oxygen inlet penetrates to the bottom of its reservoir via a Teflon gas distributor tube which provides mixing by the O_2 bubbles to facilitate oxygen saturation and thermal equilibrium.

Reactant temperatures are monitored near the center of each polyethylene bottle by a thermistor epoxied into a thin Teflon tube carrying the lead wires. The epoxy is covered with paraffin for inertness (20, 54). The leads are interrupted by a segment of varnish coated wire where they leave the cylinder to eliminate pressure leaks between the wire and insulation.

When reactant is added, it fills the reservoir through a Teflon tube ⑫ mounted outside the waterbath and ending above the highest liquid level of the internal polethylene bottle. This tube and all the Teflon tubes carrying high pressure fluid are wound with polyester fiberglass lagging, even though the bare TFE tubing (3 mm bore, 2 mm wall) survived intact an overnight pressurization to 1500 PSIG. The lagging provides a safety margin against TFE's tendency to creep and a higher barrier to heat flux. The reactant leaves the reservoir by a continuous TFE tube, ⑬ except, on oxygen solution which passes through an intervening TFE/PVC flowmeter inside the reservoir cylinder. The flowmeter is a model E25 Bearingless Flowmeter. The other two flowmeters ⑰ are model E35 and of stainless steel construction.

All cylinders bear a purging tube and valve ⑭. The purge allows any overflowed reactant to be forced out of the reservoir under gas pressure. This feature prevents contaminated liquid from reentering the reactant solution in the bottle.

The reactant solution travels from the reservoir vessels to metering valves by TFE lines ⑬. The valves ⑱ are specially constructed to meter the reactants without contamination and to withstand the operating pressure. From the Teflon valves, the reactants go through in-line temperature sensors (R3) and on to the mixer ⑲ at the beginning of the reactor tube ⑳. The mixer design is an adaptation of Berger's scheme (26) incorporating interdigitated, tangential jets at the base of a hemispherical chamber. The form of the outlet chamber forces the fluid streamlines to detach from the curved surface. The resulting wake possesses compact, intense turbulence to mix the two streams quickly.

The first reaction temperature sensor (R4) immediately follows the mixer. Each temperature sensor is a 2000Ω semiconductor thermistor emplanted one of two ways. In one method, the thermistor projects through the Teflon wall of the tube into the bulk of the flowing fluid; in the other, the thermistor is cast in an epoxy plug and held in the fluid path by a plastic "Tee" tube fitting. The inert, though mechanically disadvantageous, Teflon of which the reactor is made requires special construction techniques.

Thermistors were chosen for temperature sensing due to their large temperature coefficient of resistance and inert glass coating. (For comparison of several temperature coefficients: thermistors, 10%/°C; thermocouples, 0.6%/°C; platinum RTD, 1%/°C; --these are also prohibitively expensive). The thermometrics devices (P/N SP60 BA 252 MIB & A) chosen are well aged at elevated temperature imparting a stability of 0.01%/yr. Even in the good heat transfer conditions around the thermistors, the heatup of reacting fluid due to Joule heating of the thermistor by the measuring current is negligible since the ohmmeter (Keathley model 172) uses only femtoamp currents for resistance measurements. Having all thermistor connections soldered or by gold plated connections and having 2000Ω resistance value makes wiring resistance constant (or varying by amounts below the resolution of the ohmmeter) and low enough to allow use of the simpler two terminal methods of resistance measurement. The flow passes next through a flow selector valve ㉑ . The six-position, all Teflon valve allows the flow to be diverted to various-length reactor tubes or directly to the quencher ㉒ . The selector has ringless sliding seals to contain the pressure without contamination.

At last the reacting liquid enters the main reactor tube ⑳ . This tube is 397 cm long making the total reactor length 405 cm (maximum residence time around 6 sec.). To submerse this length tube in the thermostat for uniform starting temperature, it was coiled. Unfortunately, curvilinear flow tends to stablize laminar flowlines at higher Reynolds numbers than those which give turbulence in straight pipe. To overcome this effect, the coil is square and as large as possible (17 cm sides) so turbulence is fully developed in the straight segments between corners; furthermore, the projecting thermistors obstruct half the flow channel inducing form drag in their wake.

The thermistor spacing is close together at the entrance end of the reactor tube for catching temperature profiles which end in the tube. The sensors are further apart in the remainder of the tube.

After transiting the reactor tube the liquid passes through the complementary flow selector ㉓ and through the second mixer ㉒ . This mixer is fed by an iodine reservoir identical to the sulfur solution reservoir and connected through a flowmeter and metering valve. The mixed flow then passes to a total flowmeter and metering valve ㉔ whose purpose is maintaining a total pressure drop high enough to keep the oxygen in solution throughout the reaction zone. After the valve, the flow exits the thermostat and is accessible ㉕ for sampling for titrations before going to the drain.

The automated temperature measurement system includes the various thermistors, thermistor selection, digital ohmmeter, and microcomputer. The various thermistors are: reactant reservoirs (2), reactant lines (2), reactor tube (11), and waterbath (1). The thermistor selector receives a thermistor number (channel address) from the microprocessor under program control, decodes (actually demultiplexes) the number, and connects the specified thermistor to the digital ohmmeter which reads with a sensitivity of 0.1Ω/2000Ω and has a settling time of 2 sec (this factor being the limit on measuring speed). The actual time the program waits for settling was determined experimentally by finding when no increased wait affected the resistance reading. The measuring current is 10^{-18} A. The digital output consists of 5 x 4 lines of BCD code + 4 lines for the exponent. The microcomputer program reads these 24 lines and reassembles the resistance reading.

For calculating residence times the program needs flowrates. The three flowmeters produce an optical signal. In each flowmeter's individual converter the signal becomes an electrical square wave whose frequency is proportional to flowrate. A separate three-channel frequency to voltage converter processes the square wave for the computer's A to D converters. This circuitous route has the advantages of low pressure drop (an inert bearingless turbine), electronically smoothed output (large capacitors in the F/V integrate noise peaks in the square wave frequency), and rapid reading (by the A/D). The flowrate is correlated with the resulting readings by volumetric calibration.

The only other variables required for the calculations in the program are oxygen pressure, absolute temperature, $[S^{4+}]$, and catalyst concentration. The oxygen pressure is read (±1 PSIG) from the Heise gauge, then entered manually for calculations. The thermostat temperature is related to thermistor readings by calibration with a Beckman thermometer (to 0.002°C). The concentrations of S^{4+} and the catalyst are prepared by formulation with the S^{4+} concentration checked by iodometry previously described.

B. PROCEDURES

1. Rate from Concentration Measurement

The reaction can be influenced by inorganic and organic impurities. The organic impurities were handled by the water purification system. The silicone grease used to lubricate the shaft was regularly removed and replaced to avoid any build-up of material due to adhesion to the grease. The electrode and Teflon fittings were rinsed thoroughly with deionized water before each run. Prior to each reaction, the reactor and associated glassware were rinsed thorougly with deionized water. Periodic cleaning of the glass items with chromic acid and cleaning solution or dilute sulfuric acid, followed by several water rinses, was also performed.

The liquid volume added to the reaction was 600 ml. Added to the reactor initially was 500 ml of solution and the nitrogen flow was started in order to purge oxygen from the reactor. The stirrer was also started. All other materials were added to the reactor through the one open neck of the flask. The calcium or sodium sulfite was then weighed, along with the buffer, if it was to be used in the reaction. The dry materials were poured into the reactor and rinsed down with 100 ml of water.

The initial pH of the reaction was adjusted using the addition of either acid or base. For the buffered reactions employing succinic acid, pellets of sodium hydroxide were added. In the case of unbuffered reactions or where only minor adjustment of pH was required 1.0 M NaOH or 1.0 N H_2SO_4 was used.

Following the pH adjustment, the reactor was sealed with a ground glass stopper and preparations were made to start the reaction. Twenty-five milliter flasks containing predetermined aliquots of 0.1 N iodine solutions were readied to quench the reactions. Sodium bicarbonate required to buffer the solution during the titration and a Teflon coated stirring bar were also contained in the flask. The flasks were kept in an ice bath at all times prior to the titration. The samples at time zero were withdrawn directly from the reactor by pipette and then transferred directly to the iodine. All other samples were obtained using the sampling arm. The gas vent was closed, and after the sample tube had been purged for a few seconds, a clean test tube was used to collect the sample. From the test tube, the 5 ml aliquot was transferred to the flask containing iodine by pipette.

The reaction was then ready to start. With the stirring speed at the desired level, the nitrogen flow was cut off. A stopwatch timed the experiments starting when the oxygen flow reached operating level. The reaction was then followed by periodic sampling until sufficient data had been obtained.

2. Rate from pH Measurements

The procedure for the pH method runs was somewhat different than the procedure of the other experiments. In this method, no sampling, base, or acid addition tubes were necessary. The pH electrode was connected to the strip chart recorder, which was floated on an expanded scale to better observe the pH change in a small range. The charter recorder was then turned on just prior to starting the reaction. All other aspects of the experimental procedure were as previously described.

3. Rates From Temperature Measurement

After the reactant solutions of calcium or sodium sulfite/bisulfite and water, both of the desired pH and catalyst strength, have been prepared by the volumetric methods previously described, the following sequence of steps made up the experimental procedure.

o Change reservoirs well in advance of experiment to allow for thermal equilibrium:

-- Use N_2 purge (conveyed by flexible hose to cap) for the sulfite solution to prevent unwanted oxidation.

-- Replace plug in filler port and close off reservoir immediately when filled to prevent unwanted oxidation.

-- Overpressure the oxygen reservoir (bring pressure up slowly) to assure saturation.

o Wait for thermal steady state:

- -- Use "reservoir" section of data taking program to observe temperatures inside the reservoirs.
- -- Initiate bubbling in the O_2 reservoir or bubble periodically to aid mixing and saturation.

o When the solutions are in readiness, assure the temperature baseline of the reactor tube thermistor calibration curves is flat:

- -- Use "baseline"section of data taking program--or--
- -- Observe temperature profile of only one reactant flowing.
- -- Correct intercepts of thermistor calibration curves to compensate for any bumps.

o Collect initial sample of sulfur solution for titration.

o Begin cycling through thermistor readings a few minutes in advance of data taking to stabilize the electronics.

o Set the oxygen and nitrogen lines:

- -- Open the vent from both lines slightly to raise regulator valve off its seat (eliminating the effect of lockup).
- -- Stop the O_2 bubbling.

o From the predetermined set of observations, use:

- -- "Flows" section of the data taking program to set the required flowrate using both reactant valves and the total flow valve.
- -- Examine temperature profiles and save on file all profiles having no equipment-made flaws.

o Drain both reservoirs separately when the first one runs out:

- -- Shut off either reservoir, open the other fully to drain (avoiding contaminating of next change.
- -- Repeat for remaining reservoir.
- -- Leave total flow valve somewhat open.

C. ANALYSIS OF CALCIUM SULFITE

An analysis of the calcium sulfite solid used in the experiments is given in Table 2-1. The calcium sulfite is a product of City Chemical Corporation. There are few sources of calcium sulfite available and most of the sulfites are relatively impure. It can be seen in Table 2-1 that the calcium sulfite from City Chemical is very impure, consisting of only 50.6 mole% sulfite. The majority of the remainder is calcium sulfate, with several metal impurities also present.

Calcium sulfite was also prepared in the laboratory by bubbling SO_2 through calcium hydroxide. It was possible to obtain a much higher sulfite to sulfate purity by drying the compound carefully under nitrogen (to prevent

TABLE 2-1

ANALYSIS OF CALCIUM SULFITE SOLID

WEIGHT %

(SO_3^{2-})	50.6
Manganese	0.0062
Iron	0.0248
Copper	0.0004
Magnesium	0.0505
Cobolt	0.0008
Zinc	0.0009

Atomic Absorption Analysis by North American Exploration, Inc., Charlottesville, Virginia 22901 oxidation). Since there were several metals present in the calcium hydroxide, these were also present in the laboratory prepared sulfite; however, there was some reduction in the metal impurity levels over the commercial grade calcium sulfite. The main advantage to the laboratory prepared compound was the fact it was 85.6% sulfite, much higher than the commercial grade compound.

D. EQUILIBRIUM RELATIONSHIP FOR S^{4+} SPECIES

As noted in the introduction the presence of the various S^{4+} species depends on the pH of the solution. The mole fraction of each species is shown as a function of pH at 40°C in Figure 1-1 (170, 171).

E. IODOMETRIC TITRATION

The sulfite concentration of sulfur in the +4 valence state was determined by a difference method. An excess of iodine of a known volume and concentration was used to quench known volumes of the reacting solution. The reactions occurring during the quenching are as follows:

$$SO_2 \cdot H_2O + H_2O + I_2 \longrightarrow SO^{2-} + 2I^- + 4H^+$$

$$HSO_3^- + H_2O + I_2 \longrightarrow SO^{2-} + 2I^- + 3H^+$$

$$SO_3^{2-} + H_2O + I_2 \longrightarrow SO^{2-} + 2I^- + 2H^+$$

Arsenious acid was used in the titration in order to determine the number of moles of unreacted iodine:

$$H_3AsO_3 + I_2 + H_2O \longrightarrow H_3AsO_4 + 2I^- + 2H^+$$

A balance on the iodine can be written:

Total Iodine Added = Iodine reacting with S^{4+} +

Iodine reacting with Arsenious Acid

or $(N_I)(V_I) = N_S V_S + N_A V_A$

where N = normality $(\frac{\text{equivalents}}{\text{liter}})$

V = volume (liters)

I, S, and A represent iodine, sulfur (4+), and arsenious acid respectively.

Solving for $N_S = (N_I V_I - N_A V_A)/V_S$

In order to convert from normality to molarity,

$M_S = (N_I V_I - N_A V_A)/2V_S$

Solutions of iodine and arsenious acid were prepared according to standard methods. For all experiments, the concentration of arsenious acid was assumed to be 0.1 N. The iodine solution concentration was then determined by titrating it against the arsenious acid.

The iodine and sulfite aliquots were drawn by pipettes calibrated to 0.001 ml. In a 25 ml flask, the iodine and sulfite solutions were combined with sodium bicarbonate. A drop or two of 6 M hydrochloric acid was used to form a high-pH buffer. A magnetic stirring bar was added to each flask and the flask was then placed on a magnetic stirrer in order to perform the titration. Deionized water was employed to rinse down the sides of the flask prior to the titration. V_A was determined by adding arsenious acid from a buret calibrated to ± 0.001 ml.

As the titration proceeded, the solution changed from red to pale yellow. At this point, a small amount of starch solution was added as an endpoint indicator. The endpoint was reached when the solution went from pale purple to clear.

An examination of the possible errors in this technique indicate a maximum variance in the calculated sulfur (4+) concentration of ± 0.0002 M.

A sample calculation of the sulfur (4+) concentration follows:

$N_I = 0.088$ N

$N_A = 0.100$ N

$V_S = 4.984$ ml

$V_I = 1.993$ ml

$V_A = 1.265$ ml

$$M_S = \frac{(0.099)(1.993) - (0.1)(1.265)}{2(4.984)}$$

$M_S = 0.0071$ M

F. ANALYSIS OF DATA

1. Analysis of a Single Experiment

The results obtained from each experiment were analyzed using a Hewlett-Packard 2000C computer. A BASIC computer program, "REPORT", provided an output of conditions, data, concentrations, calculations of the rate of the reactions, fits to the integrated form of zero, first, and second order reactions, and plots of the sulfur (4+) concentration vs time.

The program required the input of the conditions for the experiment which were printed in an appropriate format. In addition to the conditions, the time, number of aliquots of iodine used, and the amount of arsenious acid used in the titration were input. These data and the concentrations in g-mol/ℓ of the sulfur (4+) species were then printed in the output. The program would then take the concentration information and determine the slope between each two data points. The slope was then output as the rate, along with the average concentration for the two points. The next part of the program used the concentration and time data in a modified version of the Hewlett-Packard library program, CURFIT called CURVIT, to provide information about the zero, first, and second order fit of the data. The final part of the program plotted the concentration vs time data and any additional comments.

The CURVIT program gave a goodness-of-fit parameter, referred to here as the index of determination. The parameter has a value of 1.0 for a perfect linear fit, and 0.0 for random scatter. It is defined as

$$R = \frac{\frac{1}{n-1}(\Sigma X_i Y_i) - \frac{n}{n-1}(XY)}{S_x S_y}$$

where n = number of points
X_i, Y_i = actual value of i point
X, Y = average values
S_x, S_y = standard deviations

The CURVIT program was employed alone to perform linear regression analysis of the log rate vs log concentration data. A Hewlett-Packard HP 25 linear regression analysis program was also used to perform some of this data reduction.

Figure 2-4 provides a listing of the REPORT, the modified CURVIT program, and a sample output of the programs.

2. Multiple Regression Analysis

MULTREG, short for multiple regression, is a program which performs a least squares curve fit of data pairs under a wide variety of I/O and processing options. The program was obtained from the Virginia Highway Research Council through Messrs. William Carpenter and Philip Harris. No listing of the actual program is included here; it is a library program for the Virginia Highway Research Council contained in the CDC CYBER 172 computer, located in Gilmer Hall at the University of Virginia. The program is in FORTRAN IV, and the data and program instructions must be prepared accordingly. The data for the rate and average concentration were obtained directly from the REPORT program described earlier. Other similar multiple regression programs are available in the Hewlett-Packard program library. Criteria for excluding data were that the time was less than 60 seconds or that the rate as recorded on

```
REPORT

10   COM N,R2,R4,Q,K[6],K$[70],T,V[50,3],M[50]
11   COM E
20   FILES SULF21,SULF22
30   DIM A[50],R[50],T[50],A$[70]
40   PRINT "TYP1 TAPO";
50   INPUT F
60   PRINT "RUN #      ";
70   INPUT Q
80   PRINT "# POINTS ";
90   INPUT N
100   PRINT "SLURRY    ";
110   INPUT K[1]
120   PRINT "TEMP      ";
130   INPUT K[2]
140   PRINT "RPM       ";
150   INPUT K[3]
160   PRINT "PH        ";
170   INPUT K[4]
180   PRINT "% O2      ";
190   INPUT K[5]
200   PRINT "LPM       ";
210   INPUT K[6]
220   PRINT "ENTERCOMMENT"
230   INPUT K$
240   PRINT #2;Q,N,K[1],K[2],K[3],K[4],K[5],K[6],K$
250   PRINT TAB(15),"DATA: TIME ',' # I ',' TITER 'RETURN'"
260   MAT  INPUT V[N,3]
270   MAT  PRINT #1;V
280   IF F=0 THEN 1530
290   IF  END #2 THEN 300
300   ASSIGN "SULF21",1,Z
310   IF  END #1 THEN 330
320   MAT  READ #1;V
330   ASSIGN "SULF21",1,Z
340   FOR P=1 TO N
350   V[P,1]=60*V[P,1]
360   PRINT #1;V[P,1],V[P,2],V[P,3]
370   NEXT '
380   PRINT LIN(4),"-",LIN(4),SPA(26),"RUN # ";Q
390   PRINT LIN(2),"CONDITIONS",LIN(1)
400   PRINT "  # DATA       % O2 @ LPM       RPM     PH      TEMP,C   SLURRY,GM/
410   PRINT  USING 420;N,K[5],K[6],K[3],K[4],K[2],K[1]
420   IMAGE3X2D,9X3D,4XD.D,6X4D,2X2D.D,5X2D,7XD.3D
430   REM B=[IODIN] C=[ARSE.ACID] D=VOL OF IODIN PIE.  F=VOL OFSAMPL
440   B=.079844
450   C=.1
```

Figure 2-4 REPORT and CURVIT Programs

```
460  D=2.03094
470  F=4.98472
480  FOR I=1 TO N
490  M[I]=(B*D*V[I,2]-C*V[I,3])/(2*F)
500  NEXT I
510  FOR J=1 TO N-1
520  A[J]=(M[J]+M[J+1])/2
530  R[J]=(M[J]-M[J+1])/(V[J+1,1]-V[J,1])
540  IF J=N=1 THEN 560
550  NEXT J
560  PRINT LIN(2),"RESULTS",LIN(1)
570  PRINT "      TIME,SEC","   # ALIQ I","   TITER,ML","   MOLARITY"
580  FOR I=1 TO N
590  PRINT  USING 600;V[I,1],V[I,2],V[I,3],M[I]
600  IMAGE 4X4D,13XD,12XD.4D,8XD.5D
610  NEXT I
620  PRINT LIN(2),"COMPUTATIONS",LIN(1)
630  PRINT "      TIME,SEC"," AV MOLARITY","      RATE,MOL/L/SEC"
640  PRINT "         0","     ---","     ---"
650  FOR I=1 TO N-1
655  IF R[I]>1.E-08 THEN 660
656  R[I]=0
660  PRINT  USING 670;V[I+1,1],A[I],R[I]
670  IMAGE5X4D,11XD.5D,8XD.7D
680  NEXT I
690  PRINT LIN(1)
700  PRINT LIN(39-2*N),TAB(62),"PAGE ";Q
710  PRINT LIN(2),"-"
720  PRINT LIN(2),"DATA REDUCTION:  INITIAL SLOPE",LIN(1)
722  IF K[1]#0 THEN 730
724  R4=930
725  R2=N
726  E=1
727  T=1
728  CHAIN "CURVIT"
730  R4=820
738  E=1
740  R2=1
750  IF M[R2] <= .005 THEN 790
760  IF R2=N THEN 790
770  R2=R2+1
780  GOTO 750
790  R2=R2-1
800  T=1
810  CHAIN "CURVIT"
820  R4=940
830  IF K[1]=0 THEN 930
840  ASSIGN "SULF22",3,Z
860  E=R2+3
880  R2=N
```

Figure 2-4. REPORT and CURVIT Programs

```
890  T=2                                        FINAL SLOPE",LIN(1)
900  PRINT LIN(1)"
910  CHAIN "CURVIT"
920  GOTO 940
930  PRINT LIN(8)
940  PRINT LIN(2),"PLOT OF CONCENTRATION VS TIME",LIN(1)
990  FOR I=1 TO N
991  A[I]=M[I]
992  NEXT I
1020  MAT T=CON
1030  MAT T=(100)*T
1032  FOR I=1 TO N
1033  T[I]=V[I,1]/60
1034  NEXT I
1040  MAT M=CON
1050  MAT M=(100)*M
1051  FOR I=1 TO N
1052  M[I]=A[I]
1053  NEXT I
1060  IF T[N] <= 20 THEN 1120
1070  IF T[N] <= 40 THEN 1150
1080  IF T[N] <= 60 THEN 1180
1090  T1=120
1100  T2=.5
1110  GOTO 1200
1120  T1=20
1130  T2=3
1140  GOTO 1200
1150  T1=40
1160  T2=1.5
1170  GOTO 1200
1180  T1=60
1190  T2=1
1200  IF M[1] <= .0099 THEN 1230
1202  IF M[1] <= .022 THEN 1222
1210  M1=.099
1220  GOTO 1240
1222  M1=.022
1223  GOTO 1240
1230  M1=.0099
1240  J=1
1250  A$=".----------!----------!----------!----------!----------!----------!"
1260  PRINT SPA(10),A$
1270  FOR I=33 TO 1 STEP -1
1280  IF I/11-INT(I/11) >= .08 THEN 1320
1290  PRINT  USING 1300;M1*I/33
1300  IMAGE#,5X.4D,"-"
1310  GOTO 1330
```

Figure 2-4. REPORT and CURVIT Programs

```
1320  PRINT SPA(10),"1";
1330  IF T[J]=100 THEN 1390
1340  IF M[J]<M1*I/33-M1/33 THEN 1390
1350  IF M[J]>M1*I/33 THEN 1390
1352  B$="*"
1353  IF K[1]=0 THEN 1368
1354  IF J<E-2 THEN 1368
1355  IF J >= E THEN 1367
1356  B$="."
1357  GOTO 1368
1360  PRINT SPA(T[J]*T2),"*";LIN(0),SPA(11);
1367  B$="#"
1368  PRINT SPA(T[J]*T2),B$;LIN(0),SPA(11);
1370  J=J+1
1380  GOTO 1330
1390  IF I=1 THEN 1420
1400  PRINT LIN(1);
1410  NEXT I
1420  PRINT LIN(0)
1430  PRINT SPA(10);A$
1440  PRINT  USING 1450;T1/6,T1/3,T1/2,2*T1/3,5*T1/6,T1
1450  IMAGE10X,"^O",8X2D,8X2D,8X2D,8X2D,7X3D,5X3D,"^"
1460  PRINT SPA(7),"[SULFUR IV]",SPA(13),"<<< TIME, MINUTES >>>"
1490  PRINT SPA(7),"MOLES/LITRE"
1500  PRINT LIN(1),"COMMENT:";K$
1510  PRINT LIN(1),TAB(59);"PAGE ";Q;".1"
1520  PRINT LIN(1),"-"
1530  END
```

Figure 2-4. REPORT and CURVIT Programs

```
CURVIT

8000  COM D,R2,R4,Q,K[6],K$[70],T,W[50,3],M[50]
8003  COM E
8006  FILES SULF21,SULF22,SULF12,SULF11
8009  DIM X[200],Y[200],U[200],V[200],A[7],B[7],C[7],S[6],F[7]
8012  DIM T[7,3]
8013  N=R2-E+1
8014  D[1]=E
8015  D[5]=R2
8016  D[2]=0
8018  FOR I=1 TO N
8021  X[I]=W[I+E-1,1]
8024  Y[I]=M[I+E-1]
8027  NEXT I
8030  MAT F=CON
8033  PRINT "CURVE TYPE","  INDEX  OF","   A","   B";"            PT#'S"
8036  PRINT " ","DETERMINATION"
8039  FOR I=1 TO 7
8042  IF (I-3)*(I-4)*(I-6)*(I-7)=0 THEN 8186
8045  MAT S=ZER
8048  GOSUB 8216
8051  IF (I-5)*(I-6)=0 THEN 8099
8054  IF (I-2)*(I-3)=0 THEN 8078
8057  FOR J=1 TO N
8060  LET V[J]=Y[J]
8063  GOSUB 8192
8066  NEXT J
8069  IF I=1 THEN 8129
8072  IF I=7 THEN 8144
8075  GOTO 8162
8078  FOR J=1 TO N
8081  IF Y[J] <= 0 THEN 8120
8084  LET V[J]=LOG(Y[J])
8087  GOSUB 8192
8090  NEXT J
8093  IF I=3 THEN 8144
8096  GOTO 8129
8099  FOR J=1 TO N
8102  IF Y[J]=0 THEN 8120
8105  LET V[J]=1/Y[J]
8108  GOSUB 8192
8111  NEXT J
8114  IF I=6 THEN 8162
8117  GOTO 8129
8120  PRINT "CAN'T FIT"
8123  LET F[I]=0
8126  GOTO 8183
8129  FOR J=1 TO N
```

Figure 2-4. REPORT and CURVIT Programs

```
8132  LET U[J]=X[J]
8135  GOSUB 8201
8138  NEXT J
8141  GOTO 8177
8144  FOR J=1 TO N
8147  IF X[J] <= 0 THEN 8120
8150  LET U[J]=LOG(X[J])
8153  GOSUB 8201
8156  NEXT J
8159  GOTO 8177
8162  FOR J=1 TO N
8165  IF X[J]=0 THEN 8120
8168  LET U[J]=1/X[J]
8171  GOSUB 8201
8174  NEXT J
8177  GOSUB 8279
8180  PRINT C[I],A[I],B[I],D[I]
8183  PRINT #(T+2);C[I],A[I],B[I]
8186  NEXT I
8189  GOTO 8348
8192  LET S[5]=S[5]+V[J]^2
8195  LET S[3]=S[3]+V[J]
8198  RETURN
8201  LET S[1]=S[1]+U[J]
8204  LET S[2]=S[2]+U[J]^2
8207  IF I>1 THEN 8210
8210  LET S[4]=S[4]+U[J]*V[J]
8213  RETURN
8216  LET K=I
8219  IF K=1 THEN 8273
8222  IF K=2 THEN 8267
8225  IF K=3 THEN 8261
8228  IF K=4 THEN 8255
8231  IF K=5 THEN 8249
8234  IF K=6 THEN 8243
8237  PRINT "7. Y=A+B*LOG(X)";
8240  RETURN
8243  PRINT "6. Y=X/(A+B*X) ";
8246  RETURN
8249  PRINT "5. Y=1/(A+B*X)";
8252  RETURN
8255  PRINT "4. Y=A+(B/X)",
8258  RETURN
8261  PRINT "3. Y=A*(X^B)",
8264  RETURN
8267  PRINT "2. Y=A*EXP(B*X)";
8270  RETURN
8273  PRINT "1. Y=A+(B*X)",
8276  RETURN
```

Figure 2-4. REPORT and CURVIT Programs

```
8279  LET B=(N*S[4]-S[1]*S[3])/(N*S[2]-(S[1]^2))
8282  LET A=(S[3]-B*S[1])/N
8285  LET S1=S[5]-(S[3]^2)/N
8288  LET S2=(B^2)*(S[2]-(S[1]^2)/N)
8291  LET C[I]=S2/S1
8294  T[I,1]=SQR((S1-S2)/(N-2))
8297  T[I,2]=T[I,1]*SQR(S[2]/(N*(S[2]-(S[1]^2/N))))
8300  T[I,3]=T[I,1]/SQR(S[2]-(S[1]^2/N))
8303  IF (I-1)*(I-4)*(I-5)*(I-7)=0 THEN 8336
8306  IF (I-2)*(I-3)=0 THEN 8327
8309  LET A[6]=B
8312  LET B[6]=A
8315  Z=T[6,2]
8318  T[6,2]=T[6,3]
8321  T[6,3]=Z
8324  RETURN
8327  LET A[I]=EXP(A)
8330  T[I,2]=EXP(T[I,2])
8333  GOTO 8339
8336  LET A[I]=A
8339  LET B[I]=B
8342  RETURN
8345  STOP
8348  CHAIN "REPORT",R4
8351  END
```

Figure 2-4. REPORT and CURVIT Programs

the REPORT program was zero. The useable data was then run through MULTREG. They were fit to the equations:

$$\log \text{Rate} = a(\log[S^{4+}]) + \log C$$

where a = order of reaction with respect to sulfur (4+) concentration, (mol/ℓ)

C = rate constant

The MULTREG program had the capability to handle more than one independent variable. In a second run of the MULTREG program, two independent variables were considered: the sulfur (4+) concentration and the catalyst concentration. In order to assure compatability with the program, catalyst concentrations had to be converted from ppm to g-mol/ℓ. This second multiple regression analysis was done for the iron catalyzed sodium sulfite oxidation, manganese catalyzed sodium sulfite oxidations, and the manganese catalyzed calcium sulfite oxidations. The same criteria were used to screen the data employed in the MULTREG program for the second analysis. The MULTREG program fit the data for each of the three cases to the following equations:

$$\log \text{Rate} = a(\log[S^{4+}]) + b([\text{Catalyst}]) + \log C$$

where a = order of reaction with respect to the sulfur$^{(4+)}$ concentration

b = order of reaction with respect to the catalyst concentration

C = rate constant

3. ANALYSIS OF pH METHOD DATA

An analysis of the sulfite oxidation rate based upon pH change was developed (based on the ideas of S. Bengtsson [24]). During sulfite oxidation, sulfite oxidized to sulfate, $SO_3^{2-} + \frac{1}{2}O_2 \longrightarrow SO_4^{2-}$. Also, the equilibrium $HSO_3^- \rightleftharpoons H^+ + SO_3^{2-}$ is established very rapidly. Thus, the pH value decreases accordingly during reaction at the pH range being studied. From the rate of change of pH the rate of oxidation can be determined.

In dilute solutions, the activities and concentrations of the ions can be equated. The following equilibrium applies:

$$\frac{[H^+][SO_3^{2-}]}{[HSO_3]} = k_s \qquad (2\text{-}1)$$

At the beginning of the test, the solution contains a known buffer concentration and $CaSO_3$ or Na_2SO_3 concentration. The pH value is set by the addition of H_2SO_4. If C_1 designates the initial concentration of (Na_2SO_3) or $CaSO_3$, and C_2 the added amount of H_2SO_4, the following concentration conditions apply:

$$[SO_4^{2-}] + [SO_3^{2-}] + [HSO_3^-] = C_1 + C_2 \qquad (2\text{-}2)$$

$$[Na^+] = 2C_1$$

The condition of electro-neutrality is:

$$2[SO_4^{2-}] + 2[SO_3^{2-}] + [HSO_3^-] + [OH^-] + [A^-] = 2C_1 + [H^+] \qquad (2\text{-}3)$$

multiply (2-2) by 2, then subtract it by (2-3), gives

$$[HSO_3^-] = [OH^-] + [A^-] - [H^+] + 2C_2$$

The equilibrium

$$k_B = \frac{[H^+][A^-]}{[HA]} = \frac{[H^+][A^-]}{[HA]_o - [A^-]}$$

is also established

$$[A^-] = \frac{K_B[HA]_o}{k_B = [H+]} \qquad (2\text{-}4)$$

Substitute (2-4) into (2-3) results in

$$[HSO_3^-] = [OH^-] + \frac{k_B[HA]_o}{k_B + [H+]} - [H^+] + 2C_1$$

The above equation is valid during oxidation. Differentiation with respect to time gives:

$$\frac{d[HSO_3^-]}{dt} = \frac{d[OH^-]}{dt} - \frac{k_B[HA]_o}{\{k_B + [H+]\}^2}\frac{d[H^+]}{dt} - \frac{d[H^+]}{dt} \qquad (2\text{-}5)$$

$$= - \{1 + \frac{(OH^-)}{[H^+]} - \frac{k_B(HA)_o}{\{k_B + [H^+]\}^2}\frac{d[H^+]}{dt}$$

$$[H^+][OH^-] = k_w, \quad \frac{d[OH^-]}{dt} = - \frac{[OH^-]}{[H+]}\frac{d[H^+]}{dt}$$

From equation (2-1)

$$\frac{d[SO_3^{2-}]}{dt} = \frac{k_S}{[H^+]^2}\{[H^+]\frac{d[HSO_3^-]}{dt} - [HSO_3^-]\frac{d[H^+]}{dt}\}$$

$$= \frac{k_S}{[H^+]^2}\{[H^+]\{- 1 - \frac{[OH^-]}{[H^+]} - \frac{k_B[HA]_o}{\{k_B + [H^+]\}^2}\} - [HSO_3^-]\}\frac{d[H^+]}{dt} \qquad (2\text{-}6)$$

Oxidation rate is

$$- \frac{dS_t}{dt} = - (\frac{d[SO_3^{2-}]}{dt} + \frac{d[HSO_3^-]}{dt}) \qquad (2\text{-}7)$$

where $S_t = [SO_3^{2-}] + [HSO_3^-]$

From (2-5), (2-6) and (2-7), we have

$$- \frac{dS_t}{dt} = \{\frac{k_S}{[H^+]} + \frac{k_S k_w}{[H^+]^3} + \frac{k_B k_S[HA]_o}{[H^+]\{k_B+[H^+]\}^2} + \frac{k_S S_t}{[H^+]\{k_S+[H^+]\}} + 1 + \frac{k_w}{[H^+]^2}$$

$$+ \frac{k_B[HA]_o}{\{k_B+[H^+]\}^2}\}\frac{d[H^+]}{dt} \qquad (2\text{-}8)$$

Taking into account that $[H^+] = 10^{-pH}$, we have, after differentiating with respect to time:

$$\frac{d[H^+]}{dt} = - 10^{-pH} \ln 10 \frac{dpH}{dt} = - [H^+]\ln 10 \frac{dpH}{dt} \qquad (2\text{-}9)$$

By substituting eq. (2-9) into equation (2-8), we get

$$-\frac{dS_t}{dt} = \{\frac{k_S}{[H^+]} + \frac{k_S k_w}{[H^+]^3} + \frac{k_B k_S [HA]_o}{[H^+\{k_B+[H^+]\}^2} + \frac{k_S S_t}{[H^+]\{k_S+[H^+]} + 1 + \frac{k_w}{[H^+]^2}$$

$$+ \frac{k_B [HA]_o}{\{k_B+[H^+]\}^2} \} \ln 10 \, [H^+] \frac{dpH}{dt} \qquad (2\text{-}10)$$

If there is no acid (HA) in the solution, the above equations can be simplified to be:

$$-\frac{dS_t}{dt} = \{ \frac{k_S S_t}{k_S+[H^+]} + \frac{k_S[OH^-]}{[H^+]} + [H^+] + \frac{[OH^-]}{[H^+]} + k_S\} \ln 10 \frac{dpH}{dt} \qquad (2\text{-}11)$$

This equation can then be used to determine the rate of reaction from the measured rate of pH change.

4. Analysis of the Flow Thermal Data

The bisulfite and sulfite oxidation are mildly exothermic giving up 29.3 and 63.2 kcal/mol respectively. Monitoring the temperature rise, therefore, is a feasible method for following the course of these reactions. The difficulties arise from the small temperature increases encountered and the inability of a method to distinguish one sulfur species from the other, a problem also shared by titration. The first problem is solved by resorting to high temperature coefficient thermistor sensors capable of distinguishing ΔT's as low as 0.001^oC. The latter difficulty can be avoided all-together if only bisulfite or sulfite is present. Initial opeartion at pH 4.6 makes bisulfite the net holder of S^{4+} while pH above 9 causes sulfite to be the dominant species.

Consider a cylindrical slice of fluid Figure 2-5 traveling away from the mixer with the conditions:

Adiabatic (qw=0)

Isobaric (Pi = Po)

Negligible viscous heating

Steady flow ($v_i = v_o$)

Homogeneous reaction ($q_r = R \cdot H_r$)

The energy balance on this volume will be:

$$\left\{\begin{array}{l}\text{Rate of}\\ \text{Accumulation}\end{array}\right\} = \left\{\begin{array}{l}\text{Rate of Input}\\ \text{by Convection}\end{array}\right\}_{\text{at i}} - \left\{\begin{array}{l}\text{Rate of Output}\\ \text{by Convection}\end{array}\right\}_{\text{at o}} + \left\{\begin{array}{l}\text{Rate of}\\ \text{Generation}\end{array}\right\} + \left\{\begin{array}{l}\text{Rate by}\\ \text{Coduction}\\ \text{Compression}\\ \text{Acceleartion}\\ \text{Dissipation}\end{array}\right\}$$

Specifically,

$$0 = \rho f\ C_p\ \Delta\ T_i - \rho f\ C_p\ \Delta\ T_o + R \cdot H_R\ \Delta lA$$

Divide by $A\Delta l$ and take the limit as $\Delta l \rightarrow 0$ and integrate

$$\frac{\Delta T}{\Delta l} = - \frac{R_A H_R}{\rho f\ C_p}$$

Evaluate:

$$A = 0.0792\ \text{cm}^2$$

$$C_p = 0.998\ \text{cal/(cal°C)}$$

$$\rho = 0.997\ \text{g cm}^{-3}$$

Sulfite = (pH $\gtrsim$ 9)

$$H_R = 63.2\ \text{kcal/mol}$$

Bisulfite = (pH = 4.6)

$$H_R = 29.3\ \text{kcal/mol}$$

The rate in the case of bisulfite then is

$$R = \frac{C_p \rho}{H_R A}\ f\ \frac{\Delta T}{\Delta l}$$

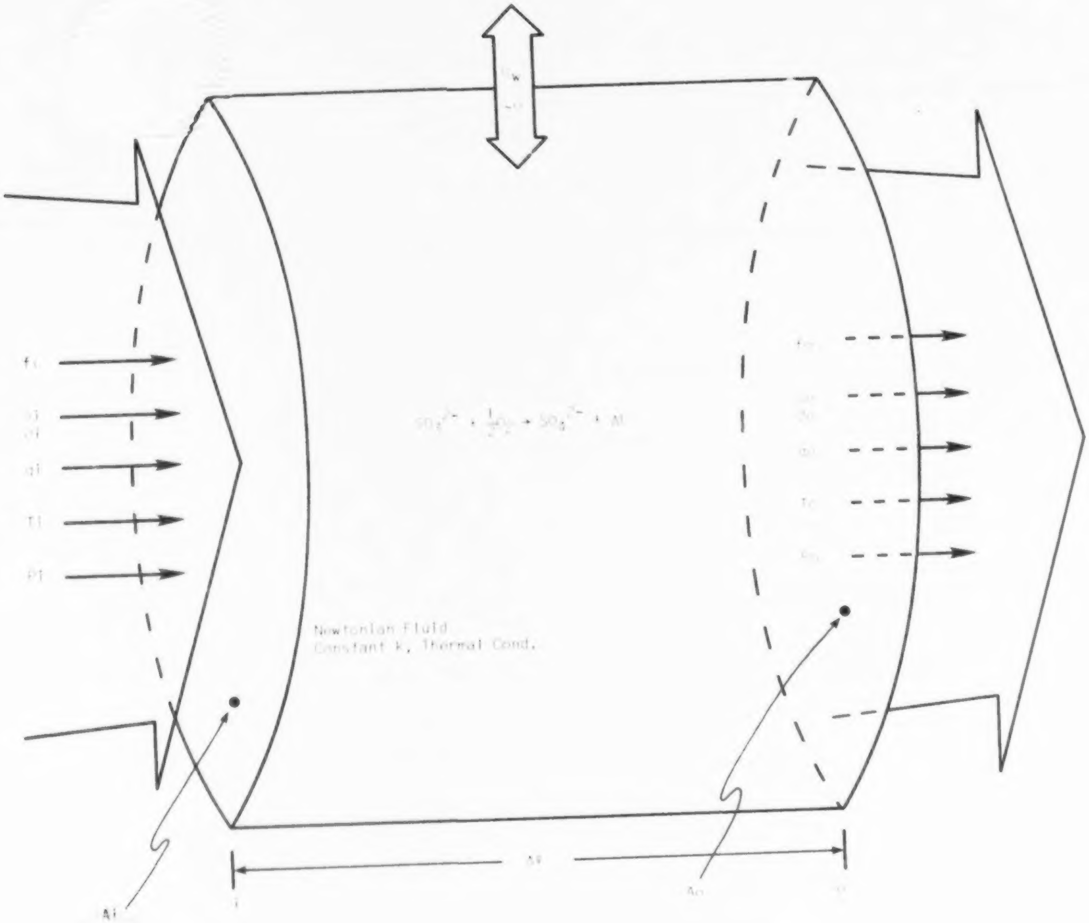
fi
Ti
Pi
$SO_3^{2-} + \frac{1}{2}O_2 \rightarrow SO_4^{2-} + \Delta H$
Newtonian Fluid
Constant k, Thermal Cond.
Ai
i
Ao
o

Figure 2-5. Element of Reacting Fluid

$$= 0.4288 \, f \, \frac{\Delta T}{\Delta l} \text{ mol/(ℓ sec)}$$

for sulfite

$$= 0.1988 \, f \, \frac{\Delta T}{\Delta l}$$

For example Figure 2-6 in run #3-23 of the flow reactor results where the conditions were:

$[HSO_3^-] = 0.0018$ mol/ℓ

$[O_2] = 0.0144$ mol/ℓ

$T_{Bath} = 25.014$°C

$f_{tot} = 6.05$ cm^3/sec

$[Mn] = 10$ ppm

The slope of the T *vs* l plot is 0.0.00025 °C/cm which gives

$$R = 0 \cdot 4288 \cdot 6.05 \cdot 0.00025$$

$$= 6.5 \times 10^{-4} \text{ mol/(ℓsec)}$$

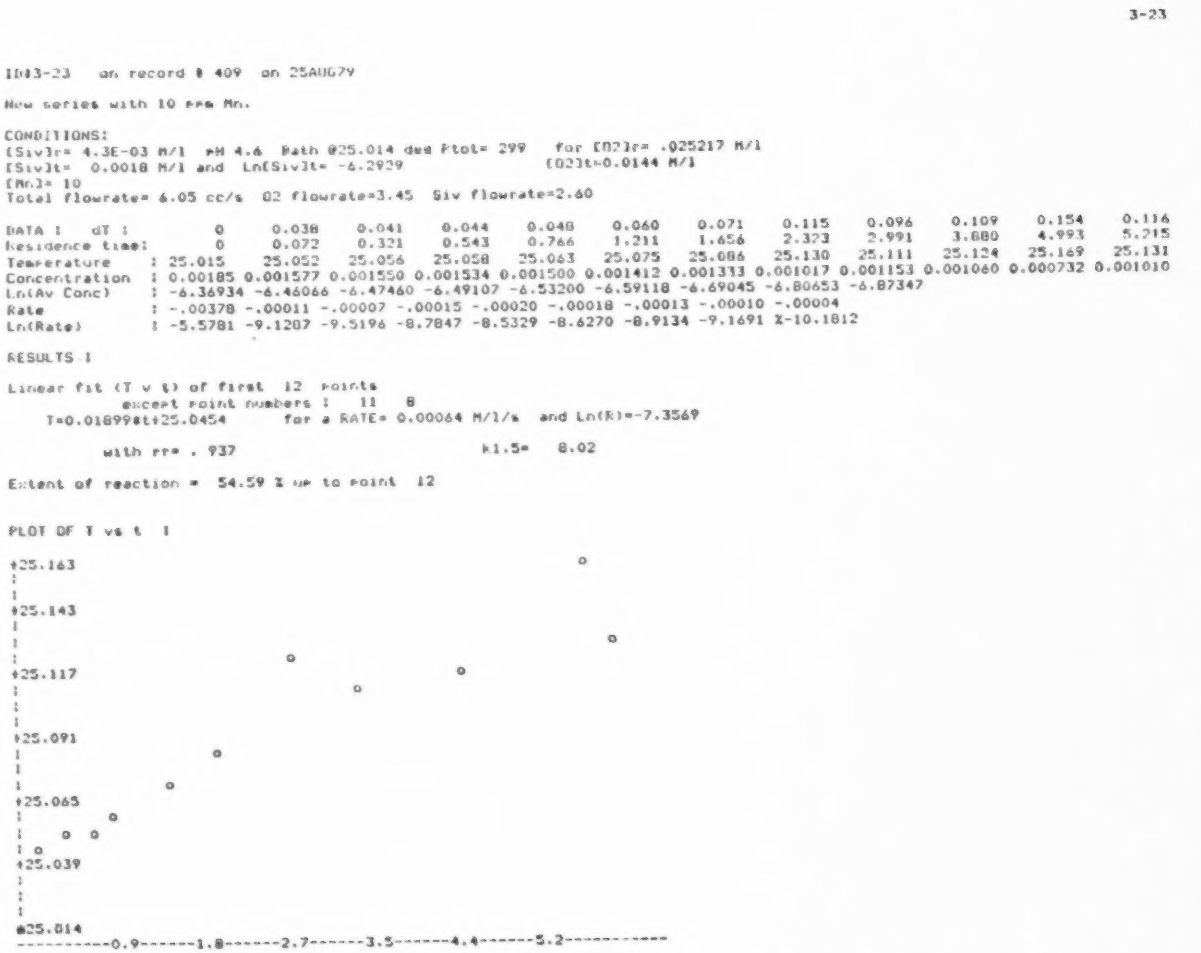

```
                                                                                                       3-23

ID#3-23   on record # 409   on 25AUG79

New series with 10 ppm Mn.

CONDITIONS:
[Siv]r= 4.3E-03 M/l  pH 4.6  Bath @25.014 deg Ptot= 299   for [O2]r= .025217 M/l
[Siv]t=  0.0018 M/l and  Ln[Siv]t= -6.2929                [O2]t=0.0144 M/l
[Mn]= 10
Total flowrate= 6.05 cc/s  O2 flowrate=3.45  Siv flowrate=2.60

DATA :   dT :           0     0.038     0.041     0.044     0.048     0.060     0.071     0.115     0.096     0.109     0.154     0.116
Residence time:         0     0.072     0.321     0.543     0.766     1.211     1.656     2.323     2.991     3.880     4.993     5.215
Temperature    : 25.015    25.052    25.056    25.058    25.063    25.075    25.086    25.130    25.111    25.124    25.169    25.131
Concentration  : 0.00185 0.001577 0.001550 0.001534 0.001500 0.001412 0.001333 0.001017 0.001153 0.001060 0.000732 0.001010
Ln(Av Conc)    : -6.36934 -6.46066 -6.47460 -6.49107 -6.53200 -6.59118 -6.69045 -6.80653 -6.87347
Rate           : -.00378 -.00011 -.00007 -.00015 -.00020 -.00018 -.00013 -.00010 -.00004
Ln(Rate)       : -5.5781 -9.1207 -9.5196 -8.7847 -8.5329 -8.6270 -8.9134 -9.1691 X-10.1812

RESULTS :

Linear fit (T v t) of first  12  points
            except point numbers :   11   8
    T=0.01899*t+25.0454        for a RATE= 0.00064 M/l/s  and Ln(R)=-7.3569

        with rr= . 937                              k1.5=   8.02

Extent of reaction =  54.59 % up to point  12


PLOT OF T vs t  :
```

Figure 2-6. Sample Output for Flow Reactor

SECTION 3

OXIDATION IN CALCIUM SULFITE SOLUTIONS

OUTLINE

A. Calcium Sulfite Oxidation (no organic acids)

B. Calcium Sulfite Oxidation in the Presence of Organic Acids

  1. Succinic Acid

    a. Effect of pH on the Rate of Oxidation

    b. Effect of Succinic Acid Concentration

  2. Adipic Acid

  3. Glycolic Acid

  4. Comparison of Rates of Oxidation with Succinic Acid, Adipic Acid, Glycolic Acid, Citric Acid, and Acetic Acid

  5. Effect of Catalyst - Manganese and Iron

    a. Succinic Acid

    b. Glycolic Acid

C. Reaction in Liquor from Penberthy Oxidation Runs at Shawnee

D. Dependence of Oxidation Rate on Stirring Speed and Oxygen Flowrate

E. Rate of $CaSO_3$ Oxidation at High Catalyst Concentration by the Flow-Thermal Method

OXIDATION IN CALCIUM SULFITE SOLUTIONS

As a basis for understanding oxidation in calcium sulfite slurries, a detailed investigation of the reaction in clear solutions was undertaken. The rate was studied as a function of temperature, pH, catalyst type and concentration, and type and concentration of organic acid inhibitors.

The pH has a strong influence on the reaction rate over the range investigated with the rate of oxidation increasing with increasing pH. For the studies with organic acid inhibitor the pH was held constant during the course of an experiment, either by the buffering action of the organic acid or by means of a pH controller. Without the organic acid this method could not be used except at the lowest pH studied (4.0) since the reaction became too fast. Therefore, a method was used in which the pH was allowed to vary throughout the experiment and the rate determined from the rate of change of pH.

The catalysts studied were manganese and iron since these are present in calcium sulfite and in sulfur dioxide scrubbing loops and are active at increasing the rate of oxidation.

The organic acids investigated all inhibited the reaction to some extent, with glycolic acid being effectively able to stop the reaction, if present in large enough quantities. These organic acids can be used in scrubbing systems to increase the sulfur dioxide absorption efficiency, and could also be used to influence the rate of oxidation.

A. CALCIUM SULFITE OXIDATION

The oxidation in clear calcium sulfite solutions was studied in a semi-batch reactor by following the pH change as described above. This method was used for intermediate reaction rates, viz., when the reaction was too fast to be studied by taking samples from the semi-batch reactor, but when the rate was somewhat slower than those investigated in the flow reactor. The studies reported in this section are thus on the oxidation of calcium sulfite without inhibitors and with the addition of no or small amounts of catalyst.

The rate of oxidation as a function of $[S^{4+}]$ at T = 25°C, 30°C, 35°C, and $40^{O}C$ is shown in Figure 3-1 and Table 3-1. The reaction is 1.5 order with respect to sulfur under these conditions and values for $k_{1.5}$ are given in Table 3-1. Similar results are presented in Tables 3-2 and 3-3 and Figures 3-2 and 3-3 for oxidation in the presence of catalyst. The catalyst levels [Mn] = 0.53 ppm and [Fe] = 1.02 ppm for the experiments of Table 3-3 and Figure 3-3 were chosen because these catalyst levels are the same as those present in liquid which is in contact with solid calcium sulfite under the conditions of the slurry oxidations described in Section IV. Thus, the rate constants obtained from Figure 3-3 are useful in the mathematical model used to interpret slurry results.

The effects of additional manganese catalyst can be seen from Table 3-4 and Figures 3-4 and 3-5.

Activation energies were obtained from the data for the three conditions (1) no added catalyst, (2) [Mn] = 0.6 ppm, and (3) [Mn] = 0.53 ppm, [Fe] = 1.02 ppm, as shown in Figure 3-6. The rate constants ($K_{1.5}$) and the rate of reaction for $[S^{4+}]$ = 0.01M were then calculated over a range of temperatures $20^{o}C$ to $80^{O}C$; these are presented in Table 3-5.

B. CALCIUM SULFITE OXIDATION IN THE PRESENCE OF ORGANIC ACIDS

A detailed investigation has been made on the effect of organic acids on the rate of oxidation in calcium sulfite solutions. These acids can be added to scrubbing loops to improve the efficiency of sulfur dioxide absorption and may be used to inhibit undesired oxidation. The oxidation was studied in the presence of succinic, adipic, glycolic, citric and acetic acids as a function of pH, acid concentration and type and catalyst concentration.

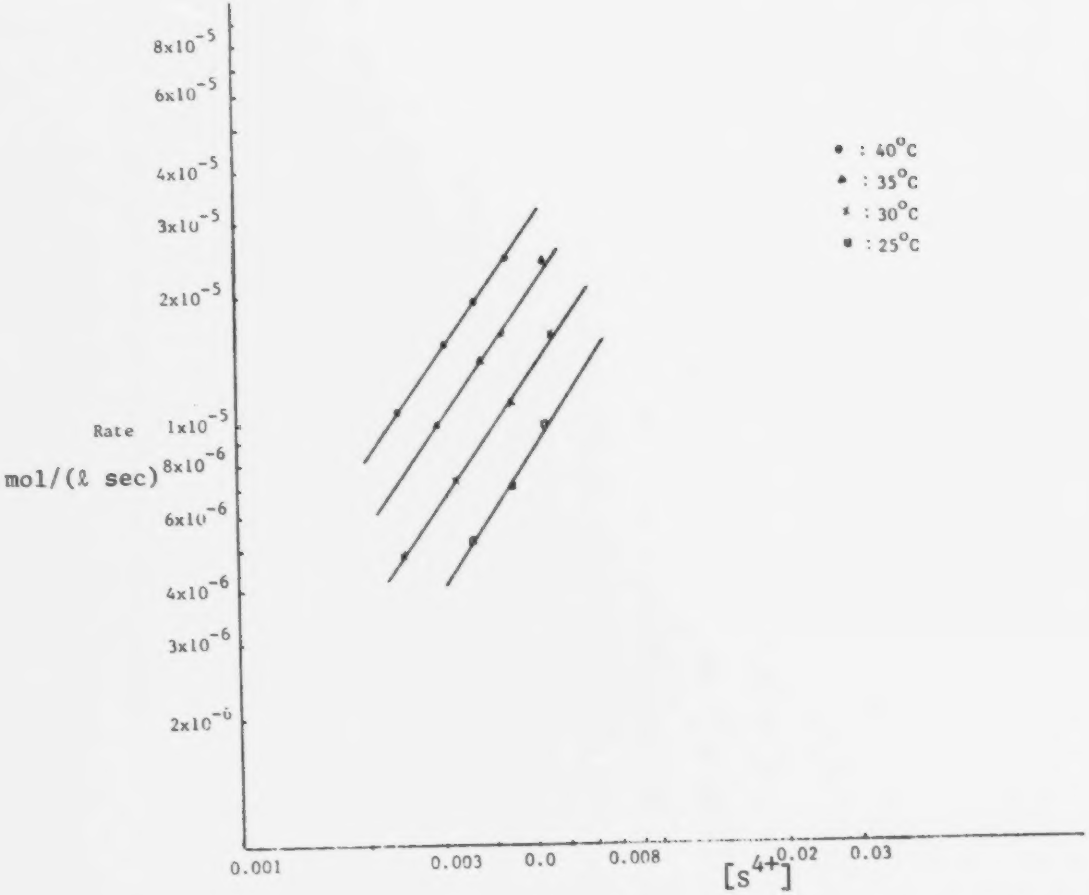

Figure 3-1. Rate of Calcium Sulfite Oxidation; No Added Catalyst Initial pH = 4.6.

TABLE 3-1. RATE OF CALCIUM SULFITE OXIDATION; NO ADDED CATALYST; INITIAL pH = 4.6.

pH = 4.60

Run No.	Initial S^{+4} Concn.	Rate mol/(ℓ sec)	Added Mn	Total Mn	Added Fe	Total Fe	Order for S^{+4}	Standard error of Order	°C Temp.	Rate Constant (for 1.5 Order)
88	0.00432	2.469×10^{-5}	0	$[Mn] = [S^{4+}] \times 13.95$ ppm/mol S^{4+}	0	$[Fe] = [S^{4+}] \times 55.8$ ppm/mol S^{4+}	1.49	0.048	40	0.0885
89	0.00364	1.95×10^{-5}	0		0		1.49	0.048	40	0.0885
90	0.00309	1.547×10^{-5}	0		0		1.49	0.048	40	0.0885
91	0.00240	1.058×10^{-5}	0		0		1.49	0.048	40	0.0885
104	0.00536	2.409×10^{-5}	0		0		1.48	0.047	35	0.061
101	0.00422	1.635×10^{-5}	0		0		1.48	0.047	35	0.061
102	0.00375	1.413×10^{-5}	0		0		1.48	0.047	35	0.061
103	0.00295	9.905×10^{-6}	0		0		1.48	0.047	35	0.061
97	0.00552	1.631×10^{-5}	0		0		1.44	0.062	30	0.039
99	0.00444	1.109×10^{-5}	0		0		1.44	0.062	30	0.039
98	0.00321	7.381×10^{-6}	0		0		1.44	0.062	30	0.039
100	0.00243	4.897×10^{-6}	0		0		1.44	0.062	30	0.039
105	0.00536	9.989×10^{-6}	0		0		1.54	0.17	25	0.025
108	0.00443	7.008×10^{-6}	0		0		1.54	0.17	25	0.025
106	0.00353	5.236×10^{-6}	0		0		1.54	0.17	25	0.025

TABLE 3-2. RATE OF CALCIUM SULFITE OXIDATION; [Mn] = 0.6 ppm

pH = 4.60

Run No.	Initial S^{4+} Concn.	Rate mol/(ℓ sec)	Added Mn	Total Mn	Added Fe	Total Fe	Order for S^{4+}	Standard error of Order	°C Temp.	Rate Constant (for 1.5 Order)
141	0.0055	3.5304×10^{-5}	0.520	0.6	0	$[Fe] = [S^{4+}] \times 55.8$ ppm Fe/mol S^{4+}	1.55	0.058	30	0.09
142	0.00441	2.658×10^{-5}	0.533	0.6	0		1.55	0.058	30	0.09
143	0.00358	1.951×10^{-5}	0.548	0.6	0		1.55	0.058	30	0.09
146	0.00456	1.769×10^{-5}	0.533	0.6	0		1.43	0.10	25	0.059
145	0.00360	1.217×10^{-5}	0.548	0.6	0		1.43	0.10	25	0.059
147	0.00249	7.402×10^{-6}	0.567	0.6	0		1.43	0.10	25	0.059
150	0.00542	1.469×10^{-5}	0.520	0.6	0		1.46	0.092	20	0.038
148	0.00436	1.057×10^{-5}	0.533	0.6	0		1.46	0.092	20	0.038
149	0.00341	8.036×10^{-6}	0.548	0.6	0		1.46	0.092	20	0.038
151	0.00252	4.712×10^{-6}	0.567	0.6	0		1.46	0.092	20	0.038

TABLE 3-3. RATE OF CALCIUM SULFITE OXIDATION; ADDED Mn AND Fe.

pH = 4.60

Run No.	Initial S^{4+} Conc.	Rate mol/(ℓ sec)	Added Mn	Total Mn	Added Fe	Total Fe	Order for S^{4+}	Standard error of Order	°C Temp.	Rate Constant (for 1.5 Order)
156	0.00275	1.2532×10^{-5}	0.497	0.53	0.888	1.02	1.44	0.013	30	0.084
153	0.00373	1.9608×10^{-5}	0.478	0.53	0.813	1.02	1.44	0.013	30	0.084
155	0.00523	3.1713×10^{-5}	0.450	0.53	0.702	1.02	1.44	0.013	30	0.084
154	0.00578	3.6497×10^{-5}	0.447	0.53	0.699	1.02	1.44	0.013	30	0.084
157	0.00276	7.4903×10^{-6}	0.497	0.53	0.888	1.02	1.56	0.024	25	0.0534
159	0.00406	1.3428×10^{-5}	0.478	0.53	0.813	1.02	1.56	0.024	25	0.0534
158	0.00526	2.0135×10^{-5}	0.450	0.53	0.702	1.02	1.56	0.024	25	0.0534
160	0.00606	2.5687×10^{-5}	0.447	0.53	0.699	1.02	1.56	0.024	25	0.0534
161	0.003033	6.623×10^{-6}	0.497	0.53	0.497	1.02	1.50	0.043	20	0.0388
163	0.004232	1.0537×10^{-5}	0.478	0.53	0.478	1.02	1.50	0.043	20	0.0388
162	0.005154	1.4583×10^{-5}	0.450	0.53	0.450	1.02	1.50	0.043	20	0.0388
164	0.00589	1.7809×10^{-5}	0.447	0.53	0.447	1.02	1.50	0.043	20	0.0388

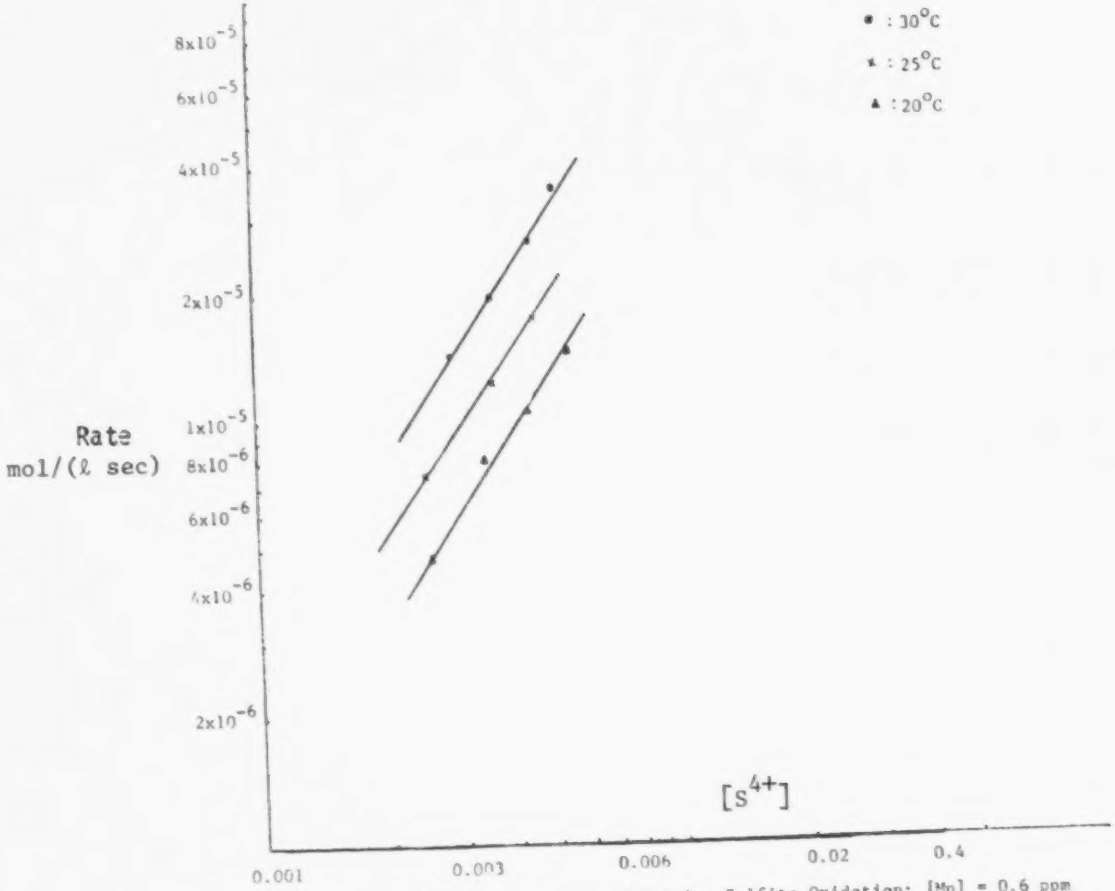

Figure 3-2. Rate of Calcium Sulfite Oxidation; [Mn] = 0.6 ppm

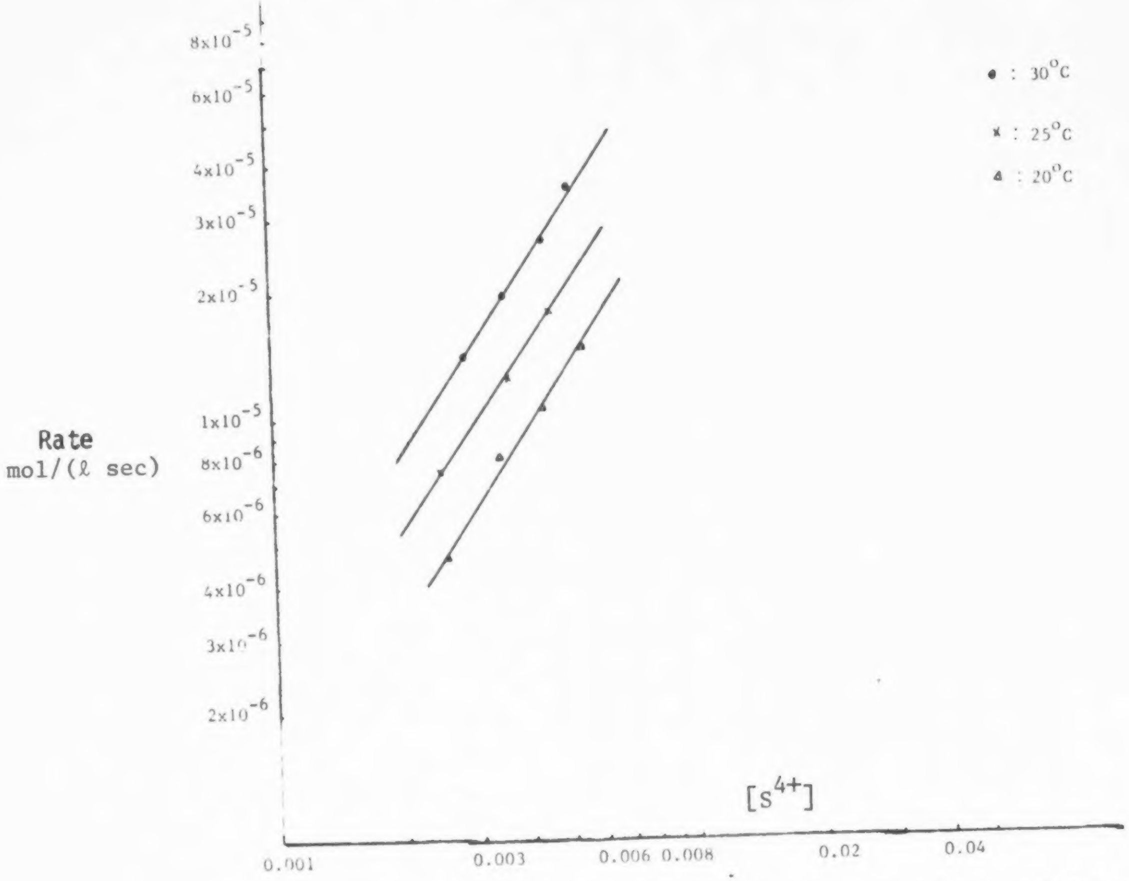

Figure 3-3. Rate of Calcium Sulfite Oxidation; [Mn] = 0.53 ppm, [Fe] = 1.02 ppm

TABLE 3-4 RATE OF CALCIUM SULFITE OXIDATION; VARIABLE [Mn]

Run No.	Initial S^{4+} Concn.	Rate mol/(ℓ sec)	Added Mn	Total Mn	Total Fe	Order for S^{4+}	Standard error of Order	Rate Constant (for 1.5 Order)
166	0.002507	$5.8112\text{x}10^{-6}$	5	5	$[Fe] = [S^{4+}] \text{ x } 55.8 \text{ ppm/mol } S^{4+}$	1.49	0.028	0.0454
165	0.003209	$8.4172\text{x}10^{-6}$	5	5		1.49	0.028	0.0454
163	0.003808	$1.0557\text{x}10^{-5}$	5	5		1.49	0.028	0.0454
164	0.005692	$1.9732\text{x}10^{-5}$	5	5		1.49	0.028	0.0454
169	0.002623	$4.2683\text{x}10^{-6}$	3	3		1.42	0.034	0.0301
167	0.003703	$6.9873\text{x}10^{-6}$	3	3		1.42	0.034	0.0301
168	0.005374	$1.2189\text{x}10^{-5}$	3	3		1.42	0.034	0.0301
170	0.006392	$1.4892\text{x}10^{-5}$	3	3		1.42	0.034	0.0301
173	0.002282	$9.2781\text{x}10^{-6}$	10	10		1.40	0.050	0.0812
171	0.003903	$2.0372\text{x}10^{-5}$	10	10		1.40	0.050	0.0812
172	0.005463	$3.1309\text{x}10^{-5}$	10	10		1.40	0.050	0.0812

No Added Fe

Temperature 20°C

pH = 4.60

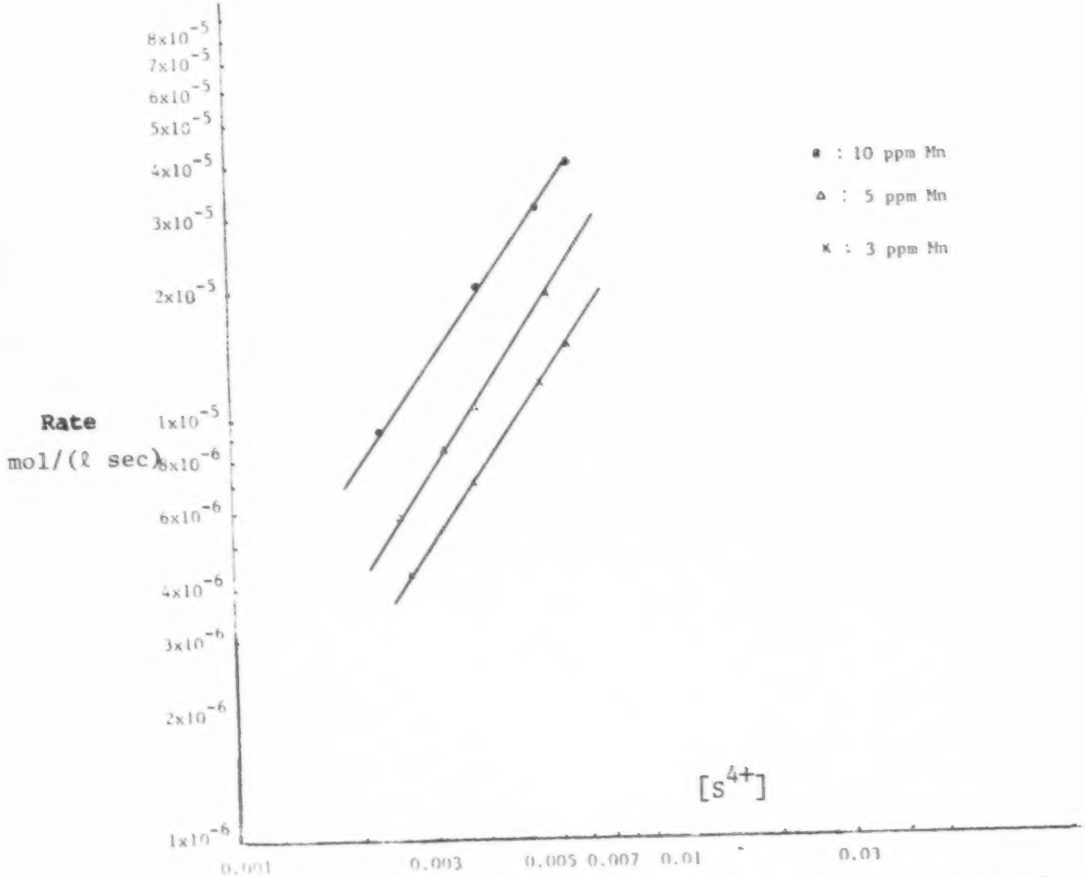

Figure 3-4. Rate of Calcium Sulfite Oxidation; Variable [Mn]

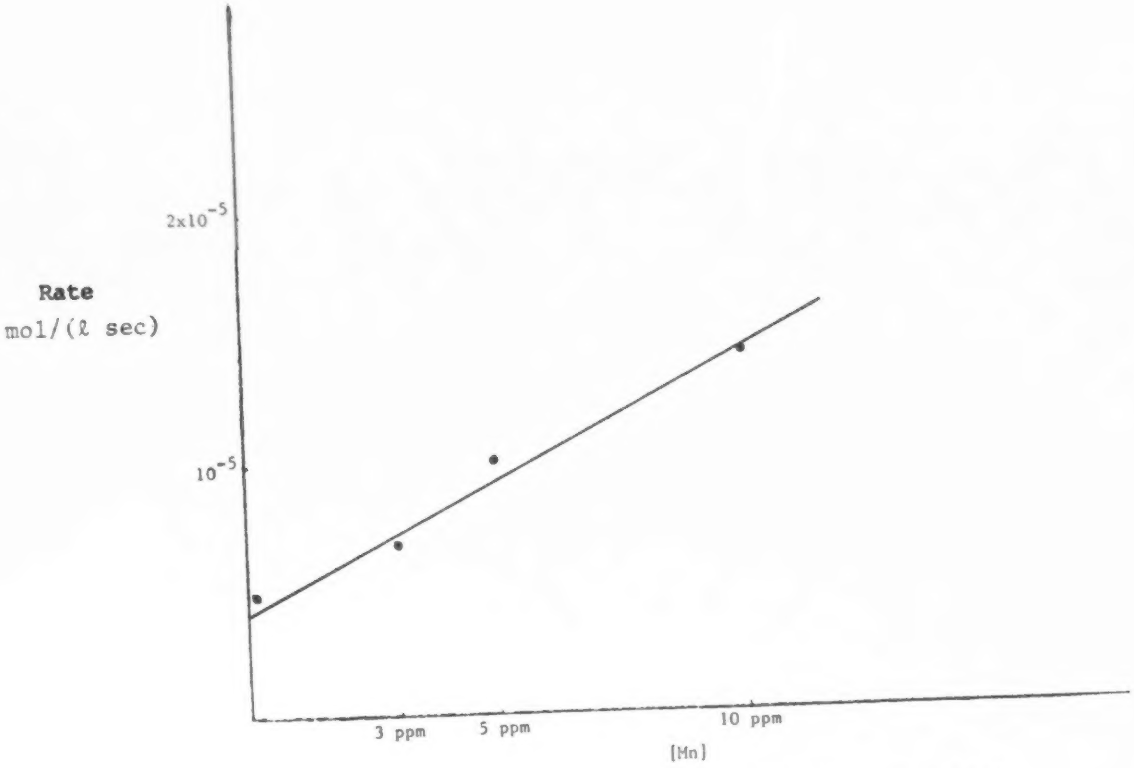

Figure 3-5. Rate of Calcium Sulfite Oxidation; Variable [Mn], $[S^{4+}]$ = 0.0037 Mol/l

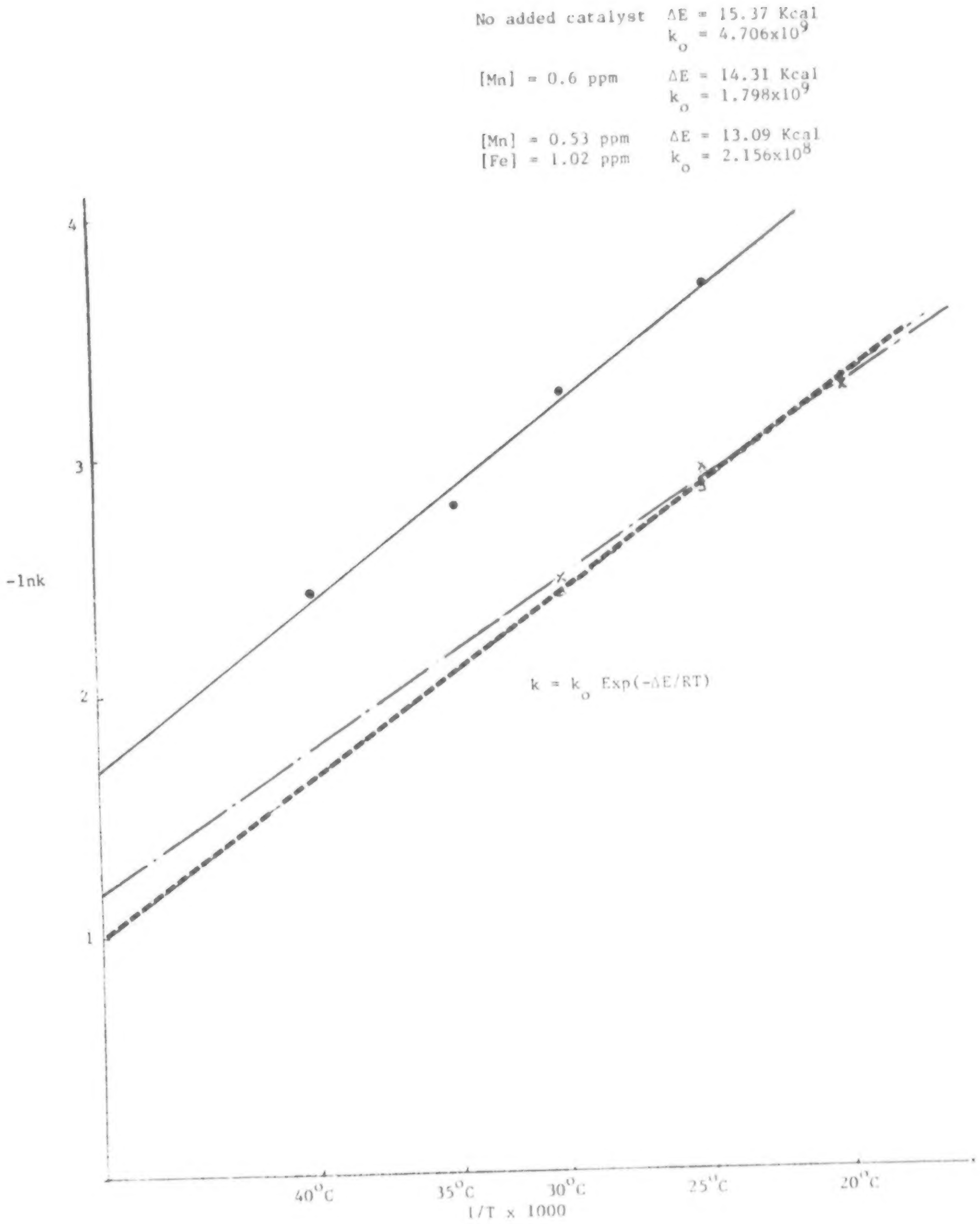

Figure 3-6. Effect of Temperature on the Rate Constant

TABLE 3-5. EFFECT OF TEMPERATURE ON THE RATE CONSTANT

Temperature (^{o}C)	Rate Constant, $k_{1.5}$	Rate of Reaction $[S^{4+}] = 0.01M$ mol/(ℓ sec)
(No Added Catalyst)		
20	0.0161	$1.6\text{x}10^{-5}$
30	0.0385	$3.9\text{x}10^{-5}$
40	0.0871	$8.7\text{x}10^{-5}$
50	0.1871	$1.87\text{x}10^{-4}$
60	0.3841	$3.84\text{x}10^{-4}$
70	0.7560	$7.56\text{x}10^{-4}$
80	1.4321	$1.43\text{x}10^{-3}$
(With Total 0.53 ppm Mn & 1.02 ppm Fe)		
20	0.03707	$3.7\text{x}10^{-5}$
30	0.07785	$7.8\text{x}10^{-5}$
40	0.1559	$1.56\text{x}10^{-4}$
50	0.2992	$2.99\text{x}10^{-4}$
60	0.5520	$5.52\text{x}10^{-4}$
70	0.9827	$9.83\text{x}10^{-4}$
80	1.6933	$1.69\text{x}10^{-3}$

1. Succinic Acid

a. Effect of pH on the Reaction Rate

Experiments were carried out on the oxidation of calcium sulfite at a temperature of 50°C in the presence of 0.2 M succinic acid. Concentration of S^{4+} was determined as a function of time by titration as described earlier. The reaction was studied over a range of pH from 4.0 to 5.5. The pH was constant to within 0.1 pH units over the course of the experiment due to the succinic acid buffer. No other pH control was required. Experiments could not be carried out by this method below pH = 4.0 because of stripping SO_2 and above 5.5, under these conditions, because of the high speed of the reaction. (Measurements at both higher and lower pH can be done in the flow reactor described earlier in this report.) In the semi-batch reactor, about 9% of the S^{4+} is vented as SO_2 in 30 minutes at a pH of 4.0 and about 60% at a pH of 3.0. Corrections to the data for SO_2 loss can be made; however, since the correction is so large at lower pH, results for pH less than 4.0 are not reported.

The results of the experiments are given in Table 3-6. Runs were made with an initial S^{4+} concentration of 0.01 M for $4.0 \leq pH \leq 5.0$. At pH = 5.5 the initial S^{4+} concentration was reduced to 0.005 M to insure complete dissolution. To compare pH = 5.0 and 5.5 experiments were also carried out at pH = 5.0, $(S^{4+})_0$ = 0.005 M, and 0.0075 M. Care must be taken in interpreting results of this type since there are impurities in the $CaSO_3$ and these impurities are the catalyst for the oxidation reaction. The catalyst strength is listed in columns 3 and 4. No catalyst was added to these solutions in addition to that already present in the $CaSO_3$. The order with respect to S^{4+} and the rate constant for that order are shown in columns 5 and 7 respectively. Within the accuracy of the results, these reactions are all 1.5

TABLE 3-6

EFFECT OF pH ON SUCCINIC ACID BUFFERED $CaSO_3$ SOLUTIONS

Initial pH	Initial S^{4+} Concentration mol/ℓ	Mn Impurity Concentration (ppm)	Fe Impurity Concentration (ppm)	Order With Respect to S^{4+}	Standard Deviation on Order	Rate Constant (k)	1.5 Order Rate Constant ($k_{1.5}$)	Run Numbers
4.0	0.01	0.14	0.56	1.35	0.10	0.0040	0.0096	566, 567
4.3	0.01	0.14	0.56	1.59	0.89	0.012	0.0074	510, 512
4.6	0.01	0.14	0.56	1.52	0.32	0.015	0.014	506, 507
4.8	0.01	0.14	0.56	1.63	0.11	0.037	0.019	511, 513
5.0	0.01	0.14	0.56	1.64	0.12	0.082	0.037	502, 514, 587, 588 3.2
5.0	0.0075	0.105	0.42	1.92	0.36	0.010	0.016	517, 518
5.0	0.005	0.07	0.28	1.25	0.12	0.0034	0.015	515, 516
5.5	0.005	0.07	0.28	1.64	0.25	0.28	0.109	520, 522

All runs were done at 50°C

1. Succinic Acid

a. Effect of pH on the Reaction Rate

Experiments were carried out on the oxidation of calcium sulfite at a temperature of 50°C in the presence of 0.2 M succinic acid. Concentration of S^{4+} was determined as a function of time by titration as described earlier. The reaction was studied over a range of pH from 4.0 to 5.5. The pH was constant to within 0.1 pH units over the course of the experiment due to the succinic acid buffer. No other pH control was required. Experiments could not be carried out by this method below pH = 4.0 because of stripping SO_2 and above 5.5, under these conditions, because of the high speed of the reaction. (Measurements at both higher and lower pH can be done in the flow reactor described earlier in this report.) In the semi-batch reactor, about 9% of the S^{4+} is vented as SO_2 in 30 minutes at a pH of 4.0 and about 60% at a pH of 3.0. Corrections to the data for SO_2 loss can be made; however, since the correction is so large at lower pH, results for pH less than 4.0 are not reported.

The results of the experiments are given in Table 3-6. Runs were made with an initial S^{4+} concentration of 0.01 M for $4.0 \leq pH \leq 5.0$. At pH = 5.5 the initial S^{4+} concentration was reduced to 0.005 M to insure complete dissolution. To compare pH = 5.0 and 5.5 experiments were also carried out at pH = 5.0, $(S^{4+})_0$ = 0.005 M, and 0.0075 M. Care must be taken in interpreting results of this type since there are impurities in the $CaSO_3$ and these impurities are the catalyst for the oxidation reaction. The catalyst strength is listed in columns 3 and 4. No catalyst was added to these solutions in addition to that already present in the $CaSO_3$. The order with respect to S^{4+} and the rate constant for that order are shown in columns 5 and 7 respectively. Within the accuracy of the results, these reactions are all 1.5

order and the rate constant for a 1.5 order reaction is shown in column 8 and graphed in Figure 3-7. The units of $k_{1.5}$ are $\ell^{0.5}\mathrm{mol}^{-0.5}\mathrm{sec}^{1}$. It can be clearly seen from Figure 3-7 that the rate of reaction increases with increasing pH with the rate increasing more rapidly above pH - 5.0. The catalyst concentration also proves to have a substantial effect.

It has been proposed by several investigators that only the sulfite ion reacts in solution. Although no conclusions on species reactivity can be drawn from this data, the results are consistent with the concept since the concentration of sulfite ion increases with pH at constant total S^{4+} concentration over the range of pH studied.

b. Effect of succinic acid concentration

The rate of oxidation was studied over a range of succinic acid concentrations from 0 to 2.0 M (23,600 ppm) at pH 4.0 and from 0.01 M to 0.2 M at pH 5.0. At pH 5.0 lower acid concentrations could not be used since the reaction rate would become too large. The reaction must proceed slowly enough so that a sufficient number of samples could be taken and the pH held approximately constant over the course of a run. At succinic acid concentrations of 0.1 M and higher, there was sufficient buffer to hold the pH constant at 4.0 without outside means; at lower concentrations a pH controller was used. The catalyst levels were constant in all cases since the initial sulfite concentration was 0.01M for all experiments. All experiments were performed at 50°C.

Typical results are shown in Figures 3-8 and 3-9 for pH 4.0 and in Figure 3-10 for pH 5.0 with varying amounts of succinic acid. From these measurements of $[S^{4+}]$ vs time, an initial reaction rate and also a rate expression were determined. The latter was obtained by the best fit of the data through the expression $r = kc^{\alpha}$. Here C is the S^{4+} concentration. The initial rate is

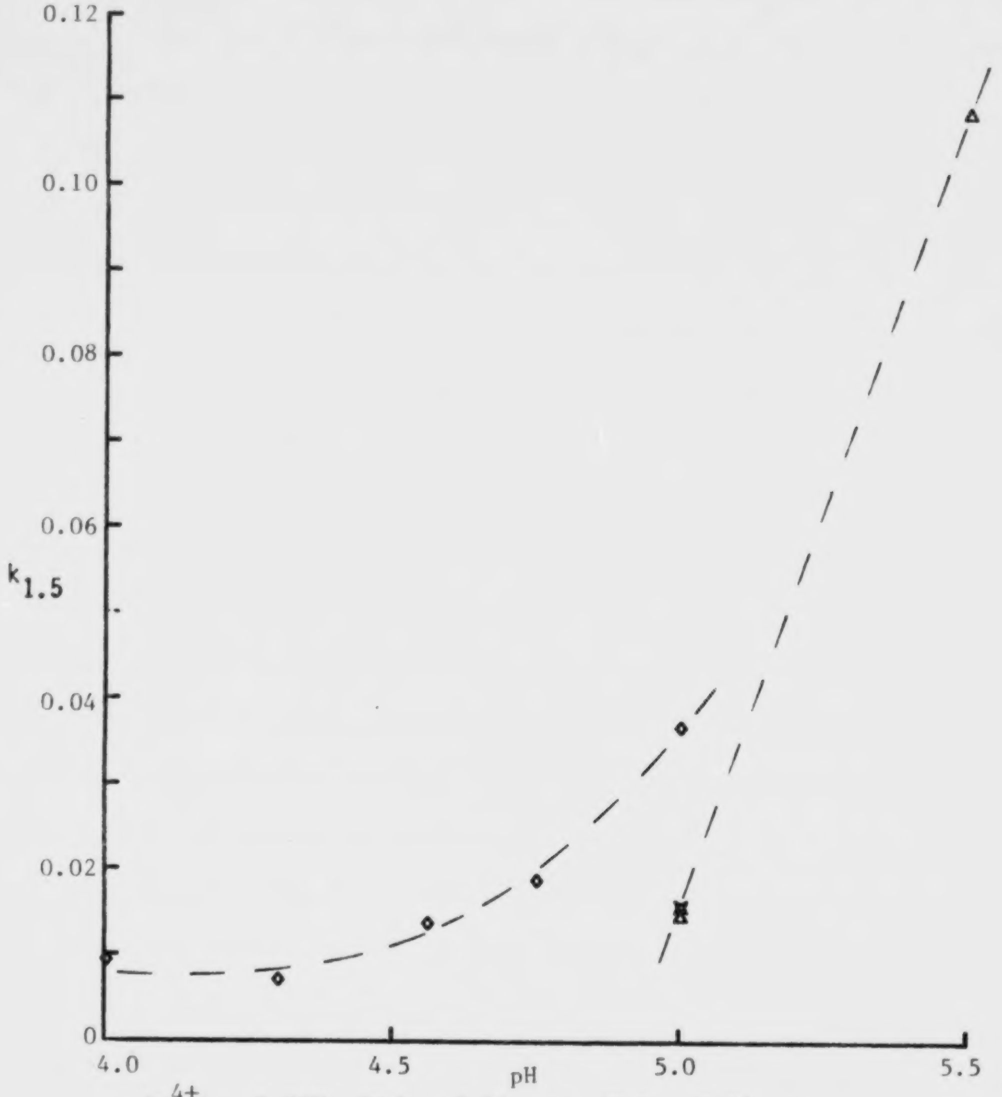

$(S^{4+})_o = 0.01M$; (Mn) = 0.14 ppm; (Fe) = 0.56 ppm

$(S^{4+})_o = 0.0075$ M; (Mn) = 0.105 ppm; (Fe) = 0.40 ppm

$(S^{4+})_o = 0.005$ M; (Mn) = 0.07; (Fe) = 0.28 ppm

T = 50°C

Figure 3-7. Effect of pH on Rate of Reaction

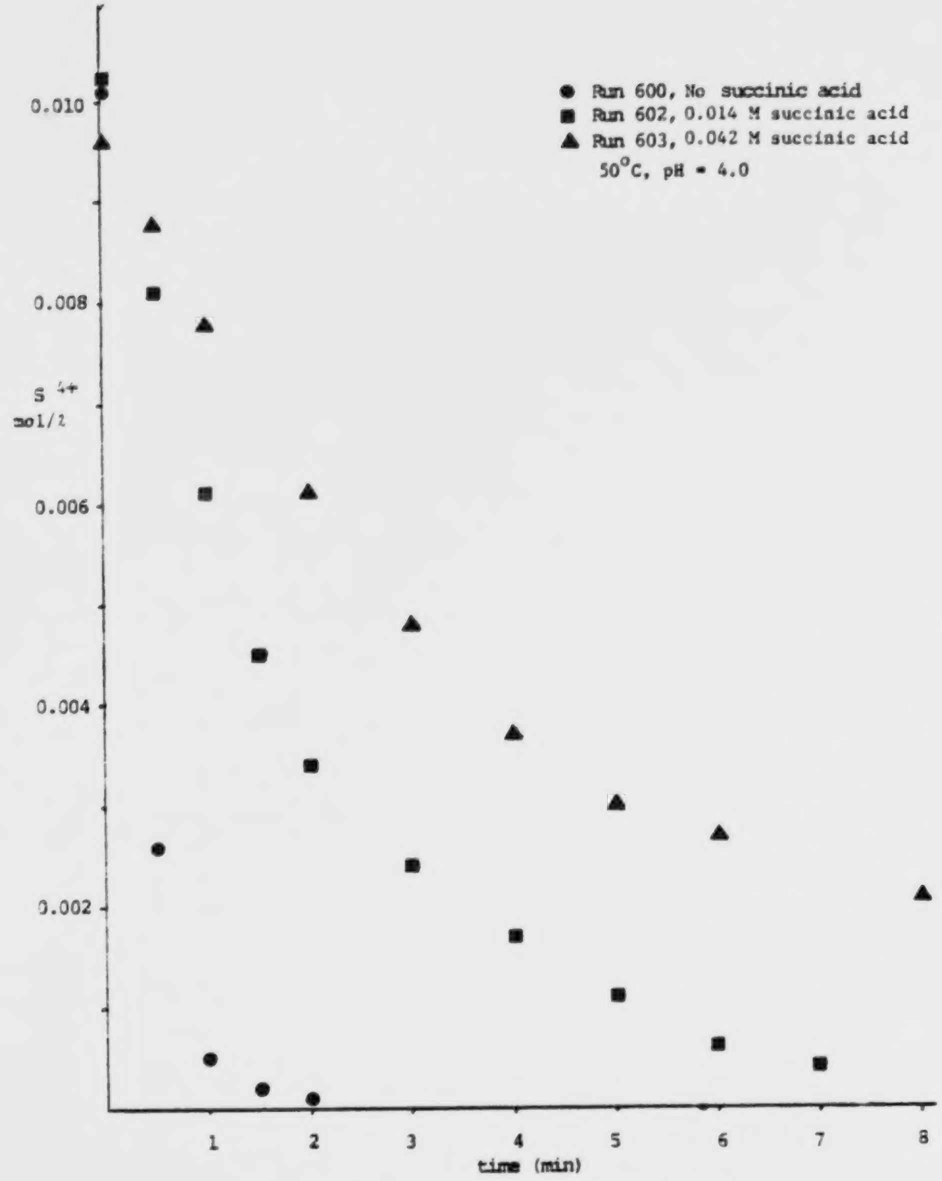

Figure 3-8. Concentration Sulfur (4+) vs Time for Various Concentrations of Succinic Acid

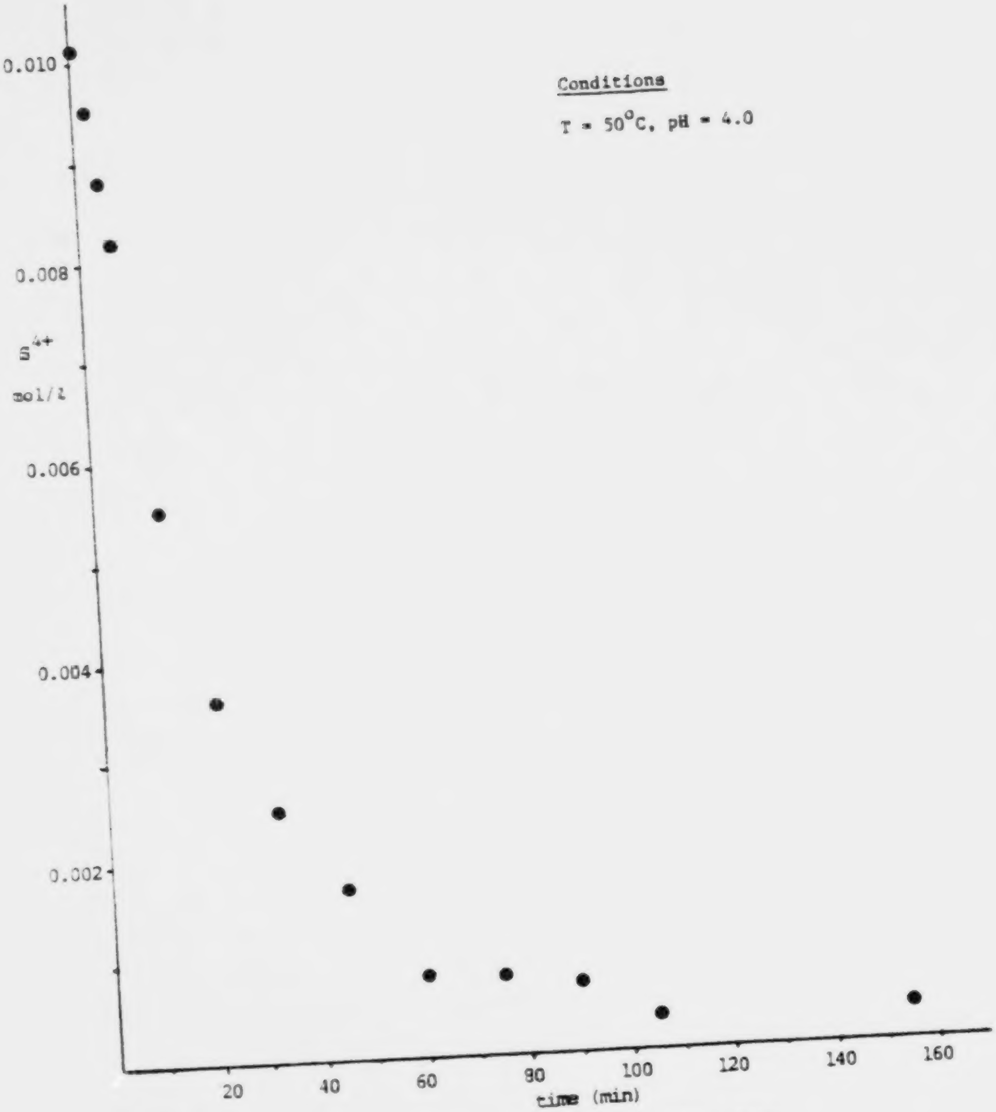

Figure 3-9. Concentration Sulfur (4+) vs Time
Run 566, 0.2M Succinic Acid

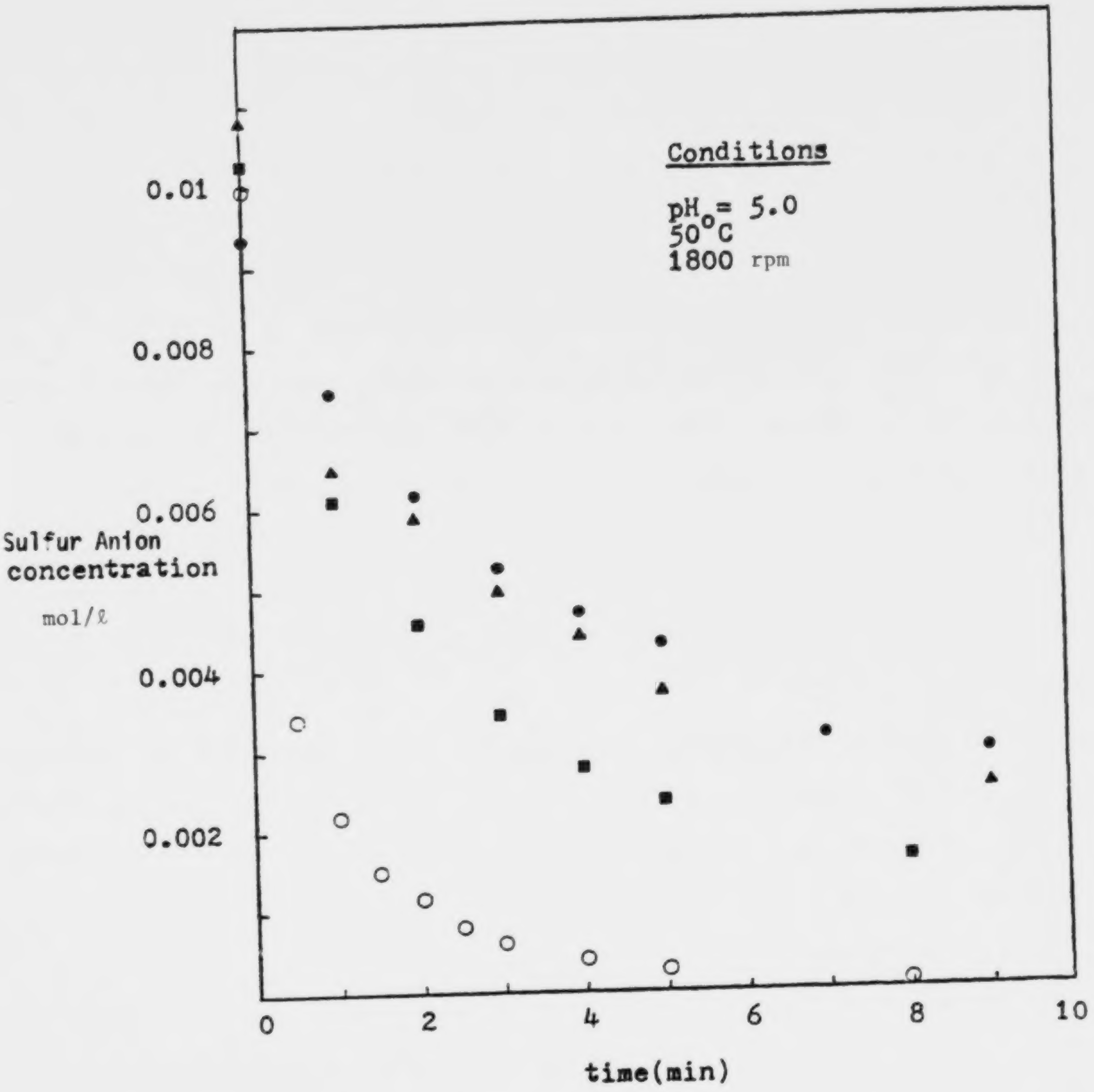

symbol	run #	composition
●	3.2	0.2 M succinic acid
▲	24.2	0.1 M succinic acid
■	25.2	0.05M succinic acid
○	26,2	0.01M succinic acid

Figure 3-10. The Inhibition of the Sulfite Oxidation Due To Succinic Acid.

shown as a function of succinic acid concentration in Figure 3-11 for pH 4.0. The strong influence of the organic acid is shown.

Summaries of the results may be found in Tables 3-7 and 3-8 for pH 4.0 and 5.0 respectively. The results without succinic acid at pH 4.0 were obtained from only 3 or 4 titration points per run and are, therefore, somewhat less reliable. It might be noted that the rate of reaction given in Table 3-7 for no organic acid and pH 4.0 is somewhat higher than that reported in Section IIA for pH 4.6. Since the rate always increases with increasing pH, under these conditions when all other parameters are held constant, the higher rate is probably caused by the higher catalyst levels present at an initial S^{4+} concentration of 0.01 M compared to the lower levels of catalyst in Section IIA. The effects of catalysts are discussed elsewhere in the report.

The order of the reaction increases with increasing pH for the ranges being studied. At pH 4.0 and low succinic acid concentrations, the reaction can be adequately described by a first order expression; however, with increasing levels of acid, the order rises above 1.0.

2. Adipic Acid

The effect of adipic acid on the rate of oxidation of calcium sulfite was studied at $T = 50^{\circ}C$ and pH = 5.0. Typical results are presented in Figure 3-12 as concentration vs time for various adipic acid concentrations. The results are summarized in Table 3-9. The reaction order is approximately 1.5 at low adipic acid concentration and rises with increasing acid concentration. All experiments were carried out with an initial S^{4+} concentration of 0.01 M.

3. Glycolic Acid

The effect of glycolic acid on the rate of oxidation was studied at $T = 50^{\circ}C$ and pH = 4.0 and pH = 5.0. Representative results are presented in

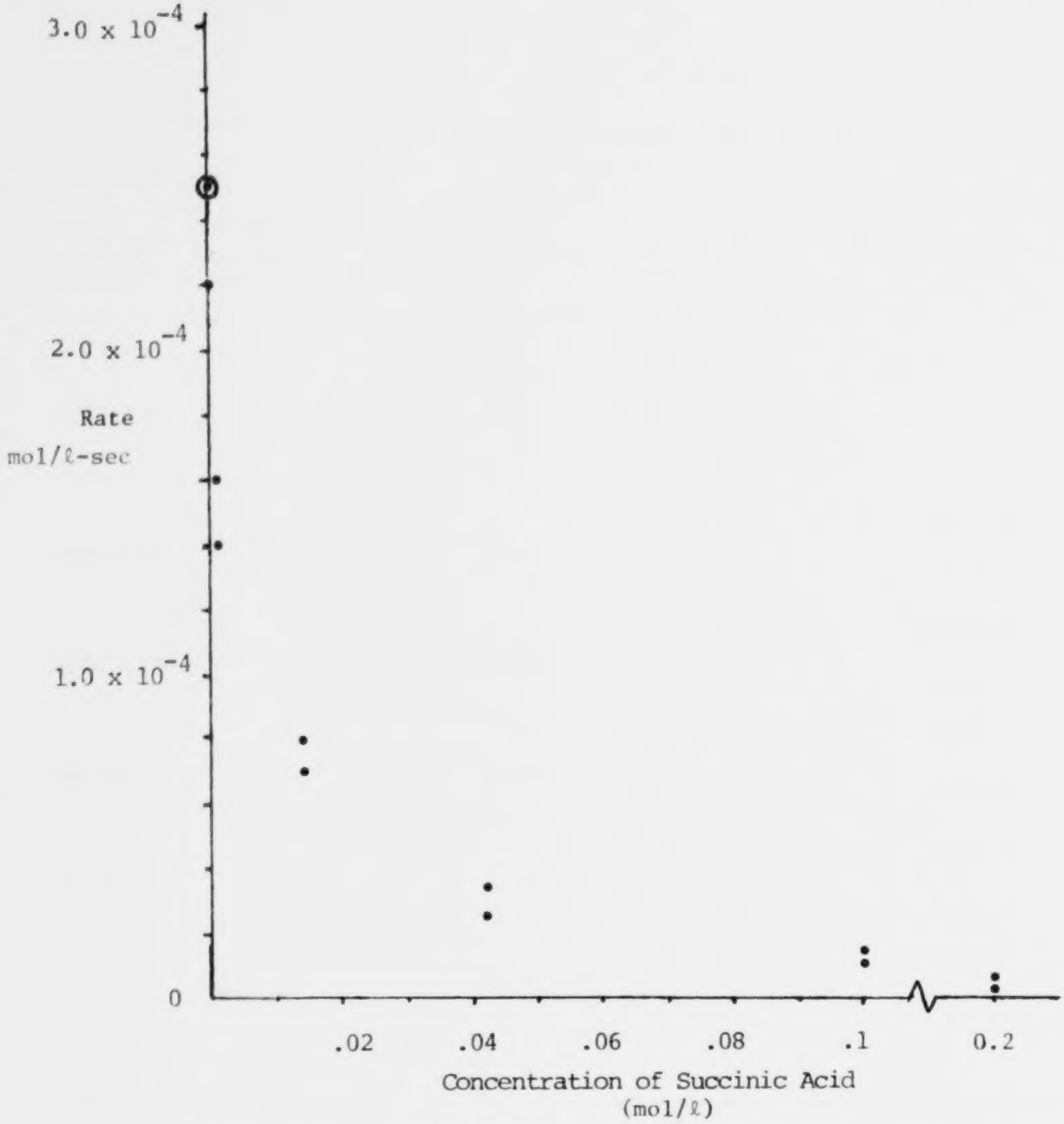

Figure 3-11. Initial Rate vs Succinic Acid Condentration

(All runs were at 50°C and an initial pH of 4.0)

TABLE 3-7

EFFECT OF SUCCINIC ACID ON OXIDATION RATE

Run #	Succinic Acid Concentration mol/ℓ	Initial Rate mol/(ℓ sec)	Order With Respect to Sulfur (4+)	Standard Deviation of Order	Rate Constant
598	0	2.45×10^{-4}	1.21	0.07	0.13613
599	0	2.21×10^{-4}			
600	0	2.49×10^{-4}			
605	0.00141	1.58×10^{-4}	0.94	0.08	0.01885
606	0.00141	1.44×10^{-4}			
601	0.01355	7.99×10^{-5}	1.19	0.08	0.02339
602	0.01355	7.02×10^{-5}			
603	0.04234	2.64×10^{-5}	1.34	0.11	0.02088
604	0.04234	3.31×10^{-5}			
585*	0.10021	1.07×10^{-5}	1.33	0.16	0.00757
586*	0.10021	1.56×10^{-5}			
566*	0.20000	3.30×10^{-6}	1.35	.10	.00397
567*	0.20000	5.40×10^{-6}			

All runs were done at 50°C and an initial pH of 4.0. The * indicates that in these runs there was sufficient succinic acid present to buffer the experiment; thus the computer was not used. (To convert mol/ℓ of succinic acid to ppm multiply by 118090.)

TABLE 3-8

RESULTS OF ORDER AND RATE DETERMINATION ANALYSIS OF DATA FOR CALCIUM SULFITE OXIDATIONS WITH VARYING CONCENTRATIONS OF SUCCINIC ACID ADDED

Concentration of succinic acid added (mol/ℓ)	Order of reaction with respect to sulfite	Standard Deviation	Rate constant Rate (=) mol/sec
0.2	1.64	0.12	0.08230
0.1	1.84	0.12	0.245
0.05	1.82	0.15	0.350
0.01	1.45	0.06	0.231

Conditions:

pH = 5.0

50°C

1800 rpm

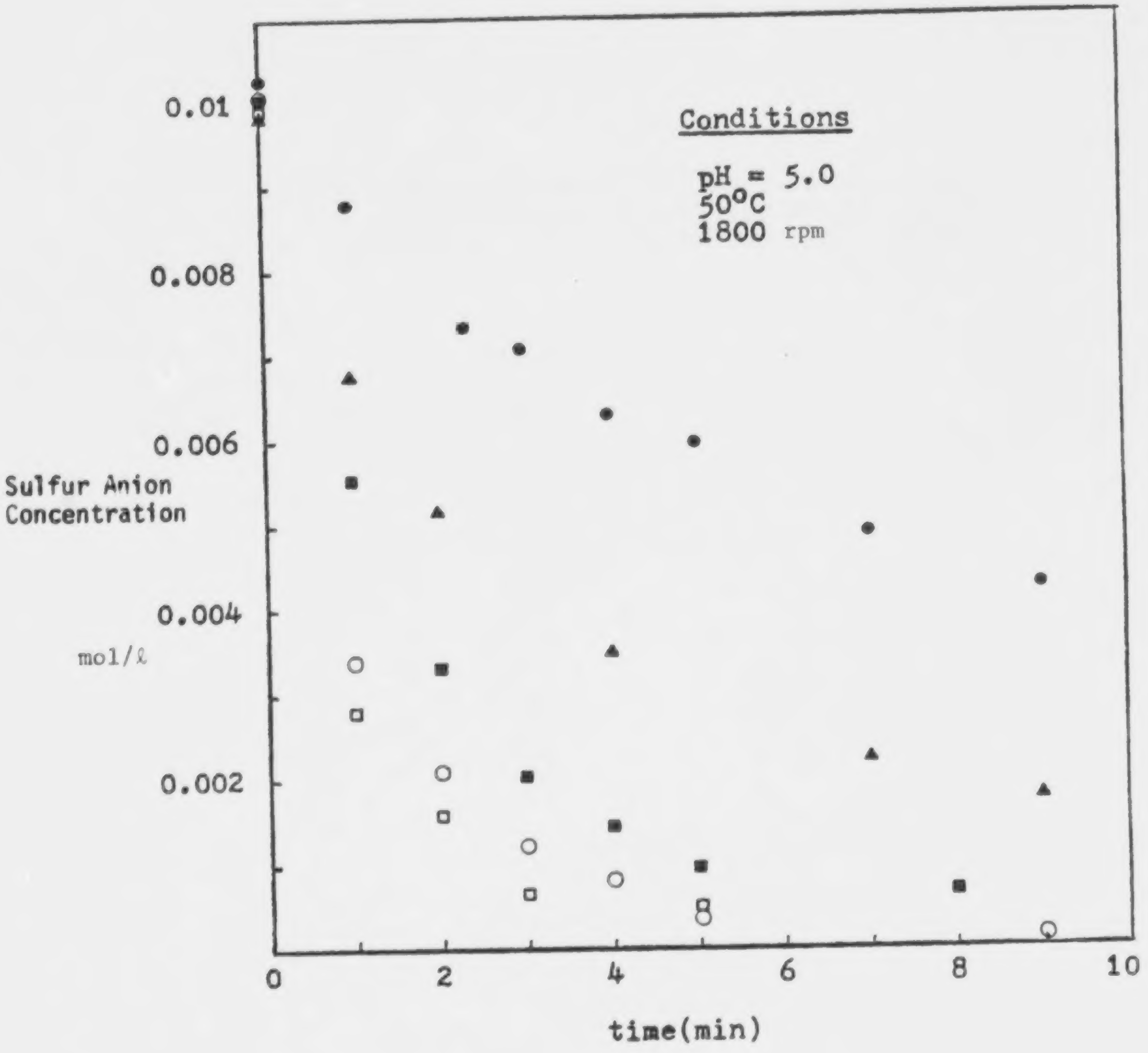

symbol	**run #**	**composition**
●	11.2	0.2 M adipic acid
▲	12.2	0.1 M adipic acid
■	27.2	0.05 M adipic acid
○	34.2	0.01 M adipic acid
□	33.2	0.005M adipic acid

Figure 3-12. The Inhibition of the Sulfite Oxidation Due To Adipic Acid.

TABLE 3-9

RESULTS OF ORDER AND RATE DETERMINATION ANALYSIS OF DATA FOR CALCIUM SULFITE OXIDATIONS WITH VARYING CONCENTRATIONS OF ADIPIC ACID (72)

Concentration of adipic acid (mol/ℓ)	Order of reaction with respect to sulfite	Standard Deviation	Rate Constant Rate = mol/sec
0.2	1.94	0.21	0.218
0.1	1.84	0.12	0.314
0.05	1.49	0.07	0.109
0.01	1.42	0.09	0.193
0.005	1.53	0.10	0.279

Conditions:

pH = 5.0

50°C

1800 rpm

Figures 3-13, 3-14, and 3-15; summaries of the results are presented in Tables 3-10 and 3-11 for pH = 4.0 and 5.0 respectively. The rate of reaction at $[S^{4+}] = 0.01$ M as calculated from the rate expression is shown in Figure 3-16 for pH 4.0 as a function of glycolic acid concentration.

Glycolic acid is a very strong inhibitor for the oxidation, much stronger than any of the other acids studied. At pH = 4.0 and no organic acid, the oxidation was completed in about one and one-half to two minutes. With an addition of 1000 ppm glycolic acid the experiment takes up to an hour or more. With a concentration of 0.2 M glycolic acid, 50% of the sulfur (4+) had not oxidized in four hours.

4. Comparison of Rates of Oxidation with Succinic Acid, Adipic Acid, Glycolic Acid, Citric Acid, and Acetic Acid

In Figures 3-17 and 3-18 a comparison is made between the succinic, adipic and glycolic acids to demonstrate which has the greatest inhibitory effect. In Figure 3-17 an acid concentration of 0.2 M was added in each run. As can be seen, glycolic acid is the greatest inhibitor followed by adipic acid then by succinic acid. In Figure 3-18 an acid concentration of 0.01 M was added. Here again the same trend of inhibitory strength (glycolic > adipic > succinic) is observed. This same information can be obtained by noting the rate constants and rate of reaction at $[S^{4+}] = 0.01$ M listed in Tables 3-12.

The structure of the organic acids may be looked at to aid in the understanding of the inhibition. It has been reported by Backstrom that alcohols inhibit the sulfite oxidation. This inhibition is due to the alcohol group reacting with free radicals in the sulfite solution (15). Several organic acids have lone alcohol groups off of the carbon chain, and all organic acids have carboxyl groups that have reactive sites similar to alcohols. The relative inhibitory strength of organic acids can be attributed to this reaction

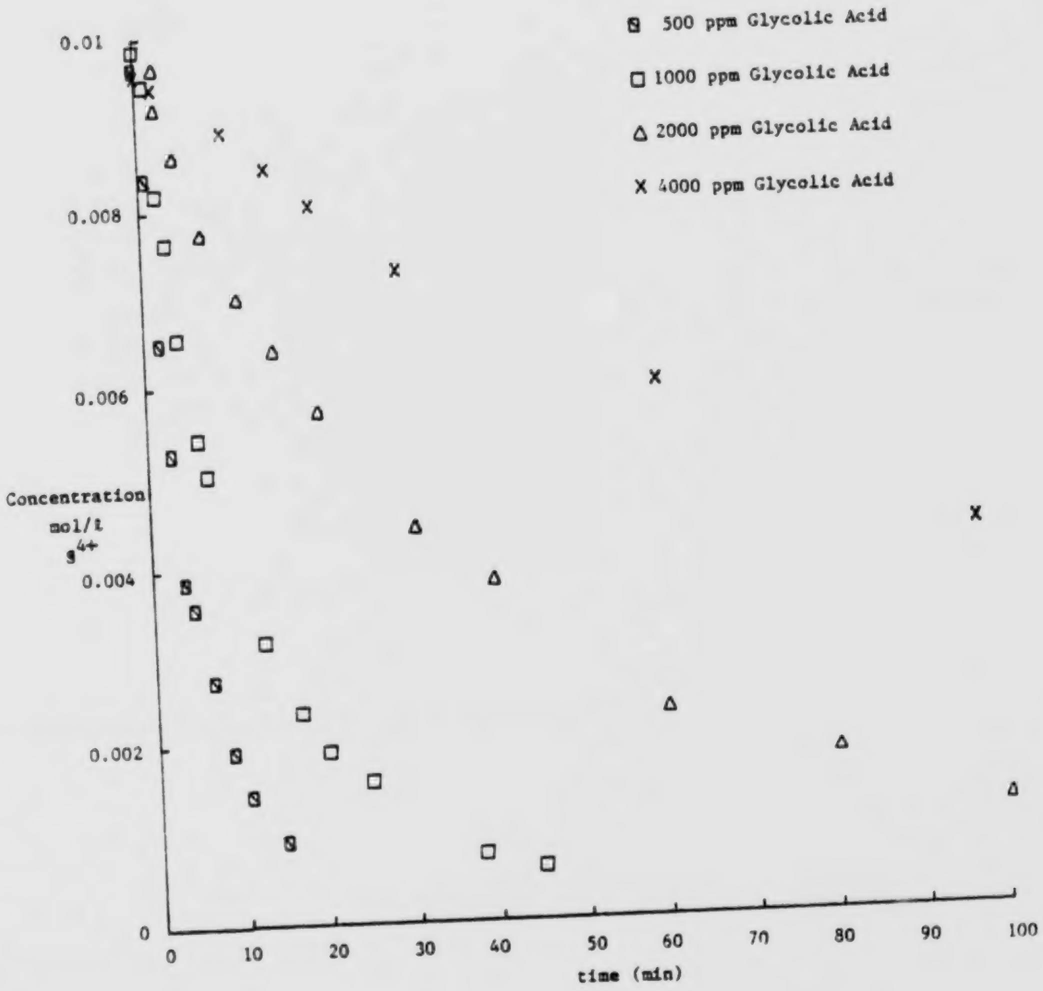

Figure 3-13. Concentration S^{4+} vs Time for Various Concentrations of Glycolic Acid

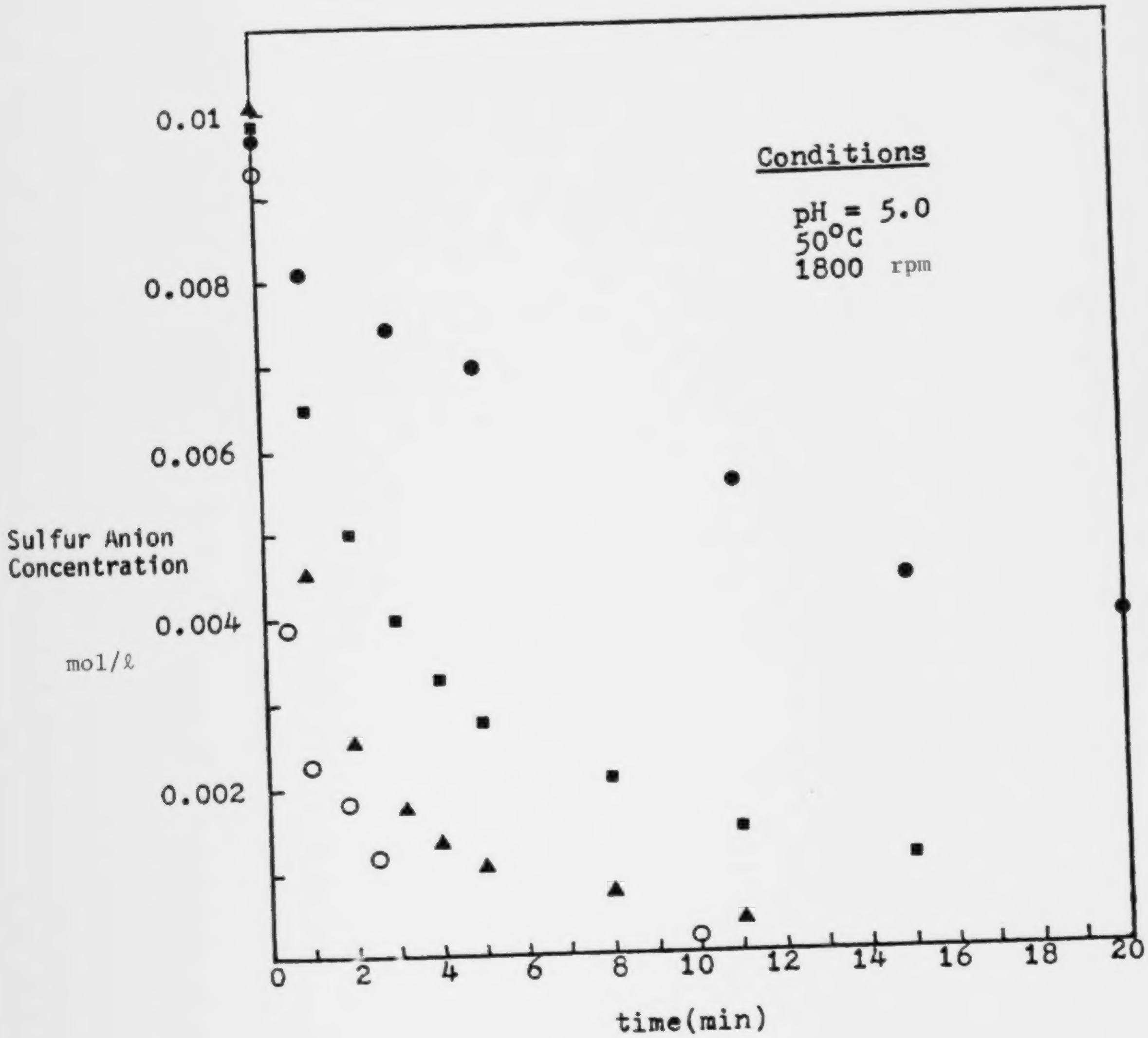

symbol	run #	composition
●	46.2	0.0263 M(2000 ppm) glycolic acid
■	38.2	0.0131 M(1000 ppm) glycolic acid
▲	37.2	0.0066 M(500 ppm) glycolic acid
○	41.2	no glycolic acid

Figure 3-14. Inhibition of the Sulfite Oxidation Due to Glycolic Acid.

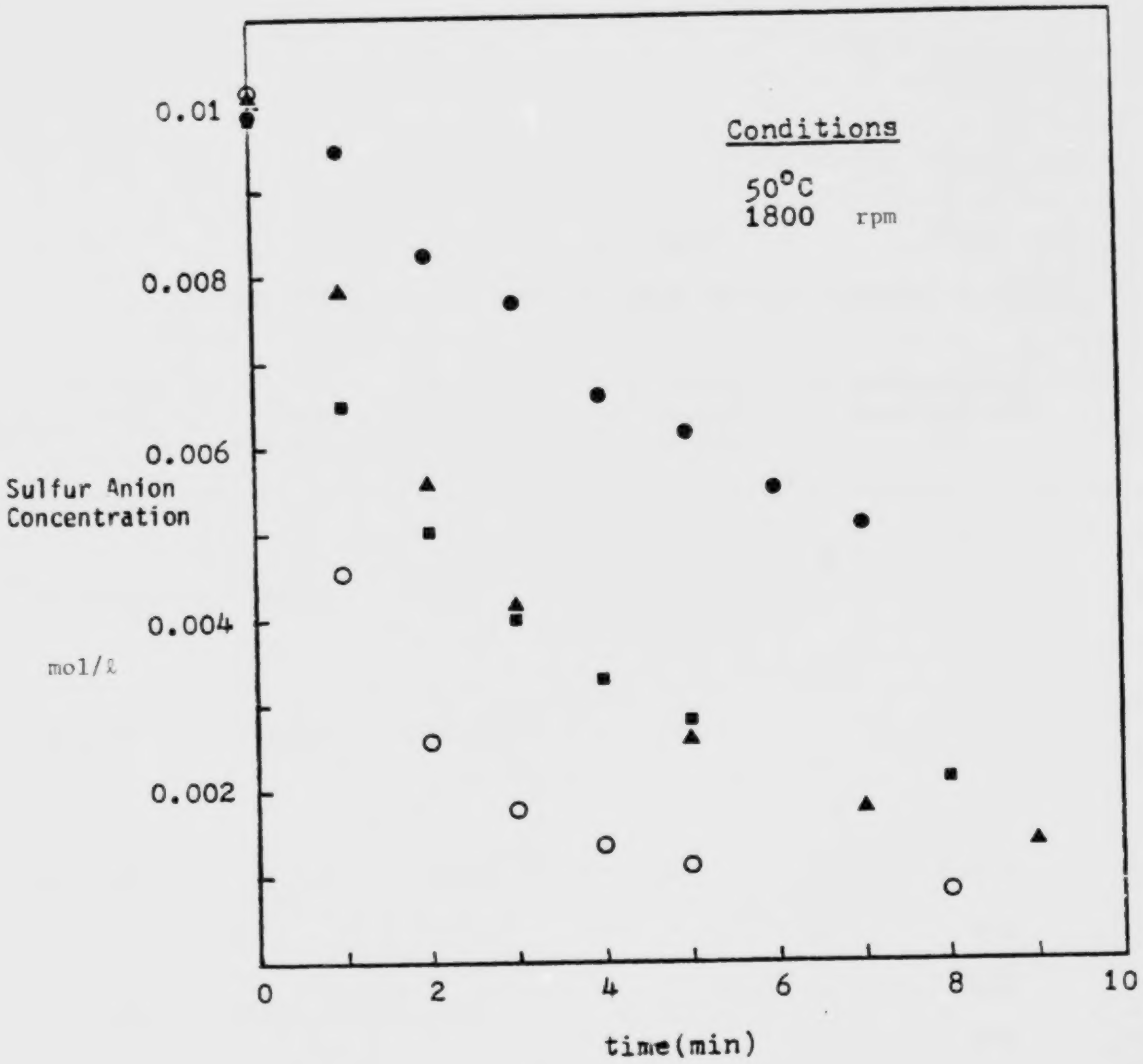

symbol	run #	composition
●	609	0.013 M(1000 ppm) glycolic acid, pH 4.0
■	38.2	0.013 M(1000 ppm) glycolic acid, pH 5.0
▲	617	0.0066 M(500 ppm) glycolic acid, pH 4.0
○	37.2	0.0066 M(500 ppm) glycolic acid, pH 5.0

Figure 3-15. The pH Effect on the Inhibition of the Sulfite Oxidation Due to Glycolic Acid.

TABLE 3-10

EFFECT OF GLYCOLIC ACID ON OXIDATION RATE OF CALCIUM SULFITE

Run#	Concentration of Glycolic Acid ppm	Order With Respect to Sulfur (4+)	Standard Deviation of Order	Rate Constant	Rate at $S^{[4+]}$ = 0.01 mol/sec
598	0	1.21	0.07	0.136	5.18×10^{-4}
599	0				
600	0				
613	500	1.48	0.10	0.046	5.05×10^{-5}
617	500				
609	1000	1.40	0.09	0.0118	1.87×10^{-5}
610	1000				
611	1000				
618	2000	1.37	0.12	0.00336	3.31×10^{-6}
619	2000				
621	4000	0.96	0.44	0.00009	1.08×10^{-6}
622	4000				
623	15200	2.03	0.88	0.0060	5.24×10^{-7}

T = 50°C; pH = 4.0. Initial concentration of sulfur (4+) is 0.01 M.

TABLE 3-11

RESULTS OF ORDER AND RATE DETERMINATION ANALYSIS OF DATA FOR CALCIUM SULFITE OXIDATIONS WITH VARYING CONCENTRATIONS OF GLYCOLIC ACID ADDED (72)

Concentration of glycolic acid added	Order of reaction with respect to sulfite	Standard Deviation	Rate constant Rate = mol/sec
0.0263 M (2000 ppm)	1.72	0.30	0.028
0.0131 M (1000 ppm)	1.83	0.10	0.270
0.0066 M (500 ppm)	1.72	0.08	0.516

Conditions:

pH = 5.0

50°C

1800 rpm

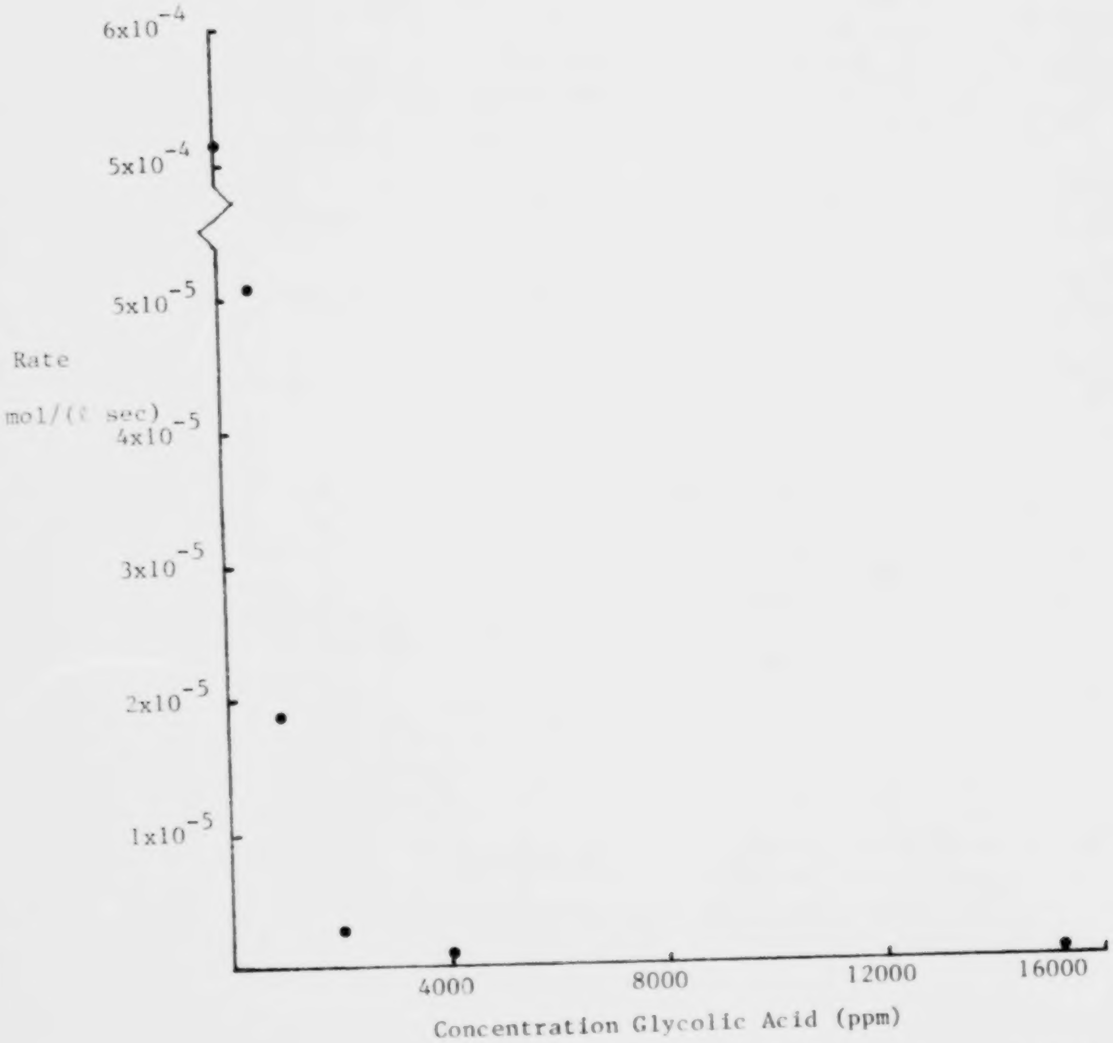

Figure 3-16. Effect of Glycolic Acid on Rate of Oxidation of $CaSO_3$ at Temperature = 50°C, pH = 4.0 $[S^{4+}]$ = 0.01 M.

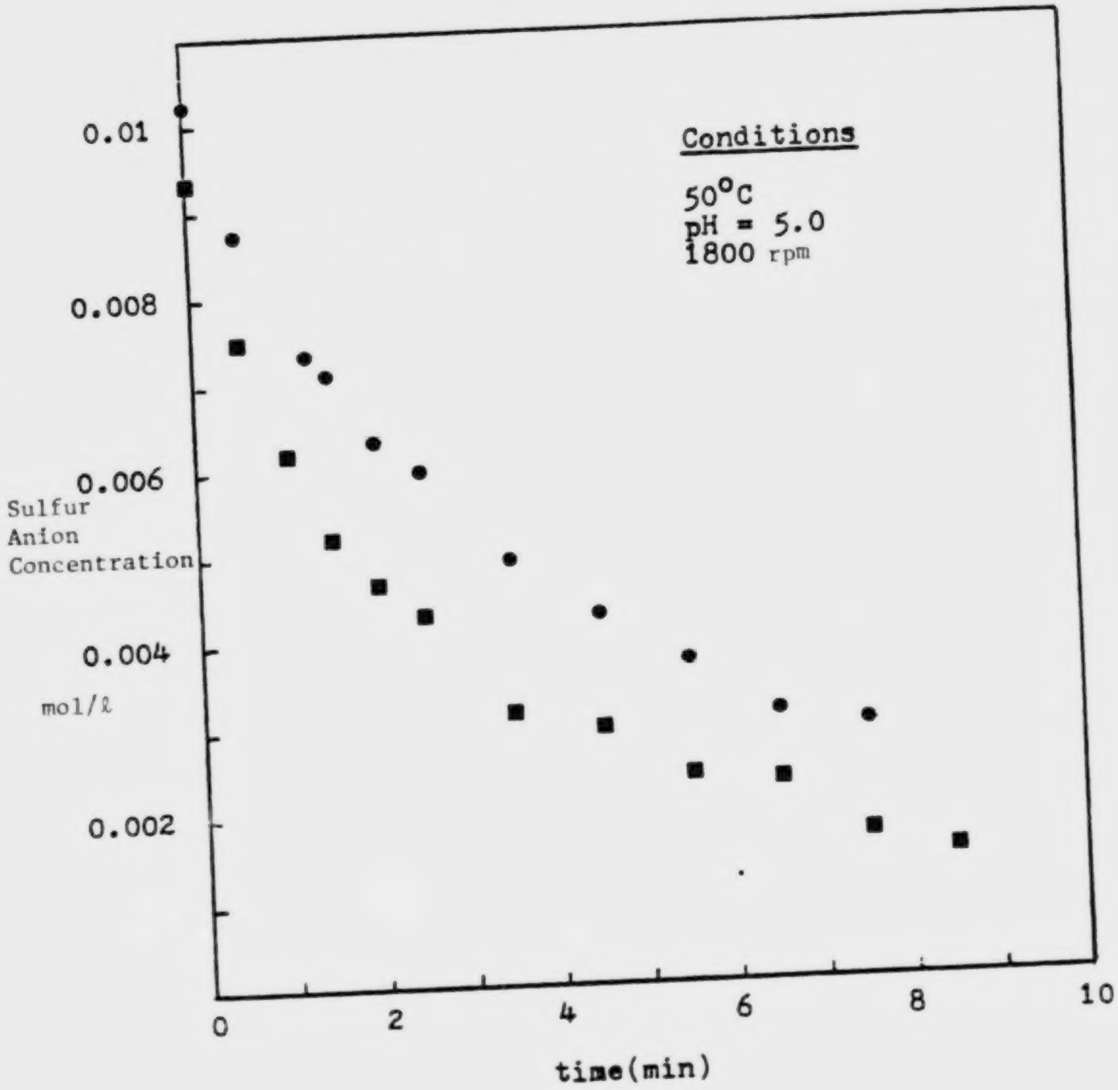

symbol	run #	composition
●	11.2	0.2 M adipic acid
■	3.2	0.2 M succinic acid
negligible reaction in 10 Minutes		0.2 M glycolic acid

Figure 3-17. Comparative Strength of Various Organic Acids as Inhibitors at 0.2 M.

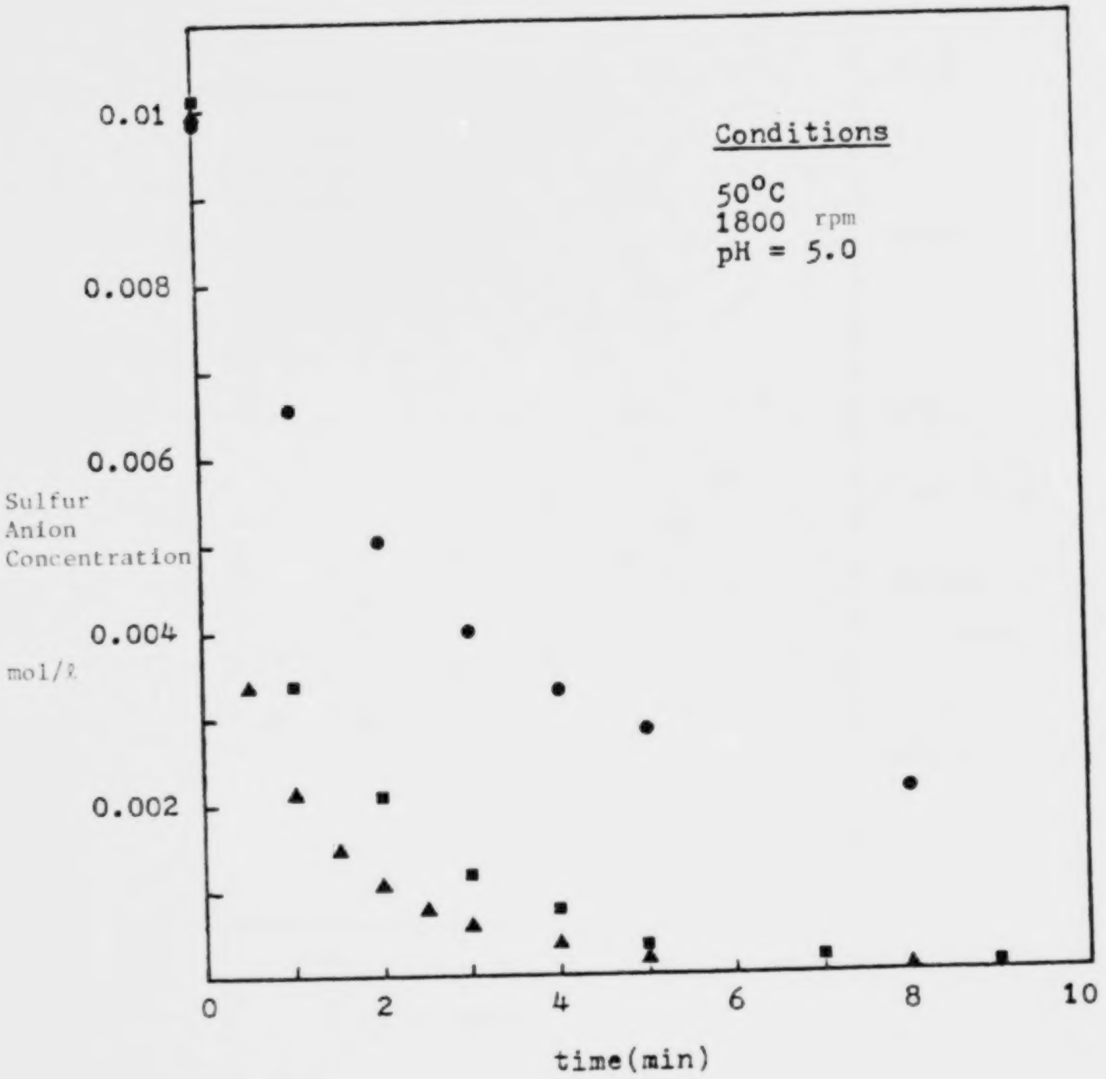

symbol	run #	composition
●	38.2	0.01 M glycolic acid
■	34.2	0.01 M adipic acid
▲	26.2	0.01 M succinic acid

Figure 3-18. Comparative Strength of Various Orgnanic Acids as Inhibitors at 0.01 M.

TABLE 3-12

EFFECT OF ORGANIC ACIDS ON OXIDATION RATE OF CALCIUM SULFITE

Run#	Acid Used	Order With Respect to Sulfur (4+)	Standard Deviation of Order	Rate Constant	Rate at $[S^{4+}] = 0.01M$, mol/sec
502,514,589,588	Succinic	1.64	0.12	0.082	4.3×10^{-5}
552,554,595,596	Adipic	1.94	0.21	0.218	2.87×10^{-5}
562,563,591,592	Citric	2.31	0.15	12.78	30.65×10^{-5}
564,565,593,594	Acetic	2.20	0.20	1.61896	6.4×10^{-5}
623	Glycolic	2.03	0.88	0.0060	5.24×10^{-7}

All runs were done at 50°C and an initial pH of 5.0. All acid concentrations are 0.2 mol/ℓ. (23618 ppm succinic, 29230 ppm adipic, 38426 ppm citric, 12000 ppm acetic, 15210 ppm glycolic.

with free radical type inhibition. Experimental work gives evidence favoring this idea. Acetic acid (CH_3COOH) was added to the reaction mixture in a concentration of 0.2 M; the reaction was completed in just less than a minute. Glycolic acid ($HOCH_2COOH$) was added to the reaction mixture in a concentration of 0.2 M also; the reaction did not proceed in 20 minutes. The difference between glycolic acid and acetic acid is simply an alcohol group (OH^-) in place of a hydrogen on the first carbon. This suggests that the alcohol group of the glycolic acid is reacting with the free radicals needed for the oxidation, thus slowing down the oxidation.

Another organic acid, citric acid, which is slightly more complex than glycolic or acetic acid was added to the reaction mixture in a concentration of 0.2 M. The sulfite oxidation was completed in about 1 minute. Citric acid does have an alcohol group extending from the carbon chain, but it also has three carboxyl groups. One possible explanation suggests that steric hinderance due to these large carboxyl groups prevents the alcohol group from reaction with the radicals and slows down the reaction. Backstrom observed a similar effect with tertiary butyl alcohol, a sterically hindered alcohol (14).

Not only do the lone alcohol groups react with the radicals in solutions, but the OH^- groups of the carboxyl group can react slightly with the radicals. This is shown with adipic and succinic acids since both inhibit the reaction to some extent. With concentrations of 0.2 M in solution the oxidation was 50% completed in four minutes with succinic acid and in five minutes with adipic acid. There is less hindrance between the groups in adipic acid because the carboxyl groups are further apart. This allows slightly more reaction between the radicals and adipic acid than with succinic acid in solution. This result is seen in the fact that adipic acid inhibits slightly more than succinic acid.

Although some inhibition is observed from organic acids without alcohol groups, more is observed from those with alcohol groups. The OH^- group of the carboxyl group does not react as much as the lone OH^- group due to the shielding by the oxygen on the carboxyl group.

5. Effect of Catalysts - Manganese and Iron

a. Succinic acid

Manganese and iron catalyze the oxidation even in the presence of the organic acids which inhibit the reaction. In discussing the effect of catalysts on the oxidation, it is important to consider both the catalysts present in the calcium sulfite as an impurity and also catalysts added to the reaction mixture. Manganese is present as are impurities also in most limestone.

A dry sample of calcium sulfite has impurity levels of 62 ppm manganese and 248 ppm iron. From this, the amount of Mn and Fe present at a given liquid sulfite concentration can be calculated. Table 3-13 shows the iron and manganese impurity levels for some initial $CaSO_3$ concentrations. Knowing the amount of Mn impurity present at 0.01 M $CaSO_3$ (for example) makes it possible to add a known amount of Mn to 0.005 M $CaSO_3$ making the total Mn concentration equal to that of the 0.01 M sulfite solution. In Table 3-14 a comparison between catalyzed and uncatalyzed runs is made. In runs 527 and 528 0.1 ppm Mn was added to bring the Mn level to that of 0.015 M $CaSO_3$. As can be seen the 0.015 M rate constants compare well to the 0.0075 M rate constants with added catalyst, while the 0.0075 M runs without catalyst have rate constants which differ. From a plot of sulfur (4+) concentration vs time (Figure 3-19) it can be seen that the 0.015 M and the catalyzed 0.0075 M have similar rates of oxidation while the 0.0075 uncatalyzed run is noticeably slower. Similar results can be seen in Table 3-9 for 0.005 M and 0.01 M runs.

TABLE 3-13

CATALYST IMPURITY LEVELS IN $CaSO_3$ SOLUTIONS

Initial S^{4+} Concentration (mol/ℓ)	Fe (ppm)	Mn (ppm)
0.005	0.279	0.070
0.0075	0.419	0.105
0.01	0.558	0.140
0.015	0.837	0.209

TABLE 3-14

EFFECT OF Mn IMPURITY ON OXIDATION RATE

Run#	Initial S^{4+} Concentration	Mn Impurity Level (ppm)	Added Mn (ppm)	Total Mn (ppm)	Order With Respect to S^{4+}	Standard Deviation of Order	Rate Constant
517,518	0.0075	0.105	0	0.105	1.42	0.36	0.0101
527,528	0.0075	0.105	0.1	0.205	1.66	0.24	0.251
525,526	0.015	0.209	0	0.209	1.74	0.17	0.346
515,516	0.005	0.070	0	0.07	1.25	0.34	0.0034
529,530	0.005	0.07	0.07	0.140	1.22	0.28	0.0076
502,514	0.01	0.140	0	0.140	1.64	0.12	0.082

Temperature = 50°C; pH = 5.0

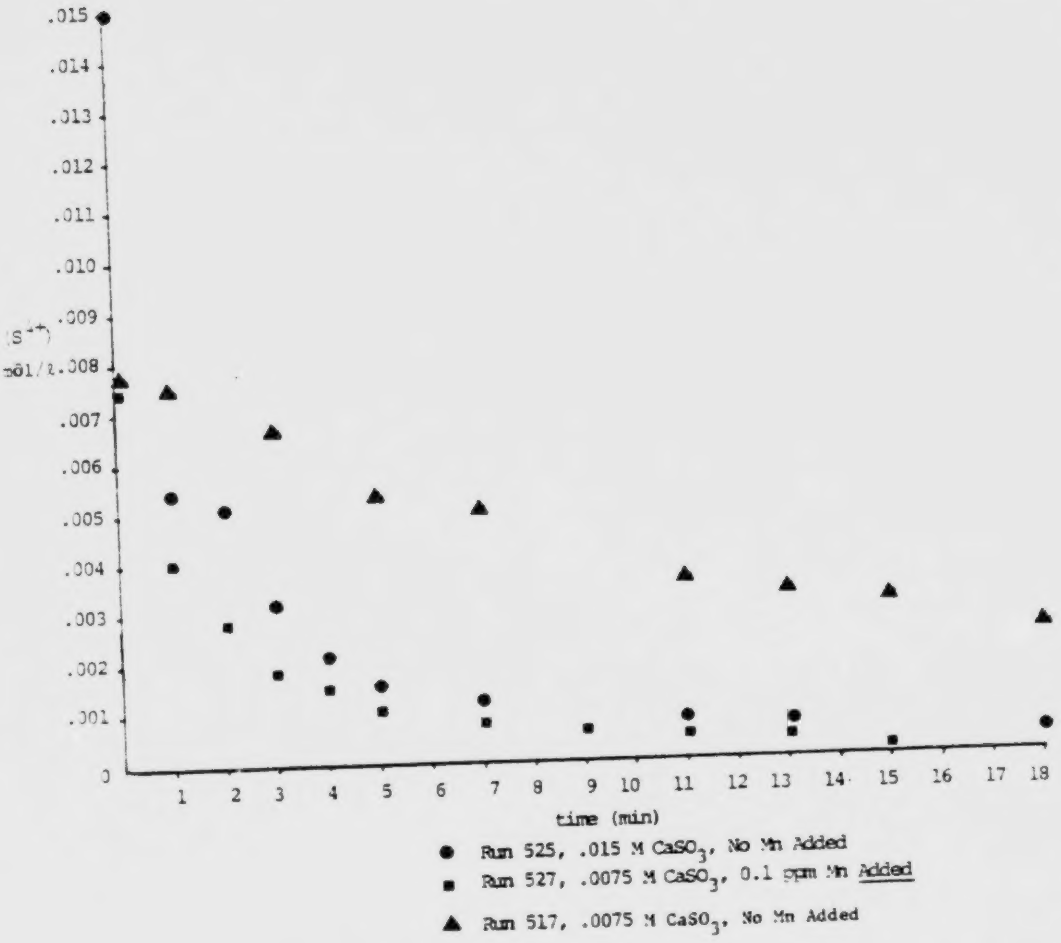

Figure 3-19. Sulfur ($_4^+$) Concentration vs Time for Various Mn Concentrations (All runs at 50°C and pH of 5.0)

Experiments were also performed keeping the initial sulfur (4+) concentration constant and varying the amount of manganese catalyst added. These experiments along with the runs mentioned earlier were analyzed using the MULTREG computer program described above. Each different set of conditions was run individually on the program to determine the order with respect to sulfur (4+). The conditions and results of these experiments are listed in Table 3-15. In the more highly catalyzed runs, the experiment was often over within the first few minutes. Thus, in these runs there were fewer points with which to make the determinations listed. This caused some scatter in the results.

The rate of reaction at $[S^{4+}] = 0.01$ M is shown in Figure 3-20 as a function of manganese concentration.

b. Glycolic acid

Experiments were run at a constant concentration of glycolic acid with varying amounts of manganese catalyst. This study was done to see if the addition of catalyst could overcome the effects of a strong organic acid inhibitor and to what degree the two additives, inhibitor and catalyst, affected the oxidation rate. All experiments were run at 50°C, initial pH of 4.0 and initial sulfur (4+) concentration of 0.01 M. A concentration of 1000 ppm glycolic acid was chosen for the organic acid additive.

Representative results are presented in Figure 3-21, where concentration vs time is plotted at various glycolic acid concentrations. The results are summarized in Table 3-16. The reaction order is between 1.0 and 1.5 for much of the range and in order to compare the behavior as a function of manganese concentration the rate of reaction at a concentration of $[S^{4+}] = 0.01$ M is given and plotted in Figures 3-22 and 3-23 (expanded scale). From the table and the plots it can be seen that the effects of both additives is

TABLE 3-15

EFFECT OF Mn CONCENTRATION ON OXIDATION RATE OF SUCCINIC ACID BUFFERED

$CaSO_3$ SOLUTIONS

Initial S^{4+} Conc. mol/ℓ	pH	Added Mn Catalyst (ppm)	Total Mn (ppm)	Order with Respect to S^{4+}	Standard Deviation of Order	Rate Constant	Rate $[S^{4+}] = 0.01M$, mol/sec
0.015	5.0	0	0.21	1.75	0.17	0.346	1.09×10^{-4}
0.0075	5.0	0.07	0.17	1.23	0.28	0.0076	2.65×10^{-5}
0.005	5.3	0.07	0.14	1.91	0.23	1.249	1.89×10^{-4}
0.005	5.5	0.07	0.14	1.78	0.22	1.078	2.97×10^{-4}
0.005	5.0	0.1	0.17	1.66	0.24	0.251	1.20×10^{-4}
0.01	5.0	0.1	0.24	1.79	0.08	0.379	9.97×10^{-5}
0.01	5.0	0.2	0.34	1.53	0.15	0.148	1.29×10^{-4}
0.01	5.0	0.3	0.44	1.41	0.27	0.0912	1.38×10^{-4}
0.01	5.0	0.4	0.54	1.47	0.23	0.173	1.99×10^{-4}
0.01	5.0	0.5	0.64	1.71	0.14	0.818	3.11×10^{-4}
0.01	5.0	1.0	1.14	1.82	0.07	2.0148	4.62×10^{-4}

Temperature = 50°C

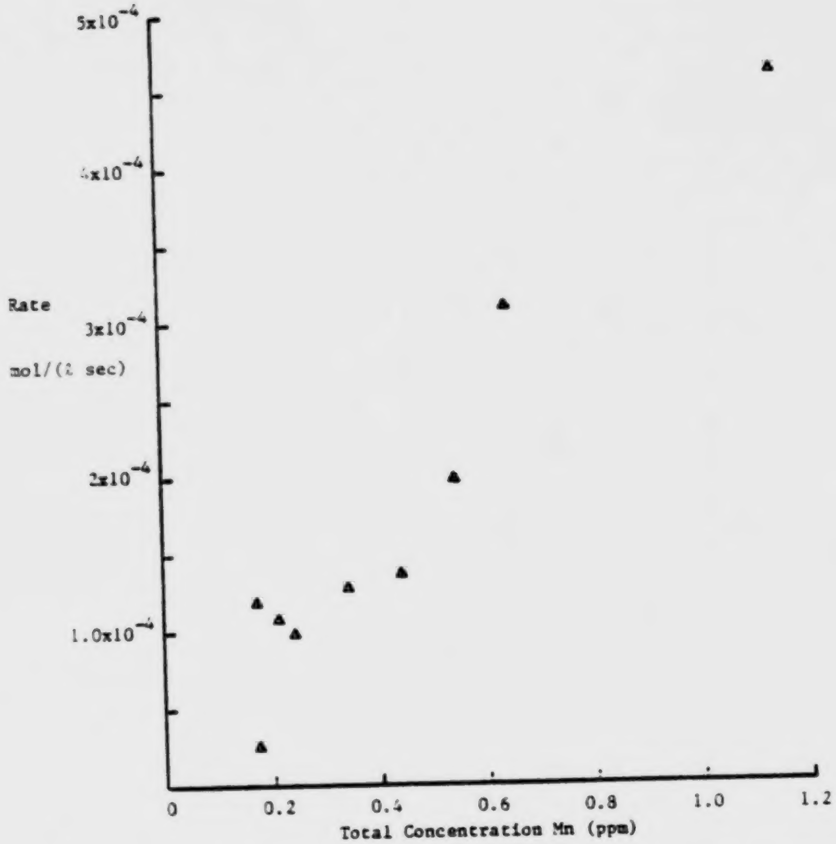

Figure 3-20. Effect of Mn on Oxidation Rate of Succinic Acid Buffered $CaSO_3$ Solutions for $[S^{4+}] = 0.01M$

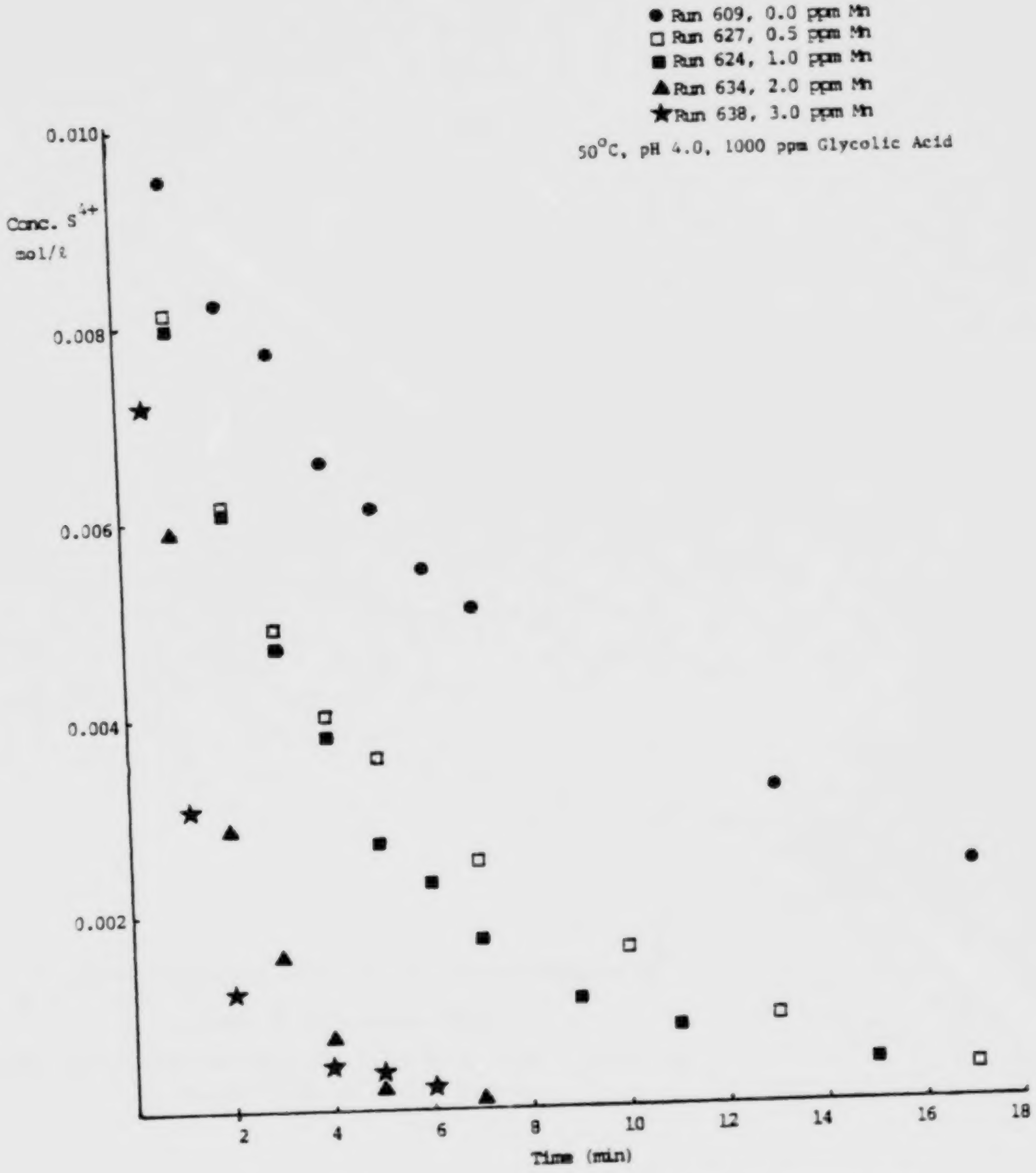

Figure 3-21. Concentration Sulfur (4+) vs Time, 1000 ppm Glycolic Acid, Various Concentrations of Mn

TABLE 3-16

EFFECT OF MANGANESE ADDITION TO GLYCOLIC ACID INHIBITED RUNS

Run#	Concentration Added Mn (ppm)	Order With Respect to Sulfur 4+	Standard Deviation of Order	Rate Constant	Rate at $[S^{4+}] = 0.01$ mol/(ℓ sec)
609	0	1.40	0.09	0.01182	1.87×10^{-5}
610	0				
611	0				
629	0.2	1.26	0.16	0.00706	2.13×10^{-5}
630	0.2				
627	0.5	1.26	0.07	0.01404	4.24×10^{-5}
628	0.5				
635	0.7	1.17	0.06	0.00908	4.15×10^{-5}
636	0.7				
624	1.0	1.23	0.07	0.14941	5.18×10^{-5}
626	1.0				
631	1.5	1.27	0.07	0.03089	8.91×10^{-5}
632	1.5				
633	2.0	1.13	0.06	0.02154	11.8×10^{-5}
634	2.0				
638	3.0	1.51	0.19	0.23892	22.8×10^{-5}
639	3.0				
640	3.5	1.60	0.29	0.463	29.2×10^{-5}
641	3.5				

All runs were done at 50°C, pH of 4.0, initial sulfur (4+) concentration of 0.01 molar and glycolic acid concentration of 1000 ppm.

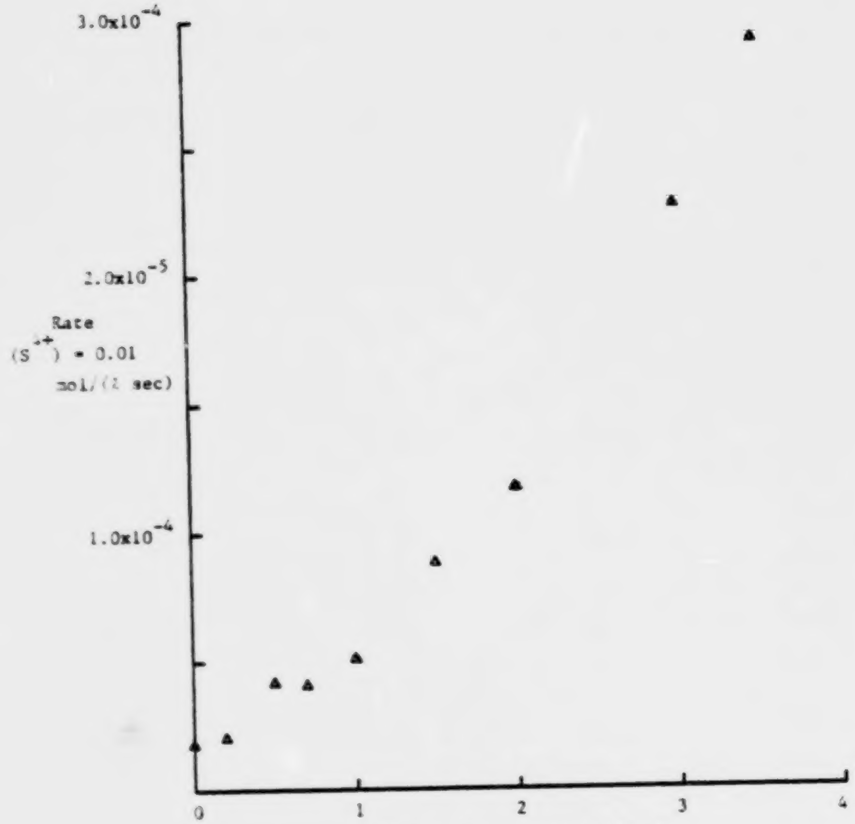

Figure 3-22. Effect of Mn Addition to Glycolic Acid Inhibited $CaSO_3$ Oxidation. Rate at $[S^{4+}] = 0.01M$.

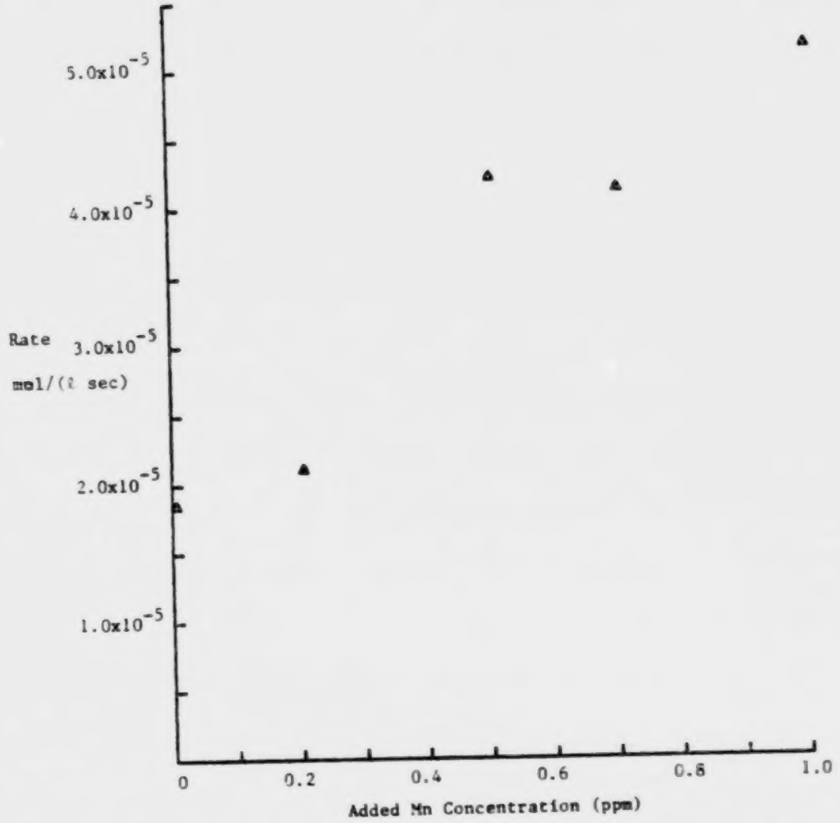

Figure 3-23. Effect of Mn Addition to Glycolic Acid Inhibited $CaSO_3$ Oxidation; Rate at $[S^{4+}] = 0.01$ M.

being observed. Adding manganese increases the oxidation rate, but the strong inhibitory effect of the glycolic acid is also apparent. With 1000 ppm glycolic acid, it takes a manganese concentration of 3.5 ppm to approach the oxidation rate of an uninhibited run. Earlier it was found with 23667 ppm (0.02 M) succinic acid only 1 ppm manganese was required for this oxidation rate. Thus the oxidation rate of an inhibited run can be increased by adding catalyst but the results of the experiment depend on the relative strength and concentrations of both the catalyst and the inhibitor added.

C. REACTION IN LIQUOR FROM PENBERTHY OXIDATION RUNS AT SHAWNEE

Oxidation studies were performed using liquor from slurry samples from the Shawnee test facility. The slurry samples were from Penberthy oxidation runs TSO-2D, TSP-2F, TSP-2G and TSP-2H. The experiments were performed to determine the degree of activity of the samples in catalyzing the oxidation of sulfite.

The experiments were carried out in the semi-batch reactor used in the majority of the work. The Shawnee samples were filtered and 0.2 M succinic acid buffer and S^{4+} as sodium sulfite were added. Even though sodium sulfite was added there is calcium in the filtrate and, therefore, these results are included in the calcium sulfite section.

Data for the oxidation of sodium sulfite in clear (filtered) Shawnee samples are collected in Table 3-17. Also listed for comparison are catalyzed and uncatalyzed sulfite oxidations in water. All reactions were performed at 50°C and buffered. The Shawnee samples can be divided into three general categories. The first type is the AP-2816 filtrate. This reacted at a rate that was convenient to follow by our procedures. The Shawnee sample has some catalytic activity but the results indicate that the rate of oxidation is less than that obtained in unsaturated clear solutions of calcium sulfite.

TABLE 3-17

OXIDATION OF SULFITE SOLUTIONS

Solvent	Solute (0.01M)	Initial Rate (first minute) (mol/ℓ sec)	Catalyst Added (ppm Mn)
Water	$CaSO_3$	5.0×10^{-5}	0
Water	$CaSO_3$	8.0×10^{-5}	0.5
Water	Na_2SO_3	1.6×10^{-5}	0
Ap-2816 Filtrate	Na_2SO_3	2.1×10^{-5}	0
2830 TSP-2D Start	Na_2SO_3	No reaction	0
2830 TSP-2D End	Na_2SO_3	$\geq 15. \times 10^{-5}$	0
2830 TSP-2F Start	Na_2SO_3	No reaction	0
2830 TSP-2F End	Na_2SO_3	$\geq 13. \times 10^{-5}$	0
2830 TSP-2G Start	Na_2SO_3	No reaction	0
2830 TSP-2G End	Na_2SO_3	$\geq 13. \times 10^{-5}$	0
2830 TSP-2H Start	Na_2SO_3	No reaction	0
2830 TSP-2H End	Na_2SO_3	$\geq 13. \times 10^{-5}$	0

The second category of the Shawnee samples contains all of the "starts" of the 2830 TSP pairs. Sulfite solutions of these samples did not oxidize at all over a 25-35 minutes period of oxygen sparging.

This behavior has been termed inhibition. In general it is a chemical effect due even to very low concentrations of certain substrates (inhibitors). The operation of inhibition takes two general paths: denying the reaction mixture of the catalyst's activity; or, interrupting the active species being oxidized. The inhibitors are usually organic molecules (although Cu^+ and CN^- show inhibitive properties) especially those bearing prominent OH^- groups. Rubber shows total inhibition in only small concentrations. Since slurry handling equipment is frequently rubber lined there are opportunities for contamination. Samples from the start of a run may have only low catalyst concentrations and ambient inhibitor levels. As the run progresses, catalyst ions may collect from successive additions of carbonate until the slurry is saturated in these constituents. This much augmented catalyst content may now overwhelm the inhibitors capacity to stop the oxidation.

The third type of Shawnee sample encountered had such a high catalytic activity that reliable rates are difficult to obtain by the methods used. These samples include all the "ends" of the 2830 TSP pairs. In oxidizing sulfite solutions in these liquors, most of the slufite had reacted between the introduction of oxygen and the first sampling one minute later. The results are meaningful, however, in that they indicate a lower boundary to the initial reaction rate. The reaction initially proceeds at least as fast as oxidation of calcium sulfite in water which contains 0.5 ppm Mn catalyst. Supplemental analysis indicated a manganese level of over 11 ppm in the liquid (see Table 3-18).

TABLE 3-18

SUPPLEMENTAL ANALYSIS OF A SHAWNEE SAMPLE*

	Ca	Cu	Co	Fe	Zn	Mn
Liquid	818	0.13	0.15	0.06	18.10	11.50
Solid	14.0%	42.02	6.67	1.28%	122.06	42.0
Combined liquid and solid	16354	4.79	0.89	1425	31.64	16.16

Total suspended solids = 110.97 g/ℓ

*Shawnee Number
2830
TSP-2H (All values are ppm unless specified)
End

Analysis done by North American Exploration Company of Charlottesville, Virginia.

D. DEPENDENCE OF OXIDATION RATE ON STIRRING SPEED AND OXYGEN FLOW RATE

The stirring speed and the oxygen flow rate must be fast enough to insure that only chemical kinetics were being studied. Therefore, each of these parameters was varied over a wide range.

Replicate runs were made at various stirring rates in order to determine the point at which mass transfer no longer limits the rate of reaction and in order to ascertain the reproducibility of the data. Oxygen was bubbled through 0.01 M (unsaturated) calcium sulfite solutions at stirring speeds ranging from 200 to 3500 rmp. These stirring speeds gave an agitation varying from a gentle swirl to a complete froth. Temperature was held constant at 50°C. The pH was maintained at 5.0 with the use of 0.2 M succinic acid buffer. A pH of 5.0 was chosen so that HSO_3^- would be the predominant sulfite species at this temperature. Data were taken as sulfite concentration vs time of oxidation and computer analysis determined rate constants and orders. Typical plots of concentration vs time are shown in Figs. 3-24 and 3-25. At low stirring rates (Fig. 3-24, 215 rpm) the reaction is mass transfer controlled and the concentration of S^{4+} decreases linearly with time. At higher speeds (500-3500 rpm) the data can be fit by a second order curve. In addition, initial rates (the decrease in sulfite concentration occurring in the first minute of reaction) were determined. (The actual order of the reaction is below 2.0 but above 1.0 as discussed above. However, a second order can be used here since it fits the data reasonably well - see Table 3-19 - and can be safely used as an internal comparison which is the only purpose of this section.) These initial rates are collected in Table 3-19. It can be concluded that mass transfer effects are unimportant at these concentrations for stirring speeds above 500 rpm.

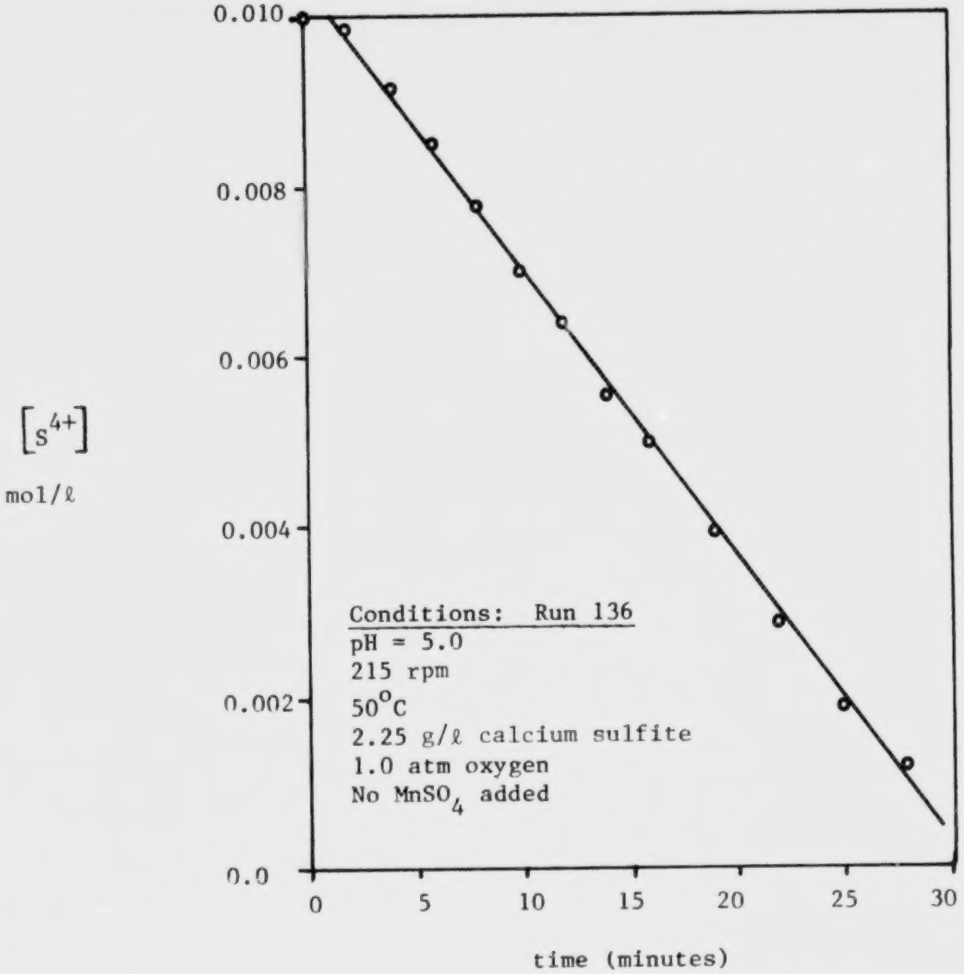

Figure 3-24. Stirring Speed = 215 rpm

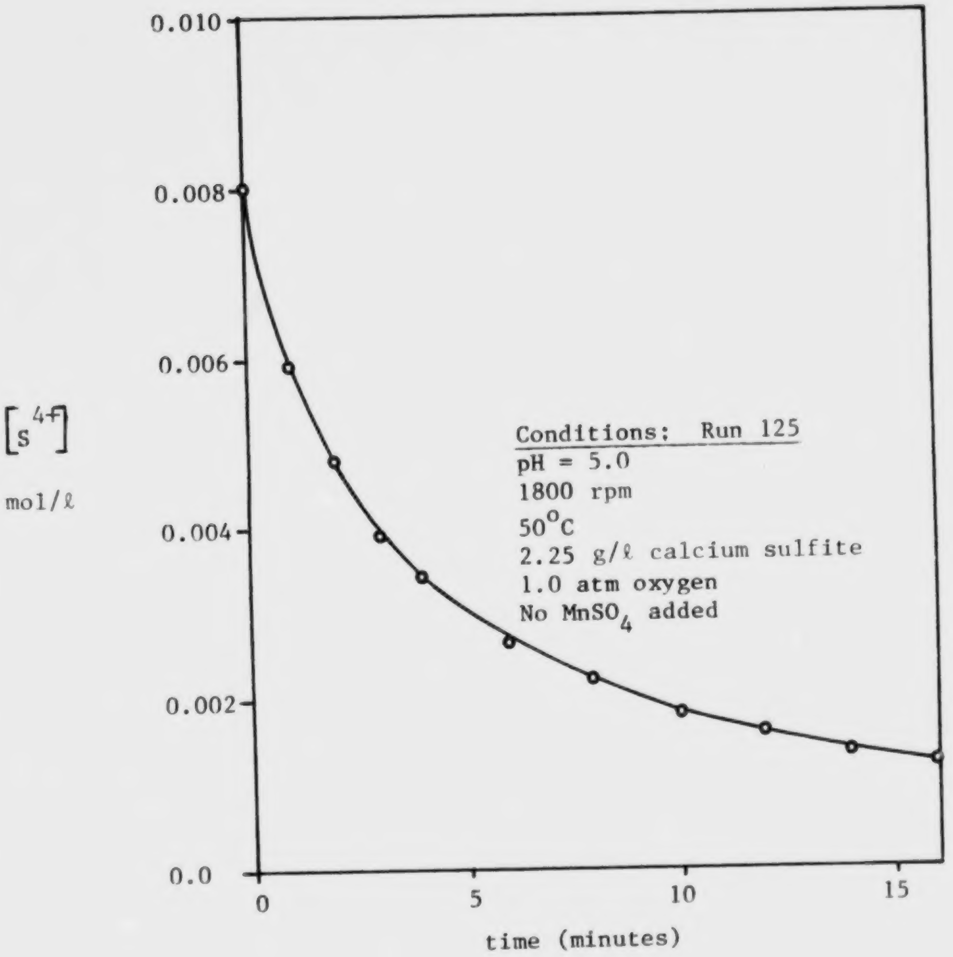

Figure 3-25. Stirring Speed = 1800 rpm

TABLE 3-19

EFFECT OF STIRRING SPEED - NO ADDED CATALYST

Run#	Stirring Speed (rpm)	Initial Rate (mol/ℓ·sec)	2nd Order Rate Constant (ℓ/mol·sec)	Index of Determination for 2nd Order Fit
121	1750	4.66×10^{-5}	0.7337	0.9999
124	1750	3.82	0.6945	0.9999
125	1750	3.45	0.7139	0.9971
126	920	3.28	0.7751	0.9964
127	920	4.55	0.7256	0.9886
128	920	5.11	0.7149	0.9955
129	500	4.28	0.6834	0.9989
130	500	4.44	0.7249	0.9990
131	500	4.51	0.7115	0.9976
132	3200	4.98	0.7485	0.9784
133	3200	4.57	0.8258	0.9987
134	3200	5.04	0.7933	0.9978
135	215	0.58		
136	215	0.38		
137	215	0.41		
138	2500	4.94	0.7083	0.9958
139	2500	5.66	0.6908	0.9930
140	2500	5.06	0.7435	0.9981
141	345	0.75		
142	345	0.48		
143	345	0.72		

Temperature = 50°C, pH = 5.0

Since an increase in agitation has no effect on the reaction rate, it would appear that under these conditions the rate is not limited by the mass transfer effects of the system. In order to further test the hypothesis that mass transfer is not controlling, experiments were made in the same reactor with manganese catalyst being added. The addition of catalyst can have a significant effect on the rate of a kinetically controlled reactor but would have no influence if mass transfer were completely limiting (i.e., fast reaction in the bulk of the liquid but diffusion resistance across a "stagnant film). As can be seen from Table 3-20 and Figure 3-26 the addition of catalyst does increase the rate of reaction for sufficiently high stirring speeds.

To further check for any mass transfer effects in the oxidation of clear solutions, studies were made on the flow rate of oxygen into the reactor. In an experiment, water is purged of oxygen by bubbling with nitrogen, then $CaSO_3$ is dissolved and the reaction started (time = 0) by turning off the nitrogen purge stream and immediately turning on the oxygen stream. Questions arose about the time delay between the start of oxygen sparging and saturation of the 600 ml solution volume. At the previous flow rate of 0.88 ℓ/min., it was estimated to take several minutes for the oxygen to displace most of the nitrogen. Therefore, runs were made at higher oxygen flow rates (from 0.77 to 7.6 ℓ/min) in order to ascertain that oxygen saturation of the liquid was rapid and complete. Results are given in Table 3-21. At higher flow rates (about 4.0 ml/min) results are somewhat less accurate since aliquots were withdrawn from the vessel, stoppers popped off, and severe splashing occurred. Also, certain runs seemed to foam for no understandable reason. All of these conditions detracted from the quality of the experimental results. Nevertheless, despite the problems, rate constants were not being significantly affected by the tenfold increase in flow rate. Therefore a flow rate of 3.0 ℓ/min was settled upon as being a satisfactory compromise.

TABLE 3-20

EFFECT OF STIRRING SPEED - 0.5 ppm Mn

Run#	Stirring Speed	2nd Order Rate Constant (ℓ/mol ·sec)	Order of Reaction
144	1750	3.141	2
145	1750	2.582	2
146	1750	4.055	2
147	1750	3.557	2
148	1750	2.517	2
149	1750	2.673	2
150	3300	3.754	2
165	920	2.711	2
166	920	2.674	2
167	500	2.915	1
168	500	2.695	1
170	500	2.585	1
171	380	1.829	0
172	250	0.138	1
173	380	1.206	1
174	2050	0.427	2
175	380	1.399	1
176	250	0.176	0
177	250	0.178	0
178	1750	2.568	2
179	1700	3.900	2
180	1700	3.716	2
181	2000	3.501	2
182	1700	4.045	2
183	1700	3.705	2
184	1700	3.176	2
187	820	3.709	2
188	820	3.058	2
189	2250	2.730	2
190	820	2.603	2

Temp = 50°C; pH = 5.0

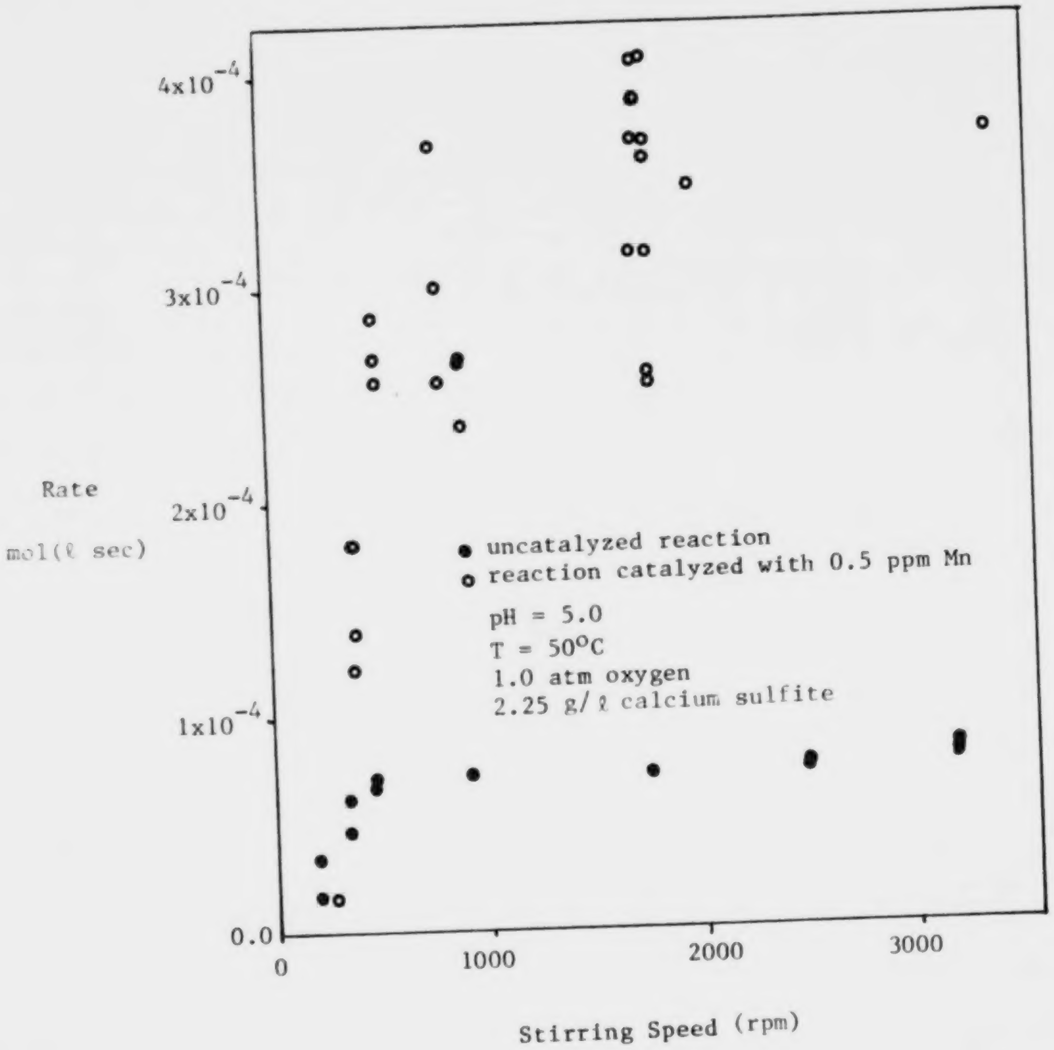

Figure 3-26. Rate at [S^{4+}] = 0.01 M vs Stirring Speed

TABLE 3-21

EFFECT OF OXYGEN FLOW RATE ON OXIDATION IN UNSATURATED SOLUTIONS

pH = 5.0 T = 50°C

Run #	2nd Order Rate Constant	Oxygen Flow Rate (ℓ/min)	Sudsing or Not
151	0.65	4.2	Yes
152	0.61	5.3	Yes
153	0.59	7.6	No
154	0.75	6.5	No
155	0.59	6.5	No
156	0.75	0.77	No
157	0.62	6.3	Yes
158	0.68	6.3	No
159	0.59	6.3	No
160	0.73	6.3	No
162	0.72	2.1	No

Filtrate Oxidations: Slurries at a pH of 4.5 and temperature of 40°C and with various densities were filtered under nitrogen after chemical equilibrium had been reached. The concentrations of manganese and iron were measured in the various filtrates. This analysis was performed by North American Exploration Company. It was felt these catalyst concentrations would be indicative of the total catalytic concentration in the filtrates. These clear liquid filtrates were then buffered to a pH of 4.5 with succinic acid and then oxidized. These experiments were conducted to study the reaction kinetics in the liquid phase of the slurry. The oxidation of these calcium sulfite slurry filtrates was very similar to work conducted by Nurmi (126). See Section V.

A linear regression analysis was performed on the concentration vs time data obtained from each filtrate oxidation to determine the reaction order with respect to the bisulfite species. Results of this analysis are given in Table 3-22 and shown in Figure 3-27.

All of the experimental data obtained from the filtrate experiments were further analyzed by a linear regression analysis. This regression analysis was made to simultaneously determine the relationship of the bisulfite concentraion and the catalytic content to the rate of oxidation. The MULTREG computer program was used to do this analysis (see Section II).

Results from this analysis showed that the iron and manganese concentrations were not independent of each other. The rate of oxidation was found to be 0.51 order with respect to the manganese concentration and 1.44 order with respect to S^{4+} which is present as bisulfite. The standard deviations and variances for S^{4+} and Mn respectively were 0.069, 0.0475, and 0.075, 0.056.

TABLE 3-22

RESULTS OF FILTRATE OXIDATIONS;

$pH_I = 4.5$ T = 40°C

Slurry Density	ppm Mn in Filtrate	Run #	Order	1.4 Order Rate Constant
4.33		331	1.72	0.0192
4.4	0.2	345	1.80	0.020
10		341	1.62	0.0158
10	0.66	348	1.64	0.02361
20	0.91	342	1.32	0.0271
35		354	1.24	0.04265
50	1.71	332	1.46	0.02554
50		343	1.49	0.0370
80	2.66	344	1.42	0.0422
80		351	1.74	0.0426

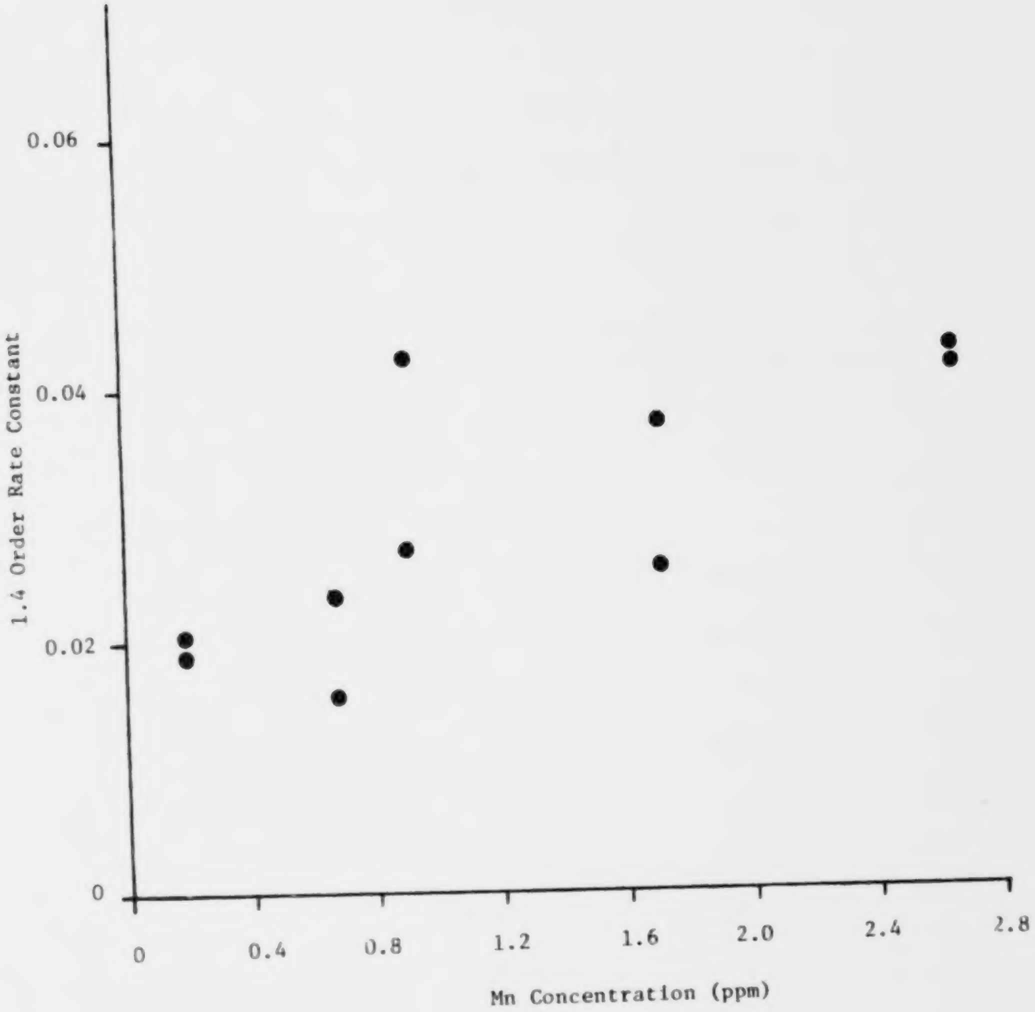

Figure 3-27. 1.4 Order Rate Constant *vs* Mn Concentration in $CaSO_3$ Filtrate Oxidations

Because of these results, the experimental data were forced through a 1.4 order reaction model to give 1.4 order rate constants. These calculated rate constants, graphed against the manganese concentration found in the filtrates are shown in Figure 3-27.

E. RATE OF $CaSO_3$ OXIDATION AT HIGH MANGANESE CONCENTRATIONS BY FLOW-THERMAL METHOD

Clear bisulfite solutions having calcium as the spectator cation oxidize too rapidly for the time scale of the batch method. In the flow ractor even highly catalyzed calcium bisulfite solutions oxidize at a readily measured rate. In this way the data needed to describe the oxidation in the clear solution surrounding slurry particles where the manganese may be present at a few ppm is obtained as well as rates in extremely catalyzed solutions. The extremely catalyzed solutions reveal the rates of oxidation in the set of experiments performed to observe overall limitation by rate of mass transfer (to assess the mass transfer coefficient).

The results of a flow-thermal experiment is a temperature vs time graph. The T vs t curve (eg. Figure 3-28) is determined from the concentrations of reactants and catalyst, pH, and initial temperature. In this set of experiments the pertinent conditions were:

pH:	3.8 - 4.6	
$[S^{4+}]$:	0.00136 - 0.00456	mol/ℓ
$[O_2]$:	0.00642 - 0.0172	mol/ℓ
[Mn]:	10 - 2000	ppm (wt.)
$T_{initial}$:	25 ± 0.02	°C

Most experiments were performed at pH 4.6 with an excursion to lower values since in the flow reactor, stripping does not occur. The rates for these experiments came from the method described in Section II. That method of analysis is based on only one type of sulfur species reacting;

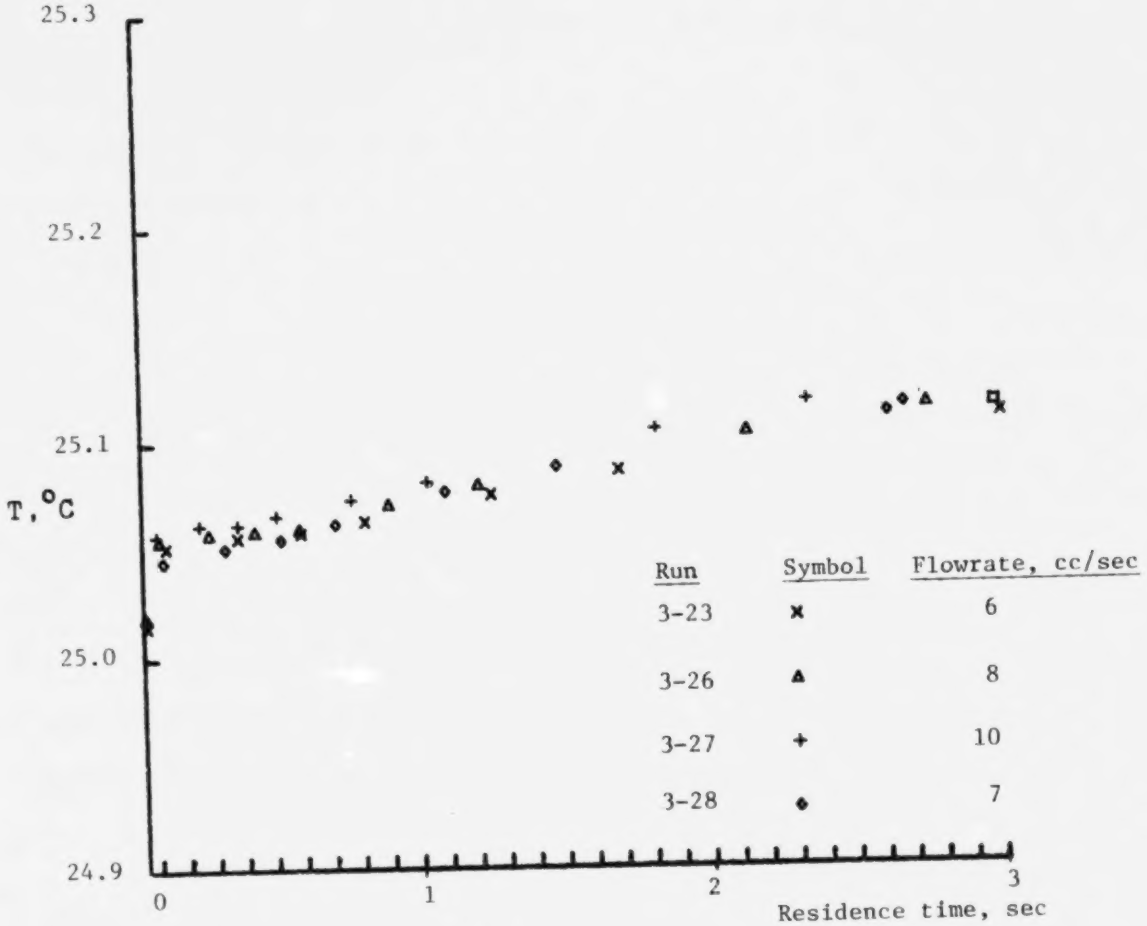

Conditions: pH = 4.6

[Mn] = 10 ppm

$[S^{4+}]$ = 0.002 M

$[O_2]$ = 0.012 M

T = 25°C

Figure 3-28 Representative T vs t Results for $CaSO_3$ Oxidation

and, as such only applies to bisulfite solutions initially at pH 4.6 where all the S^{4+} is in the form of bisulfite and only then to their initial moments of reaction before the pH drops. However, for rough comparisons with the lower pH values tested, this method is also good enough. The rates encountered under the conditions in the list above range from 0.0004 to 0.017 mol/(ℓ sec).

The results in Figure 3-29 represent the effect of Mn^{2+} concentrations at 10, 200, 1000, and 2000 ppm. The rates coming from these oxidation are listed in Table 3-23.

Because very low pH oxidation sometimes is important and in the flow reactor there is no loss of reactant at low pH as there is in open-system batch reactors, the pH over the range 3.3 to 4.7 was examined. The results are in Table 3-24.

Although these experiments were all performed at 25°C it is likely the results here are similar enough to those from the batch pH method that the activation energy (E_A) may be accepted for converting the rates found here to any temperature by using the Arrhenius relation

$$\text{Rate}(T) = \text{Rate}(25^{o}) \times \exp(-E_A/RT).$$

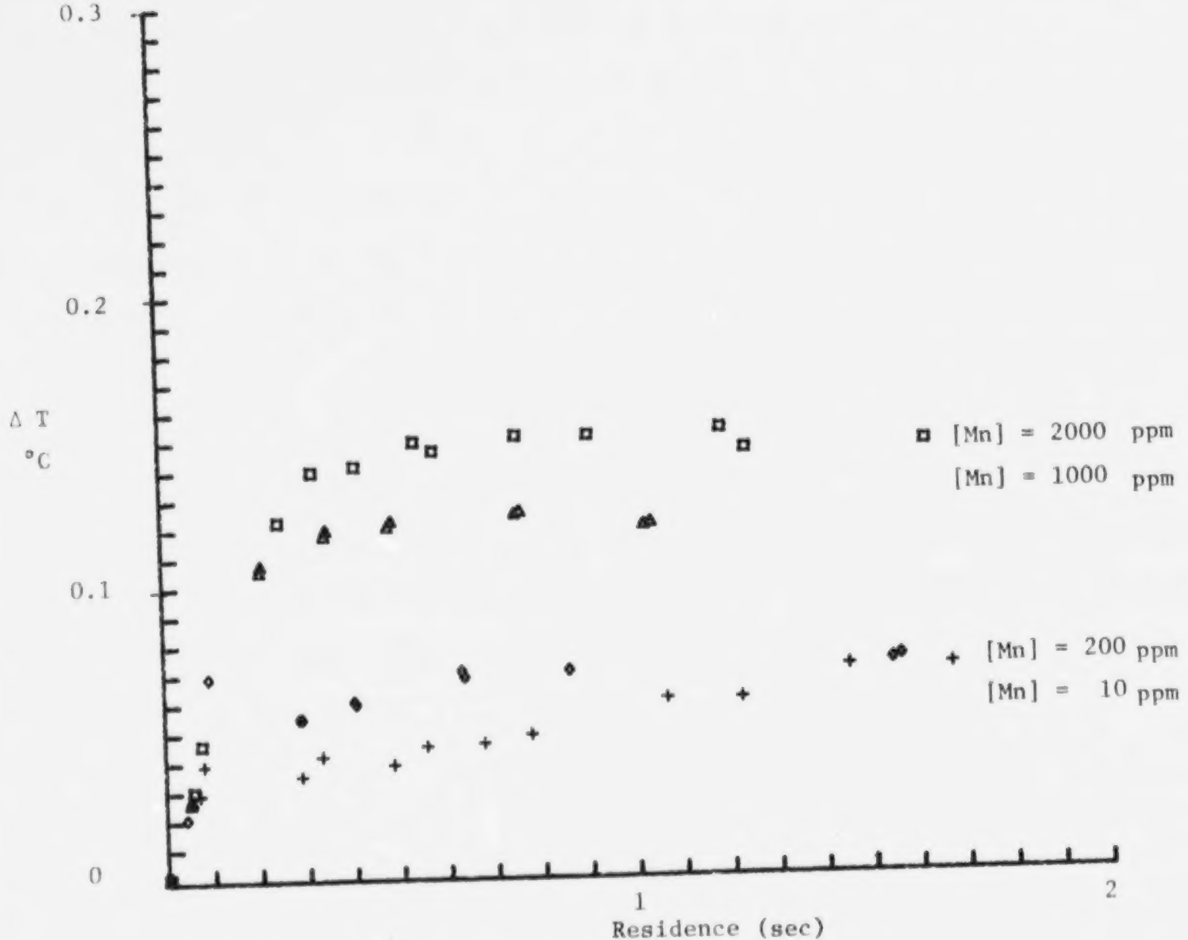

Conditions: $[S^{4+}]$ = 0.002 M

$[O_2]$ = 0.013 M

pH = 4.6

T = 25°C

Figure 3-29 Effect of [Mn] on Oxidation Rate

TABLE 3-23

EFFECT OF HIGH Mn CONCENTRATIONS ON $CaSO_3$ OXIDATION RATE

[Mn] ppm	Rate mol/(ℓ sec)	Conditions
10	0.006	pH = 4.6
200	0.007	T = 25°C
1000	0.012	$[S^{4+}]_{AV} = 0.003$ M
2000	0.014	$[O_2]_{AV} = 0.01$ M

TABLE 3-24

EFFECT OF pH ON THE RATE OF Mn CATALYZED $CaSO_3$ OXIDATIONS

pH	Rate, mol/(ℓ sec)
3.3	0.00048
3.8	0.00051
4.5	0.00059
4.6	0.00078
4.7	0.00105

Conditions

[Mn] = 10 ppm

$[S^{4+}]_{AV}$ = 0.003 M

$[O_2]$ = 0.01 M

T = 25°C

SECTION 4

OXIDATION IN SLURRIES

OUTLINE

- IV. Oxidation in Slurries
  - A. Experiment
    - 1. Solubility Studies
      - a. Theoretical Analysis
      - b. Experimental Results
    - 2. Oxidation in Calcium Sulfite Slurries
    - 3. Oxygen Flow Rate Studies
    - 4. pH and Temperature Studies
    - 5. Slurry Density Studies
    - 6. Catalyzed Slurry Oxidation Studies
    - 7. Liquid Phase Slurry Behavior
    - 8. pH Behavior During Reaction
    - 9. Slurry Reactions with and without pH Controller
    - 10. Liquid Phase Catalyst Studies
  - B. Mathematical Model
    - 1. General Description of Model
    - 2. Physical Description of Particles
      - a. Electron Micrograph
      - b. Particle Size Distribution
    - 3. Derivation of Spherical Model
    - 4. Solutions of the Spherical Model
    - 5. Derivation of the Flat Plate Model

OXIDATION IN SLURRIES

A. EXPERIMENTAL

Experiments were conducted to determine the effect of several different experimental parameters on the rate of oxidation in calcium sulfite slurries. These experimental parameters included temperature, stirring speed, initial pH, slurry density, and added manganese catalyst. Both total and liquid sulfite concentrations were examined during these studies. Other experiments were run to determine whether the reacting system was limited by the mass transfer of oxygen or by reaction of sulfur (4+). Those experimental results have been simulated by a computer-programmed mathematical model.

1. Solubility Studies

The solubility of calcium sulfite in water is a function of temperature, pH, and ionic strength. It is very important and necessary for the liquid phase kinetic studies, solid-liquid mass transfer studies, and the mathematical modeling of slurry oxidation reaction. Therefore it has been investigated by both theoretical analyses and experiments.

a. Theoretical Analysis

The solids used, even before oxidation, are a mixture of calcium sulfite and calcium sulfate. A detailed computer program is available for calculating the solubility of these solids (22). Approximate values, however, can be obtained with the following equations:

$$[Ca^{2+}]\ [SO_3^{2-}] = K_{sp1} \qquad (4.1)$$

$$[Ca^{2+}]\ [SO_4^{2-}] = k_{sp2} \qquad (4.2)$$

$$[H^+]\ [OH^-] = K_w \qquad (4.3)$$

These equations ignore ion-pair formation, $CaSO_3°$ and $CaSO_4°$, which are not significant. During the course of dissolution, the equilibrium is established rapidly. Then we have

$$HSO_3^- \rightleftharpoons H^+ + SO_3^{2-}$$

$$HSO_4^- \rightleftharpoons H^+ + SO_4^{2-}$$

and

$$\frac{[H^+][SO_3^{2-}]}{[HSO_3^-]} = k_s \qquad (4.4)$$

$$\frac{[H^+]\ [SO_4^{2-}]}{[HSO_4^-]} = K_2 \qquad (4.5)$$

The condition of electro-neutrality is:

$$2[Ca^{2+}] + [H^+] = [OH^-] + 2[SO_4^{2-}] + 2[SO_3^{2-}] + [HSO_3^-] + [HSO_4^-] \qquad (4.6)$$

At 40°C we have

$k_{sp1} = 2.76 \times 10^{-7}$ (156) $(mol/\ell)^2$

$k_{sp2} = 1.2 \times 10^{-6}$ (180) $(mol/\ell)^2$

$k_w = 10^{-13.5348}$ (181) $(mol/\ell)^2$

$k_s = 4.94 \times 10^{-8}$ (25) (mol/ℓ)

$k_2 = 6.4565 \times 10^{-3}$ (mol/ℓ)

At a fixed pH value, we thus have 6 equations and 6 unknowns (i.e., $[Ca^{2+}]$, $[OH^-]$, $[SO_4^{2-}]$, $[SO_3^{2-}]$, $[HSO_3^-]$) and $[HSO_4^-]$). In all cases, molar concentrations are used in favor of activities since the activity coefficients are very close to 1.0 (Handbook of Chemistry and Physics, e.g. section D-205) at our low concentrations (less than 0.01M). Those equations can then be solved to give the saturation concentration of sulfite which is the sum of $[SO_3^{-2}]$ and $[HSO_3^-]$. The result is shown in Figure 4-1. Although the equations are approximate, the results fit experimental data reasonably well.

b. Experimental Results

Experiments to get the saturation concentration of calcium sulfite in water were performed at different pH values. The experimental conditions were as follows:

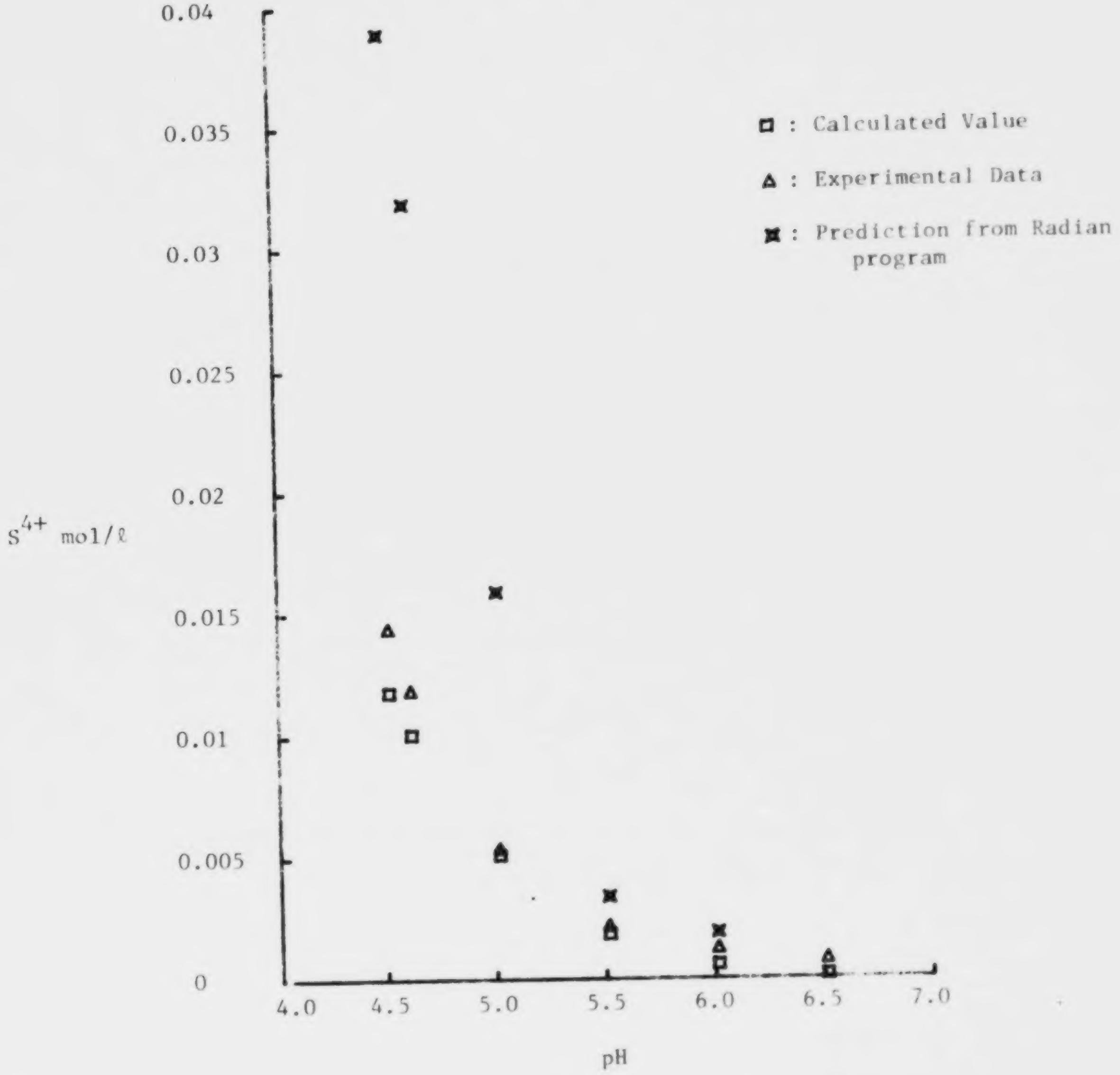

Figure 4-1. Solubility of Calcium Sulfite at 40°C

Temperature = 40^oC
Slurry density = 10 g/ℓ (and 20 g/ℓ)
Stirring Speed = 1800 rpm

The reactor was nitrogen sparged so that the S^{4+} would not be oxidized ($P_{02} = 0$). Stripping of SO_2 is minimal at pH = 4.5 and above. A pH controller kept the pH of the slurry at a fixed value by pumping in H_2SO_4 as needed. The slurry stirred for more than three hours to make sure that thermal and chemical equilibrium had been reached before making measurements. Clear solution samples were thus taken by letting the slurry flow through a Millipore filter. The saturation concentration of sulfite was then determined by iodometric titration. The result is shown in Figure 4-1 in which values from the BMREP (22) computer program predictions are also given for comparison. It can be seen that the experimental values are much lower than the computer predictions. Further, the changes of slurry density have no influence on the saturation concentration (Figure 4.2).

A power function of Cs = 1676.84 ($pH^{-7.791}$) was found to best fit these data.

2. Oxidation in Calcium Sulfite Slurries

When the calcium sulfite slurries were oxidized, the total concentration vs time data obtained were very similar regardless of the experimental conditions used. An example of the data obtained from the slurry oxidations is shown in Figure 4-3. The reaction curves consisted of two distinct sections. The first section of the curve in Figure 4-3 shows a very rapid initial reaction rate. At some time during the slurry oxidation, the rate of oxidation suddenly becomes much slower as shown by the the difference of the slopes of two line segments shown in Figure 4-3.

3. Oxygen Flow Rate Studies

In an experiment, water is purged of oxygen by bubbling with nitrogen, then $CaSO_3$ is dissolved and the reaction is begun (time = 0) by switching the

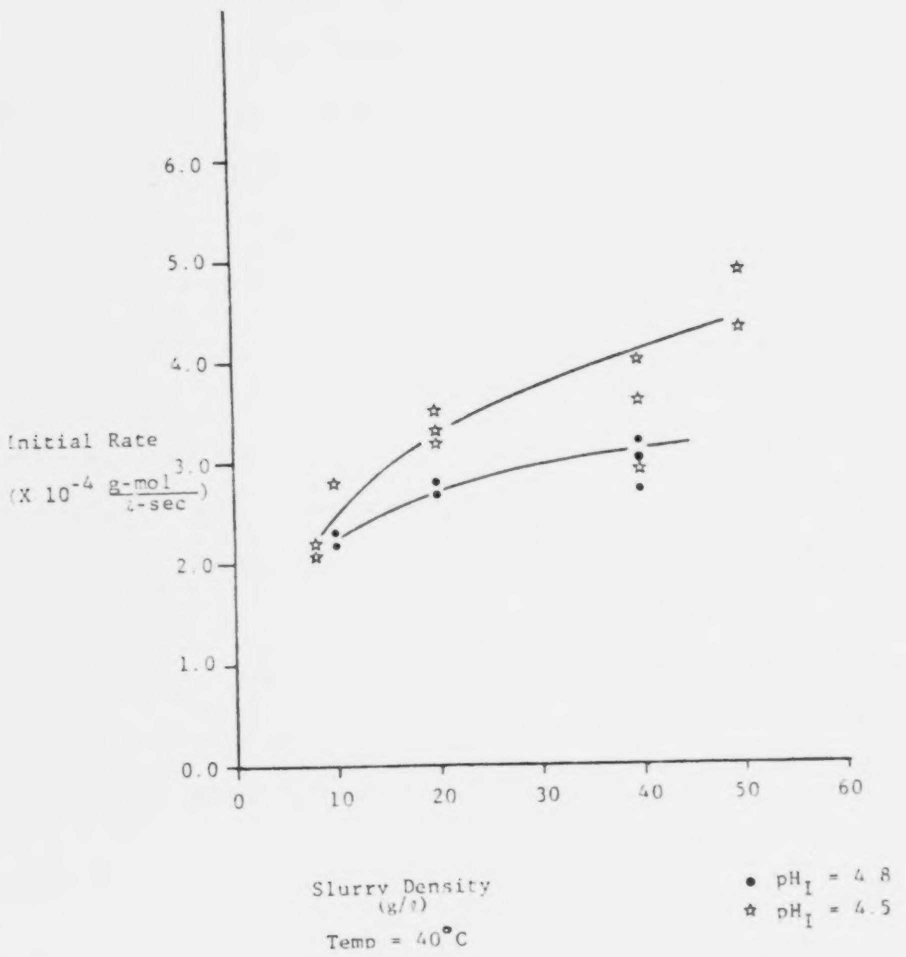

Figure 4-2. Effect of Slurry Density on Oxidation Rate

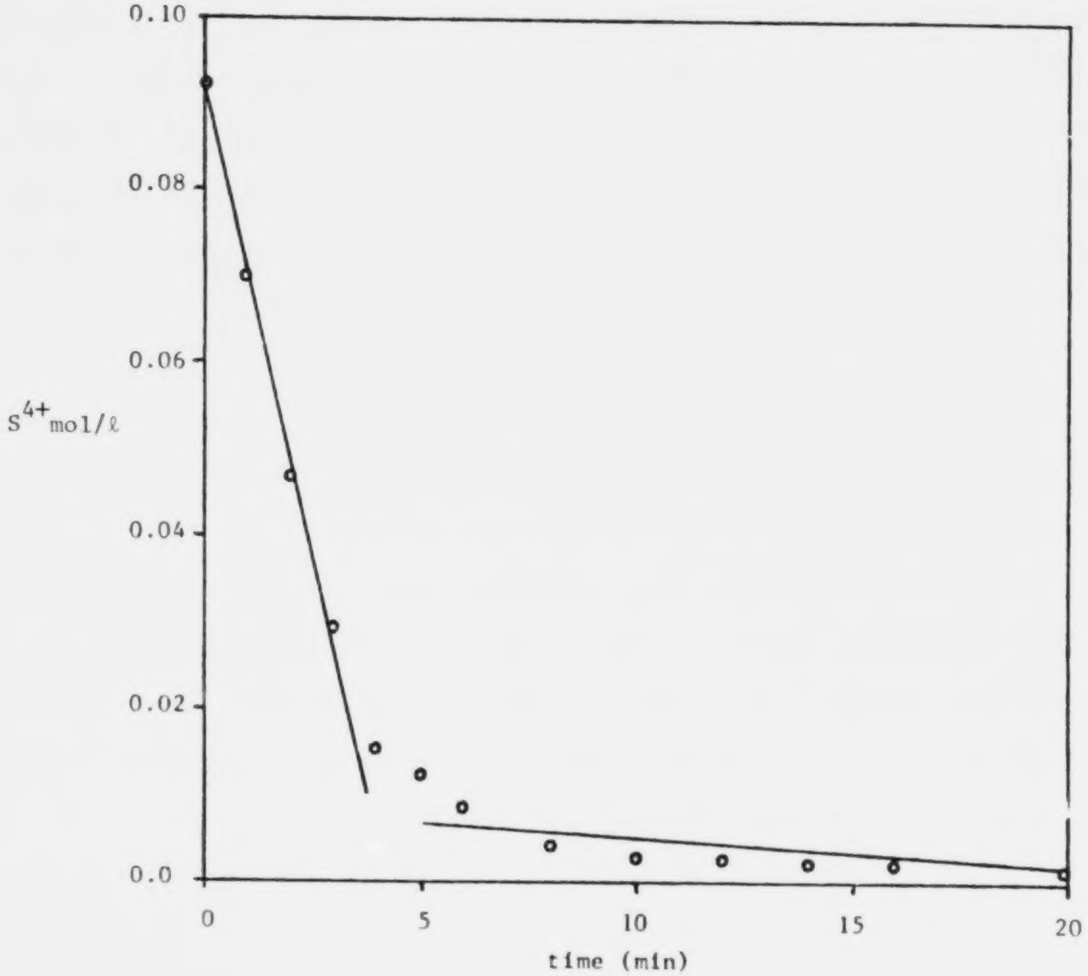

Run #221 pH_I = 5.1, 50°C, 1800 rpm, 3.0 ℓ/min O_2

Figure 4-3. Typical Slurry Reaction Curve

nitrogen purge stream and the oxygen stream. Questions arose about the time delay between the start of oxygen sparging and saturation of the 600 ml solution volume. At flow rate of 0.77 ℓ/min, it was estimated to take several minutes for the oxygen to displace most of the nitrogen. Therefore, runs were made at higher oxygen flow rates (from 0.77 to 7.6 ℓ/min) in order to test that oxygen saturation of the liquid was rapid and also complete.. At higher flow rates (above 4.0 ml/min) results are somewhat less accurate since, when aliquots were withdrawn from the vessel by momentarily closing off the gas escape vent, problems were encountered (stoppers popping off and severe splashing). Also, certain runs seemed to foam for no clear reason. Nevertheless, despite the problems, rate constants were not being significantly affected by the tenfold increase in flow rate. Therefore a flow rate of 3.0 ℓ/min was settled upon as being a satisfactory compromise.

Slurries with 2000 ppm added manganese catalyst were oxidized with different oxygen flow rates. If the oxidation was being hindered by gas to liquid mass transfer, an increase in the oxygen flow rate should have increased the rate of oxidation. However, as seen below in Figure 4-4, no increase in the slurry oxidation rate was observed.

4. pH and Temperature Studies

Slurry oxidations were conducted over a range of initial pH's to determine the effect of pH on the initial reaction rate. The pH's used in this study varied from 6.0 to 4.3. Experiments were conducted at both 40°C and 50°C. All experiments used a slurry density of 20 g/ℓ, an oxygen flow rate of 3 ℓ/min and a stirring speed of 1800 rpm. Examples of the experimental data obtained in this study are given by the total concentration vs time data in Figures 4-5 to 4-7. The initial reaction rate from these experiments as a function of pH and temperature is shown in Figure 4-8. Table 4-1 provides a list of the experiments used in this study.

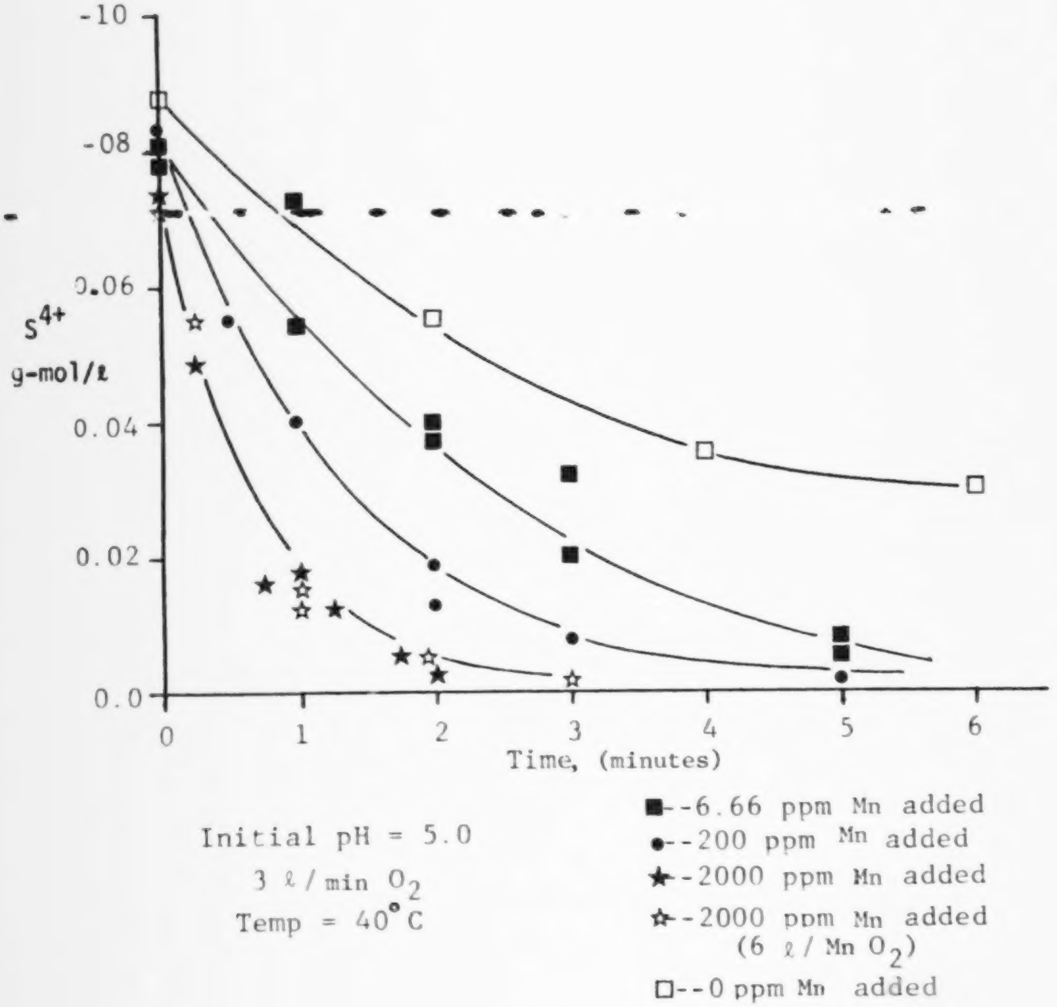

Figure 4-4 Effect of Mn Catalyst on Slurry Oxidation Rate

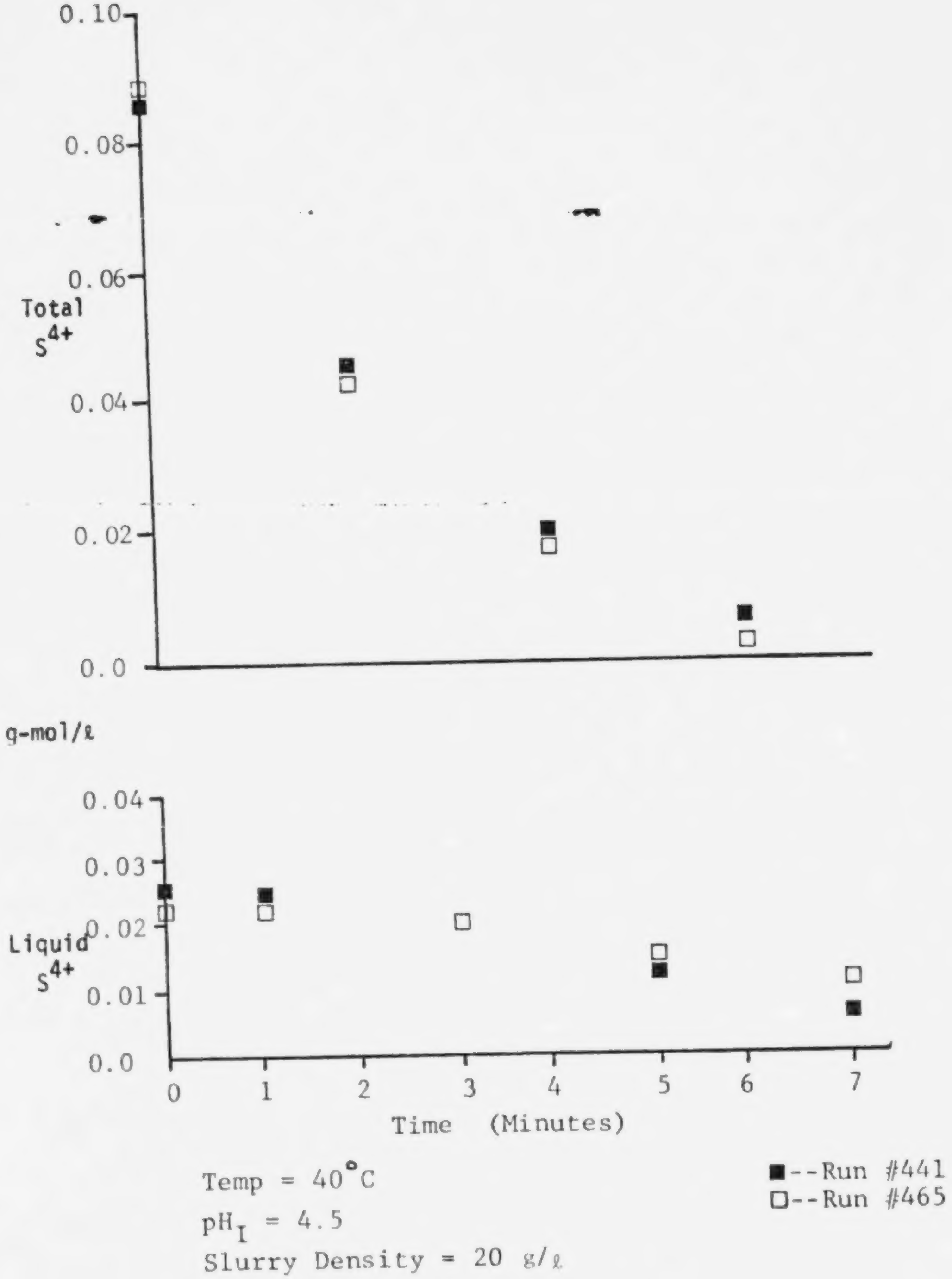

Temp = 40°C

$pH_I = 4.5$

Slurry Density = 20 g/ℓ

Figure 4-5. Slurry Oxidation, pH = 4.5 (182)

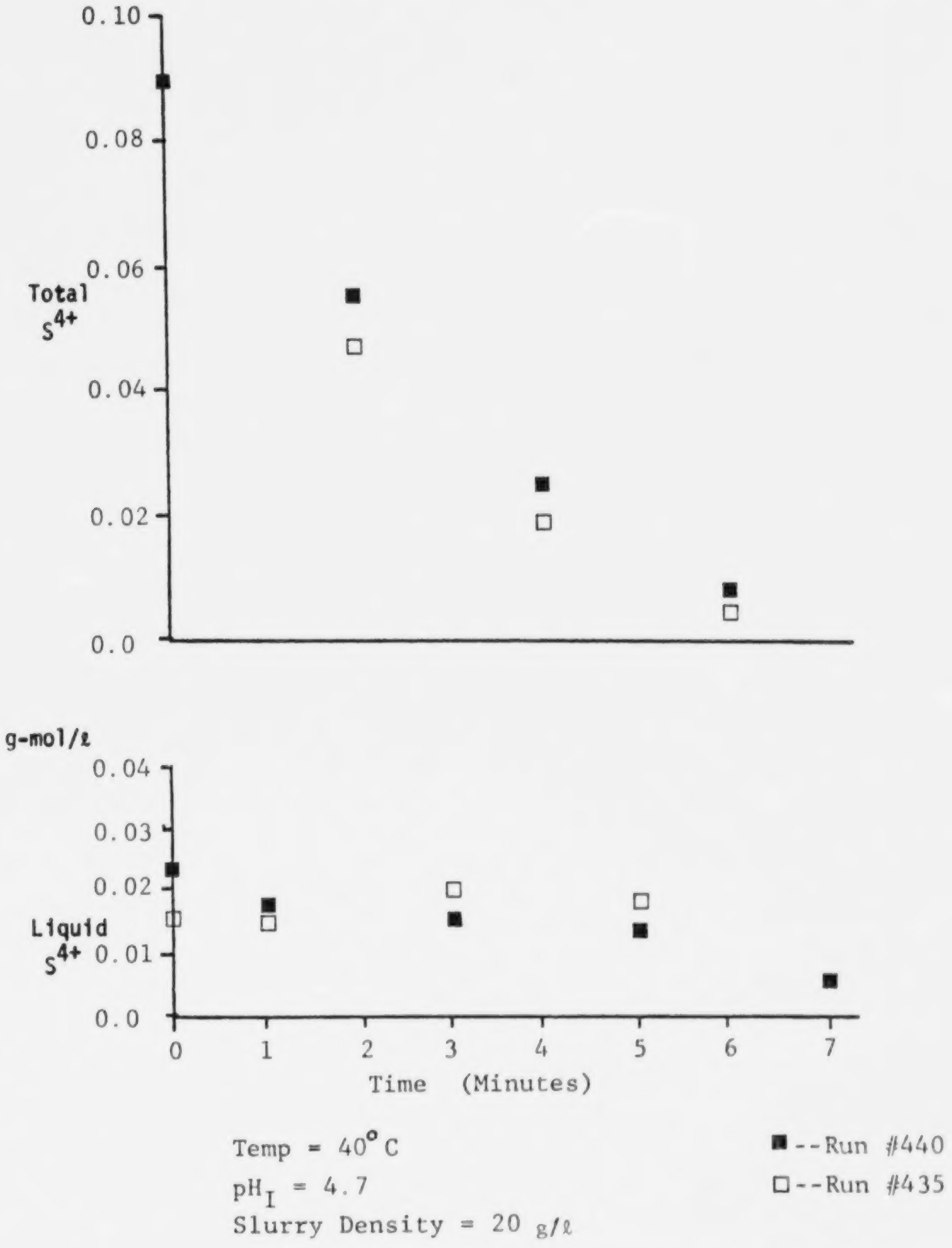

Temp = 40°C
pH_I = 4.7
Slurry Density = 20 g/ℓ

Figure 4-6 Slurry Oxidation, pH = 4.7 (182)

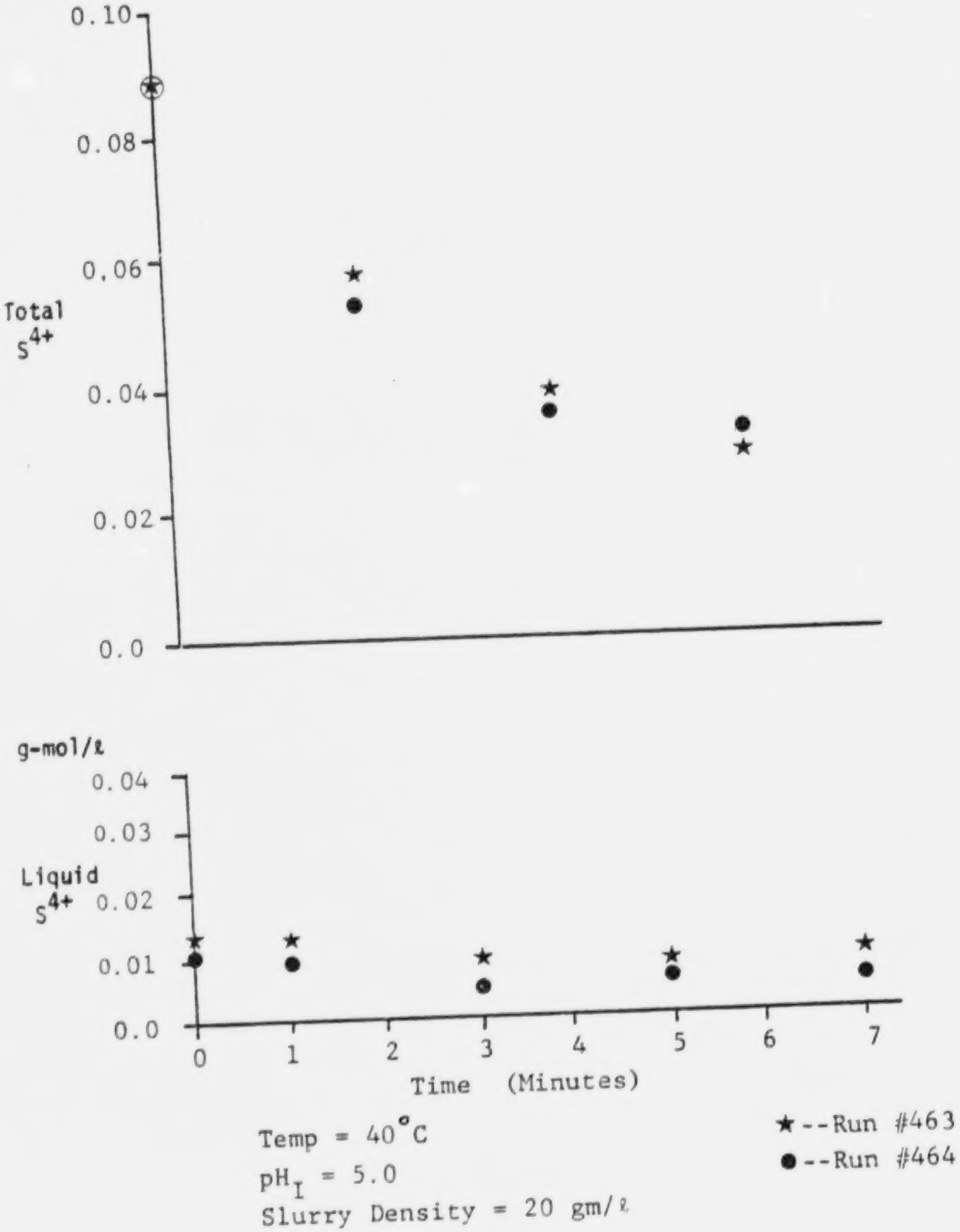

Temp = 40°C

pH_I = 5.0

Slurry Density = 20 gm/ℓ

Figure 4-7 Slurry Oxidation, pH = 5.0 (182)

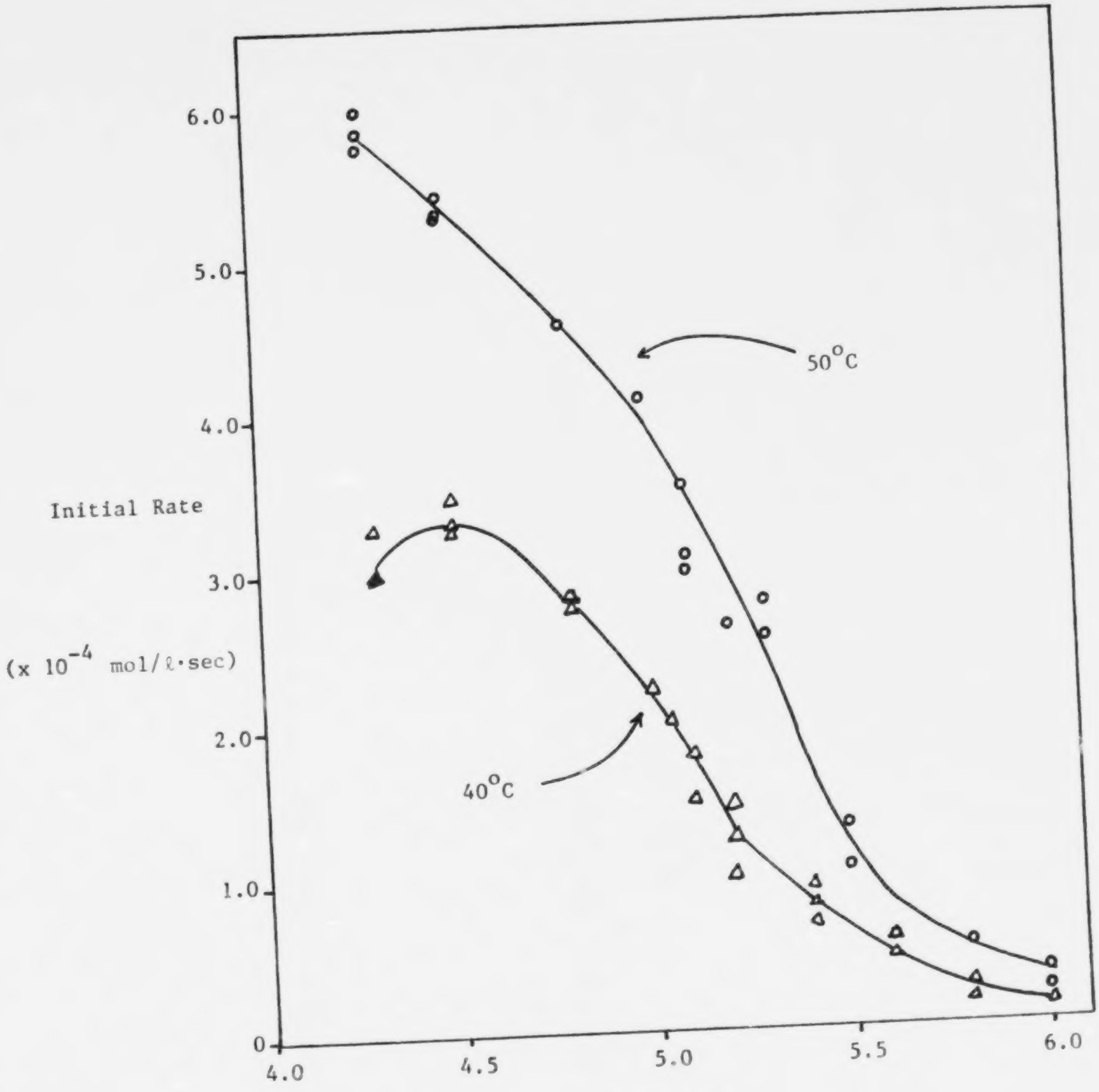

Figure 4-8 Effect of pH on Slurry Oxidation Rates

(All runs at 1800 rpm and 3.0 ℓ /min O_2)

TABLE 4-1

RESULTS OF STUDIES SHOWING EFFECT OF INITIAL pH ON OXIDATION (182)

Run #	pH_I	Temperature (°C)	Initial Rate $\times 10^{-4}$ mol/(ℓ sec)
235	4.3	50	5.97
237	4.3	50	5.86
238	4.3	50	5.76
227	4.5	50	5.41
228	4.5	50	5.31
229	4.5	50	5.34
241	4.8	50	5.42
245	4.8	50	4.60
223	5.0	50	4.10
220	5.1	50	3.08
221	5.1	50	3.54
222	5.1	50	2.95
244	5.2	50	2.62
242	5.3	50	2.77
243	5.3	50	2.77
232	5.5	50	1.07
234	5.5	50	1.33
253	6.0	50	0.61
251	4.3	40	3.27
257	4.3	40	2.99
264	4.3	40	3.00
256	4.5	40	3.25
263	4.5	40	3.46
250	4.5	40	3.29
255	4.8	40	2.75
258	4.8	40	2.83
259	5.0	40	2.23
260	5.1	40	1.50
261	5.1	40	1.73
262	5.2	40	1.24
265	5.2	40	1.00
248			
266	5.4	40	0.68
267	5.4	40	0.92
252	5.4	40	0.83
268	5.6	40	0.47
269	5.6	40	0.58
270	5.8	40	0.15
271	5.8	40	0.27
272	6.0	40	0.12
441	4.5	40	3.76*
465	4.5	40	3.33*
440	4.7	40	3.57*
435	4.7	40	3.00*
463	5.0	40	3.00*
464	5.0	40	2.63*

*not shown in Figure 4-3

5. Slurry Density Studies

Slurries with densities of 8, 10, 20, 40, 50 g/ℓ were oxidized to determine the effect of slurry density on the initial reaction rate. Experiments were made with initial pH's of 4.8 and 4.5 and a temperature of 40°C. The stirring speed used was 1750 rpm and the oxygen flow rate was 3 ℓ/min. Examples of the experimental data obtained from these experiments are given below by the total concentrations vs time data in Figures 4-9, 4-10, 4-5. Table 4-2 gives a list of the experiments used in this study. A graph of the initial reaction rate as a function of slurry density is shown in Figure 4-2.

6. Catalyzed Slurry Oxidation Studies

By increasing the rate of one step in an overall process such as the oxidation of sulfur (4+), the relative importance of the several steps involved, reaction, absorption of oxygen, and dissolution of solids can be determined. This information is necessary in developing a model of the process. The model is discussed in more detail later.

Initial experiments were conducted in which 8 ppm manganese catalyst (Mn^{2+}) was added. The slurry load in the experiments was 20 g/ℓ. Experiments had an initial pH of 4.5 and 5.1 and two temperatures 40°C and 50°C. The results are listed in Table 4-3. The results for some representative runs are shown in Figure 4-11. As expected the addition of catalyst speeds up the reaction. It should be noted that the shapes of the catalyzed and uncatalyzed runs are similar, the difference being in the rate of the process. The effect of catalyst on the pH of the slurry during the course of the reaction is shown in Figures 4-12 and 4-13. At an initial pH of 4.5, Mn simply speeds up the pH drop. However, at an initial pH of 5.1 the general shape of the pH curve is altered.

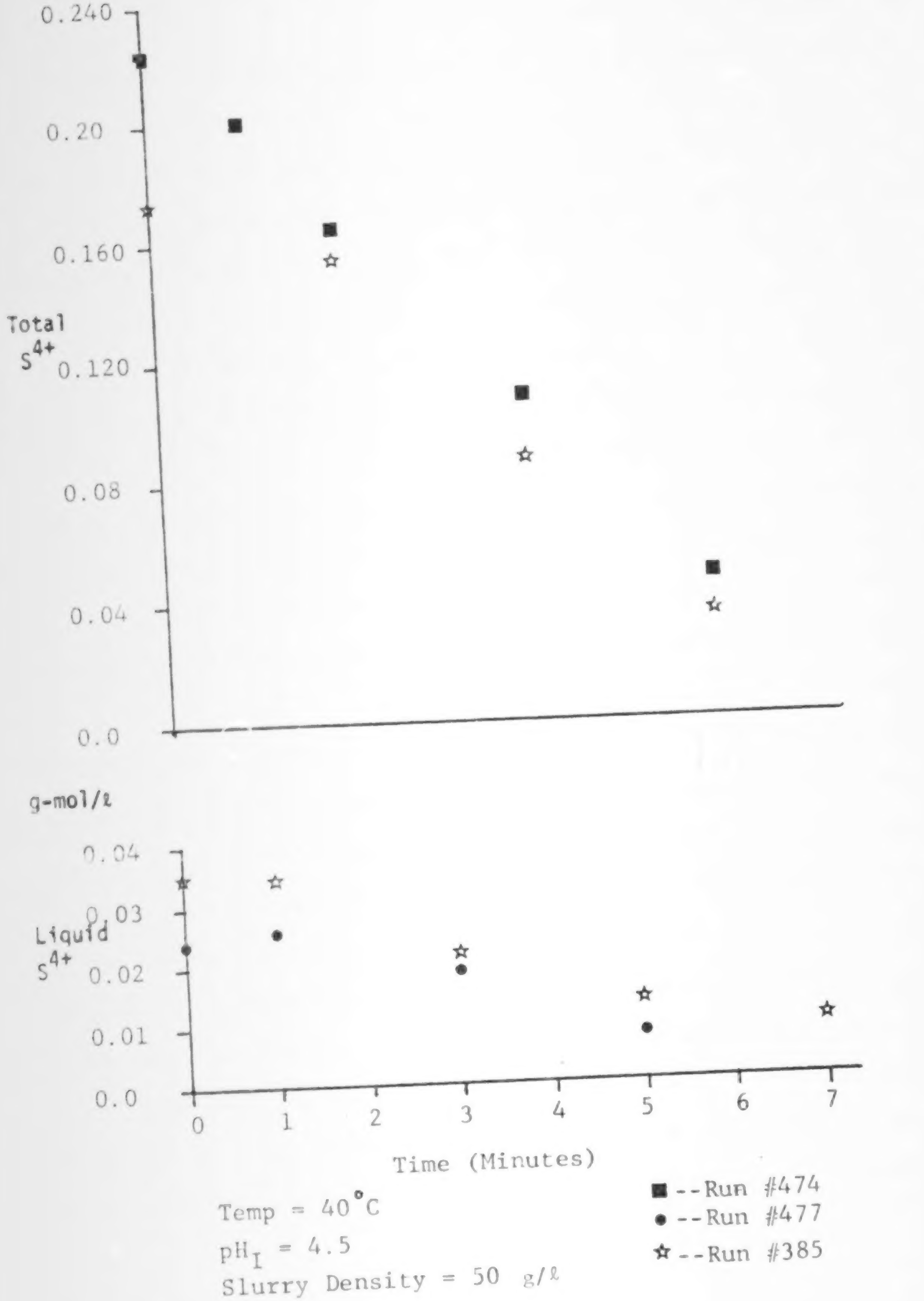

Figure 4-9. Slurry Oxidation, pH = 4.5 (182)

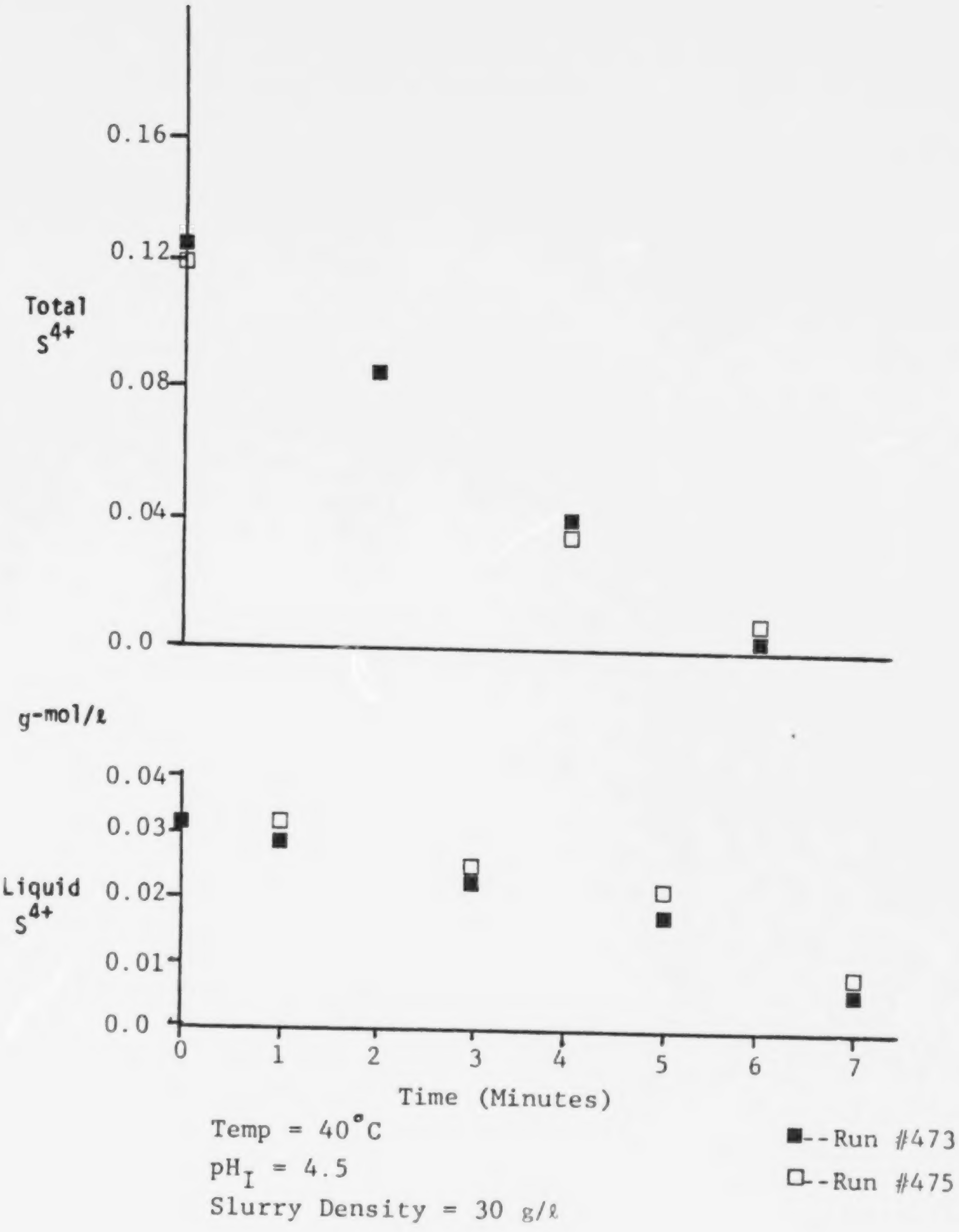

Temp = 40°C

pH_I = 4.5

Slurry Density = 30 g/ℓ

Figure 4-10. Slurry Oxidation, pH = 4.5 (182)

TABLE 4-2

EFFECT OF SLURRY LOAD ON OXIDATION RATE AT 40°C (182)

Initial pH	Initial Slurry Concentration g/ℓ	Initial Rate mol/ℓ · sec	Stirring Speed (rpm)	Run #
4.8	40	2.5×10^{-4}	1750	306
4.8	40	3.2	1750	307
4.8	40	3.0	1750	313
4.8	20	2.7	1750	249
4.8	20	2.8	1750	255
4.8	20	2.8	1750	258
4.8	10	2.3	1750	304
4.8	10	2.2	1750	305
4.5	50	4.3	1750	315
4.5	50	4.9	1750	316
4.5	40	4.0	1750	311
4.5	40	3.0	1750	309
4.5	40	3.6	1750	312
4.5	20	3.5	1750	250
4.5	20	3.2	1750	256
4.5	20	3.3	1750	263
4.5	10	2.2	1750	308
4.5	10	2.8	1750	310
4.5	8	2.1	1750	318
4.5	8	2.2	1750	319
4.5	50	4.8	2800	321
4.5	8	2.5	2800	320
4.5	8	2.1	2800	322
4.5	50	4.7	1800	474*
4.5	50	4.5	1800	385*
4.5	30	3.3	1800	473*
4.5	30	3.1	1800	475*
4.5	20	3.3	1800	441*
			1800	465*

*Not shown in Figure 4-2

TABLE 4-3

EFFECT OF CATALYST ON SLURRY OXIDATION RATE

40°C

Run #	Initial pH	conc. Mn (ppm)	Initial Rate mol/(ℓ sec)
250	4.5	0	3.4×10^{-4}
256	4.5	0	3.2
299	4.5	8	6.6
300	4.5	8	6.2
275	5.0	0	1.83
259	5.0	0	2.22
282	5.0	0	2.55
274	5.0	8	2.79
276	5.0	8	2.90
247	5.1	0	1.5
261	5.1	0	1.8
301	5.1	8	3.0
302	5.1	8	3.0
303	5.1	8	2.8

50°C

233	4.5	0	5.4×10^{-4}
228	4.5	0	5.31
229	4.5	0	5.34
290	4.5	8	6.5
291	4.5	8	6.9
233	5.1	0	3.0
296	5.1	0	2.8
297	5.1	0	3.0
298	5.1	0	3.0
288	5.1	8	5.0
293	5.1	8	5.2
294	5.1	8	4.8

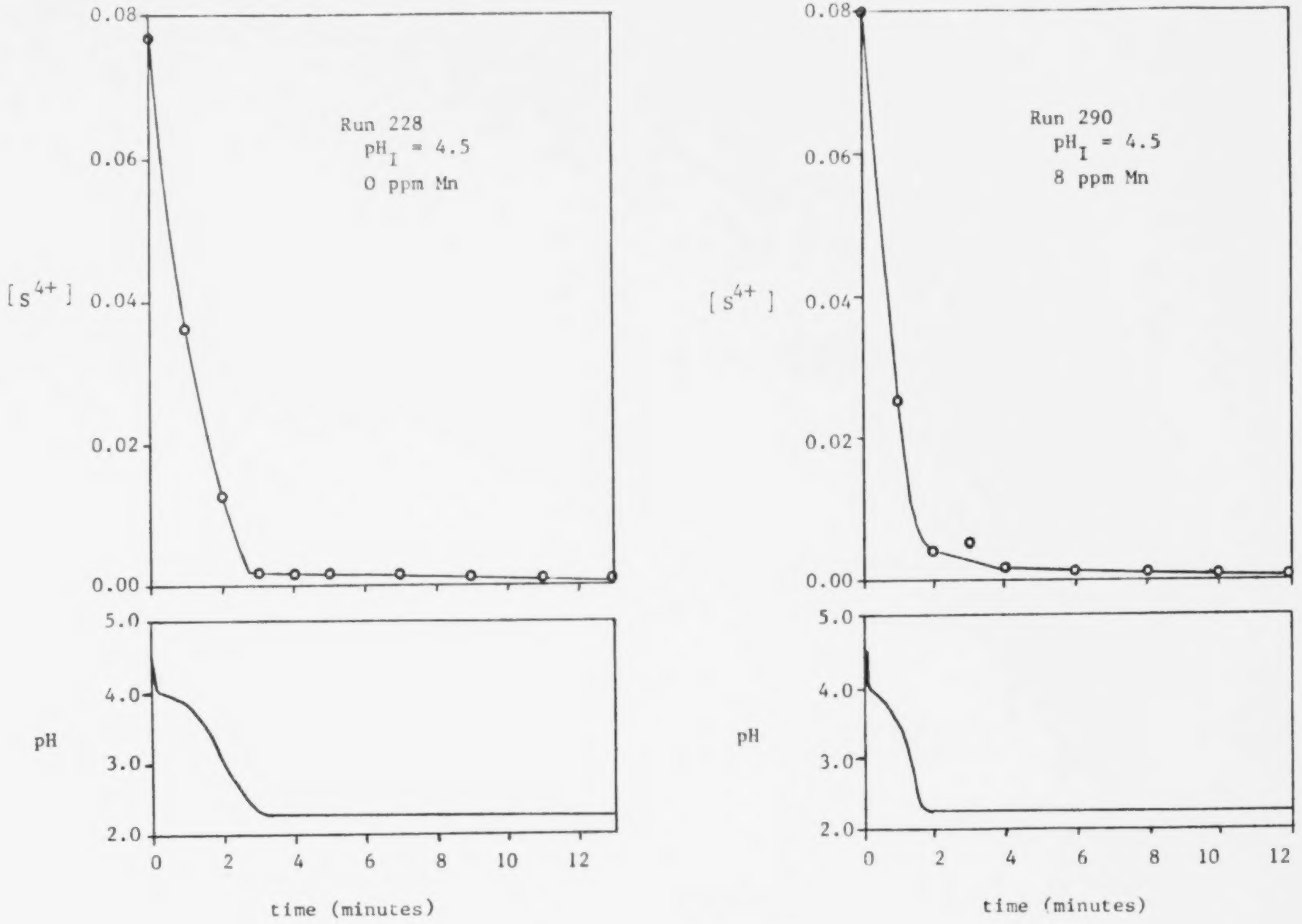

Figure 4-11. Catalyzed & Uncatalyzed Oxidations in Slurries at 50°C

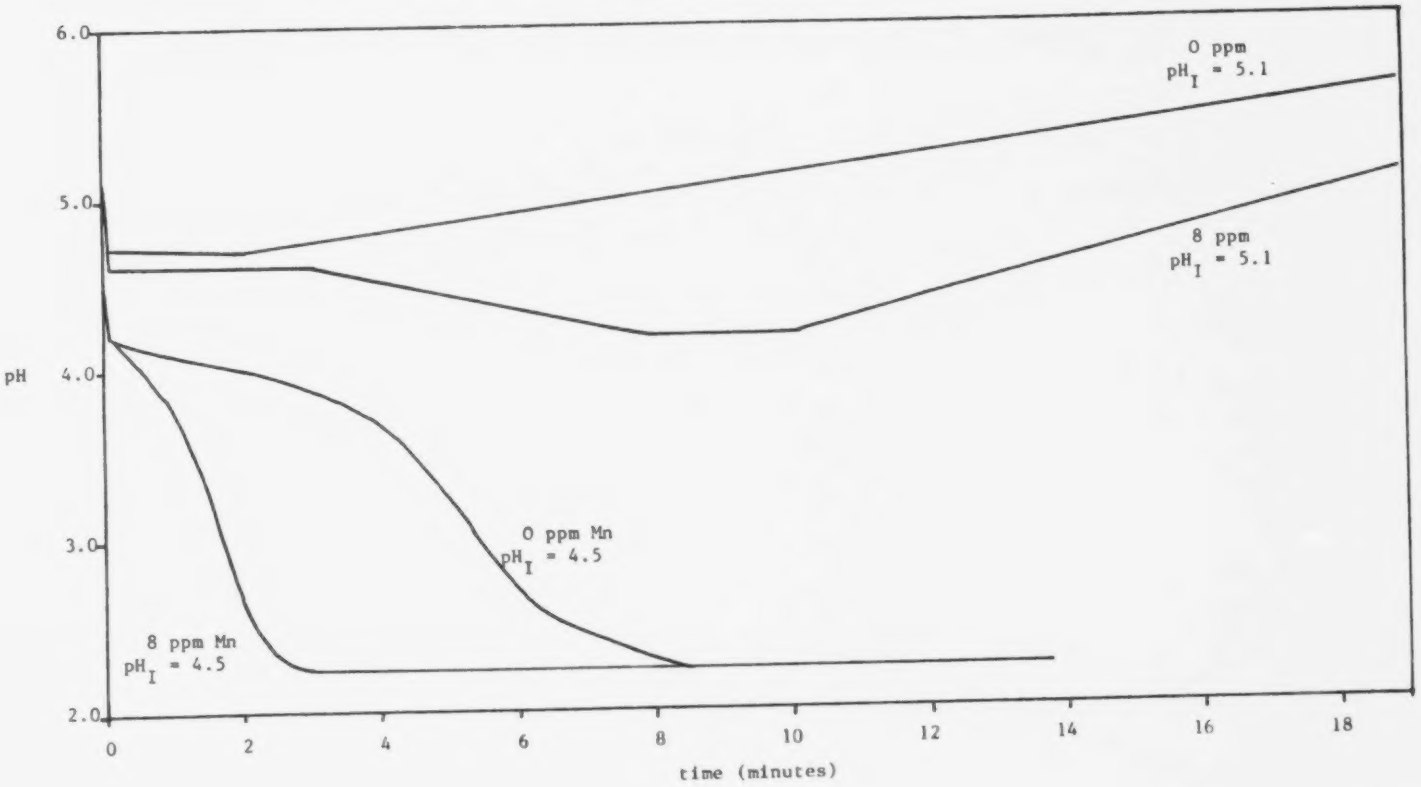

Figure 4-12. Effect of Catalyst on pH Behavior
(40°C)

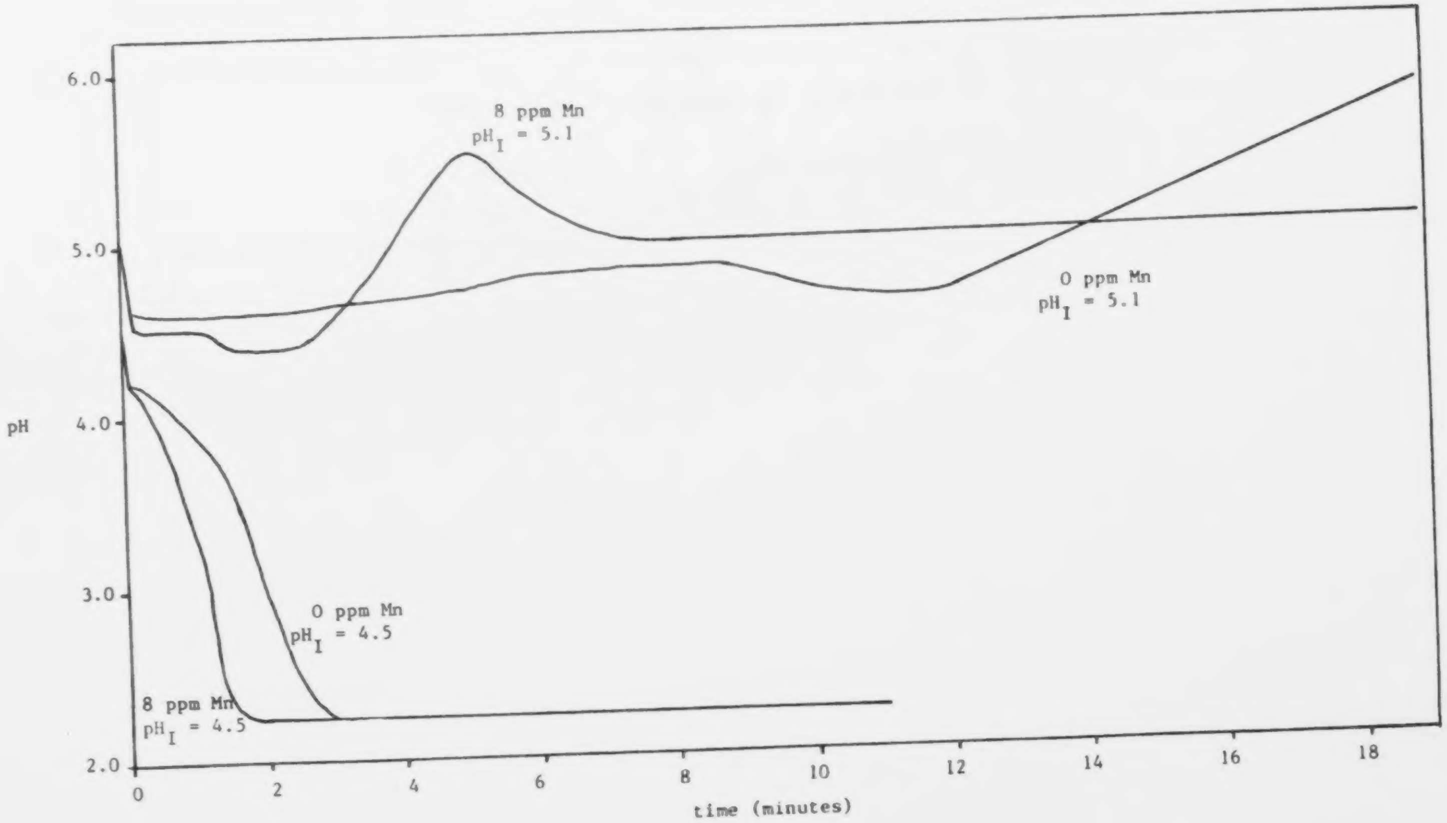

Figure 4-13. Effect of Catalyst on pH Behavior (50°C)

Experiments were also conducted in which manganese concentrations of 6.66, 200, and 2000 ppm were used. The operating conditions used were a 20 g/ℓ slurry density, 1800 rpm stirring speed, initial pH of 5.0, and temperature of $40^{\circ}C$. Table 4-4 lists the experiments used in this study. Examples of the data obtained in this study are shown in Figure 4-4. Figure 4-4 shows that the slurry reaction rate is strongly influenced by added manganese catalyst.

7. Liquid Phase Slurry Behavior

A series of slurry oxidations were run in which both the total and liquid sulfite concentrations were measured as a function of time. Table 4-5 gives the operating conditions used in these experiments. The results are shown in Figures 4-5 to 4-7, 4-9, 4-10, 4-14 to 4-17.

The pH vs time response curves for these slurry oxidations are shown in Figures 4-18 to 4-20.

8. pH Behavior During Reaction

In all cases, there is an abrupt drop in slurry pH upon the introduction of oxygen. This occurs within the first five seconds and is always between 0.3 and 0.5 pH units. From here, the pH will (a) continue dropping at a much slower rate, or (b) flatten out and begin to rise, or (c) a combination of (a) and (b), depending on the initial pH. At a pH below 5, curve type (a) is observed while at a pH above 5.1 type (b) is observed. The changeover between (a) and (b) (i.e. type c) occurs between 5.0 and 5.1. The exact reasons for the differing behaviors are not fully understood; however, it is the result of a complex relationship between $CaSO_3$ solubility, pH, and oxidation rate.

9. Slurry Reactions with and without pH Controller

As was mentioned before, there is an abrupt drop in the initial pH as soon as the reaction begins; thereafter, the pH varies according to the ini-

TABLE 4-4

EXPERIMENTS MADE IN Mn CATALYST STUDY (182)

Slurry Density = 20 g/ℓ   Stirring Speed = 1800 rpm

pH_I = 5

Run #	Mn Added	O_2 Flow Rate
450	200 ppm	3 ℓ/min
459*	200 ppm	"
468	200 ppm	"
470	2000 ppm	"
471	2000 ppm	6 ℓ/min
486	2000 ppm	"
485	2000 ppm	3 ℓ/min
400	6.66 ppm	"
401	6.66 ppm	"

* not shown in figure IV- 4

TABLE 4-5

EXPERIMENTAL CONDITIONS USED IN SLURRY OXIDATIONS SHOWN IN FIGURE 4-5 to 4-7, 4-9, 4-10, 4-14 to 4-17

Figure	Material Oxidized	Mn Added	Slurry Density	pH_I	Run #
IV-5	Calcium Sulfite	200 ppm	20 g/ℓ	5.0	461 468
IV-6	"	200 ppm	20 g/ℓ	4.5	487 488
IV-7	"	None	50 g/ℓ	4.5	474 477 385
IV-8	"	"	30 g/ℓ	4.5	473 475
IV-9	"	"	20 g/ℓ	4.5	441 465
IV-10	"	"	20 g/ℓ	4.7	440 435
IV-11	"	"	20 g/ℓ	5.0	463 464
IV-12	Laboratory Prepared Calcium Sulfite	200 ppm	12 g/ℓ	5.0	453 454 455 458 466 467
IV-13	"	None	12/ g/ℓ	5.0	469 476

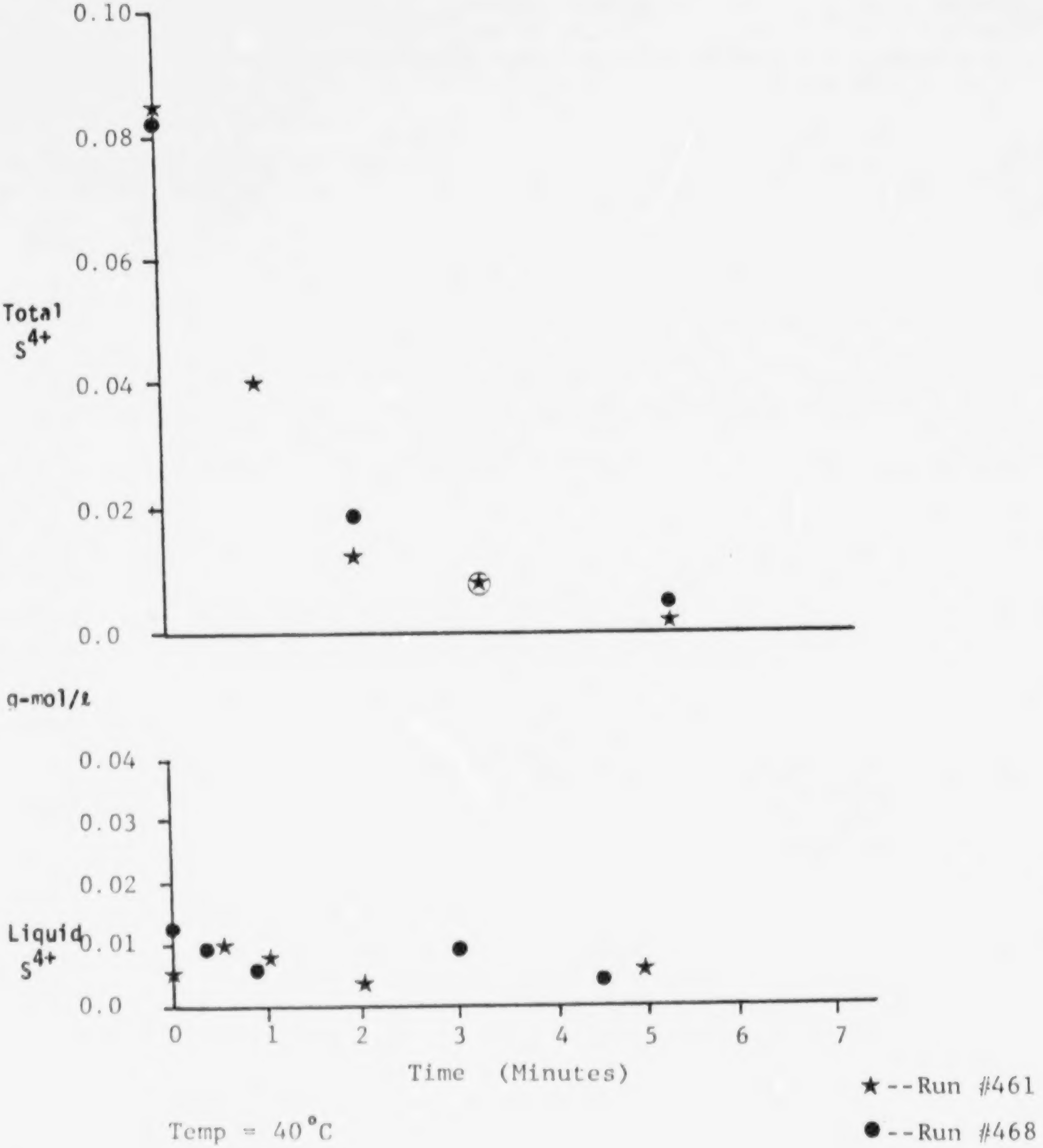

Temp = 40°C

pH_I = 5.0

Slurry Density = 20 g/ℓ

200 ppm Mn Added

Figure 4-14. Slurry Oxidation, 200 ppm Mn, pH = 5.0 (182)

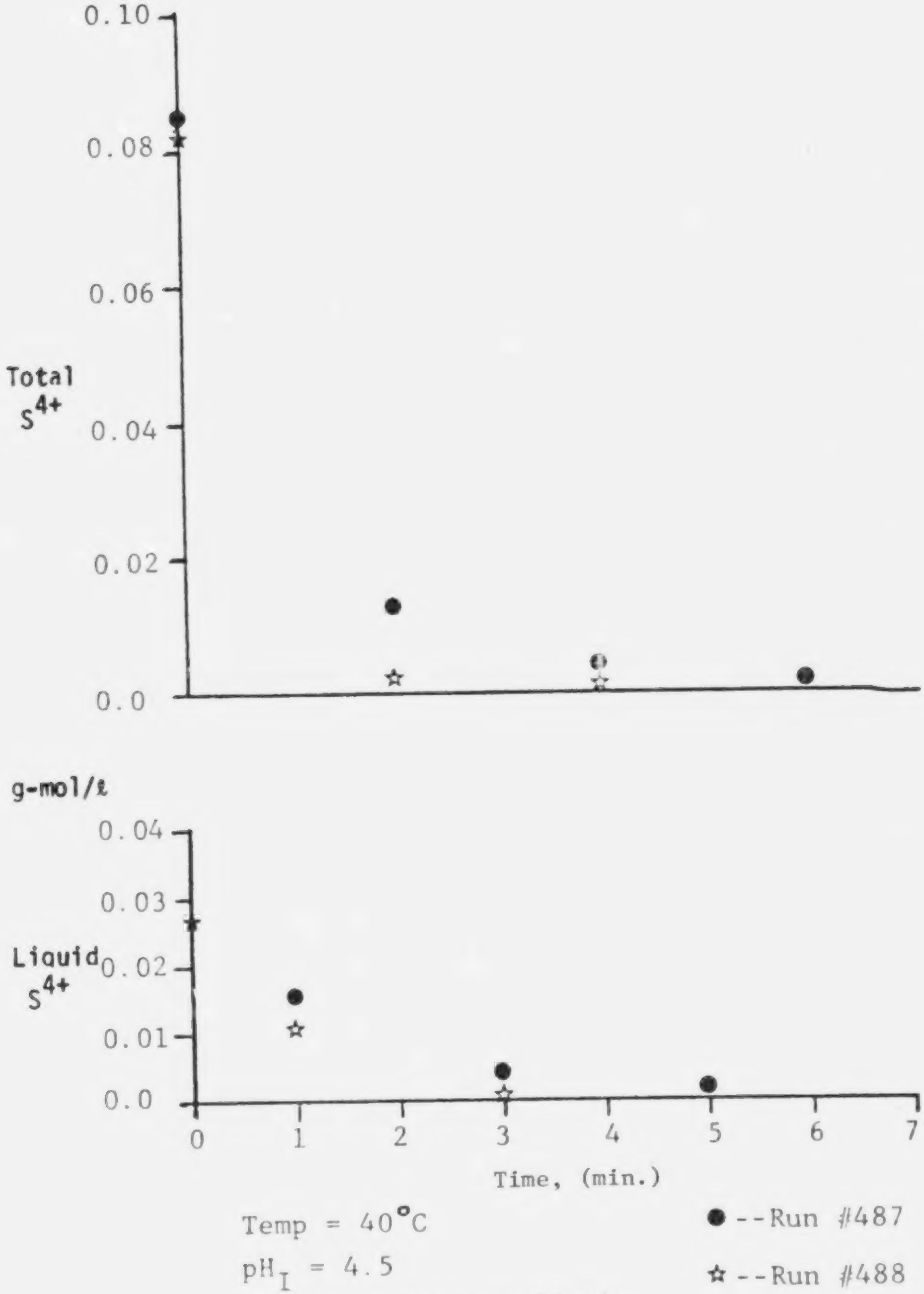

Temp = 40°C
pH_I = 4.5
Slurry Density = 20 g/ℓ
200 ppm Mn Added

Figure 4-15. Slurry Oxidation, 200 ppm Mn, pH = 4.5 (182)

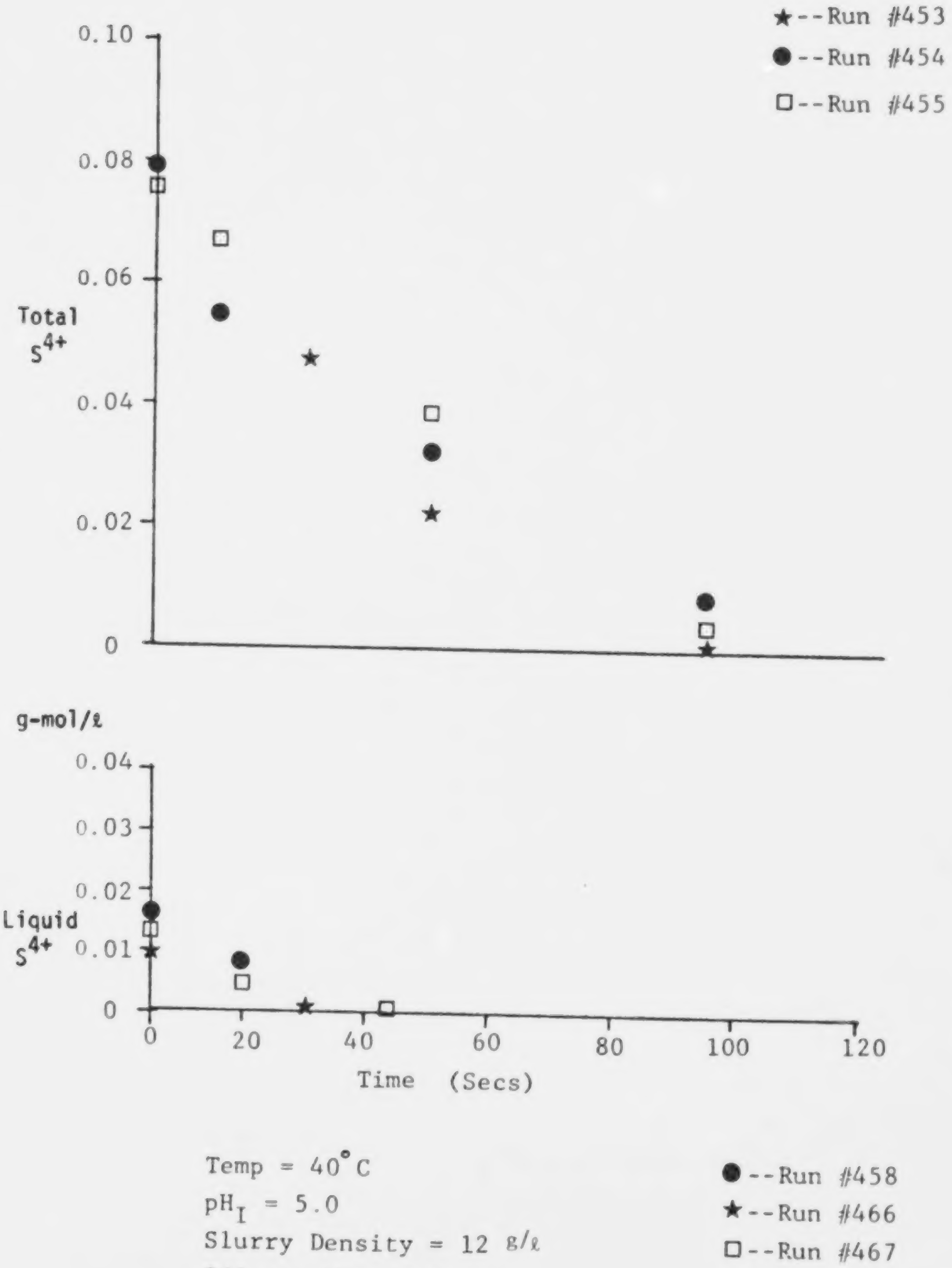

Temp = 40°C
pH_I = 5.0
Slurry Density = 12 g/ℓ
200 ppm MN Added
Laboratory Prepared Calcium Sulfite

Figure 4-16. Slurry Oxidation, 200 ppm Mn, pH=5.0 (182)

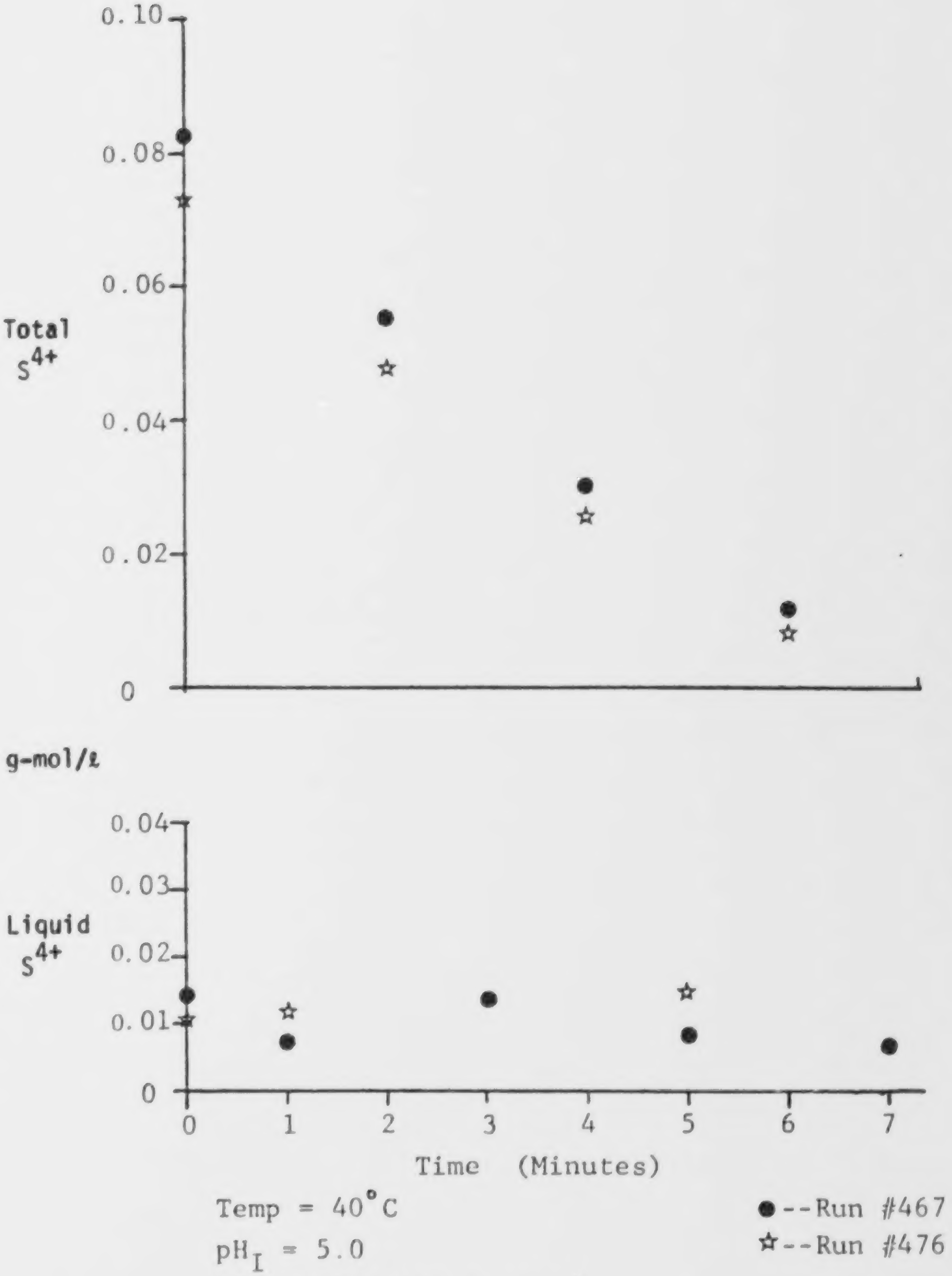

Temp = 40°C

pH_I = 5.0

Slurry Density = 12 g/ℓ

Laboratory Prepared Calcium Sulfite

Figure 4-17. Slurry Oxidation, pH = 5.0 (182)

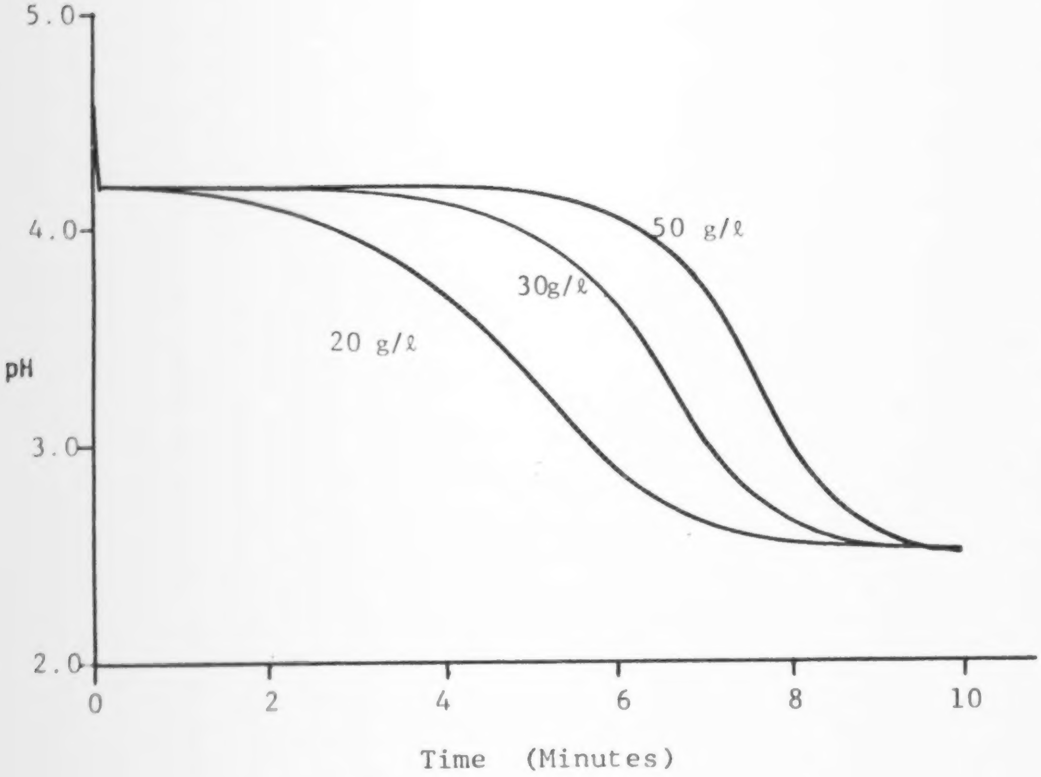

Temp = 40°C
pH_I = 4.5

Figure 4-18. pH Behavior During Slurry Oxidations; Effect of Slurry Density (182)

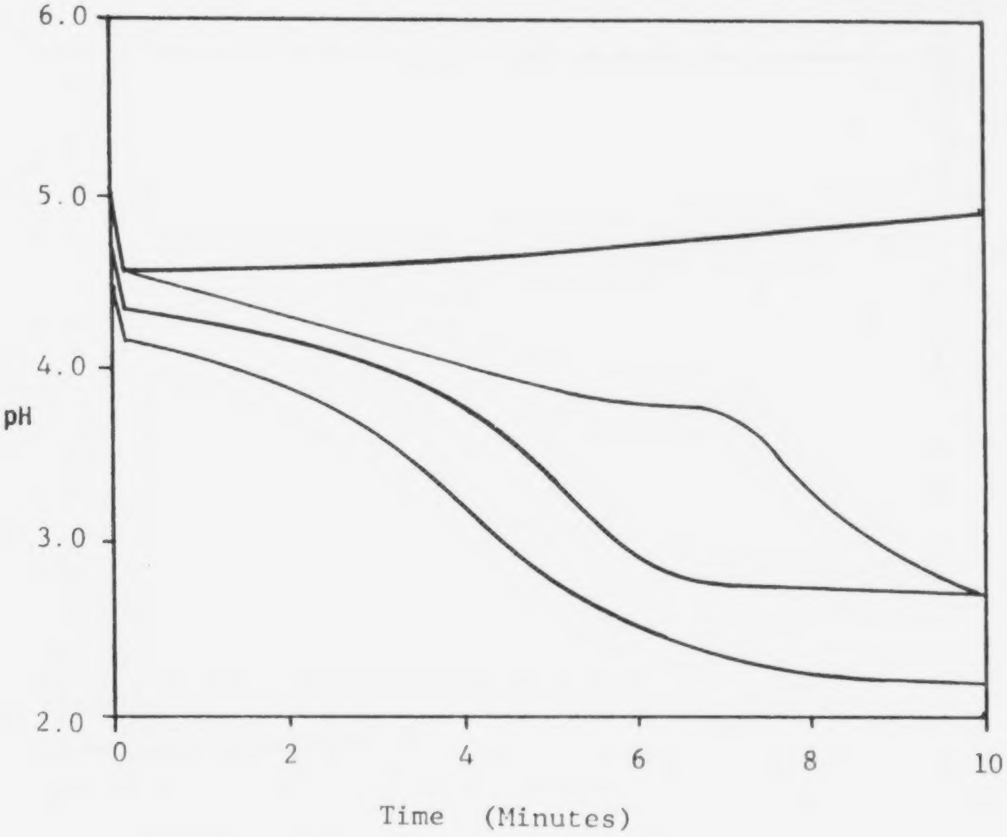

Temp = 40°C

Slurry Density = 20 g/ℓ

a) pH_I = 5.0

b) pH_I = 5.0 (Laboratory prepared calcium sulfite, Slurry Density = 12 g/ℓ

c) pH_I = 4.7

d) pH_I = 4.5

Figure 4-19. pH Behavior During Slurry Oxidations; Effect of Initial pH (182)

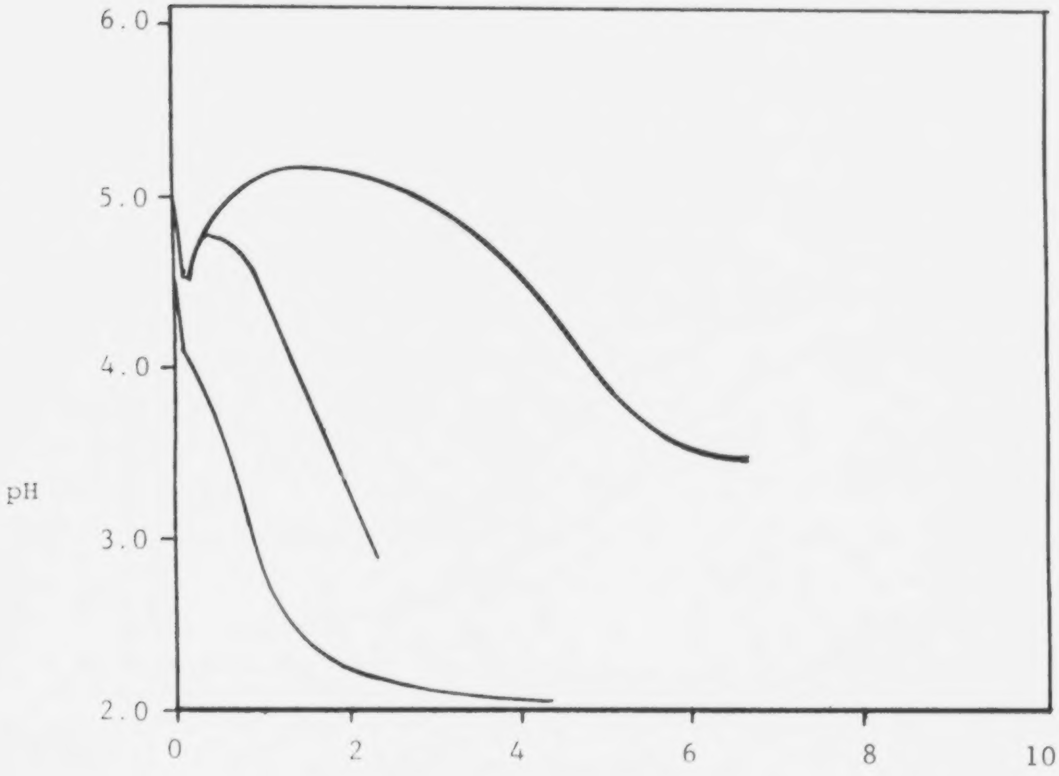

Temp = 40°C

a) 200 ppm Mn Added, Slurry Density = 20 g/ℓ

b) Laboratory Prepared Calcium Sulfite, 200 ppm Mn Added, Slurry Density = 12 g/ℓ

c) 200 ppm Mn Added, Slurry Density = 20 g/ℓ

Figure 4-20. pH Behavior During Slurry Oxidations; Highly Catalyzed Runs (182) tial conditions. Experiments were run by using a pH controller (to control the pumping of acid or base) to keep the pH of the solution at a fixed value in order to obtain reaction data at a constant pH over a longer period. The experimental conditions were:

Temperature = $40^\circ C$
Slurry Density = 20 g/ℓ
Stirring Speed = 1800 rpm
Initial pH = 5.0
Controlled pH = 4.6
Flow Rate of 100% O_2 = 3 ℓ/min

Both total and liquid sulfite concentrations were measured. The results were shown in Figure 4-21 which will be used for simulation by a mathematical model described below. Results of experiments under the same conditions but without using a pH controller were also shown in Fig. 4-21 for comparison. The reaction rate of the pH uncontrolled case is a little bit faster than that of the pH controlled case. But the difference is almost unnoticeable.

10. Liquid Phase Catalyst Study

A 20 g/ℓ slurry with an initial pH of 5.0 at $40^\circ C$ was oxidized. Filtered samples were periodically taken from the reactor and analyzed for manganese catalyst by North American Exploration Company. The results shown in Figure 4-22 show that the manganese concentration in the liquid phase of the reactor increases as the oxidation proceeds.

B. MATHEMATICAL MODEL

1. General Description of Model

A mathematical model was developed to predict both the liquid-phase and total sulfite behavior during slurry oxidations. The model was developed in general terms so that it could be used to simulate any experimental condi-

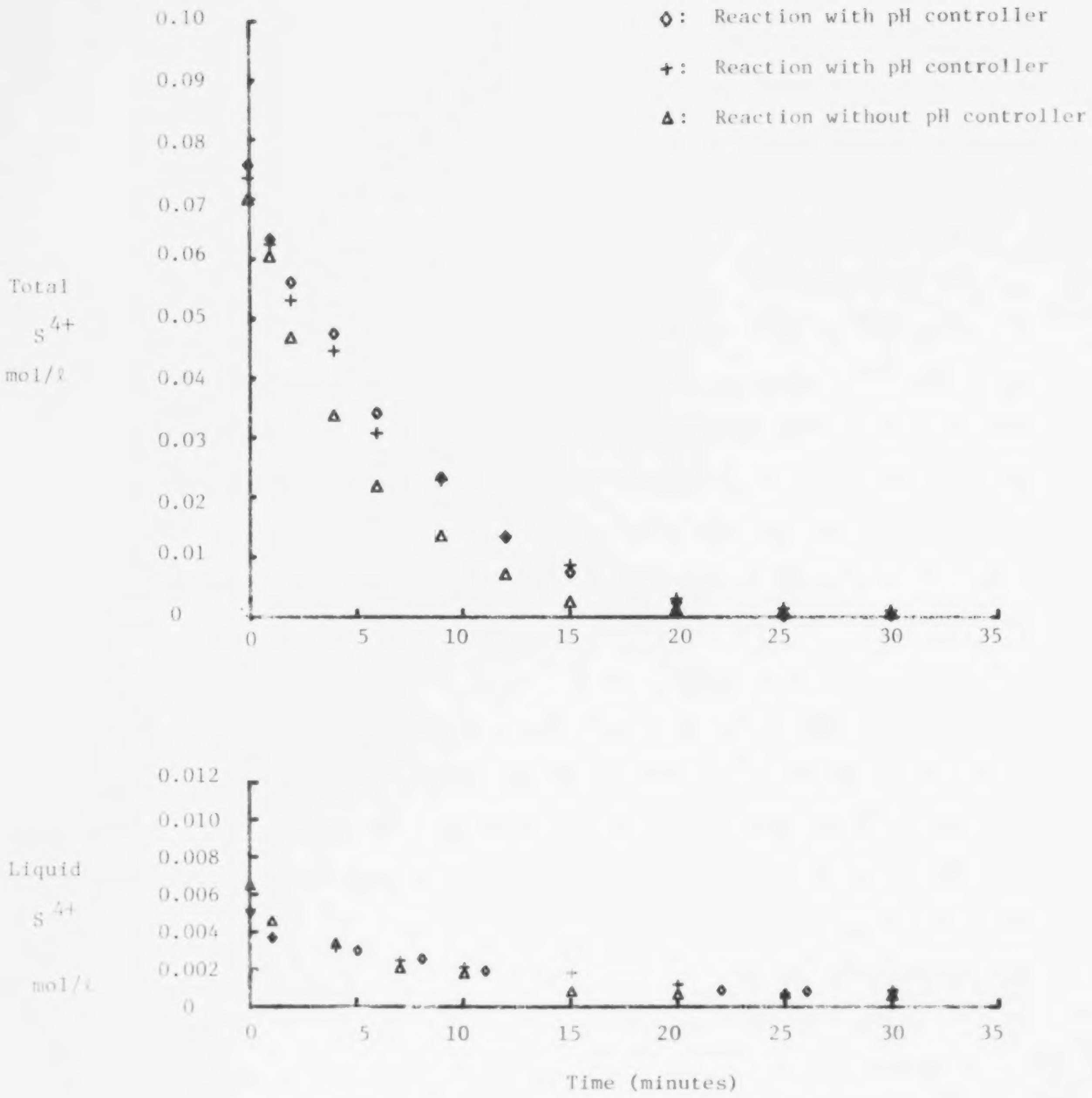

Temp = 40°C Stirring speed = 1800 rpm

pH = 5.0 Slurry Density = 20 g/ℓ

Figure 4-21. Slurry Oxidation with No Mn Added

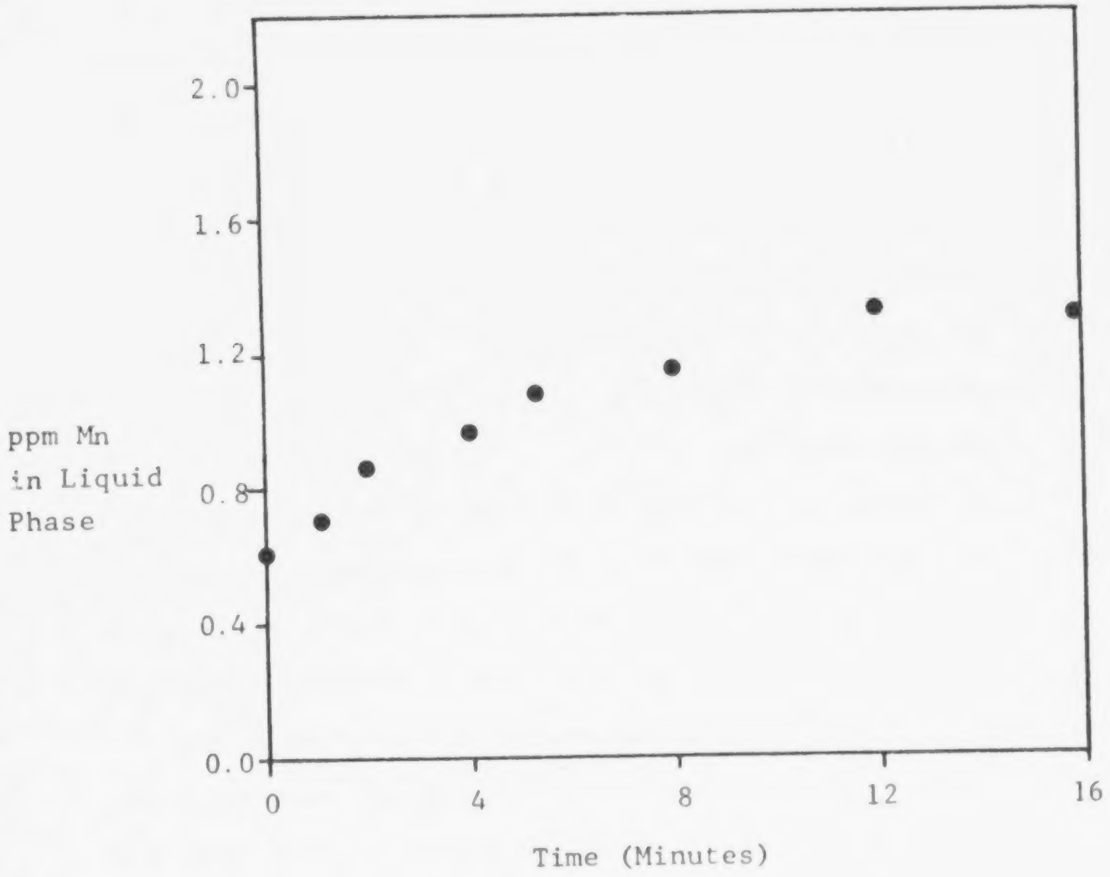

Temp = 40°C

pH_I = 5.0

Slurry Density = 20 g/ℓ

Figure 4-22. Liquid Phase Catalyst Behavior During Slurry Oxidations (182)

tions. This model is based on three simplifying assumptions. These assumptions can be relaxed if the model is further developed at a later date.

The first assumption is that the only loss of sulfite from the slurry occurs from the liquid phase oxidation of sulfite. It is also assumed that the oxygen concentration is constant at saturation at all times during the oxidation. Finally, the assumption is made that the hydrogen ion concentration is constant througout the liquid phase at all times during the oxidation of the slurry.

2. Physical Description of Particles

a. Electron micrograph

Electron micrographs were made of the crystals in the calcium sulfite slurries. A slurry with a density of 20 g/ℓ was prepared and the pH of the slurry was adjusted with sulfuric acid to a value of 4.5. A sample of this slurry was taken, filtered under nitrogen, washed with acetone, and dried in a vacuum oven. A JEOL JSM-35 scanning electron microscope set to magnifications of 3,000 X and 10,000 X was used to study the crystal structure of the calcium sulfite in the slurries. Electron micrographs obtained from this examination are presented in Figures 1-2 and 1-3. The general shape of the particles can be seen in Figure 1-2 while the features of the surface are shown in Figure 1-3. These solids, even before oxidation are a mixture of $CaSO_3$ (50% by weight) and $CaSO_4$. The flat platelike crystals are calcium sulfite and the large cylindrical crystals are calcium sulfate (162). The average aspect ratio of flat plates was found to be 8.46 : 3.7 : 1 (182). It can be seen from these figures that particles of calcium sulfite and calcium sulfate aggregate together and exist in the solution as rough spheres.

b. Particle size distribution

The particle size distribution, before oxidation, was determined by means of a Coulter counter using a electrolyte of 5% LiCl in methanol. The equivalent spherical diameter and the volume fraction are given in Table 4-6 for a typical sample. This initial size distribution was used in the mathematical model for the case of spherical particles as will be stated in subsection (3) below. For flat plates an equivalent size distribution was calculated by using the aspect ratio of 8.46 : 3.7 : 1.

3. Derivation of the Spherical Model

In the instant case the solid particles are rough spherical aggregates made up of tiny, flat platelike sulfite and cylindrical sulfate crystals. The model was thus developed for the case of spherical particles. The analysis for the case of all particles being flat plates is given in subsection (5).

The liquid phase concentration of sulfite in the slurry is governed by two competing mechanisms. Sulfite in the liquid is lost due to the oxidation reaction but is replenished by the dissolution of the solid calcium sulfite. This system of competing mechanisms can be represented by a differential equation of the form

$$\frac{d(VC_\ell)}{dt} = -VR_R + VR_m \tag{4.7}$$

where V = reactor volume
$C = [S^{4+}]$ liquid
R_R = reaction rate
R_m = disssolution rate

The kinetic rate expression has already been shown to be

$$R_R = -k\,C_\ell^{1.5} \tag{4.8}$$

The mass transfer of S^{+4} ions from solid to liquid can generally be given by

$$R_m = k_\ell\,a(C_s - C_\ell) \tag{4.9}$$

TABLE 4-6

SIZE DISTRIBUTION OF CALCIUM SULFITE PARTICLES
(COULTER METHOD)

Equivalent Spherical Diameter (μm)	Volume Fraction
2.52	.9
3.18	1.5
4.	2.3
5.04	4.6
6.35	9.6
8.	17.
10.08	19.3
12.7	20.1
16.	14.5
20.16	7.3
25.4	2.1
32	.7
40.32	.1
50.8	0.
64.	0.
80.64	0.

Geometric Mean Diameter	11.62 μm
Median	11.94 μm
Mode	13.07 μm
Standard Deviation	1.59 μm

Substitution of (4-8) and (4-9) into (4-7) gives the equation
where k_1 = mass transfer coefficient

a = interfacial area
C_s = saturation concentration

$$\frac{d(VC_\ell)}{dt} = - VkC_\ell^{1.5} + Vk_\ell\, a(C_s - C_\ell) \tag{4.10}$$

The volume of the reactor can be cancelled out of this expression as it remains constant

$$\frac{dC_\ell}{dt} = - k\, C_\ell^{1.5} + k_\ell\, a(C_s - C_\ell) \tag{4.11}$$

where a, the interfacial area of particles per unit volume, changes with time as the particles shrink and also as the smallest particles in the original size distribution dissolve away. It can be represented as

$$a = \frac{\sum_{i=1}^{n} 4\pi\, \gamma^2_i\, N_{t=0}\, h_i\, f_i}{V} \tag{4.12}$$

where γ_i = the radius of i type particles which is a function of time
$N_{t=0}$ = the initial total numbers of particles
h_i = No. fraction of i type particles
f_i = fraction of original number of i type particles remaining in reactor, f_i equals to 1 or 0
n = the number of particle size being considered. In this work, n is equal to 13.

Therefore

$$a = \frac{4\pi\, N_{t=0} \sum_{i=1}^{13} \gamma_i^2\, h_i\, f_i}{V} \tag{4.13}$$

Substitution of (4-13) into (4-11) gives the equation for liquid phase behavior in the slurry.

$$\frac{dC_\ell}{dt} = - kC_1^{1.5} + \frac{4\pi N_{t=0}\, k_\ell\, (C_s - C_\ell)}{V} \sum_{i=1}^{13} \gamma_i^2\, h_i\, f_i \qquad (4.14)$$

The rate of mass transfer from solid particle to liquid phase is given by the expression

$$\frac{d(\text{Total moles})}{dt} = - VR_m \qquad (4.15)$$

or

$$\frac{d(\text{Total moles})}{dt} = - Vk_\ell\, a(C_s - C_\ell) \qquad (4.16)$$

Multiplying by the molecular weight of calcium sulfite yields

$$\frac{dW}{dt} = - Vm\, k_\ell\, a(C_s - C_\ell) \qquad (4.17)$$

where

m = molecular weight of calcium sulfite
w = total mass of solid particles

$$= \rho\, V$$

$$= \rho \sum_{i=1}^{13} \frac{4}{3}\, \pi\gamma_i^3\, N_{t=0}\, h_i\, f_i$$

$$= \frac{4}{3}\, \pi\rho\, N_{t=0} \sum_{i=1}^{13} \gamma_i^3\, h_i\, f_i \qquad (4\text{-}18)$$

Substitution of (4-13) and (4-18) into (4-17) gives (4-19)

$$\frac{4}{3}\, \pi\rho\, N_{t=0}\, \frac{d}{dt} \left\{\sum_{i=1}^{13} \gamma_3^3\, h_i\, f_i\right\} = - 4\pi m k_\ell N_{t=0}(C_s - C_\ell)\left\{\sum_{i=1}^{13} \gamma_i^2\, h_i\, f_i\right\}$$

Equation (4-19) can be split into 13 equations corresponding to 13 types of solid particles

$$\frac{d\gamma_i}{dt} = - \frac{m\, k_\ell}{\rho}\, (C_s - C_\ell) \qquad (4\text{-}20) - (4\text{-}32)$$

$i = 1, 2, 3, ---, 13$

These equations describe the time rate of change of particle sizes.

The total concentration of sulfite at any time t is the sum of liquid phase and solid phase concentrations remaining in the solution.

$$C_T = C_\ell + \frac{\text{Total moles of solid sulfite}}{\text{Volume of Reactor}}$$

$$= C_\ell + \frac{\sum_{i=1}^{13} \frac{4}{3}\pi\gamma_i^3 \frac{\rho}{m} N_{t=0}\, h_i\, f_i}{V}$$

$$= C_\ell + \frac{\frac{4}{3}\pi\rho\, N_{t=0}}{Vm} \left\{\sum_{i=1}^{13} \gamma_i^3\, h_i\, f_i\right\} \tag{4-33}$$

Equations (4-14), (4-20), - (4-32) can be solved simultaneously to give C_ℓ and γ_i. Then from equation (4-33) the total concentration of sulfite, C_T can also be calculated.

4. Solutions of the Spherical Model

In solving the model, the loss of particles due to dissolution must be taken into account. The total number of particles remains constant until the smallest portion of particles in the original distribution dissolve away. The new number of particles can then be calculated by subtracting the number of particles in the lost portion from the original number of particles. The initial particle size distribution and the total number of particles can be found in Table 4-6 which is the result from Coulter counter analysis. The solution of the model will continue in this stepwise manner until all solid calcium sulfite is dissolved.

In the slurry oxidation reaction, as was noted before, there is a sharp drop in the initial pH as soon as the oxidation begins. Because of this sharp drop in the pH the initial liquid phase concentration of S^{4+} will no longer be equal to the saturation concentration of S^{4+}. Therefore, in the model, the initial liquid phase concentration is taken to be equal to the saturation concentration at time equal zero and initial pH. For times greater than zero, the saturation concentration in the model will be the saturation concentration at the average pH of the slurry as it oxidizes. For reactions without adding Mn catalysts, a pH controller was used to keep the pH at a fixed value during the course of reaction. Thus the saturation concentration at this pH can be used in the model.

A Runge-Kutta-Gill algorithm was chosen to solve this system of simultaneous differential equations. This model programmed in the BASIC language with the Runge-Kutta-Gill algorithm (program B-30) is shown in Figure 4-23. An example calculation of this program is shown in Figure 4-23.

The model was first used to determine the solid-liquid mass transfer coefficient. Computer runs were made to model the 2000 ppm Mn catalyzed slurry oxidation shown in Figure 4-4. From Section III we know that the liquid phase oxidation is 1.5 order. Computer curves were generated using a variety of mass transfer coefficients and a rate constant of 85 $\ell^{0.5}$/g-mol$^{0.5}$ sec as shown in Figure 4-24. A mass transfer coefficient of 0.02 cm/sec was seen to most closely fit the experimental data.

Using the mass transfer coefficient of 0.02 cm/sec, the model was then tested against the slurry oxidations with 0, 6.66, and 200 ppm added Mn catalysts. Results are presented in Figure 4-25, 4-26 and 4-27. The 1.5 order rate constants for 0, 6.66 and 200 ppm Mn added reactions are 0.35, 2.0, and 4.5 $\ell^{0.5}$/g-mol$^{0.5}$sec. The corresponding values of 1.5 order rate constants from experiments (Section III) are 0.162, 0.35, and 0.8 ~ 5 $\ell^{0.5}$/g-mol$^{0.5}$sec.

The liquid phase S^{4+} concentrations predicted by the model using k_ℓ = 0.02 cm/sec for the 0 ppm Mn added case were also compared to the experimental data as shown in Fig. 4-28. It can be seen that the predicted results don't fit the experimental data well. The liquid S^{+4} concentration profiles pre-

```
B30

10  REM                           B30
20  REM                         23MAY79
30  REM
40  REM THIS PROGRAM MODELS SISSOLUTION & REACTION IN CASO4 SLURRIES
50  REM -------------------- INPUT SECTION-------------------------
60  REM DENSITY
70  R7=2.29
80  REM CHEMICAL REACTION RATE CONSTANT(1.5 ORDER)
90  A=5
100  REM    MASS TRANSFER COEFFICIENT
110  K=0
120  REM INITIAL NUMBER OF PARTICLES
130  M=1.34E+10
140  A1=0
150  REM COEF :RHO*4/3*M*PI/MOL WT/RXR VOL
160  Z=R7*.0541*M
170  REM SATURATION CONCENTRATION OF THE LIQUID AT THE INITIAL PH
180  C=.01
190  REM INITIAL TIME
200  T1=0
210  REM FINAL TIME
220  T2=420
230  REM  STEP SIZE
240  E=.5
250  REM NUMBER OF ITERATIONS PER STEP
260  N2=10
270  REM  FRACTION OF EACH STEPSIZE ON THE HISTOGRAM
280  DIM W[15],P[14],X[15],Q[15],D[14],B[14]
290  W[1]=.2018
300  X[1]=1.26
310  W[2]=.1674
320  X[2]=1.59
330  W[3]=.129
340  X[3]=2
350  W[4]=.129
360  X[4]=2.52
370  W[5]=.1345
380  X[5]=3.175
390  W[6]=.1191
400  X[6]=4
410  W[7]=.0676
420  X[7]=5.04
430  W[8]=.0352
440  X[8]=6.35
450  W[9]=.0127
460  X[9]=8
470  W[10]=.00319
480  X[10]=10.08
500  W[11]=.00046
510  X[11]=12.7
520  W[12]=.000077
530  X[12]=16
540  W[13]=.000005
550  X[13]=20.16
560  X[14]=.0055
570  DIM R[16]
580  MAT  READ R
590  DATA 0,.5,0,.5,.5,.292893,1.70711,.166667
```

Figure 4-23 B30 Program and Sample Calculation

```
 600  DATA 2,1,1,2,.5,.292893,1.70711,.5
 610  REM
 620  REM-------- INITIAL VALUES NEEDED ------
 630  C5=0
 640  REM FLAG FOR FIRST PASS THROUGH PROGRAM
 650  F7=0
 660  REM Y IS A COUNTER FOR HISTOGRAM STEPS
 670  Y=1
 680  REM   F IS THE FRACTION OF PARTICLES REMAINING
 690  F=1
 700  REM INITIAL SULFUR +4 CONCENTRATION TOTAL
 710  C7=.0822
 720  REM VARIOUS VARIABLES INITIALIZED
 730  FOR I=1 TO 14
 750  X[I]=X[I]*.0001
 760  Q[I]=0
 770  D[I]=0
 780  B[I]=1
 790  NEXT I
 800  X[14]=.0055
 810  REM INITIAL TIME
 820  T=T1
 830  REM COUNTER VARIABLE
 840  N3=N2
 850  REM
 860  REM ----------------------- HEADING --------------------------
 870  PRINT
 880  PRINT "SOLUTION ON ";T1;" TO ";T2;"SEC BY";E;"SEC PRINTED EA ";E*N2;"
 890  PRINT
 900  PRINT "RATE CONSTANT                (L90)            A=";A
 910  PRINT "MASS TRANSFER COEF           (L110)           K=";K
 920  PRINT "INITIAL # PARTICLES          (L130)           M=";M
 930  PRINT "SATURATION CONC              (L180)           C=";C
 935  PRINT "INITIAL TOTAL CONC           (L710)          C7=";C7
 940  PRINT "INITIAL LIQUID CONC          (L560)      X(14) =";X[14]
 945  PRINT
 950  PRINT "TIME ";TAB(12);"TOTAL S+4";TAB(27);"S+4 IN SOLN";
 960  PRINT TAB(41);"BIGGEST XTAL";TAB(55);"FRACTION LEFT"
 970  PRINT
 980  REM
 990  REM------------------------- CALCULATIONS --------------------------
1000  GOTO 1160
1010  FOR J=1 TO 4
1020  T=T+R[J]*E
1030  REM    SUBROUTINE CALL FOR EFFECT OF HISTOGRAM
1040  GOSUB 1290
1050  FOR I=Y TO 14
1060  S=R[J+4]*(D[I]-R[8+J]*Q[I])
1070  X[I]=X[I]+E*S
1080  Q[I]=Q[I]+3*S-R[12+J]*D[I]
1090  NEXT I
1100  C5=0
1110  NEXT J
1120  FOR I=Y TO 13
1130  C5=C5+X[I]^3*W[I]
1140  NEXT I
1150  C7=C5*Z+X[14]
1160  IF N3-N2<0 THEN 1260
1170  N3=0
1180  REM
1190  REM----------------------- OUTPUT -------------------------------
1200  REM
1210  PRINT INT(T);
1220  PRINT TAB(12);C7;TAB(27);X[14];
1230  PRINT TAB(41);X[13];TAB(55);F
1240  PRINT
```

Figure 4-23 B30 Program and Sample Calculation

```
1250  REM--------- END OF LOOP -----
1260  N3=N3+1
1270  IF T-T2<0 THEN 1010
1280  STOP
1290  REM
1300  REM------------------- SUBROUTINE --------------------  ------------
1310  REM
1320  REM DETERMINES K FROM HISTOGRAM
1330  FOR I=Y TO 13
1340  IF X[I]>0 THEN 1400
1350  B[I]=0
1360  Y=Y+1
1370  X[I]=0
1380  F=F-W[Y-1]
1390  GOTO 1410
1400  NEXT I
1410  IF F<.000005 THEN 1430
1420  GOTO 1440
1430  F=0
1440  REM THIS IS THE SET OF FOURTEEN GOVERNING EQUATIONS
1450  FOR I=Y TO 13
1460  D[I]=-B[I]*K*.05633*(C-X[14])
1470  NEXT I
1480  A1=0
1490  FOR I=Y TO 13
1500  A1=A1+W[I]*X[I]^2
1510  NEXT I
1520  D[14]=-A*X[14]^1.5+A1*K*M*12.566*(C-X[14])/600
1530  RETURN
1540  END
```

Figure 4-23 B30 Program and Sample Calculation

Sample Calculation

```
90 A=20
110 K=0.008
130 M=1.16E10
180 C=0.012
710 C7=0.07



RUN
B30

SOLUTION ON  0     TO  420  SEC BY .5          SEC PRINTED EA  5     SEC

RATE CONSTANT              (L90)           A= 20
MASS TRANSFER COEF         (L110)          K= .008
INITIAL # PARTICLES        (L130)          M= 1.16000E+10
SATURATION CONC            (L180)          C= .012
INITIAL TOTAL CONC         (L710)         C7= .07
INITIAL LIQUID CONC        (L560)    X(14) = .0055

TIME        TOTAL S+4      S+4 IN SOLN    BIGGEST XTAL   FRACTION LEFT

 0           .07            .0055          .002016        1

 5           5.78475E-02    1.94055E-03    1.99436E-03     1

 10          4.97928E-02    1.79136E-03    1.97152E-03     1

 15          .042669        1.64645E-03    1.94836E-03     1

 20          3.64141E-02    1.50611E-03    1.92487E-03     1

 25          3.09583E-02    1.37228E-03    1.90107E-03     1

 30          .026223        1.24701E-03    1.87698E-03     .7982

 35          2.21298E-02    1.12986E-03    1.85262E-03     .6308

 40          1.86077E-02    1.02028E-03    .001828        .6308

 45          1.55933E-02    9.18142E-04    1.80315E-03     .5018

 50          1.30272E-02    8.22961E-04    1.77807E-03     .5018

 55          1.08547E-02    7.35504E-04    1.75279E-03     .3728

 60          9.02356E-03    6.54963E-04    1.72731E-03     .3728

 65          7.48844E-03    5.81645E-04    1.70167E-03     .3728

 70          6.20423E-03    5.16100E-04    1.67586E-03     .2383

 75          5.13367E-03    4.56256E-04    1.64992E-03     .2383

 80          4.24517E-03    4.02797E-04    1.62385E-03     .2383

 85          3.50686E-03    3.56470E-04    1.59766E-03     .1192

 90          2.89307E-03    3.14528E-04    1.57138E-03     .1192
```

Figure 4-23 B30 Program and Sample Calculation

```
95          2.38594E-03    2.76438E-04    .001545      .1192
100         1.96842E-03    2.42906E-04    1.51855E-03    .1192
105         1.62346E-03    2.14327E-04    1.49203E-03    5.16001E-02
110         1.33784E-03    1.88613E-04    1.46544E-03    5.16001E-02
115         1.10293E-03    1.65146E-04    1.43880E-03    5.16001E-02
120         9.10928E-04    1.44219E-04    1.41211E-03    5.16001E-02
125         7.54061E-04    1.26295E-04    1.38538E-03    5.16001E-02
130         6.24711E-04    1.11525E-04    1.35861E-03    1.64001E-02
135         5.17282E-04    9.84341E-05    1.33181E-03    1.64001E-02
140         4.28522E-04    8.64308E-05    1.30498E-03    1.64001E-02
145         3.55763E-04    7.55250E-05    1.27812E-03    1.64001E-02
150         2.96447E-04    6.58617E-05    1.25124E-03    1.64001E-02
155         2.48060E-04    5.76447E-05    1.22434E-03    1.64001E-02
160         2.08136E-04    5.10263E-05    1.19743E-03    3.70005E-03
165         1.74703E-04    4.54171E-05    1.17050E-03    3.70005E-03
170         1.46657E-04    4.03409E-05    1.14356E-03    3.70005E-03
175         1.23251E-04    3.56746E-05    1.11660E-03    3.70005E-03
180         1.03851E-04    3.14083E-05    1.08964E-03    3.70005E-03
185         8.78620E-05    2.75745E-05    1.06267E-03    3.70005E-03
190         7.47100E-05    2.42269E-05    1.03569E-03    3.70005E-03
195         6.38342E-05    2.14349E-05    1.00870E-03    3.70005E-03
200         5.46983E-05    1.92097E-05    9.81709E-04    5.10053E-04
205         4.69002E-05    1.73375E-05    9.54712E-04    5.10053E-04
210         4.02028E-05    1.56727E-05    9.27711E-04    5.10053E-04
215         3.44502E-05    1.41508E-05    9.00706E-04    5.10053E-04
220         2.95233E-05    1.27446E-05    8.73698E-04    5.10053E-04
225         2.53211E-05    1.14448E-05    8.46687E-04    5.10053E-04
230         2.17520E-05    1.02517E-05    8.19673E-04    5.10053E-04
235         1.87297E-05    9.17095E-06    7.92656E-04    5.10053E-04
240         1.61717E-05    8.21200E-06    7.65638E-04    5.10053E-04
245         1.39981E-05    7.38694E-06    7.38617E-04    5.00532E-05
250         1.21346E-05    6.68743E-06    7.11594E-04    5.00532E-05
255         1.05246E-05    6.07580E-06    6.84570E-04    5.00532E-05
```

Figure 4-23 B30 Program and Sample Calculation

Reproduced from best available copy.

```
260        9.12890E-06    5.52662E-06    6.57545E-04    5.00532E-05
265        7.91825E-06    5.02473E-06    6.30518E-04    5.00532E-05
270        6.86981E-06    4.56117E-06    6.03491E-04    5.00532E-05
275        5.96450E-06    4.13083E-06    5.76462E-04    5.00532E-05
280        5.18575E-06    3.73107E-06    5.49433E-04    5.00532E-05
285        4.51858E-06    3.36087E-06    5.22402E-04    5.00532E-05
290        3.94921E-06    3.02040E-06    4.95371E-04    5.00532E-05
295        3.46468E-06    2.71067E-06    4.68339E-04    5.00532E-05
300        3.05276E-06    2.43340E-06    4.41306E-04    5.00532E-05
305        2.70178E-06    2.19090E-06    4.14273E-04    0
310        2.40076E-06    1.98351E-06    3.87239E-04    0
315        2.14048E-06    1.80465E-06    3.60205E-04    0
320        1.91393E-06    1.64819E-06    3.33171E-04    0
325        1.71576E-06    1.50960E-06    3.06136E-04    0
330        1.54177E-06    1.38555E-06    2.79101E-04    0
335        1.38861E-06    1.27353E-06    2.52065E-04    0
340        1.25354E-06    1.17166E-06    2.25030E-04    0
345        1.13429E-06    1.07852E-06    1.97994E-04    0
350        1.02895E-06    9.93049E-07    1.70958E-04    0
355        9.35874E-07    9.14453E-07    1.43922E-04    0
360        8.53619E-07    8.42144E-07    1.16885E-04    0
365        7.80715E-07    7.75703E-07    8.98487E-05    0
370        7.16623E-07    7.14843E-07    6.28120E-05    0
375        6.59712E-07    6.59383E-07    3.57751E-05    0
380        6.09237E-07    6.09232E-07    8.73811E-06    0
385        5.64329E-07    5.64329E-07    0             0
390        5.24210E-07    5.24210E-07    0             0
395        4.88221E-07    4.88221E-07    0             0
400        4.55816E-07    4.55816E-07    0             0
405        4.26532E-07    4.26532E-07    0             0
410        3.99983E-07    3.99983E-07    0             0
415        3.75838E-07    3.75838E-07    0             0
420        3.53814E-07    3.53814E-07    0             0
```

Figure 4-23 B30 Program and Sample Calculation

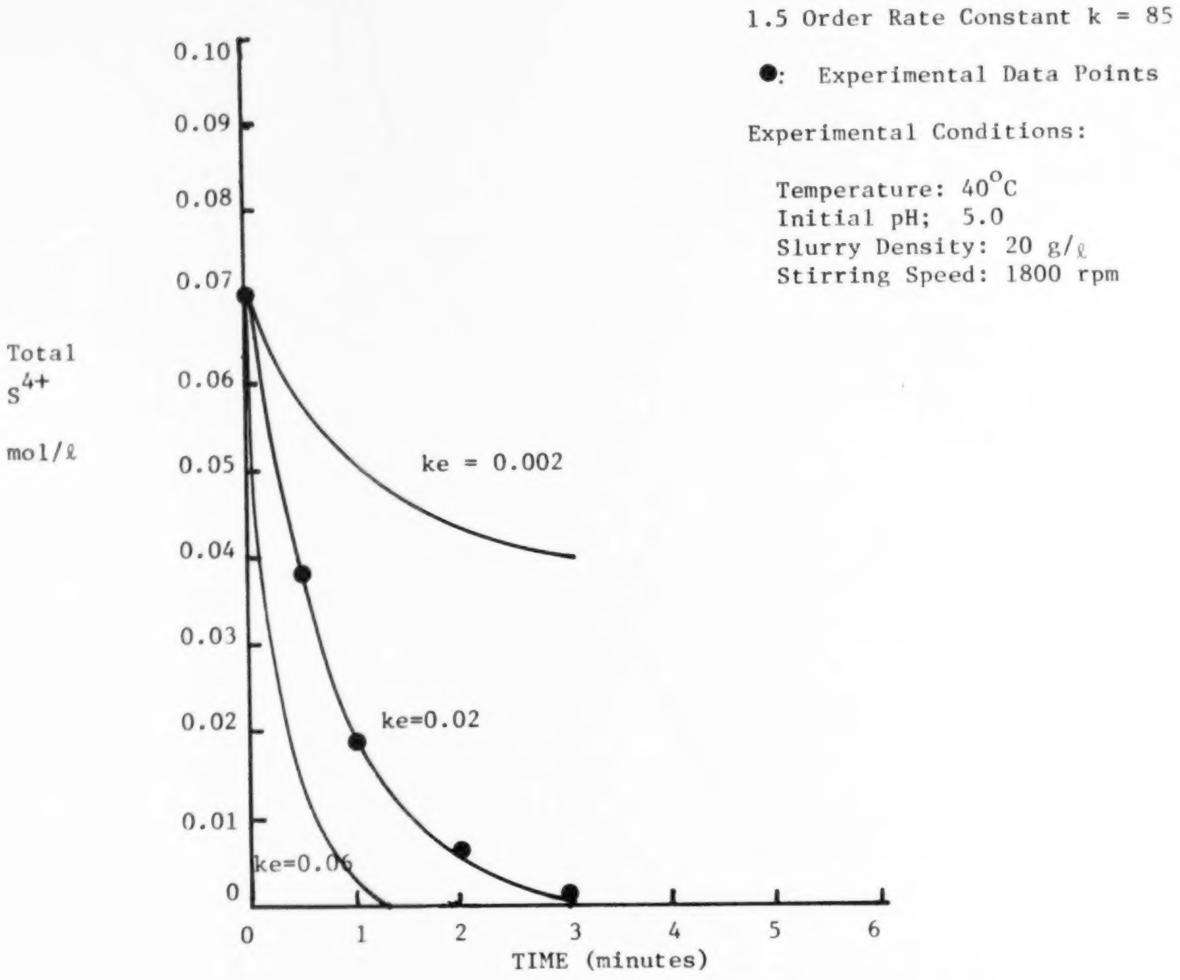

1.5 Order Rate Constant k = 85

●: Experimental Data Points

Experimental Conditions:

Temperature: 40°C
Initial pH; 5.0
Slurry Density: 20 g/ℓ
Stirring Speed: 1800 rpm

Figure 4-24. Determination of ke from Highly Catalyzed Slurry Data (2000 ppm Mn Added)

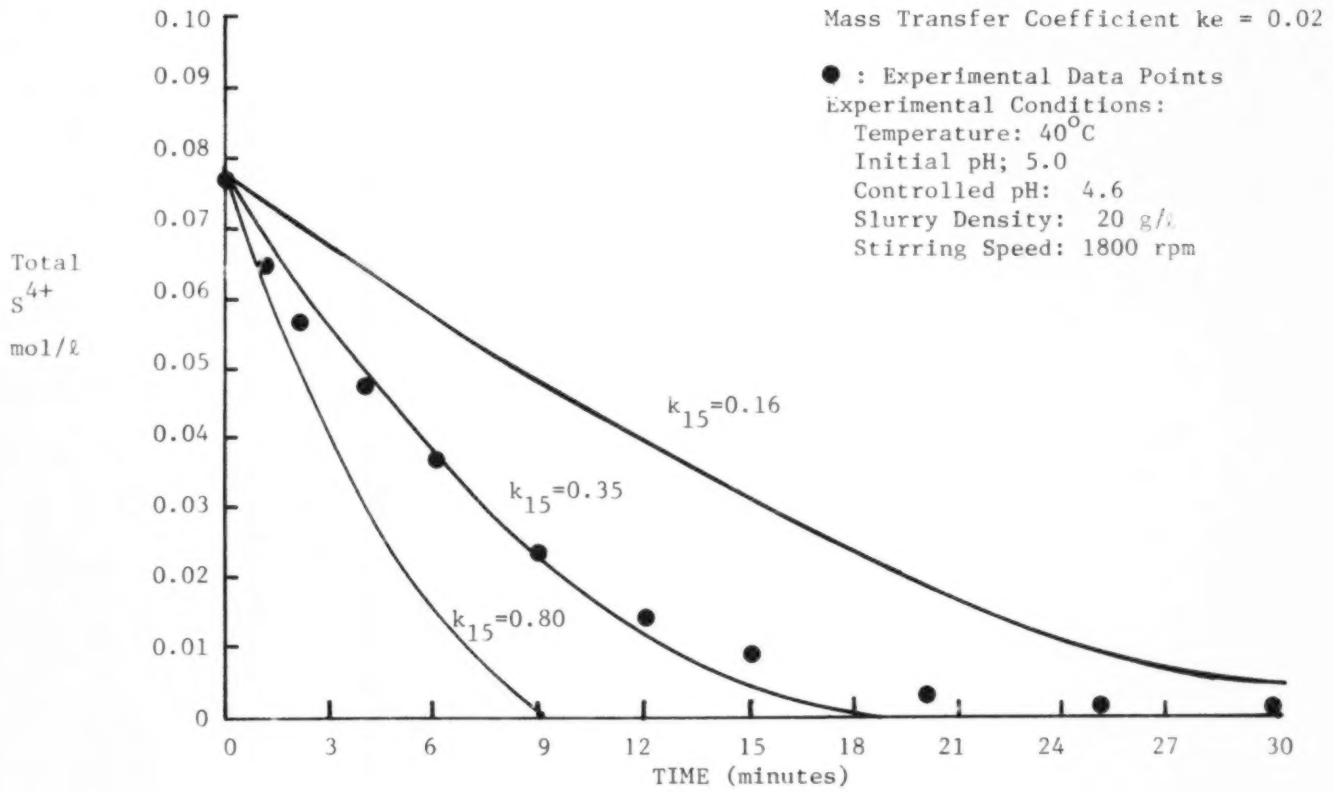

Figure 4-25. Comparison of Total S^{4+} from Model to Experimental Slurry Oxidation Data for No Added Mn.

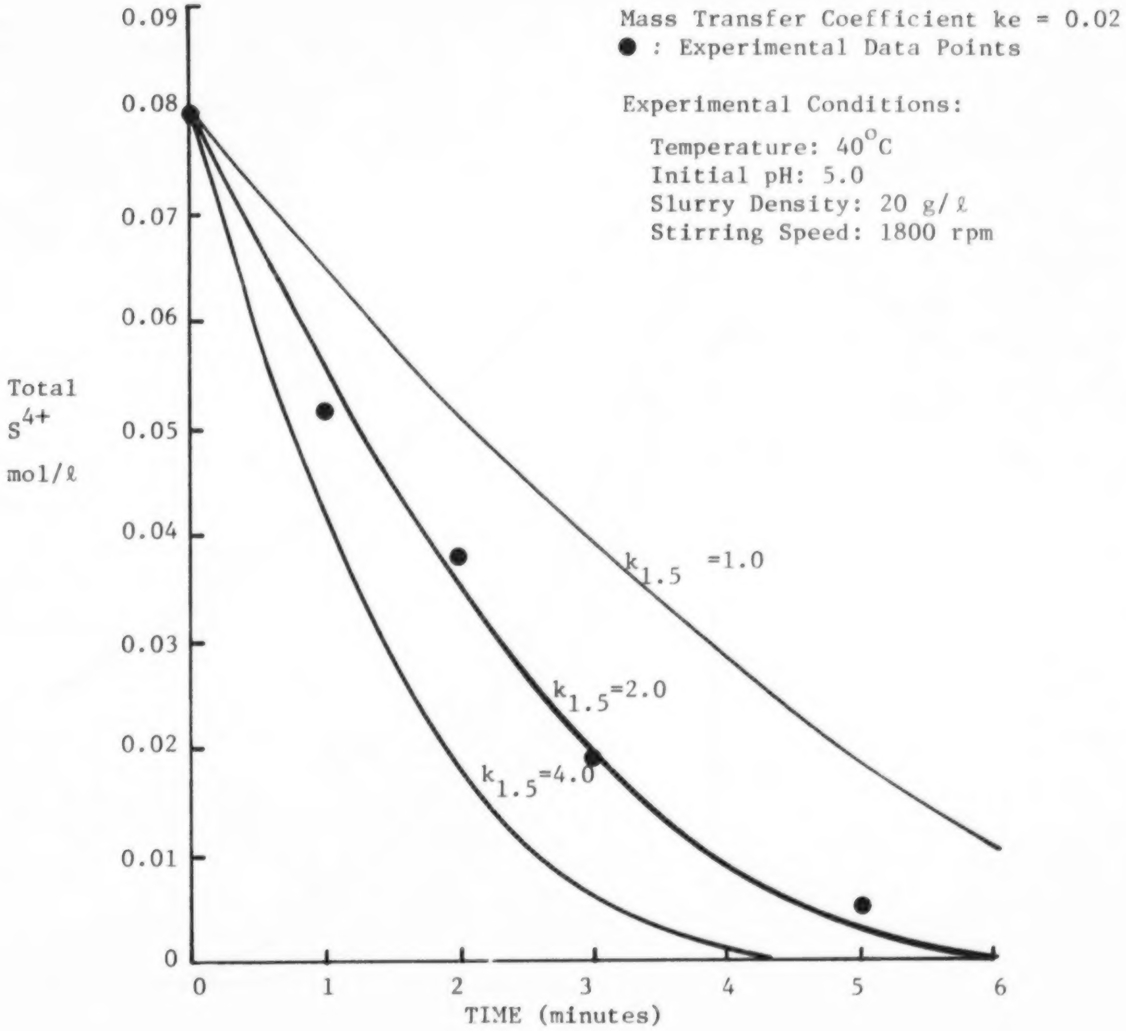

Figure 4-26. Comparison of Model to Experimental Slurry Oxidation Data for 6.66 ppm Mn Added

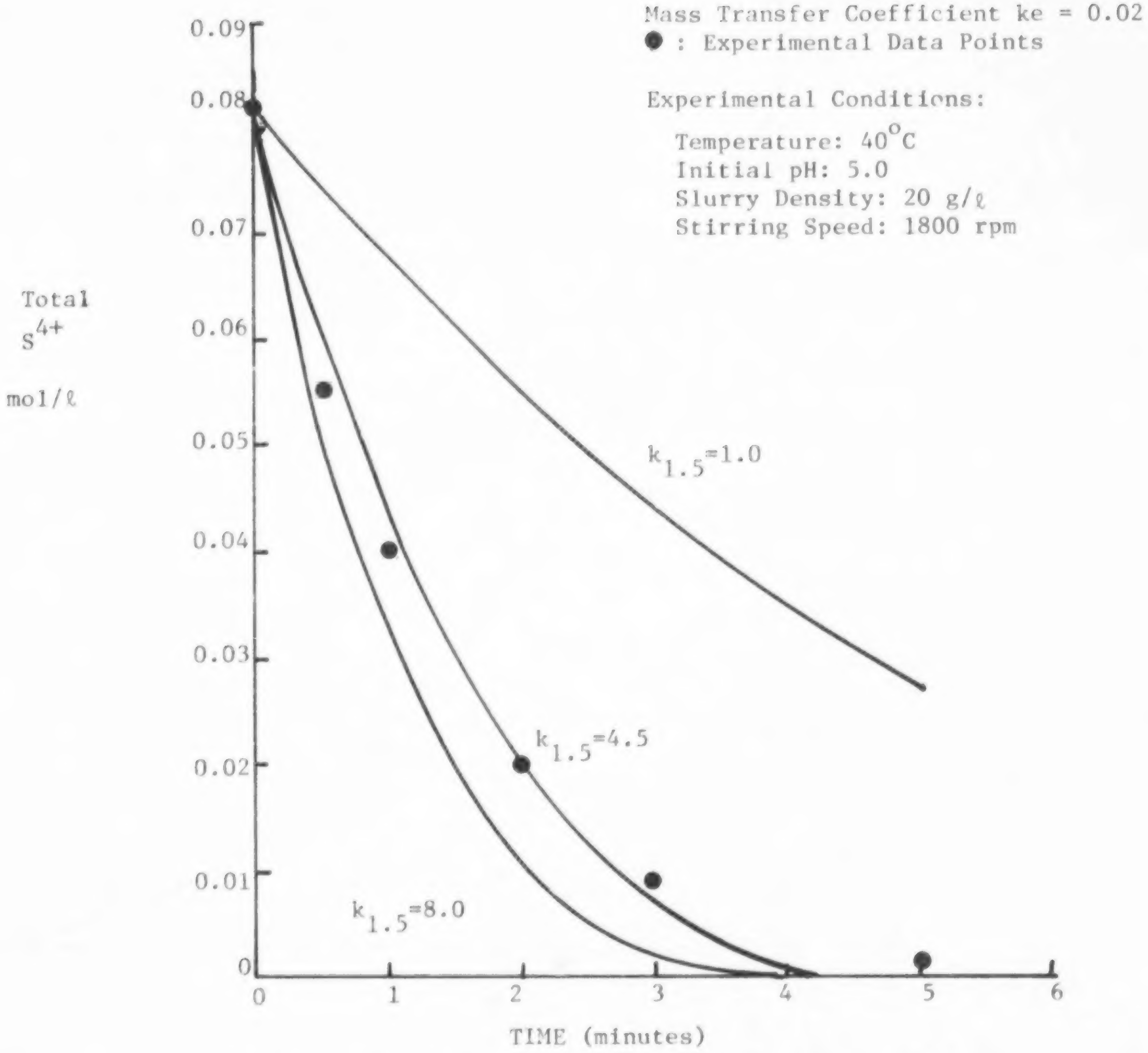

Figure 4-27. Comparison of Model to Experimental Slurry Oxidation Data for 200 ppm Mn Added.

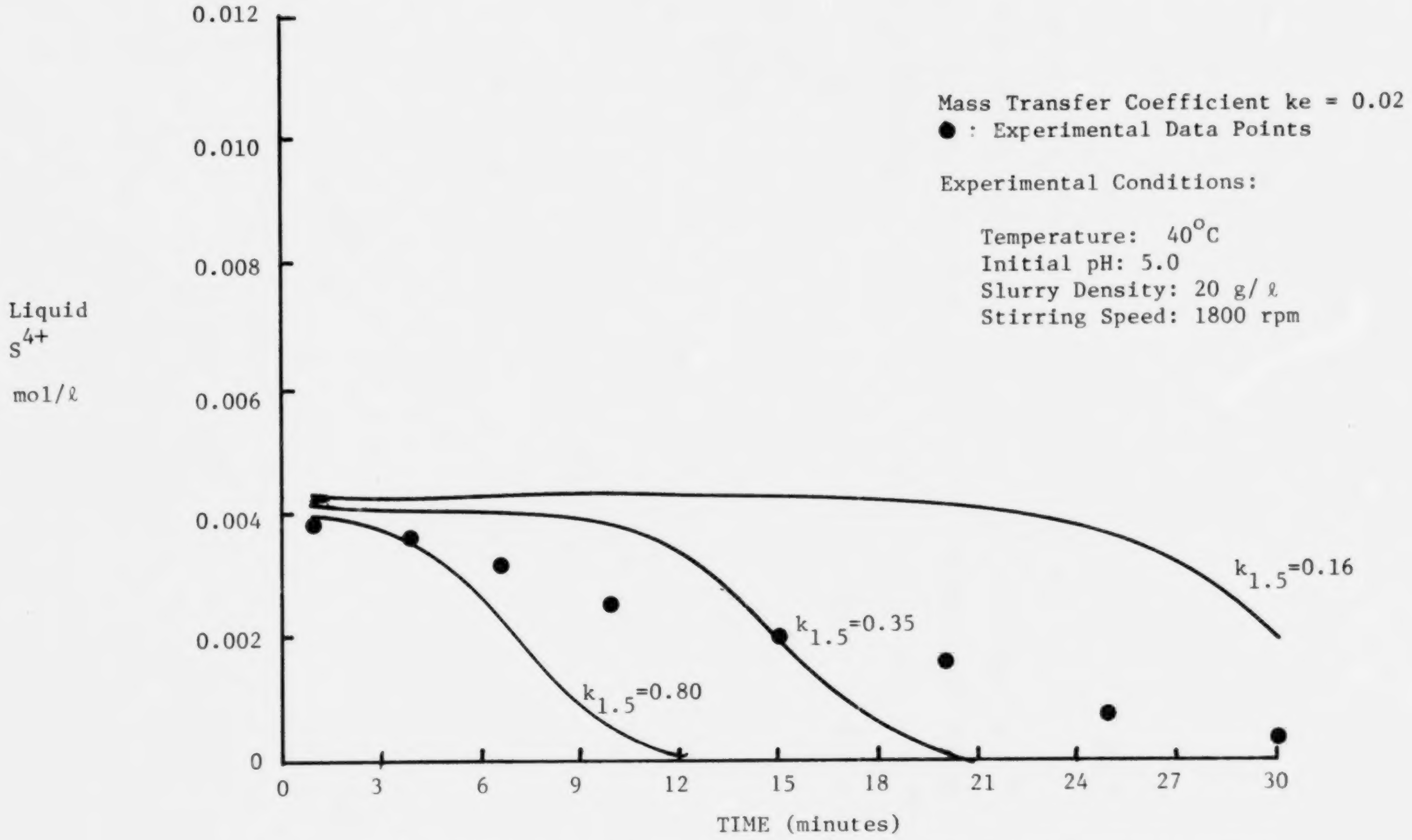

Figure 4-28 Comparison of Liquid S^{4+} from the Model to Experimental Slurry Oxidation Data for No Mn Added.

dicted by the model for 0, 6.66, 200, and 2000 ppm Mn added cases, using the best 1.5 order rate constants obtained from earlier graphs, are also shown in Fig. 4-29 for reference.

5. Derivation of the Flat Plate Model

The model was also derived for the solid particles being flat plates. The following assumptions were made in developing this model. The particles were all flat plates with a mean aspect ratio of 8.46 : 3.7 : 1. By neglecting the surface areas offered by four edges, the total surface area, Ap, of each plate was defined to be that of the two large surfaces. It was also assumed that there was negligible mass transfer from the edges of the crystals. Therefore Ap remained constant as the particle dissolves. The particle size distributions (including surface area and thickness) were calculated from the Coulter counter's data (spheres) by using the aspect ratio of 8.46 : 3.7 : 1.

Following these assumptions and also the assumptions made in subsection (3) above, the model for the flat plate crystals is

$$\frac{dC_\ell}{dt} = - kC_\ell^{1.5} + \frac{N_{t=0}\, k_\ell\, (C_s - C_\ell)}{V} \sum_{i=1}^{13} Ap_i\, h_i\, f_i \qquad (4\text{-}34)$$

$$\frac{H_i}{dt} = - \frac{2mk_\ell}{\rho} (C_s - C_\ell) \qquad (4\text{-}35) - (4\text{-}47)$$

$i = 1, 2, 3, ---, 13$

$$C_T = C_\ell + \frac{\rho N_{t=0}}{2mV} \sum_{i=1}^{13} Ap_i\, H_i\, h_i\, f_i \qquad (4\text{-}48)$$

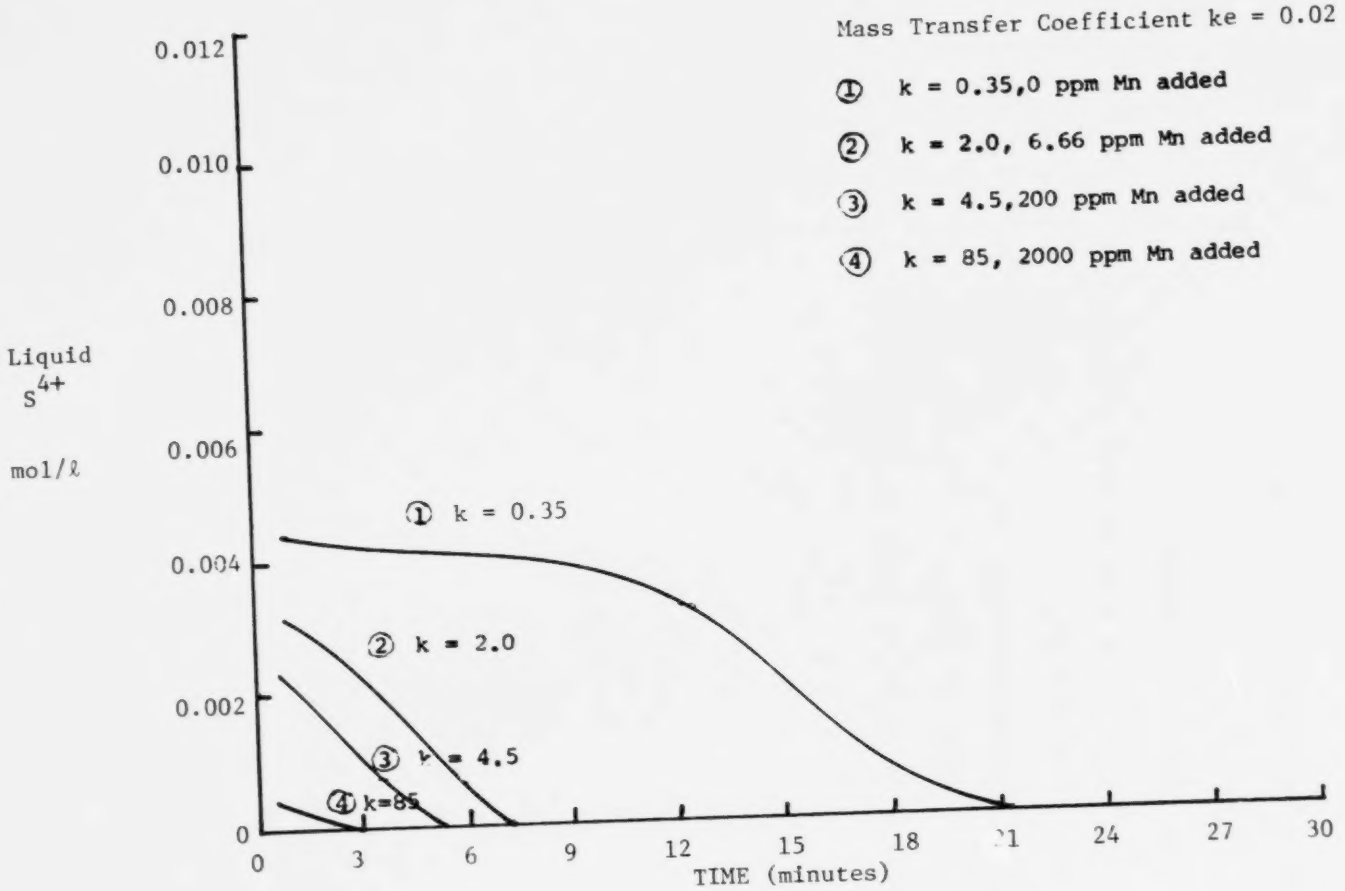

Figure 4-29. Computer Predicted Liquid $[S^{4+}]$ Profiles

SECTION 5

OXIDATION IN SODIUM SULFITE SOLUTIONS

OUTLINE

V. Oxidation in Sodium Sulfite Solutions
    A. Na_2SO_3 oxidation
        1. Manganese Catalyst
    B. Na_2SO_3 Oxidation with Succinic Acid Buffer
        1. Iron Catalyst
        2. Manganese Catalyst
        3. Mixed Catalysts
    C. Rate of Na_2SO_3 Solution Oxidation by the Flow-Thermal Method

OXIDATION IN SODIUM SULFITE SOLUTIONS

The oxidation of sodium sulfite was studied in the presence of either iron or manganese catalysts and with a mixture of the two. It was of interest to supplement the calcium sulfite studies described above with sodium sulfite work, since the calcium sulfite (commercial and laboratory produced) contains numerous impurities while the sodium sulfite (reagent grade) is much purer. Therefore, using sodium sulfite, the effects of the added catalyst can be determined more precisely.

A. SODIUM SULFITE OXIDATION

The rate of sodium sulfite oxidation without organic acid buffer was determined using the pH method described above.

1. Manganese Catalyst

The rate of reaction at $T = 40^{\circ}C$ and $pH = 4.6$ is given in Table 5-1 for various concentrations of $[S^{4+}]$ and manganese. A rate expression was determined for each manganese concentration by means of a regression analysis, and the order is given in Table 5-1. Results for $[Mn] = 2.67$ ppm are also presented in Figure 5-1. The reaction is very close to second order for all manganese concentrations and the second order rate constants are also presented in Table 5-1. Note that this is a different order than observed for $CaSO_3$. Under the conditions of these experiments the rate is only weakly influenced by the manganese concentration as can be seen in Figure 5-2.

B. SODIUM SULFITE OXIDATION WITH SUCCINIC ACID BUFFER

1. Iron Catalyst

Since the calcium sulfite was found to have significant concentrations of iron, sodium sulfite was used to examine the catalytic effect of iron on the oxidation of the sulfite. Ferric sulfate was selected to be the catalyst.

TABLE 5-1

Na_2SO_3 OXIDATION

Run No.	Iniital $[S^{4+}]$ Constant of Sulfite	Rate	[Mn]	[Fe]	Order	Index for Order	Rate Constant of 2.0 Order
49	0.092	$2.928x10^{-6}$	0.5	0	2.09	0.999	0.000376
52	0.140	$6.621x10^{-6}$	0.5	0	"	"	"
50	0.210	$1.630x10^{-5}$	0.5	0	"	"	"
51	0.354	$4.860x10^{-5}$	0.5	0	"	"	"
46	0.092	$2.826x10^{-6}$	1.33	0	2.05	0.999	0.000384
63	0.129	$5.730x10^{-6}$	1.33	0	"	"	"
47	0.202	$1.480x10^{-5}$	1.33	0	"	"	"
48	0.354	$4.972x10^{-5}$	1.33	0	"	"	"
57	0.082	$2.761x10^{-6}$	2.67	0	2.05	0.999	0.000436
64	0.117	$5.810x10^{-6}$	2.67	0	"	"	"
60	0.180	$1.433x10^{-5}$	2.67	0	"	"	"
59	0.425	$9.093x10^{-5}$	2.67	0	"	"	"
70	0.060	$1.191x10^{-6}$	4.0	0	2.16	0.996	0.000434
71	0.190	$1.185x10^{-5}$	4.0	0	"	"	"
72	0.354	$5.685x10^{-5}$	4.0	0	"	"	"
74	0.075	$1.976x10^{-6}$	6.0	0	2.10	0.0995	0.000410
65	0.125	$5.283x10^{-6}$	6.0	0	"	"	"
75	0.211	$1.409x10^{-5}$	6.0	0	"	"	"
76	0.392	$6.626x10^{-5}$	6.0	0	"	"	"
67	0.087	$2.641x10^{-6}$	8.0	0	2.15	0.994	0.000415
68	0.184	$1.115x10^{-5}$	8.0	0	"	"	"
66	0.243	$2.326x10^{-5}$	8.0	0	"	"	"
69	0.326	$4.650x10^{-5}$	8.0	0	"	"	"
53	0.095	$2.348x10^{-6}$	0	0	2.34	0.998	0.000375
54	0.221	$1.866x10^{-5}$	0	0	"	"	"
73	0.251	$2.247x10^{-5}$	0	0	"	"	"
55	0.333	$4.667x10^{-5}$	0	0	"	"	"
56	0.383	$5.906x10^{-5}$	0	0	"	"	"

T= 40°c, pH = 4.6

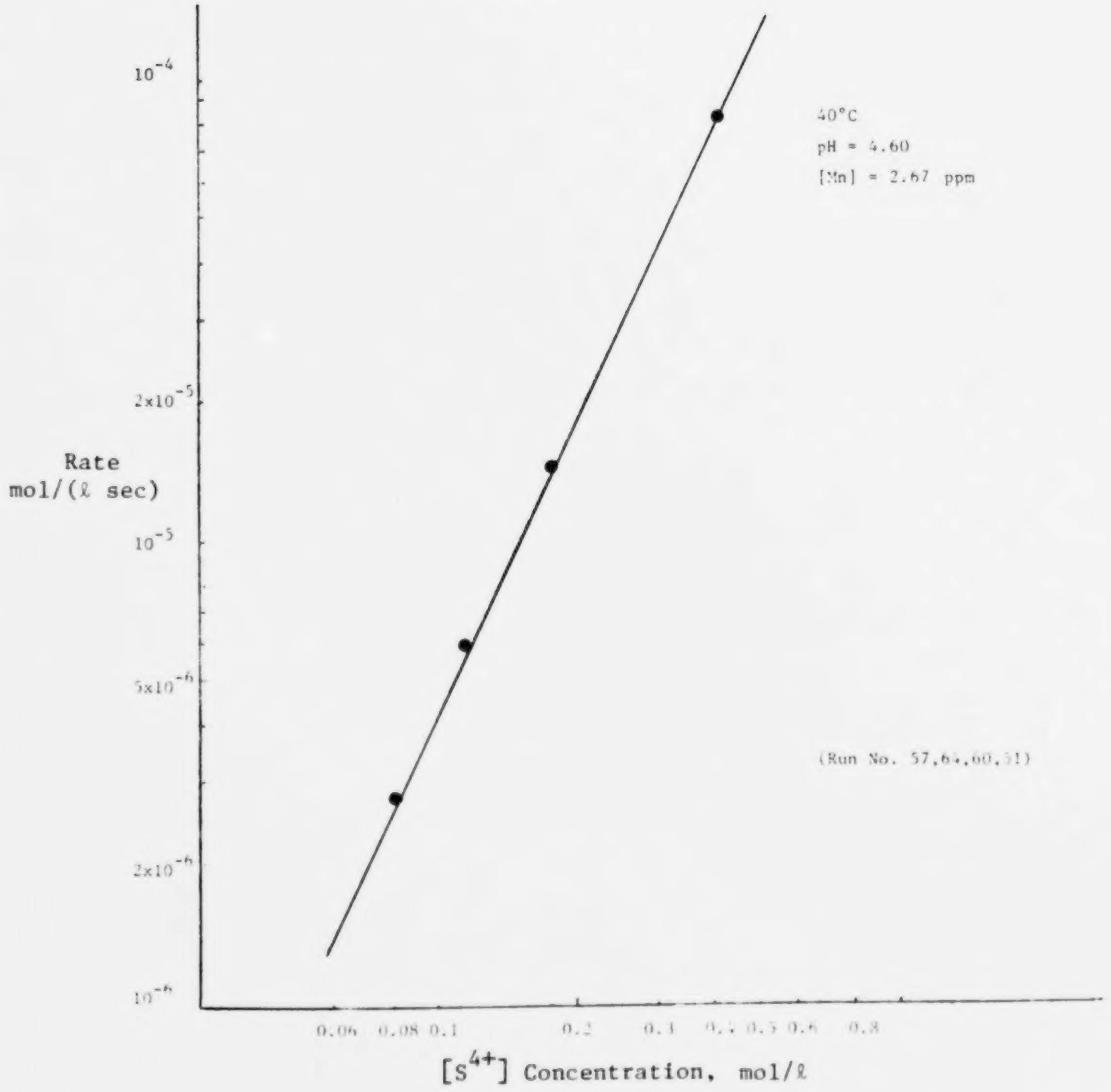

Figure 5-1. Dependence of Rate on Sulfite Concentration

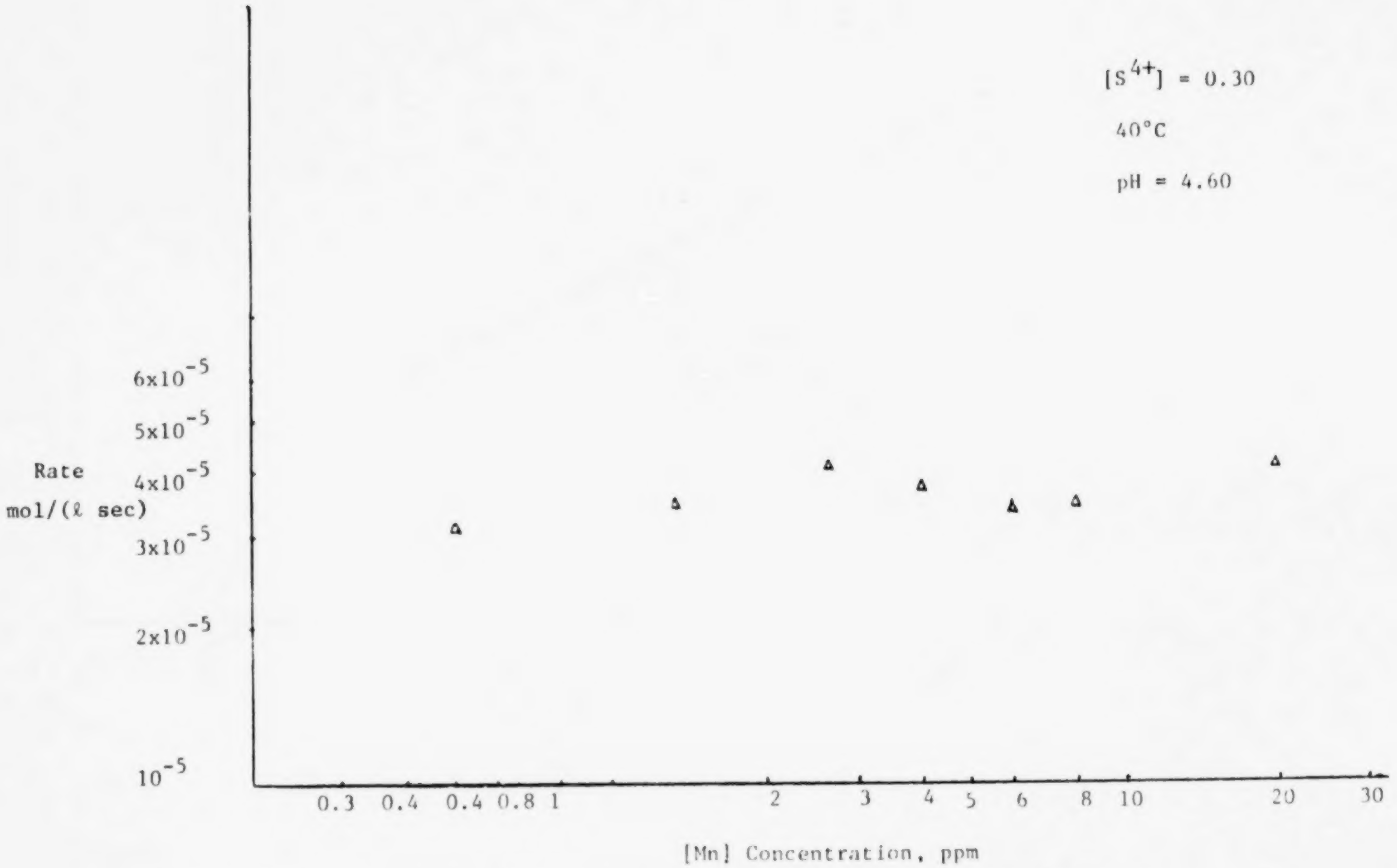

Figure 5-2. Dependence of Rate on Manganese Concentration

Ferric sulfate was found to be soluble in the reacting solution at concentrations less than 6.0 ppm at a temperature of 40°C and a pH of 4.6. A stock slurry was employed throughout the experiments. It was kept well mixed in order to assure that the concentrations of iron added to the reacting solution were uniform.

The initial sulfite concentration in the reactor ranged from 0.0045 to 0.0483 M. Oxygen was maintained at a flow rate of 3.0 ℓ/min. The concentration of iron added to the reacting solution ranged from 0 to 10 ppm. The temperature of the reactions was either 30, 40, or 50°C. Stirring speed was 1620 rpm. A buffer to maintain the pH within 0.25 pH units of the initial pH, 4.6, throughout the course of the reaction was prepared using 14.2 g of succinic acid per 600 ml of water or catalyst solution. NaOH pellets were used to adjust the initial pH of the reacting solution.

The iron catalyzed sodium sulfite oxidations can be better understood if they are broken down into three sets. The first set of experiments consisted of varying only the concentration of ferric sulfate added to the reactor. The temperature of the water bath was varied in the second set of experiments. Iron concentration in the reactor was maintained at 5 ppm. In the third set of experiments the bath temperature was maintained at 40°C, the added iron concentration was 5 ppm, and the initial sulfite concentration added to the reactor was varied.

Typical data from experiments in which the concentration of ferric sulfate was varied are presented in Figure 5-3 where the total concentration of the sulfur (4+) species vs time is plotted. It can be seen that 1 ppm Fe increases the rate of oxidation significantly, but increasing concentrations of iron up to 10 ppm does not have such a dramatic effect upon the rate of oxidation. An initial analysis of the data fit the data to zero, first, and

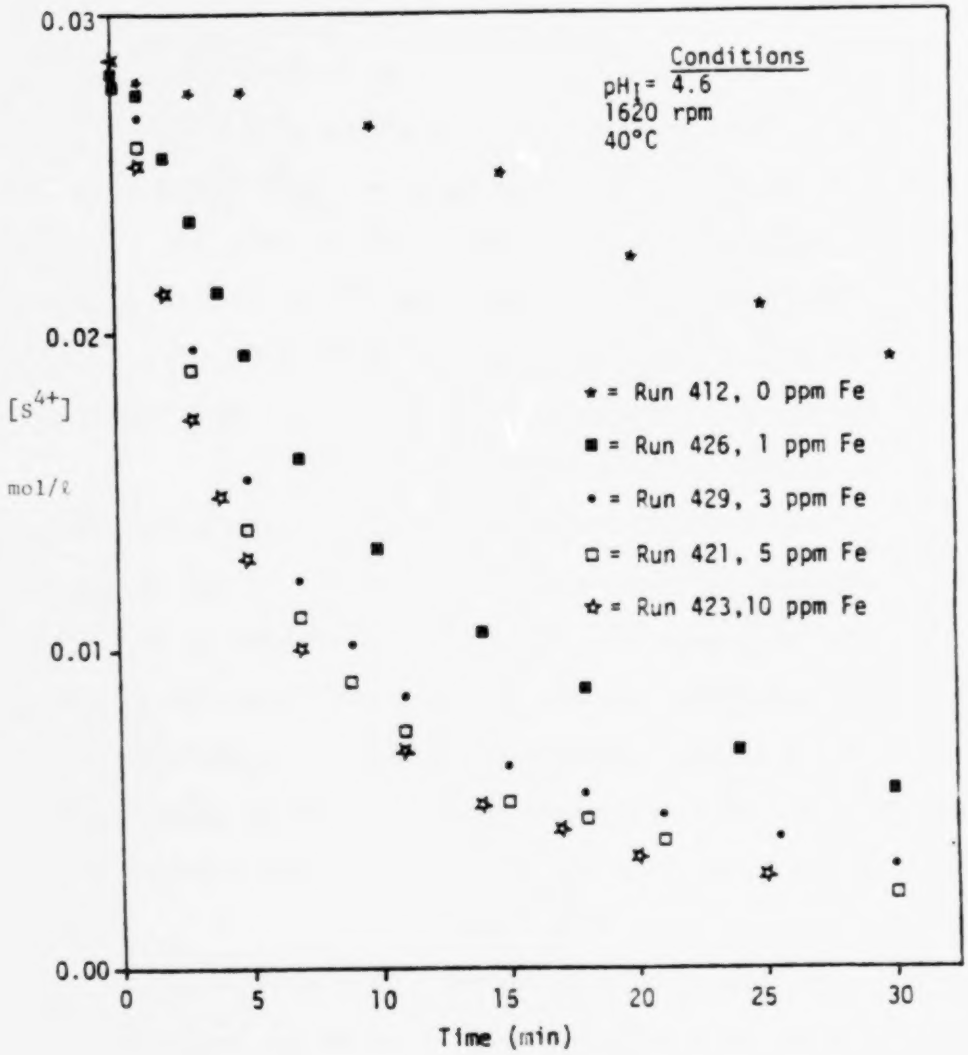

Figure 5-3. Sulfur (4+) Concentration vs Time for Iron Catalyzed Na_2SO_3 Oxidations (126)

second order models. Of the integer values the iron catalyzed oxidations fit a second order model best although a non-integer order is superior as noted below. Table 5-2 presents a listing of the second order rate constants, the index of determination used to provide an indication of the theoretical curve's goodness-of-fit, and the calculated order of the reaction with respect to the sulfite concentration.

Figure 5-4 is a plot of the reaction rate at $[S^{4+}] = 0.028$ M calculated from the second order rate expression.

The data obtained from experiments performed at various temperatures are shown in Figure 5-5 where the concentration of sulfur (4+) vs time is plotted for typical reactions. Analysis by the REPORT program indicated that the second order model fit the data better than zero or first order at the three different temperatures. These data are given in Table 5-3. An activation energy of 18.8±0.8 kcal/(g mol) was calculated by the linear regression analysis of a plot of ln(ℓ/sec order rate constant) vs $(\text{temperature})^{-1}$ presented in Figure 5-6.

The third set of experiments was performed at 40°C, 5 ppm iron were added to the reactor. The initial concentration of the sulfite was varied in order to make a second determination of the order of the reaction with respect to the sulfite. Table 5-4 contains data obtained from the REPORT program. A second order model fit the data better than zero or first. This information indicated that the reactions maintained consistent behavior over the range of sulfite concentrations considered.

The lower values for the second order rate constants calculated for both the lowest and higher concentrations of sulfite used are probably due to measurement limitations at low concentrations, and the inability of the buffer to control the pH of the reacting solution at high concentrations.

TABLE 5-2

RESULTS OF SODIUM SULFITE OXIDATION WITH IRON CATALYST ADDED (126)

Run #	Initial S^{+4} g-mol/ℓ	Iron Concentration Added (ppm)	Second Order Rate Constant (ℓ/mol sec)	Index Of Determination	Rate at $[S^{4+}] = 0.028$ mol/(ℓ sec)
412	0.0280	0	0.0119	0.982	9.33×10^{-6}
413	0.0266	0	0.0133	0.991	1.04×10^{-5}
425	0.0290	1	0.0750	0.995	5.88×10^{-5}
426	0.0283	1	0.0805	0.998	6.31×10^{-5}
427	0.0278	3	0.128	0.956	1.00×10^{-4}
429	0.0286	3	0.147	0.995	1.15×10^{-4}
421	0.0278	5	0.202	0.977	1.58×10^{-4}
422	0.0277	5	0.181	0.990	1.42×10^{-4}
442	0.0281	5	0.166	0.988	1.30×10^{-4}

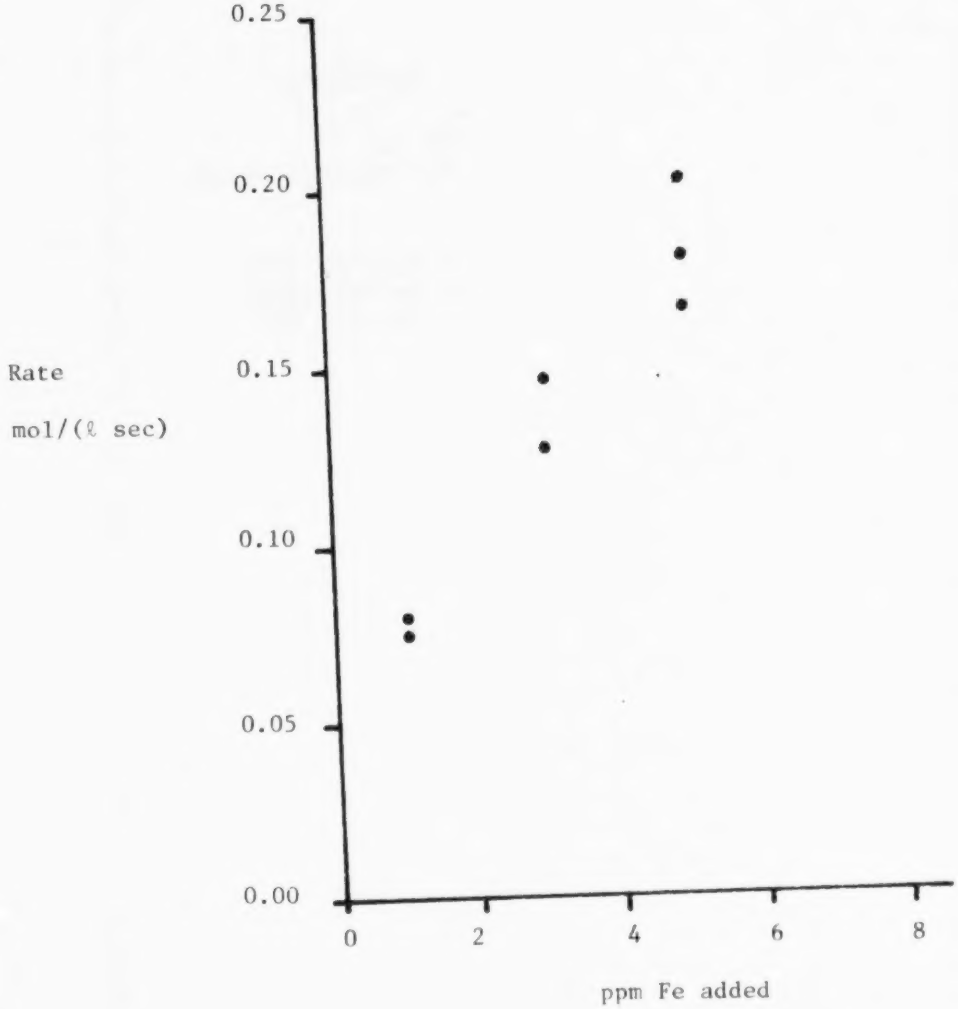

Figure 5-4. Rate at $[S^{4+}] = 0.028$ **M** **vs Concentration** Iron Added for Sodium Sulfite Oxidations (126)

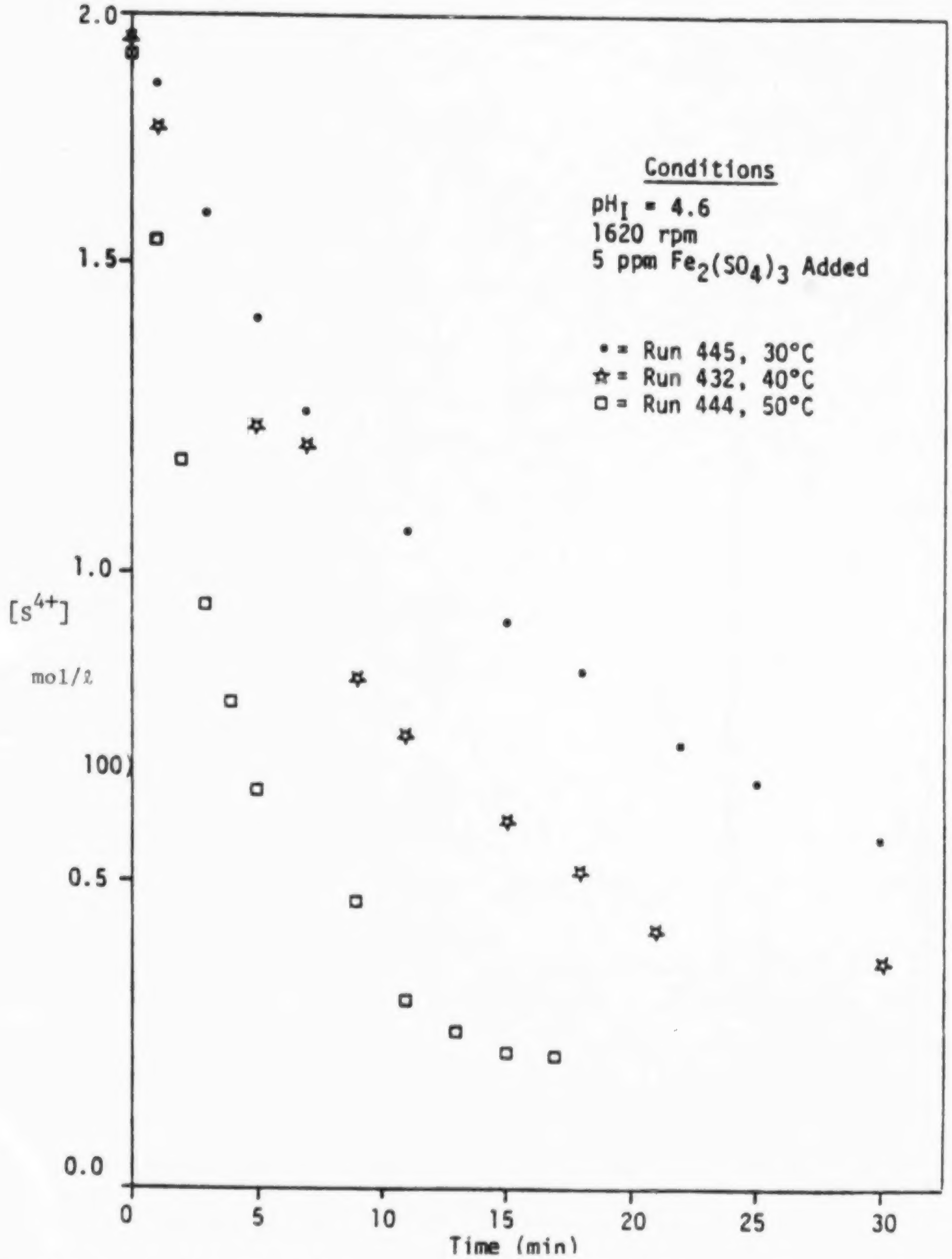

Figure 5-5. Sulfur (4+) Concentration vs Time for Iron Catalyzed Oxidations at Various Temperatures Using Na_2SO_3 (126)

TABLE 5-3

RESULTS OF IRON CATALYZED REACTIONS AT VARIOUS TEMPERATURES USING SODIUM SULFITE (126)

Run	Temp °C	Second-Order Rate Constant ℓ/(mol sec)	Index of Determination
445	30	0.0675	0.998
446	30	0.0605	0.997
421	40	0.202	0.977
422	40	0.181	0.990
442	40	0.166	0.988
443	50	0.511	0.973
444	50	0.426	0.988

Conditions:	Stirring Speed	1620 rpm
	Initial pH	4.6
	5 ppm Fe Added	

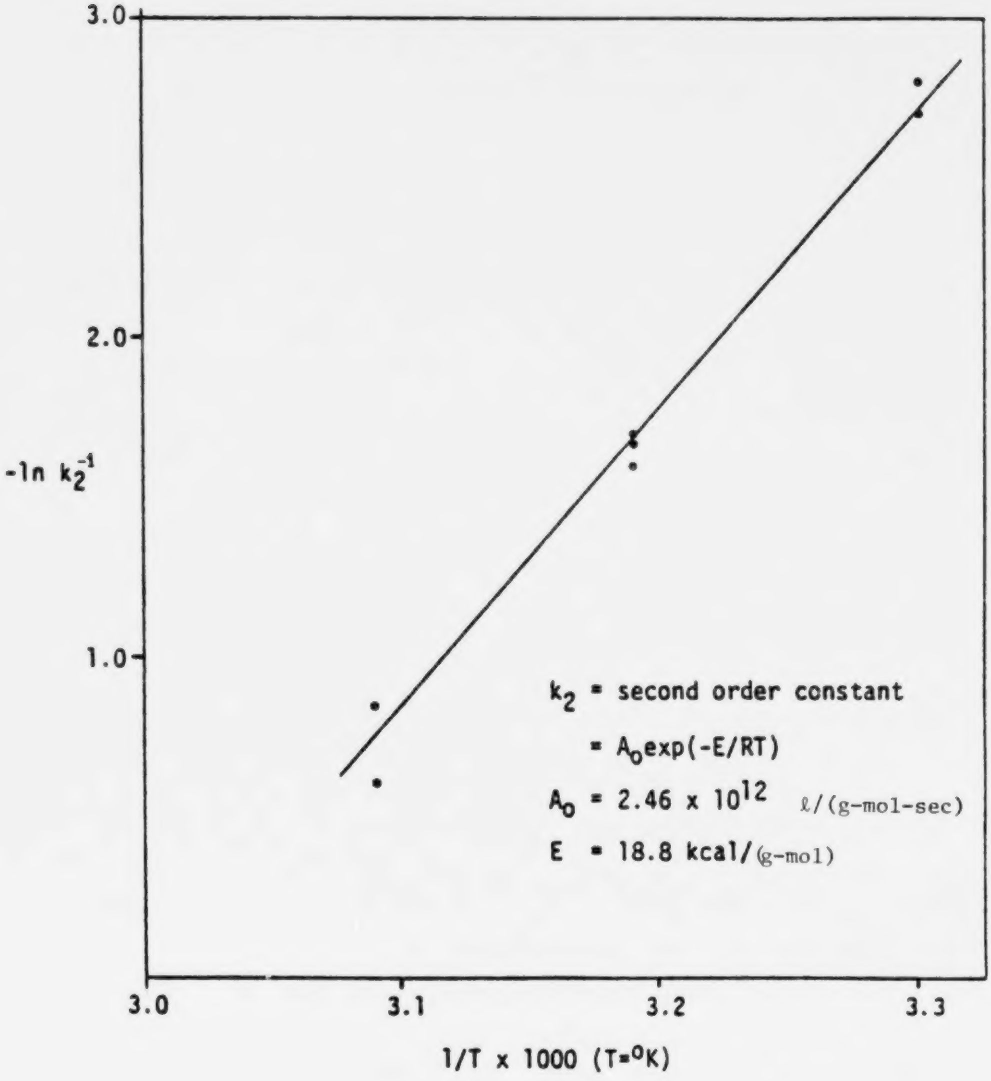

Figure 5-6. Activation Energy Determination for Fe Catalyzed Na_2SO_3 Oxidations (126)

TABLE 5-4

RESULTS OF SODIUM SULFITE OXIDATIONS WITH VARYING INITIAL SULFITE CONCENTRATION AND 5 ppm IRON ADDED (126)

Run	Initial S^{+4} g-mol/ℓ	Second Order Rate Constant ℓ/(mol sec)	Index of Determination
451	0.0045	0.114	0.902
452	0.0046	0.062	0.922
434	0.0094	0.142	0.996
436	0.0096	0.160	0.990
432	0.0186	0.147	0.991
433	0.0181	0.188	0.987
421	0.0278	0.202	0.977
422	0.0277	0.181	0.990
442	0.0281	0.166	0.988
437	0.0370	0.165	0.990
439	0.0379	0.158	0.994
448	0.0483	0.067	0.997
449	0.0473	0.059	0.997

Conditions:

Temperature = 40°C

Initial pH = 4.6

Stirring Speed = 1620 rpm.

5 ppm Fe Added as $Fe_2(SO_4)_3$

The use of a constant succinic acid concentration over a wide sulfite concentration was observed to cause problems in pH control. At an initial sulfite concentration of 0.0438 M the pH dropped 0.27 units, but at 0.0277 M the pH drop was only 0.14 units during the reaction.

Regression analysis of the data for Fe concentrations of 1.0, 3.0, and 5.0 ppm was done to determine the dependence of the rate of reaction at each of these iron concentrations. The results are presented in Table 5-5.

A multiple regression analysis of all iron catalyzed experiments performed at 40°C was done in order to determine the order of the reaction with respect to iron and sulfur(4+) concentrations simultaneously. Data at time greater than sixty seconds were used in the analysis. (See section on MULREG Analysis). Based on 184 data points, the order of the sodium sulfite oxidation with respect to the sulfur(4+) concentration was 1.69 with a standard deviation of 0.06. The order with respect to the iron concentration was 0.18 with a standard deviation of 0.08. The rate of reaction of sodium sulfite with iron catalyst at T=40°C and pH=4.6 is therefore given by

$$\text{rate}=0.155\ [\text{Fe}]^{0.18}\ [\text{S}^{4+}]^{1.69}$$

where [Fe] has units of moles per liter. Figure 5-7 is a plot of rate vs iron concentration at $[\text{S}^{4+}] = 0.028$ M and pH 4.6.

2. Manganese Catalyst

Reactions using buffer, sodium sulfite solutions of approximately the same initial concentration were performed under the conditions described in Table 5-6. A solution of manganese sulfate was added to the water in the reactor in concentrations ranging from 0 to 4.00 ppm Mn. The reactions had an induction period of about four minutes. During this period, the concentration of sulfite decreased only slightly. After the induction period, the reaction proceeded significantly faster. The sulfur(+4) species were consumed more

TABLE 5-5

MULTREG RESULTS FOR IRON CATALYZED Na_2SO_3 OXIDATIONS

Fe Concentration Added (ppm)	Number Of Data Points	Order With Respect to $[S^{4+}]$	Standard Deviation
1.00	21	1.78	0.10
3.00	19	1.78	0.10
5.00	123	1.68	0.08

Conditions:

$pH_I = 4.6$

Temperature = 40°C

Stirring Speed = 1620 rpm

Fe added as $Fe_2(SO_4)_3$

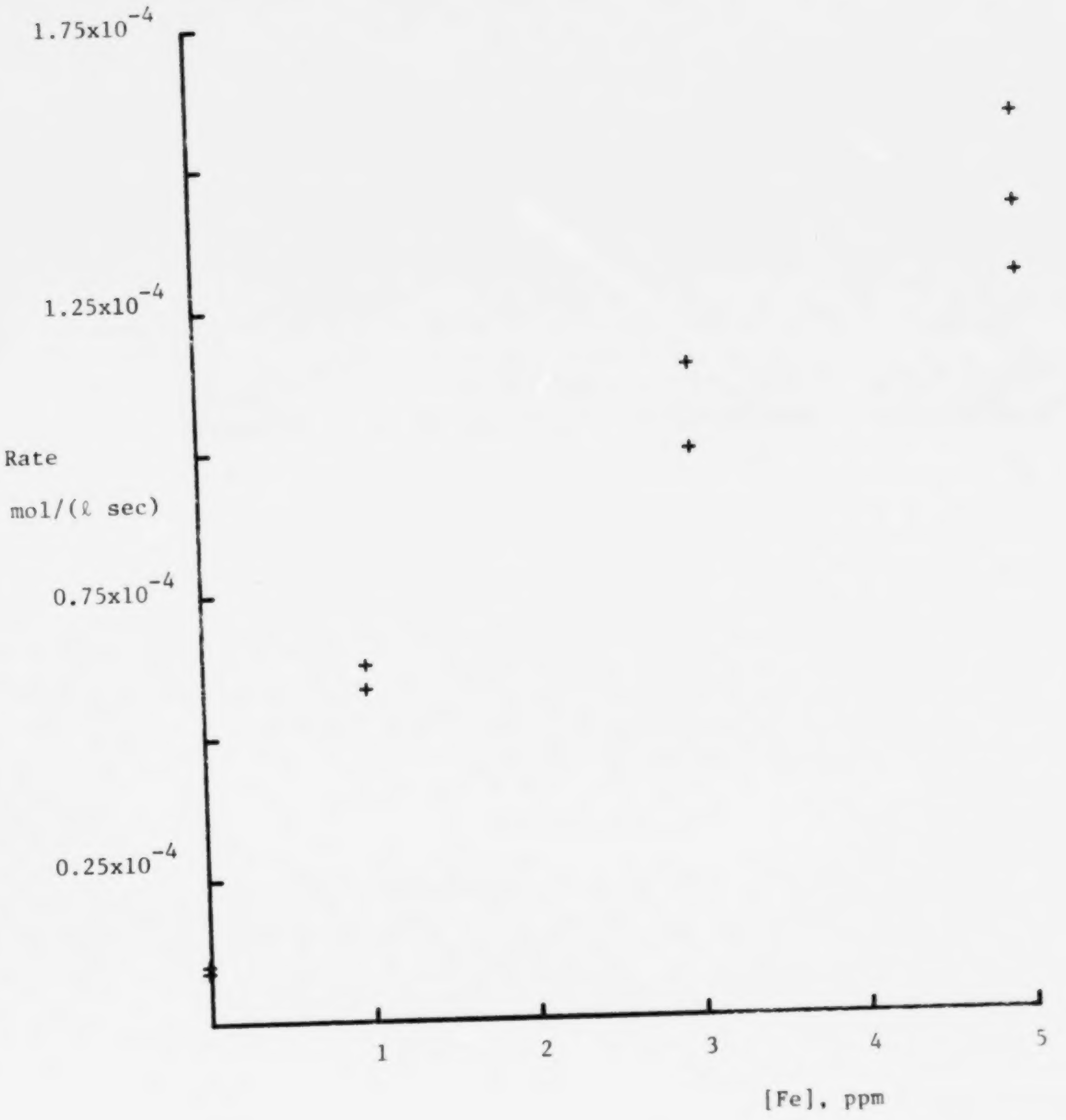

Figure 5-7. Rate at $[S^{4+}] = 0.028m$ vs Concentration Fe

(Temp = 40°C; pH = 4.6)

TABLE 5-6

RESULTS OF SODIUM SULFITE OXIDATIONS WITH MANGANESE ADDED (126)

Run #	Initial Sulfite g-mol/ℓ	Conc. Mn Added (ppm)	First Order Rate Constant*	Index of Determination	Rate at $[S^{4+}] = 0.028$ mol/(ℓ sec)
412	0.0280	0.00	$2.40 \times 10^{-4} (\text{sec})^{-1}$	0.985	6.72×10^{-6}
413	0.0366	0.00	1.81×10^{-4}	0.966	5.07×10^{-6}
405	0.0262	0.08	4.18×10^{-4}	0.914	1.17×10^{-5}
407	0.0264	0.08	4.68×10^{-4}	0.987	1.31×10^{-5}
415	0.0279	0.50	8.66×10^{-4}	0.990	2.42×10^{-5}
417	0.0283	0.50	8.81×10^{-4}	0.989	2.47×10^{-5}
419	0.0281	0.83	9.25×10^{-4}	0.989	2.59×10^{-5}
418	0.0281	0.83	1.06×10^{-3}	0.983	2.968×10^{-5}
404	0.0266	1.33	2.51×10^{-3}	0.969	7.03×10^{-5}
406	0.0259	1.33	2.22×10^{-3}	0.994	6.22×10^{-5}
408	0.0268	2.67	5.23×10^{-3}	0.973	1.46×10^{-4}
409	0.0266	2.67	4.45×10^{-3}	0.987	1.246×10^{-4}
410	0.0264	4.00	1.05×10^{-2}	0.838	2.94×10^{-4}
411	0.0268	4.00	1.05×10^{-2}	0.898	2.94×10^{-4}

* The rate constant is based on curve fitting of data for times greater than three minutes.

Conditions:

Temperature = 40°C

Initial pH = 4.6

Stirring Speed = 1620 rpm.

Mn Added as $MnSO_4$ Solution

rapidly as the manganese concentration was increased throughout the range investigated. Figure 5-8 is a plot of the concentration of the sulfur(4+) species vs time for typical reactions performed.

The induction period was neglected in the analysis. Data at times greater than four minutes were analyzed using an HP 2000C library program, CURFIT, in order to check the fit of the data to a zero, first and second order model. In all cases where manganese was added to the solution, the data fit the first order case best. The rate of reaction at $[S^{4+}] = 0.028$ M is shown in Table 5-6 for both catalyzed and uncatalyzed runs and the results are plotted in Figure 5-9.

A linear regression analysis was done to determine the order with respect to sulfur (4+) for each concentration of manganese. These are presented in Table 5-7. With the manganese runs there was an induction period as reported earlier. In the analysis of this data the induction period was neglected and only points after the induction period used in the analysis.

A multiple regression analysis of all manganese catalyzed experiments, performed at 40°C, was done in order to determine the order of the reaction with respect to the manganese and sulfur(4+) concentrations simultaneously. Results from the time of the maximum rate until the end of the reaction were used in the analysis. Seventy-eight data points were used in the analysis and the order of the reaction with respect to sulfur(4+) concentration was 0.94 with a standard deviation of 0.04. The order with respect to manganese was found to be 0.67 with a standard deviation of 0.04. The rate of oxidation for sodium sulfite with manganese catalyst at 40°C and pH = 46 is the given by

$$\text{Rate} = 2.141\ [\text{Mn}]^{0.67}\ [S^{4+}]^{0.94}$$

where [Mn] has units of moles per liter.

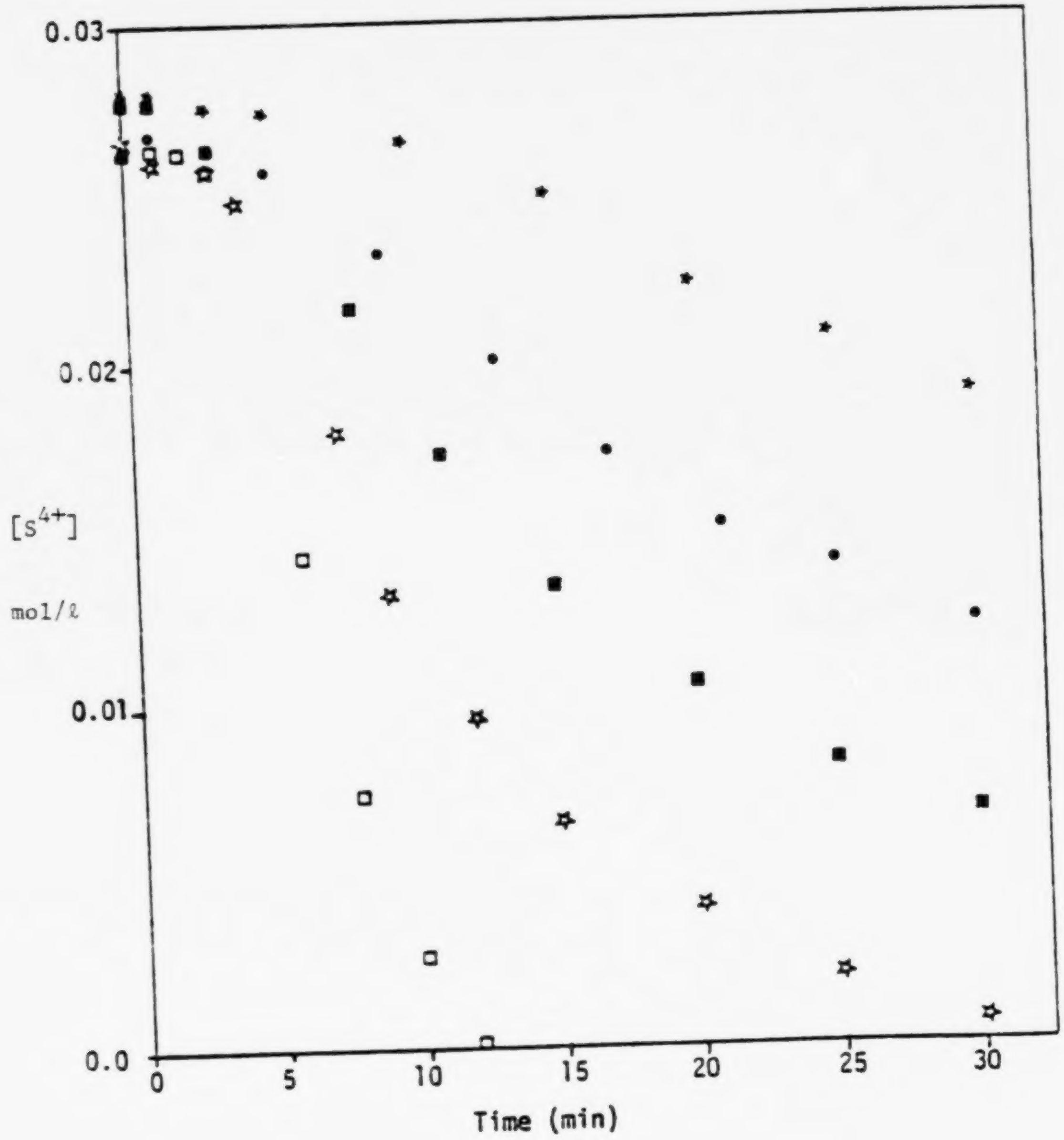

Figure 5-8. Sulfur (4+) Concentration vs Time for Manganese Catalyzed Oxidations of Na_2SO_3 Solutions. (Conditions and Key for Symbols on Next Page) (126)

Conditions

$pH_I = 4.6$

1620 rpm

40°C

$MnSO_4$ solution used as catalyst

Key of Symbols

Symbol	Run #	ppm Mn added
★	412	0.08
●	407	0.08
■	415	0.50
☆	404	1.33
□	410	4.00

Figure 5-8 (continued)

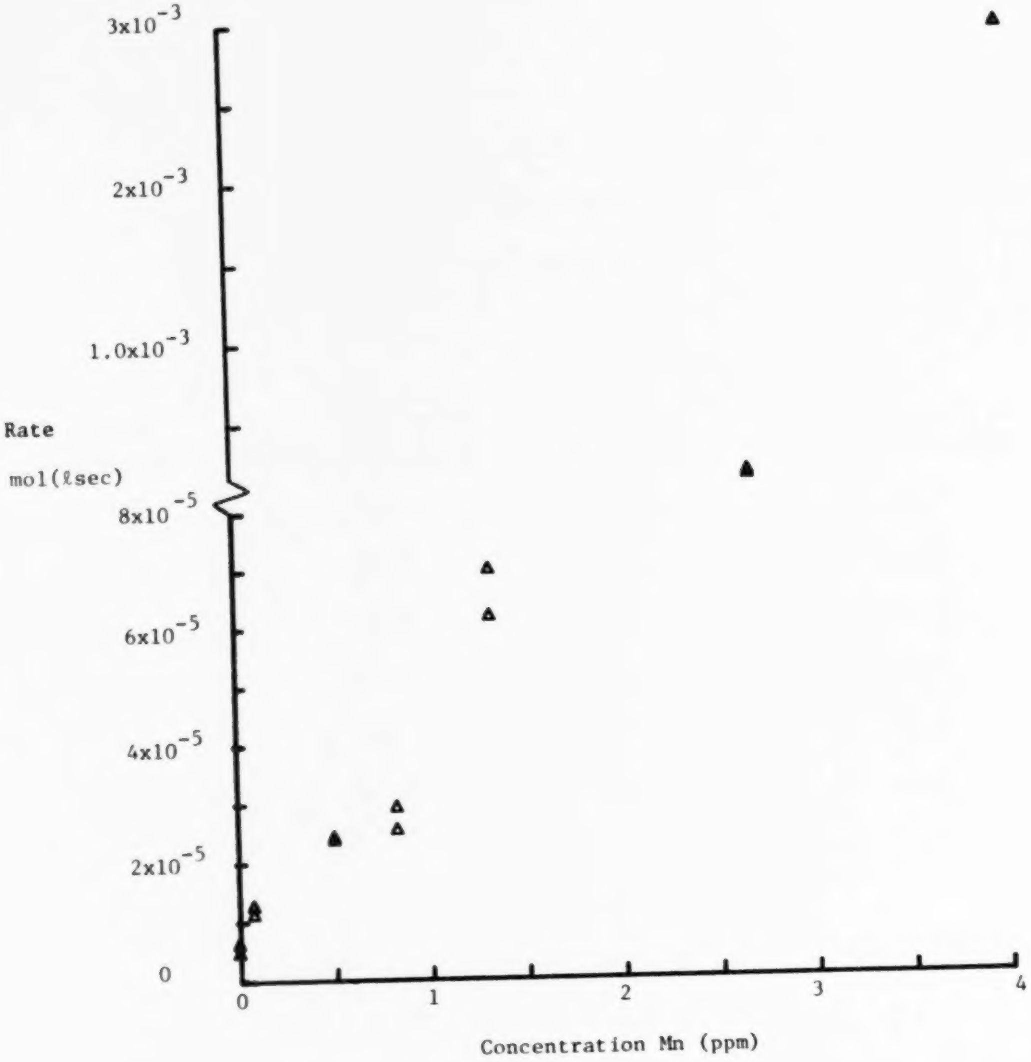

Figure 5-9. Rate at S^{4+} = 0.028M vs Mn Concentration
Temp = 40°C; pH = 4.6

TABLE 5-7

REGRESSION ANALYSIS OF MANGANESE CATALYZED Na_2SO_3 OXIDATIONS (126)

Mn Concentration Added (ppm)	Number Of Data Points	Order With Respect to $[S^{4+}]$	Standard Deviation
0.08	12	2.31	0.30
0.50	10	1.64	0.07
0.83	21	0.91	0.14
1.33	14	0.90	0.06
2.67	11	1.03	0.08
4.00	10	0.96	0.09

Conditions:

$pH_I = 4.6$

Temperature = 40°C

Stirring Speed = 1620 rmp

Mn added as $MnSO_4$

3. Mixed Catalyst

An inspection of the data obtained from the iron and manganese catalyzed sodium sulfite oxidations led to speculation concerning the effect of combining the two catalyst materials in the same reacting solution. Various combinations of the catalysts were added to solutions 0.03 M Na_2SO_3. At an initial pH of 4.6 and temperature of 40^oC the reactions showed an induction period. Concentrations of manganese and iron similar to those found in the buffered calcium sulfite solutions were used in the experiments. Figure 5-10 is a plot of the reduced sulfur (4+) concentration, $[S^{4+}]/[S^{4+}]o$, vs time for some typical experiments. There is no real similarity to the reactions.

In order to investigate the observed results further, a comparison of the mixed catalyst oxidations for two different concentrations of catalysts was made with the manganese catalyzed Na_2SO_3 oxidations. Table 5-8 contains a comparison of first order rate constants determined by the REPORT program for the mixed catalyst oxidations.

All of the experiments done with mixed catalysts were found to have an induction period. The rate and average concentration data from the REPORT program were used to determine the order of the sulfur (4+) concentration. Data were taken from the point where the rate increased indicating the end of the induction period.

A multiple regression analysis was performed on the mixed catalyst data to determine the order with respect to sulfur (4+), manganese, and iron. The results are presented in Table 5-9. As can be seen the order with respect to iron can be considered to be 0. Thus, a second multiple regression was done where the mixed catalyst experimental data were used but orders were only determined for S^{4+} and Mn. These are also reported in Table 5-9. These results show little change in the orders with respect to S^{4+} and Mn.

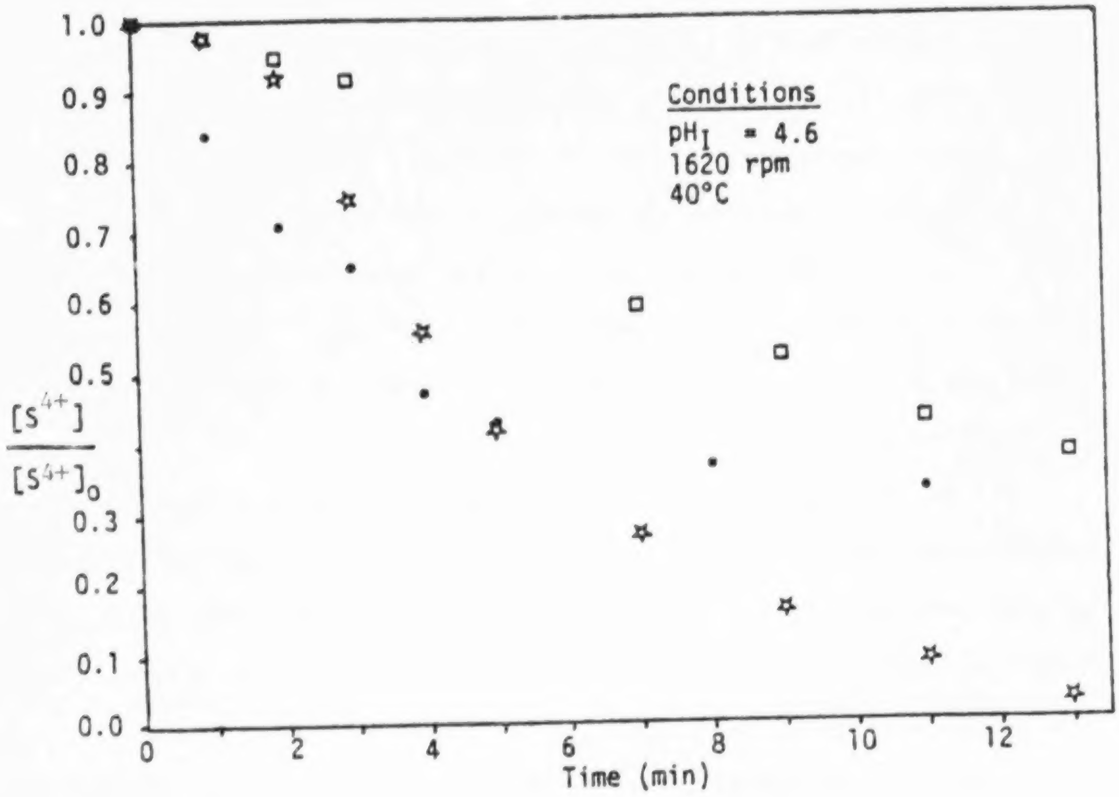

Symbol	Run #	Composition
☆	91.1	Na_2SO_3, 2 ppm Mn & 2 ppm Fe Added
•	65.1	$CaSO_3$, No Catalyst Added
□	93.1	Na_2SO_3, 0.5 ppm Mn & 3 ppm Fe Added

Figure 5-10. Reduced Sulfur (4+) Concentration vs Time for Comparison of Oxidation Reactions

TABLE 5-8

RESULTS OF SODIUM SULFITE OXIDATION WITH IRON AND MANGANESE ADDED

Run #	ppm Fe added	ppm Mn added	First Order Rate Constant	Index of Determination
101.1	1.0	0.50	8.01×10^{-4}	0.982
102.1	1.0	0.50	8.60×10^{-4}	0.989
90.1	2.0	2.0	4.31×10^{-3}	0.977
91.1	2.0	2.0	4.82×10^{-3}	0.970
93.1	3.0	0.50	1.11×10^{-3}	0.988
94.1	3.0	0.50	1.34×10^{-3}	0.988
97.1	6.0	3.0	5.88×10^{-3}	0.938
98.1	6.0	3.0	5.78×10^{-3}	0.929

TABLE 5-9

MULTIPLE REGRESSION RESULTS FOR MIXED CATALYST SODIUM SULFITE OXIDATIONS

Order with Respect to S^{4+}	Standard Deviation	Order with Respect to Fe	Standard Deviation	Order with Respect to Mn	Standard Deviation	Rate Constant
0.96	0.03	0.04	0.07	0.94	0.06	71.6589
* 0.96	0.03	-	-	0.06	0.05	60.2560
0.94	0.05	-	-	0.67	0.04	2.1406

Temp = 40°C, pH = 4.6

* In these runs both catalyst were present, but in the analysis of the data it is assumed that the reaction is zero order in iron.

However, from the results of the manganese only catalyzed runs, iron does seem to have an effect on the influence of manganese concentration on the rate. The rate expression obtained from the manganese only catalyzed runs was: Rate $= 2.141\ [Mn]^{0.67}\ [S^{4+}]^{0.94}$.

The results obtained from the experiments wth manganese only (no iron) are also presented in Table 5-9 for comparison. It is noted that although the order of the reaction with respect to iron is zero, the results obtained with and without iron are different. Therefore, iron does influence the rate of reaction, but that rate does not depend on the amount of iron for Fe > 1 ppm.

C. RATE OF Na_2SO_3 SOLUTION OXIDATION BY THE FLOW-THERMAL METHOD

Sodium sulfite/bisulfite solutions have long been employed to study the oxidation kinetics of aqueous S^{4+} ions. These sodium salts are much more soluble, less expensive, and available in purer lots than the corresponding calcium salts. Several studies have shown the sodium cation to have no effect on the oxidation rate (21, 91, 95). No mechanism proposed to date involves the spectator cation (Na or Ca) in a kinetically important step. So the important effects of catalysts, $[S^{4+}]$, or inhibitors may profitably be studied in the experimentally more advantageous sodium solutions. Furthermore, the results of sodium sulfite oxidations may have direct application in sodium-based wet scrubbing processes for sulfur dioxide removal from stationary sources.

The conditions selected for the sodium bisulfite/sulfite oxidations were therefore in two parts: low pH and high pH.

pH:	4.5, 5, 6	11
$[S^{4+}]$:	0.05 - 0.14	0.009 - 0.09 mol/ℓ

$[O_2]$: 0.004 - 0.015 mol/ℓ

[Mn]: 10, 100, 1000 ½, 0.4-0.6, 1, 3 ppm

T: 25±0.02 °C

The rates encountered for sodium sulfite oxidations span a broader range than the range for calcium sulfite oxidation. The greater solubility of sodium salts especially at higher pH values, results in much faster oxidations. In the current work rates ranged from 0.0002 to 0.7 mol/(ℓ sec).

Table 5-10 contains the results of varying the Mn concentration over a small, but likely range. In this range, tripling the catalyst concentration, doubles the reaction rate. This range of ½ to 3 ppm is a likely range for solutions made from commercial salts.

The effect of a rise in pH is to increase the homogeneous reaction rate. For the $NaHSO_3$ oxidation the results of varying pH from 4.5 to 5 to 6 are in Table 5-11. At pH 4.5 the rates for [Mn] at all concentrations were too low to measure. The increase of rate with [Mn] is greater than linear for both pH 5 and 6.

The reactant orders for the high pH experiments were examined by Multiple Regression Analysis for the conditions:

$$[S^{4+}] = 0.0086\text{-}0.0781 \text{ M}, \ [O_2] = 0.0043\text{-}0.0118 \text{ M}, \ [Mn] = 0.5 \text{ ppm}$$

The results were:

Sulfite Order = 1.49±0.17 Oxygen Order = 0.49±0.19 So the order is about 3/2 in sulfur and 1/2 in oxygen. The figure for oxygen varied in several multiple regressions varying as far as 0.43±0.6.

The oxidation state of the catalyst, Mn^{2+} or Mn^{+}, is important in determining the rate of the reaction. To see what effect the two oxidation states

TABLE 5-10

EFFECT OF [Mn] on Na_2SO_3 OXIDATION RATE

[Mn], ppm	Rate, mol/(ℓ sec)
3	0.404
1	0.2004
0.5	0.148

Conditions:

pH: 11

$[S^{4+}]$: 0.01 mol/ℓ

$[O_2]$: 0.015 mol/ℓ

T: 25°C

TABLE 5-11

EFFECT OF pH

$NaSO_3$ OXIDATION RATES

[Mn] ppm \ pH	4.5	5	6
1	too low	-	-
10	-	-	0.0206
100	too low	0.00022	0.298
1000	too low	0.0112	-

These rates are in mol/(ℓ sec)

Dashes indicate conditions not tested

Conditions:

$[S^{4+}]$: 0.05 - 0.14 mol/ℓ

$[O_2]$: 0.008 - 0.013 mol/ℓ

T: 25°C

might have, the Mn catalyst at 1 ppm was put alternately in the sulfite reservoir (Mn^+) and the oxygen reservoir (Mn^{2+}). The difference is notable and shown in Figure 5-11. Faster initial temperature rise is observed when Mn is added to the sulfur side, indicating a greater rate.

Although these experiments were done at 25°C, the similarity with the pH method results suggests the rates may be calculated for higher temperatures with the Arrhenius relation using the pH method activation energy.

Conditions: [S] 0.05 M
$[O_2]$ 0.008 M
[Mn] 1 ppm
pH 11
T 25°C

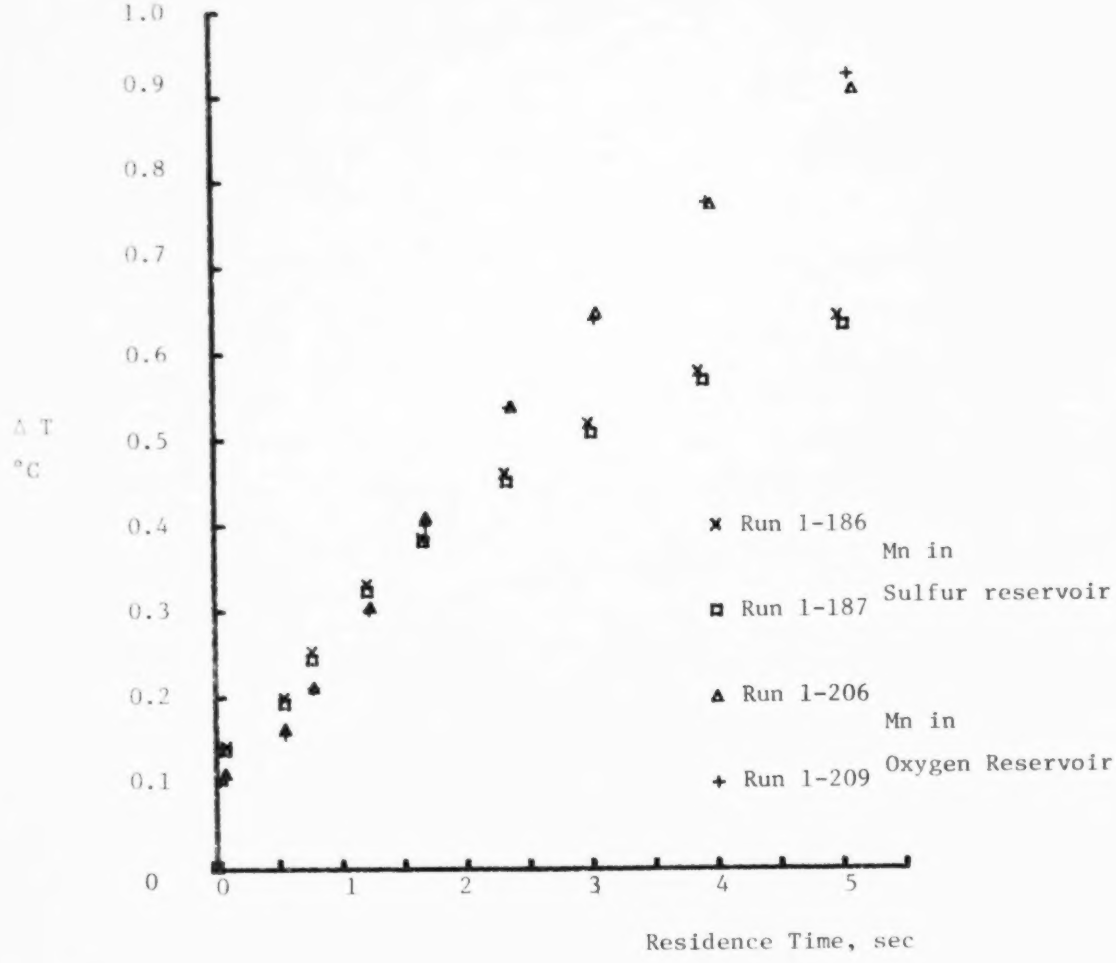

Figure 5-11. Comparison of Mn Added only to Oxygen Side or Only to Sulfur Side

SECTION 6

CONCLUSION

For convenience and rapid comparison, this section is a synopsis of this study of aqueous sulfur dioxide oxidation. It is organized by the sections of the report, and in each section, the findings of the subsections are given in order.

Section 1: Introduction

- The conditions surrounding aqueous sulfur dioxide oxidation: incidence, physical considerations, and kinetics are treated in an extensive literature review having 190 references.
- Some individual articles were commented upon or amplified; most notably, the work by Gladkii in Russia. For this work there are detailed comparisons with the instant work.

Section 2: Experiments

- The batch reactor and experiments included many details to ensure kinetically-limited oxidation free from uncontrolled catalysis and physical variations.
- The flow reactor represents an advance in the application of automated flow calorimetry to chemical kinetics by incorporating the capacity for high pressures with a completely inert flow circuit.
- The materials used and reacting solutions which resulted were all examined for composition. The calcium sulfites contained much sulfate as well as catalytic impurities.
- Analyses of experimental results were by several means: a comprehensive computer program was prepared to format all data reduction to aid

in comparison of 0, 1st, and 2nd order rate expressions as well as varying experimental parameters; for specific experimental sequences, a multiple regression program gave results for reactant orders and rate constants.

For the pH method considerable extensions and corrections of Bengtsson's ingenious scheme were employed. The flow thermal experiments gave rates via an enthalpy balance on the reacting fluid.

Section 3: Oxidation in Calcium Sulfite Solutions

- The reaction order of the oxidation of clear calcium sulfite solutions is 1.5 by the pH method. Tables 3-1 to 3-5 give the 1.5 order rate constants under different reaction conditions.
- The reaction order of oxidation of calcium sulfite with the presence of succinic acid is also 1.5 and the $k_{1.5}$ are shown in Table 3-6. It can be seen from Figure 3-7 that the rate of reaction increases with increasing pH with the rate increasing more rapidly above pH = 5.0.
- At pH = 4.0 and low succinic acid concentrations, the reaction is adequately described by a first order expression; however, with increasing levels of acid, the order rises above 1.0.
- The effects of adipic acid on calcium sulfite oxidation are summarized in Table 3-9. The reaction order is approximately 1.5 at low adipic acid concentration and rises with increasing organic acid concentration.
- Glycolic acid is a very strong inhibitor for the oxidation, much stronger than any of the other acids studied. Summaries of the results are presented in Tables 3-10 and 3-11.
- The trend of inhibitory strength is:

glycolic acid>adipic acid>succinic acid

o The oxidation rate of an inhibited run is increased by adding catalyst (i.e. manganese and iron) but the results of the experiment will depend on the relative strength and concentrations of both the catalyst and the inhibitor added.

o Oxidation studies were performed using liquor from slurry samples from Penberthy Oxidation Runs at the Shawnee Test Facility. The experiments were to determine the degree of activity of the samples in catalyzing the oxidation of sulfite.

o Experiments were made to find the safe (kinetics limited not mass transfer limited) range of the operating parameters. At low stirring speeds (Figure 3-24, 215 rpm) the reaction is mass transfer controlled and the concentration of S^{4+} decreases linearly with time. At higher stirring speeds (500-3500 rpm) mass transfer effects are unimportant.

o Experiments of $CaSO_3$ oxidation at high manganese concentrations (10, 200, 1000, and 2000 ppm) were conducted by flow-thermal method. The results are listed in Table 3-23 and 3-24, with a range of pH from 3.3 to 4.7.

Section 4: Oxidation in Slurries

o Solubilities of $CaSO_3$ under different pH were obtained by both theoretical calculation and experimentation. The data agree with each other well. A power function of $Cs = 1676.84\ (pH^{-7.791})$ fits the experimental data well. There is notable difference between these results and the predictions of the Radian equilibrium program.

o An oxygen flow rate of 3 ℓ/min was used in the oxidation reaction after showing that there is not gas-liquid mass transfer control during the reaction at these conditions.

- The initial rate of reaction increases with decreasing initial pH or increasing slurry density.
- Figure 4-4 shows that the slurry reaction rate is strongly influenced by added manganese catalyst.
- In all cases there is an abrupt drop in slurry pH upon the introduction of O_2. From this lowered value, the pH will (a) continue dropping at a much slower rate, or (b) flatten out and begin to rise, or (c) a combination of (a) and (b), depending on the initial pH. At a pH below 5, curve type (a) is observed while at a pH above 5.1 type (b) is observed. The changeover between (a) and (b) occurs between 5.0 and 5.1.
- Figure 4-22 shows that the manganese concentration, in the liquid phase of the reactor increases, as the oxidation proceeds and the solids dissolve. These changes in catalyst concentration have a strong effect on the rate of reaction.
- A mathematical model for the slurry reaction predicts the concentrations of both total sulfite and liquid phase sulfite as a function of time as the reaction proceeds.
- By modeling the slurry oxidation with 2000 ppm Mn added, a mass transfer coefficient of 0.02 cm/sec was found.
- From this mathematical model, the $k_{1.5}$ for 0, 6.66, and 200 ppm Mn added reactions are 0.35, 2.0, and 4.5 $\ell^{0.5}/\text{g mol}^{0.5}$ sec. The corresponding experimental values are 0.162, 0.35, and 0.8-5.0 $\ell^{0.5}/\text{gmol}^{0.5}$ sec.
- The mathematical model predictions for total sulfite concentration agree very well with experimental observation, but the prediction of liquid phase sulfite concentration differ significantly from experimental results.

Section 5: Oxidation in Sodium Sulfite Solution

o For examining bisulfite/sulfite kinetics, sodium salts may be used as well as calcium, especially because of their higher solubility and lower impurity level

o With manganese catalyst, $T = 40^{o}C$, $pH = 4.6$, $[Mn] = 2.67$ ppm the rate expression is about second order in sulfur with a rate constant of 0.0004 ℓ/(mol/sec). Under these conditions, these results of the pH method show only a weak dependence of rate on [Mn] on the range 0.3-30 ppm.

o Various organic acids have been used as buffers for this reaction system. One of these same acids has been suggested to improve limestone solubility. The kinetics with these acids present was studied:

o Ferric sulfate solubility in the reacting solution is less than 6 ppm at 40°C and pH 4.6. On the range $T = 30^{o}$ to $50^{o}C$, the activation energy is 18.8 ± 0.8 kcal/mol. The best integer order for $[S^{4+}]$ is two with an average rate constant of 0.14 ℓ/(molsec). On the range 0-5 ppm, the slope of the Rate vs [Fe] line is 0.025--not a strong dependence. By multiple regression analysis, the rate law is:

$$\text{Rate} = 0.155\ [Fe]^{0.18}\ [S^{4+}]^{1.69}$$

o Buffered manganese experiments on the range 0-4 ppm[Mn] showed a 4-minute "induction period." After the induction period the reaction is nearly first order in sulfur (pH: 4.6, $T = 40^{o}C$) with a rate constant depending on [Mn]. Multiple regression analysis showed

$$\text{Rate} = 2.141\ [Mn]^{0.67}[S^{4+}]^{0.94}$$

o Commercial sulfites and limestone contain mixed profiles of iron and manganese. The experiments showed an induction period followed by rates similar to manganese-only catalyzed reactions. Multiple regression analysis confirmed the absence of an iron order; however, the presence of iron changes the dependence on [Mn] to 0.67 though not affecting the sulfur order.

o The effect of oxygen concentration and higher pH may not be studied in the batch reactors. The flow-thermal method is suited for these studies. At pH 5 and 6 the increase of rate with [Mn] is greater than linear. At pH 11 the slope of rate vs [Mn] was 0.67. Multiple regression analysis show the order in sulfur to be approximately 1.5 (1.49 ± 0.17) and the oxygen order to be about 0.5 (0.49 ± 0.19). When manganese is added to the reaction mixture in the +1 oxidation state, the rate is half again faster than it is for manganese in the +2 state.

REFERENCES

1. Abcor, "Carbonate Absorption Process," Wilmington, Mass.

2. Abel, E., "Zur Anionkatalyse der Autoxydation," Monatsch. fur Chemie, 87, 113 (1956).

3. Abel, E., "Uber die Thermische Autoxydation von Sulfit," Monatsch. fur Chemie, 85, 1003 (1954).

4. Abel, E., "Zur Theorie der Oxydation von Sulfit zu Sulfat durch Sauerstoff," Monatsch. fur Chemie, 82, 815 (1951).

5. "Activated Magnesia Method Rids Stack of Sulfur Dioxide in Japanese Process," Chemical and Engineering News, Vol. 47, September 8, 1969, pp. 48, ASTI.

6. Aerojet-General Corporation Contract PH 86-68-77, "Applicability of Aqueous Solutions to the Removal of SO_2 from Flue Gases," prepared by L. E. Gressingh, A. F. Graeffe, F. E. Miller, and H. Barber for the National Air Pollution Control Administration, October 1970.

7. Alper, E., "Kinetics of the Oxidation of Sodium Sulfite Solution," Trans. Inst. Chem. E., 51(2), 159 (1973).

8. Altwicker, E. R. "The Role of Inhibitors in the Kinetics of Sulphite Oxidation," Trans I Chem E, 55, 281 (1977).

9. Amdur, M. O., "Toxicologic Appraisal of Particulate Matter, Oxides of Sulfur, and Sulfuric Acid," J. Air Control Assn., 19, 638 (1969).

10. Anderson, D. O., "Effect of Air Contamination on Health," Can. Med. Assn. J., 97, 528 (1967).

11. Andrieu, "Measurements of Interfacial Area in a Packed Column by the Sulfite Oxidation Method Comparison with Wetted Area," Chem. Eng. Sci , 29 (5), 1263, (1974) Eng.

12. Astarita, G., and G. Marrucci, "Gas Absorption with Zero Order Chemical Reaction," I E C Fund, 2, 4 (1963).

13. Babcock and Wilcox Company report 5153, "Magnesia Base Wet Scrubbing of Pulverized Coal Generated Flue Gas--Pilot Demonstration,: prepared by W. Downs and A. J. Kubasco, September 28, 1970.

14. Backstrom, H. L., "The mechanism of Inhibition in Autoxydation Reactions," Trans. Faraday Soc., 24, 601 (1928).

15. Backstrom, H. L., "The Chain Reaction Theory of Negative Catalysis," JACS, 49, 1460 (1927).

16. Backstrom, H. L., and H. N. Alyea, "Inhibitory Action of Alcohols on the Rate of Oxidation of Sodium Sulfite," JACS, 51, 90 (1929).

17. Baly, E. C., and R. A. Bailey, "Equilibrium in Aqueous Solutions of the Alkali Metal Bisulfites," JCS, 121, 1813 (1922).

18. Barron, C. H., "Reaction Kinetics of the Oxidation of Sodium Sulfite by the Rapid Mixing Flow Method," Thesis, University of Virginia (1963).

19. Barron, C. H., and H. A. O'Hearn, "Reaction Kinetics of the Oxidation of Sodium Sulfite by the Rapid Mixing Flow Method," Chem E Sci, 21, 397 (1966).

20. Bassett, H., and A. J. Henry, "The Formation of Dithionate by the Oxidation of Sulfurous Acid and Sulphites," JCS, 914 (1935).

21. Bassett, H., and W. G. Parker, "The Oxidation of Sulphurous Acid," JCS, 1540 (1951).

22. Bechtel Modified Radian Equilibrium Computer Program, obtained from R. Borgwardt of E. P. A., (1977).

23. Beilke, S. and D. Lamb, "Remarks on the Rate of Formation of HSO_3^- in Aqueous Solution," AIChEJ, 21, 402, (1975).

24. Bengtsson, Sune, Ph.D. Dissertation, Technical University of Munich, (1974)

25. Bengtsson, S., and Bjerle, I., Catalytic Oxidation of Sulfite in Dilute Aqueous Solution, Chem. Eng. Sci. 30 (1975), 1429-1435.

26. Berger, R. L., Balks, B., and Chapman, H., "High Resolution Mixer for the Study of the Kinetics of Rapid Reactions, Rev Sci Inst. 39 493 (68).

27. Bienstock, D., et al. "Removal of SO_2 from Flue Gas with Alkalized Alumina at Elevated Temperatures," ASME Trans. Ser. A., July, (1964), Vol. 86, pp. 353-8, ASTI.

28. Bjerle, I. S. Bengtsson, and K. Farnkvist, "Absorption of SO_2 in $CaCO_3$ Slurry in a Laminar Jet Absorber," CES, 27, (10), (1972).

29. Borgwardt, R. H., "Effect of Forced Oxidation on Limestone /SO_x Scrubber Performance," EPA, (1977).

30. Borgwardt, R. H. Combustion, p. 37, (October 1975).

31. Borgwardt, R. H., "IERL-RTP Scrubber Studies Related to Forced Oxidation," Flue Gas Desulfurization Symposium, EPA, New Orleans.

32. Borgwardt, R. H., "Limestone Scrubbing of SO_2 at EPA/RTP Pilot Plant," Progress Report 23, (April 1976)

33. Borgwardt. R. H., "Limestone Scrubbing of SO_2 at EPA/RTP Pilot Plant," Progress Report 24,(May 1976).

34. Borgwardt, Robert H., "Limestone Scrubbing of SO_2 at EPA/RTP Pilot Plant," Progress Report 25,(June 1976).

35. Borgwardt, R. H., "Limestone Scrubbing of SO_2 at EPA/RTP Pilot Plant," Progress Report 26,(July 1976).

36. Borgwardt, R. H., "Limestone Scrubbing of SO_2 at EPA/RTP Pilot Plant," Progress Report 27,(August 1976).

37. Borgwardt, R. H., D. C. Drehmel, T. A. Kittleman, D. R. Mayfield and J. S. Bowen, "Alkaline Additives for Sulfur Dioxide Control," EPA Cincinnati Annual Report, July 1968-December 1970, DSC/RLB-71-1 (1971).

38. Borgwardt, R. H., "Kinetics of the Reaction of SO_2 with Calcined Limestone," Environmental Science and Technology, 4, 59-63 (1970).

39. Bretsznajder, S., "Katalityczne Utlenianie Dwutlenku Siarki Zaabsorbowanego W Roztworze Zasadowego Siarczanu Glinowego," Roczniki Chem, 29, 227, (1955).

40. Brian, P., J. Hurley, and E. Hasseltine, "Penetration Theory for Gas Absorption Accompanied by a Second Order Chemical Reaction, A.I.Ch.E.J. 7 (1961), 226-231.

41. Brian, P., R. Baddour, and D. Matiatos, "An Ionic Penetration Theory for Mass Transfer with Chemical Reaction," A.I.Ch.E.J. 10 (1964), 727-733.

42. Catipovic, N. M., "Kinetics of Catalyzed and Uncatalyzed Oxidation of Sulfur Dioxide in Aqueous Solution," Thesis, University of Illinois, Urbana (1974).

43. Chalk, A. J., and J. F. Smith, Nature 174, 802 (1954).

44. Chen, T-I., and C. H. Barron, "Some Aspects of the Homogenous Kinetics of Sulfite Oxidation," I E C Fund, 11(4), 466 (1972).

45. Chertkov, B. A., "Theory of Oxidation of Sulfite-Bisulfite Solutions," Zh Prikl Khim, 32, 2609 (1960).

46. Cheng, Robert T., Morton Corn and John O. Frohliger, "Contribution to the Reaction Kinetics of Water Soluble Aerosols and SO_2 in Air at ppm Concentrations," Atmospheric Environment, 5, 987-1009, (1971).

47. Chowdhury, A. K., "Gas-Liquid Reactions Formulation as Initial Value Problems," CES, 28, 658-63, (1973).

48. Coughanowr, D. R., and F. E. Krause, "The Reaction of SO_2 and O_2 in Aqueous Solutions of $MnSO_4$," I E C Fund, 4(1), 61 (1965).

49. Cortelyou, C. G., "Commercial Processes for SO_2 Removal," CEP, 65 (9), 69-77, (1969).

50. Counterman, Paul, E. R. Altwicker, "Inhibition of Oxidation of Sulfur Dioxide During Alkaline Scrubbing," Prep. Paper Nat Meet Div Water Air Waste Chem ACS 12(21), 43-9 (72) Eng.

51. Danckwerts, P. V., Gas-Liquid Reactions, McGraw-Hill, New York, 1970.

52. Danckwerts, P. V. and A. J. Gillham, Trans. Instn. Chem. Engrs. 44, T42 (1966).

53. Danielson, John A., Air Pollution Engineering Manual, Ch. 9, U. S. Dept. of HEW, USGPO, (1967).

54. DeWaal, K. J., and J. C. Okeson, "The Oxidation of Aqueous Sodium Sulfite Solutions," Chem E Sci, 21, 559 (1966).

55. "Desulfurization Process Uses Electrodialysis," C & EN, 519, 23, (1977).

56. Draemel, Dean, "An EPA Overview of Sodium-Based Double Alkali Processes Part 1. A View of the Process Chemistry of Identifiable and Attractive Schemes," EPA Flue Gas Desulfurization Symposium, New Orleans, May 14-17, (1973).

57. Duprey, R. L., "The Status of SO_x Emission Limitations," Chemical Engineering Progress 68, 70-76 (1972).

58. Emmert, "A Study of Gas Absorption in Falling Liquid Films O_2 and CO_2," ChE Prog. 50, 87 (1954).

59. Engdahl, Richard B., "A Critical Review of Regulations for the Control of Sulfur Oxide Emissions," Journal of the Air Pollution Control Association 23, 364-375 (1973).

60. EPA, "National Public Hearings on Power Plant Compliance with SO_x Air Pollution Regulations," Submitted to Administrator of EPA, January (1974).

61. EPA, "National Strategy for Control of Sulfur Oxides from Electric Power Plants," Report 10 Jul (1974).

62. Erwin, J., "Sulfur Dioxide Oxidation," Thesis, University of Illinois, (1975).

63. Foskett, N. L. and Lowrance, E. G., "Stone and Webster Ionics SO_2 Removal and Recovery Process," EPA Flue Gas Desulfurization Symposium, New Orleans, May 14-17, (1973).

64. Foster, P. M., "The Oxidation of Sulfur Dioxide in Power Station Plumes," Atmospheric Environment, 3, 157 (1969).

65. Frydaman, G. N., Torsten, R., and Sillen, L. G., "Some Solution Equilibrium $CaCO_3$ and $CaSO_3$," Acta Chem. Scand., 12, 878 (1958).

66. Fuller, E. C., and R. H. Crist, "The Rate of Oxidation of Sulfite Ions by Oxygen," JACS, 63, 1644 (1941).

67. Fuzzi, Sandro, "Study of the Iron (III) Catalyzed Sulfur Dioxide Oxidation in Aqueous Solution Over a Wide Range of pH."

68. Gall, R. L., E. J. Pasecki, W. Michael, "Removing SO_2 from Stack Gases by a Double Alkali: Wet Scrubbing Process," AICHE Meeting, Washington D.C., (Dec. 1974).

69. Gifford , D. C., "Operation of a Limestone Wet Scrubber," CEP, 69 (6), (1973).

70. Gladkii, Working Group on Stationary Source Air Pollution Control Technology; State Scientific Research Institute of Industrial and Sanitary Gas Cleaning, USSR, Moscow, (1974).

71. Goodwin, R. W., "Oxidation of Flue Gas Desulfurization Waste and the Effect on Treatment Modes," J. Air Pollution Control Assn. 28, 35, (1978).

72. Gorman, David N., B. S. Thesis, University of Virginia, (1979).

73. Graff, Robert A. and Robert Pfeffer and Arthur M. Squires, "Capturing Sulfur with Calcined Dolomite," Second International Clean Air Congress in Washington, D.C., Dec. 6-11, (1970).

74. Graffeo, Harpel, and Hsu, "Kinetics of $CaSO_4$ Crystallization Applied to FGD Problems," AIChE Meeting, Washington D.C., Dec. (1974).

75. Gunn, D. J., and A. Saleem, "Absorption and Liquid Phase Oxidation of Sulfur Dioxide," Trans. Inst. Chem. E., 48, T46 (1970).

76. Haber, F., and F. Braun, "Uber die Autoxydation. II," Z Phys. Chem., 35, 84 (1900).

77. Harpel, W. I., et al., "The Chemistry of Scrubbers," Comb. p. 33, March, (1976)

78. Harvey, R. D., Frost, R. R. and Thomas, Josephus, Jr., "Use of Carbonate Rocks for Control of Sulfur Dioxide in Flue Gases," Part I., EGN 55, Illinois State Geological Survey, August (1972).

79. Harvey, R. D. and Steinmetz, John D., "Petrographic Properties of Carbonate Rocks Related to their Sorption of Sulfur Dioxide," EGN50, Illinois State Geological Survey, September (1971).

80. Hartley, Edwin M. and Michael J. Matteson, "Catalytic Oxidation of Sulfur Dioxide at 3000-5000 ppm and Various Temperatures by Aqueous Solutions of Manganese Sulfate," 165th ACS National Meeting, Division of Industrial and Engineering Chemistry (1973).

81. Hatfield, J. D., Y. K. Kim, and R. C. Mullins, "Study of the Effect of Organic Acids on the Wet-Limestone Scrubbing Process," Report for the Environmental Protection Agency, Contract # T-V-34425A, Feb. 24, (1972).

82. Hatfield, J. D. and J. M. Potts, "Use of Weak Acids to Improve Absorption by Limestone Slurries," 72nd National Meeting of AIChE, May 21-24, (1972).

83. Head, N. N., S. C. Wang, and R. T. Keen, "Results of Lime and Limestone Testing with Forced Oxidation at the RPA Alkali Scrubbing Test Facility," Bechtel Corp., (1977).

84. Higginson, W. C., "Equivalence Changes in Oxidation-Reduction in Solution. Some Aspects of Sulfurous Acid," *JCS*, 447 (1957).

85. Hikita, H. and M. Asai, "Gas Absorption with (m,n)th Order Irreversible Chemical Reaction," *Int. Chem. Eng. 4* (1964), 332-340.

86. Hoather, R. C., and C. F. Goodeve, "The Oxidation of Sulphurous Acid," *Trans. Faraday Soc.*, *30*, 626, 1149 (1934).

87. Horlacher, W. R., "Four SO_2 Removal Systems," *Chem E. Prog*, *68(8)*, 43 (1972).

88. Johnson, N. M., and R. C. Reynolds, "Atmospheric Sulfur," *Science*, *177* 514 (1972).

89. Johnstone, Field, and Tassler, "Gas Absorption and Aerosol Collection in a Venturi Atomizer," *IEC* *46*, 1601 (54).

90. Johnstone, H. F. and A. D. Singh, "Recovery of Sulfur-Dioxide from Waste Gases, Design of Scrubbers for Large Quantities of Gases," *IEC* *29*, 286 (1937).

91. Johnstone, H. F., and A. J. Moll, "Formation of Sulfuric Acid in Fogs," *I E C*, *52* 861 (1960).

92. Johnstone, H. F., and Singh, A. D., "The Recovery of Sulfur Dioxide from Dilute Waste Gases by Chemical Regeneration of the Absorbent," *I E C*, *32*, 1037 (1946).

93. Johnstone, H. F., and D. R. Coughanowr, "Absorption of Sulfur Dioxide from Air," *I E C*, *50*, 1169 (1958).

94. Judeikis, H. S. 1976.

95. Junge, C. E., and T. G. Ryan, "The Study of SO_2 Oxidation in Solution and its Role in Atmospheric Chemistry," *Quart J. Roy Meterol Soc.*, 84, 46 (1958).

96. Kaplan, Norman, "An EPA Overview of Sodium-Based Double Alkali Processes, Part II. Status of Technology and Description of Attractive Schemes," EPA Flue Gas Desulfurization Symposium, New Orleans, May 14-17, (1973).

97. Kellogg, W. W., R. D. Cadle, E. R. Allen, A. L. Lazrus, and E. A. Martell, "The Sulfur Cycle," Science, 175, 587 (1972).

98. Kerr, Clayton P., "Sulfur Dioxide Removal in Venturi Scrubbers," EPA Office of R & D.

99. Kerr, C. P. "Aqueous Sodium Sulfite Bisulfite and Sulfate Equilibriums," AIChEJ, 20(6), 12-13-15 (1974), Eng.

100. Kesler, R. B. and Han, S. T., "Solubility and Neutralization Equilibria in the Magnesium-Base Sulfite Acid System" Tappi, 45(7), (July 1962).

101. Kikuchi, S., K. Honda, and S. Kim, "Removal of Dissolved Oxygen by Sodium Sulfite," Bull. Chem. Soc. Jap., 27, 65 (1954).

102. King, C. J., "Turbulent Liquid Phase Mass Transfer to a Free Gas-Liquid Interphase," IEC Fund, 5, 1 (1966).

103. La Mantia, C. R., E. R. Bangel, T. J. Lamb and R. Phillips, "Sulfur, Sulfuric Acid and Pollution Problems...and Control for Small Scale Facilities," American Institute of Chemical Engineers Sixty-third Annual Meeting Held in Chicago, Illinois on November 29-December 3, (1970).

104. Lee, J. C. and Meyrrek, D. L., "Gas-liquid Interfacial Areas in Salt Solutions in an Agitated Tank," Trans. Inst. Chem. Engrs., 48, pt37 (1970).

105. Leo, P. P. and J. Rossoff, "Catalytic Concentrations in Scrubber Liquor," EPA-600/7-76-018, (October 1976).

106. Likens, Gene E., "Acid Precipitation," C & EN, Nov. 22, 29 (1976).

107. Linek, V., "The Oxidation of Aqueous Sulfite Solutions," Chem. E. Sci., 26, 491 (1971).

108. Linek, V., and J. Mayrhoferova, "The Kinetics of Oxidation of Aqueous Sodium Sulfite Solutions," Chem. E. Sci., 25, 787 (1970).

109. Linek, V., and J. Tvrdik, "Generalization of Kinetic Data on Sulfite Oxidation Systems," Biotech Bioeng, 13(3), 353 (1971).

110. Little, A. D., Inc., "Sulfur Dioxide Control Process Study-Sodium Scrubbing with Lime Regeneration," a Report to Illinois Institue for Environmental Quality, (January 1972).

111. Loading, J. W. and J. G. Patel, CRP 71, 85, (1975).

112. Mason, R. B., and J. H. Mathews, "The Effect of UV Light on the Oxidation of Sodium Sulfite by Atmospheric Oxygen," J. Phys Chem, 30, 414 (1926).

113. McKay, H. A., Atmospheric Environment, 5, 7 (1971).

114. McMichael, W., L. Fan, C. Wen, "Analyais of SO_2 Wet Limestone from Pilot Plant Spray and TCA Scrubbers, Ind. Eng. Chem. Process Dev. Des. 15 (1976), 459-467.

115. Milbauer, J., and J. Pazourek, "L'Oxydation des Sulfites en Solution Concentratees," Bull. Soc. Chim Fr. 31, 676 (1922).

116. Mishra, G. C. and R. D. Srivastava, "Homogeneous Kinetics of Potassium Sulfite Oxidation," CES, 31, 969 (1976).

117. Mishra, G. C. and R. D. Srivastava, "Kinetics of Oxidation of Ammonium Sulfite by Rapid Mixing Method," CES 30 1387 (1975).

118. Miyamatto, S., "The Effect of Alkali on the Oxidation of Sodium Sulfite with Air," Bull. Soc. Chim Jap, 2, 74 (1927).

119. Miyamatto, S., and T. Kaya, "On the Rate of Solution of Oxygen into Water, Part VI," Bull. Soc. Chim Jap, 6, 264 (1931).

120. Miyamatto, S. and T. Kaya, "On the Dissolution Velocity of O_2 in H_2O," Bull. Ch Soc. Jap 5 321 (1930).

121. "Monsanto Co. Removal System," Chemical and Engineering News, Vol. 20, July 20, 1970, p. 20, CENI.

122. Morgan, O. M., and O. Maas, "An Investigation of the Equilibria Existing in Gas-Water Systems Forming Electrolytes," Can. J. Res., 5, 162 (1931).

123. Murthi, Kotturi S., Douglas Harrison, Raymond K. Chan, "Reaction of Sulfur Dioxide with Calcined Limestones and Dolomites," Environmental Science and Technology 5, (9) 776-781 (1971).

124. Nannen, L. W., R. E. West, and F. Kreith, "Removal of SO_2 from Low Sulfur Coal Combustion Gases by Limestone Scrubbing," JAPCA, 24(1), (1974).

125. Nash, L. K. Elements of Statistical Thermodynamics, Addison Wesley, Don Mills, Ontario (1968).

126. Nurmi, D., M.S. Thesis, University of Virginia, (1978).

127. Okabe, "Auto-oxidation of Sulfite and its Redox Potential," Japan Chem Soc J81, 1818 (60) (Jap).

128. Oldenkamp, R. D. and E. O. Margolin, "The Molten Carbonate Process for Sulfur Oxide Emissions," CEP, 65 (11) 73-76 (1969).

129. Onda, K., H. Takeuchi, and Y. Maeda, "The Absorption of Oxygen into Sodium Sulfite Solutions in a Packed Column," Chem. E. Sci., 27(2), 449 (1972).

130. Onda, K., T. Kobayashi, and M. Fujine, "Behavior of the Reaction Plane Movement in Gas Absorption Accompanied by Instantaneous Chemical Reaction," Chem. E. Sci., 26, 2009 (1971).

131. Phillips, D. H., and M. J. Johnson, "Oxygen Transfer in Agitated Vessels," I E C, 51(1), 83 (1959).

132. Phillips, Robert J., "Sulfur Dioxide Emmission Control for Industrial Power Plants," Project Engineer Paper, G. M. Tech. Center, 603-638, (1971).

133. Pitzer, Kenneth S., "Thermodynamics of Electrolytes. 1. Theoretical Basis and General Equations," J. Phys. Chem., 77, (2) 268-277.

134. Potts, J., et al., "Removal of Sulfur Oxides from Waste Gases," Report by Tennessee Valley Authority, Applied Research Branch, (1972), 22-39.

135. Powell, R. H., "Kinetics of SO_2 Oxidation," Thesis, University of Illinois, Urbana (1973).

136. Pritchett, P. W., "The Catalyzed Reaction of Oxygen with Sulfurous Acid with its Effects on the Absorption of Oxygen into Water," Thesis, University of Delaware (1961).

137. Rabe, A., "Vapor-Liquid Equilibrium Data for the Binary System: SO_2/H_2O," J. of Ch. Data, 8 333, (1963).

138. Ramachandran, P. and M. Sharma, "Absorption with Fast Reaction in a Slurry Containing Sparingly Soluble Fine Particles," Chem. Eng. Sci. 24 (1969), 1681-1686.

139. Rand, M. C. and S. B. Gale, "Kinetics of the Oxidation of Sulfites by Dissolved Oxygen," Rudolfs Research Conference, Rutgers State Univ. 380 (1967).

140. Reinders, W., and S. T. Vles, "Reaction Velocity of Oxygen with some Inorganic Salts III," Rec Trav Chim, 44 249 (1925).

141. Reith, T., and W. J. Beek, "The Oxidation of Aqueous Sodium Sulfite Solutions," Chem. E. Sci., 28, 1331 (1973).

142. Rochelle, Gary T. and Judson King, "The Effect of Additives on Mass Transfer in $CaCO_3$ or CaO Slurry Scrubbing of SO_2 from Waste Gases," IEC Fund, 16, No. 1, (1977).

143. Rodinov, A. I., "Determination of Phase Contact Surface During the Oxidation of Sodium Sulfite Solutions by Atmospheric Oxygen in a Grid Plate Column," Izu. Vyssh Ucheb Zaved Khim Teknol, 13(12), 1805, (1970).

144. Ross, L. and H. Lewis, "Reaction of Sulfur Oxides with Phosphate Rock," Ind. & Eng. Proc. Design, Vol. 6 Oct., (1967), pp. 407-8, ASTI.

145. Sada, E., H. Kumozawa, and M. A. Buti, "Chemical Absorption into a Finite Slurry," CES, 34, 715-718, (1979).

146. Sappok, R., and P. Walker, "Removing Sulfur Dioxide form Flue Gases Using Carbon at Elevated Temperatures," Air Pollution Control Association Journal, Vol. 19, November (1969), pp. 856-861, ASTI.

147. Sawataki, K. "Antioxidants for Sulfites," Kokai, 66, 595 (1973).

148. Sawicki, J. E., "Reaction Kinetics of Heterogeneous Oxidation of Sodium Sulfite," Thesis, University of Virginia, (1972).

149. Sawicki, J. E., and C. H. Barron, "On the Kinetics of Sulfite Oxidation in Heterogeneous Systems," Chem. E. J. (Lusanne), 5(2), 153 (1973).

150. Schroeter, L. C., "Sulfurous Acid Salts as Pharmaceutical Antioxidants," J. Pharm. Sci., 50, 891 (1961).

151. Scriven, L. E., "Absorption into a Accelerating Film," AIChEJ, 4, 382, 439, (1958).

152. Schroeter, L. S. "Potentiometric Determination of Sulfite Oxidation Rates," J. Pharm. Sci., 52(6), 654 (1963).

153. Schroeter, L. D., "Kinetics of Air Oxidation of Sulfurous Acid Salts," J. Pharm. Sci., 52(6), 559 (1963).

154. Schmidt, M., "World Health Organization Project US3100," U. S. Air Poll Contr Admin (1970).

155. Schultz, J. S., and E. L. Gaden, "Sulfite Oxidation as a Measure of Aeration Effectiveness," I E C, 48(12), 2209 (1956).

156. Seidell, A., "Solubilities of Inorganic and Metal Organic Compounds," D. Van Nostrand Co., Inc., New York, 3rd ed. 328, (1940).

157. Shah, Y. T. and C. N. Kenney, "Application of Penetration and Film Theories to the Catalysis of Gas Reactions by Liquid Catalysts: the Oxidation of Sulphur Dioxide," CES, 27, 1-10, (1972).

158. Shah, I. S. and Quigley, C. P., "Magnesium Base SO_2 Recovery Process A Prototype Installation at Boston Edison Company and Essex Chemical Company," American Institute of Chemical Engineers, Atlantic City, New Jersey, (Aug. 1971).

159. Sherwood, T. K., "Performance of Pack Towers," Trans AIChE 36, 39, (1940).

160. Singh, D. K., R. N. Sharma, and R. D. Srivastava, "Kinetics of Oxidation of Sodium Dithionite by Flow Thermal Method," AIChEJ 24, 232 (1978).

161. Slack, A., and L. Falkenberg, "Sulfur Dioxide Removal from Power Plant Gases by Limestone Injection, (TVA)," Combustion Magazine, Vol. 41, December (1969), pp. 15-21, ASTI.

162. "Sludge Oxidation in Limestone FGD Scrubbers," Interagency Energy--Environment Research and Development Report, EPA-600/7-7-061 (1977).

163. Srivastava, R. D., A. F. McMillan, and I. J. Harris, "The Kinetics of Oxidation of Sodium Sulfite," Can. J. Chem. E., 46, 181 (1968).

164. Stites, J. G., Jr., et al., "Catalytic Oxidation System for Removing Sulfur Dioxide from Flue Gas," Combustion Magazine, Vol. 40, May 1969, p. 20, Vol. 41, December 1969, pp. 23-24, ASTI.

165. Struck, Robert T., Metro D. Kulik and Everett Gorin, "Removal of Sulfur Dioxide from Stack Gases by a Modified Claus Process," Env. Sci. & Tech., 5(7), 626-630, (1971).

166. Summers, Peter W. and Brian Hitchon, "Source and Budget of Sulfate in Precipitation from Central Alberta, Canada," J. of the Air Pollution Control Association, 23, 194-199 (1973).

167. Tartar, H. V., and H. H. Garretson, "The Thermodynamic and Ionization Constants of Sulfurous Acid at 25°C," JACS, 63, 808 (1941).

168. Terjesen, Sven G., "Mass Transfer with Chemical Reaction," Kem-Tek, 2, Congress, (Nov. 4).

169. Thomas, W. J., "The Abosorption of Sulphur Dioxide in Water Part I--Theory," Trans. Instn. Chem. Engrs., 42, T3-T6, (1964).

170 Thomas, W. J., "The Absorption of Sulphur Dioxide in Water Part II--Experimental Analysis," Trans. Instn. Chem. Engrs., 42, T7-T12, (1964).

171. Titoff, A., "Beitrage zue Kenntnis der Negativen Katalyse in Homogenen System," Z Phys Chem., 45, 614 (1903).

172. Tsirlin, A., V. N. Trushanov, and G. Y. Khodov, "The Use of Cobalt Sulfate as a Catalyst of Sodium Sulfite Oxidation in Aqueous Solution," Zh Prikl Khim, 46(10), 2167 (1973).

173. Uchida, S., H. Moriguchi, H. Maejimo, K. Koide and S. Kageyama, "Absorption of Sulfur Dioxide into Limestone Slurry in a Stirred Tank Reactor," Can. J. ChE., 56, (1978).

174. Uchida, S., C. Y. Wen, "Rate of Gas Absorption into a Slurry Accompanied by Instantaneous Reaction," CES, 32(11) 1277-1281, (1977).

175. Uchida, S., C. Y. Wen, and W. J. McMichael, "Role of Holding Tank in Lime and Limestone Slurry Sulfur Dioxide Scrubbing," I & EC Proc. Des. and Dev, 15, 88, (1976).

176. Uno, T., S. Fukui, M. Atsukawa, M. Higashi, H. Yomada, and K. Kamel, "Sacle-Up of a SO_2 Control Process," CEP 66 61-65 (1970).

177. Villiers-Fisher, John F., "Removal of Sulfur-Dioxide from Gas Streams," U.S. Pat: 3-833-711.

178. Vivian, J. E., "Liquid Side Resistance in Gas Aborption," AIChEJ, 2, 437 (1956).

179. Walter, P. E., "SO_2 Oxidation Kinetics," Thesis, University of Illinois, Urbana (1972).

180. Weast, R., "Handbook of Chemistry and Physics," CRC Press, 56th ed., B-236 (1975-1976).

181. Weast, R., "Handbook of Chemistry and Physics," CRC Press, 56th ed., D-152 (1975-1976).

182. Weisnicht, William L., M. S. Thesis, University of Virginia (1978).

183. Wen, C. Y. W. J. McMichael, R. D. Nelson, Jr., "Scale Control in Limestone Wet Scrubbing Systems," EPA-650/2-75-031 (1975).

184. Wen, C., W. McMichael, R. Nelson, "Scale Control in Limestone Wet Scrubbing Systems," Report to U.S. EPA by A. D. Little, Inc., (1975), 37-57.

185. Wesselingh, J. A., and A. C. Van't Hoog, "Oxidation of Aqueous Sulfite Solutions," Trans. Inst. Chem. E., 48, T69 (1970).

186. Winter, E. R., and H. Briscoe, "Oxygen Atom Transfer During the Oxidation of Aqueous Sodium Sulfite," JACS, 73, 496 (1951).

187. Yagi, S., and H. Inoe, "The Absorption of Oxygen into Sodium Sulfite Solution," Chem. E. Sci., 17, 411 (1962).

188. Young, S. L., "The Inhibition of Chemical Reaction by Foreign Substances," JACS, 24, 297 (1902).

189. Yui, T., "Dissociation Constant of Sulfurous Acid," Tokyo Inst. P. Chem. Bull., 19, 1229 (1940).

190. Zagorski, Z. P., K. Sehested, S. O. Nielsen, "Pulse Radiolysis of Aqueous Alkaline Sulfite Solutions," J. Phys Chem, 75(23), 3510 (1971).